VOLUME 46, NUMBER 12

December, 1958

published monthly by The Institute of Radio Engineers, Inc.

Proceedings of the IRE®

contents

DECEMBER

published monthly by The Institute of Radio Engineers, Inc.

Proceedings of the IRE®

continued

COVER

Unusual interference patterns can be produced by reflecting colored light from the grooves of a revolving phonograph record modulated at a single frequency. By measuring the distance between certain of the irregular dark lines that run upward through the white lines, the modulation amplitude of the grooves can be calculated, as described in the IRE Standards on page 1940.

PROCEEDINGS OF THE IRE, published monthly by The Institute of Radio Engineers, Inc. at 1 East 79 Street, New York 21, N. Y. Manuscripts should be submitted in triplicate to the Editorial Department. Responsibility for contents of papers published rests upon the authors, and not the IRE or its members. All republication rights, including translations, are reserved by the IRE and granted only on request. Abstracting is permitted with mention of source.

Thirty days advance notice is required for change of address. Price per copy: members of the Institute of Radio Engineers, one additional copy $1.25; non-members $2.25. Yearly subscription price: to members $9.00, one additional subscription $13.50; to non-members in United States, Canada, and U. S. Possessions $18.00; to non-members in foreign countries $19.00. Second-class postage paid at Menasha, Wisconsin, under the act of March 3, 1879. Acceptance for mailing at a special rate of postage is provided for in the act of February 28, 1925, embodied in Paragraph 4, Section 412, P. L. and R., authorized October 26, 1927. Printed in U.S.A.

December, 1958
Vol. 46 No. 12

Proceedings of the IRE

Poles and Zeros

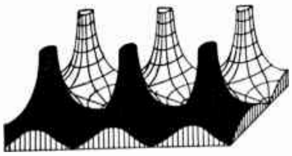

Engineering Shortage, 1962? Passing almost without notice is the fact that last year's college class of freshman engineers increased only about one per cent over that of 1956. Scattered early reports this fall indicate no significant increase over 1957 and possibly a drop. This does not bode well for the accuracy of predictions which showed our graduations of 1961 and 1962 on an upward trend.

Countering this downward enrollment is a shift to larger electrical engineering enrollments where, under the impact of electronics, many of our departments have made advances in removing the hardware and are attacking the subject at a high science level. Of course you can hear that these boys are attracted to electrical engineering only by the glamor, that the field will not be able to support so many, and they will inevitably return to the older engineering disciplines as more sound and solid. We seem to recall having heard that once before, and isn't electronics now our fifth largest industry?

Good students go where they see the greatest intellectual challenge, and electrical engineering seems to be that field. Another overlooked straw in the wind is that science enrollments generally went up this fall. Does this indicate a greater challenge from the science field to the young student? Do non-electrical branches of engineering appear less glamorous, more stultified, more tied to techniques of this earth than does electrical engineering or science? Has our renovation of engineering education been too long debated and delayed on many campuses, and has it thus placed us in the position of running behind in meeting the desires and aspirations of the good students? Are we going to miss our opportunity and remain a profession of quasi-technicians?

Or does it mean that the electrical engineers are going to have to do the whole job—witness digital computer applications to machine tools or highway cuts and fills (Scanning the TRANSACTIONS, page 1972 this issue).

Shows and Symposia. An extensive complex of shows and exhibits, accompanied by technical symposia, has grown up in the electronics profession around IRE sponsorship. Since the first National Electronics Conference in Chicago in 1944 we have added WESCON, NEREM, SWIRECO, MAECON, Dayton PGANE, and others. In recent weeks after attendance at the Cedar Rapids event and NEC, and a near miss at the Canadian Eighth Region Exhibition, we have been impressed with the "taking it to the grass roots" aspects of these services to the electronic profession.

The National Electronics Conference is probably the oldest such event, having just run its fourteenth version. Started in 1944, it already has traditions among which is the story that it was planned in a cocktail lounge with only fuzzy memories and the minutes on a napkin. After it was swamped with an attendance of 3000 in wartime Chicago after advance preparations for 400, the statement now is that if you stood in line all day for a hotel room, after having confirmed reservations, you are properly a Founder, and if you then slept in the swimming pool you are a Charter Member. The NEC has continued to prosper, and this year had the foresight to sign up in May as a luncheon speaker the man who reciprocated by selecting the NEC weekend to fire the first moon shot that got away—Dr. Simon Ramo.

In operating conferences and shows for service to the profession we have also developed a breed of young volunteer show and convention managers who know how to stage such events properly—who sell the exhibit space, sort the abstracts to find the papers most suited to today's technical interests, sandbag the banquet speakers into speaking, and then start the sessions on time and know how to properly greet and introduce a speaker.

It does not appear that our counterparts in other technical fields have developed these skills in handling guests, nor in conveying apparatus and information to the hinterlands. Perhaps it is the easy portability of much electronics hardware, but we are more inclined to suspect the continuing technical hunger of alert and young scientifically trained minds. The recent shows again contribute to the feeding of these appetites, with improvements in measuring equipment, further sophistication in computing and data handling, and the continuing ascendance of the transistor.

Who attends these symposia and shows? The answer points to the man concerned with technical projects or responsibilities, there to hear papers which will aid him in the solution of his problem, or to find a new Mark II widget, half as large, one fourth as heavy, and ten times as fast as the old 1957 Mark I he has been using. Does he actually attend? Incomplete figures show attendance around the country in excess of 115,000 last year. Considering an IRE membership of 68,000 and a *Fortune* estimate of 100,000 as the electronic engineering population of the country, it seems fair to conclude that these exhibits and programs do serve our profession.

New Members, Anyone? Realizing that an EMF E does not produce a rapid response in circuits of high L, or that an impulse does not instantaneously move a heavy body, or that an application blank is not always to be had when the will to sign is, you will find a membership application ready for filling out and signing following page 6 of the new IRE DIRECTORY, so conveniently placed you need not even lift the DIRECTORY.
—J.D.R.

Elmer H. Schulz

Director, 1958-1959

E. H. Schulz (A'38–SM'46–F'58), assistant director of Armour Research Foundation of Illinois Institute of Technology, was born in Lockhart, Tex., on October 30, 1913. He was graduated from the University of Texas in Austin with the B.S. degree in electrical engineering in 1935 and the M.S. degree in 1936. He received the Ph.D. degree from the Illinois Institute of Technology in Chicago in 1947.

From 1936 to 1942 he taught electrical engineering at the University of Texas. In 1942 he joined the staff of Illinois Institute of Technology, where he taught senior and graduate courses in radio engineering and was in charge of war-training programs in electronics and radio.

He became assistant chairman of the electrical engineering research department of Armour Research Foundation in 1946, and the following year was named chairman of the electrical engineering department. Later he became manager of the physics and electrical engineering division. His advancement to assistant director of the Foundation in 1953 put him in charge of the research activities of nearly 900 scientists and engineers in nine departments.

He is co-author of "Experiments in Communications and Electronic Engineering," and the author of a number of technical papers. His present position in the IRE is director for the Fifth Region. He served as chairman of the Chicago Section in 1949–1950, and has been on the National Education Committee and the National Industrial Electronics Committee.

Dr. Schulz is a past president of the National Electronics Conference and the Radio Engineers Club of Chicago. He is a Fellow of the American Institute of Electrical Engineers and a member of the Western Society of Engineers and the American Association for the Advancement of Science.

Scanning the Issue

General Power Relationships for Positive and Negative Nonlinear Resistive Elements (Pantell, p. 1910)—Considering the key role that nonlinear devices have long played in radio and electronics, it may seem surprising that our theoretical understanding of nonlinear circuits has not been more fully developed long ago. Although the difficulty of analyzing nonlinear phenomena has caused progress to come slowly, the emergence of more sophisticated devices has provided considerable incentive in recent years for learning more about fundamental properties of nonlinear circuit elements. As a result, a number of important papers have been published on the subject just in the past several years. One of these, which appeared in PROCEEDINGS two years ago, investigated some general power relations which govern nonlinear reactance modulators, yielding equations that have proven to be of far-reaching significance in the study of modulators, demodulators, harmonic generators, and parametric amplifiers. The present paper extends this work to include nonlinear resistors, deriving some important relationships concerning modulation efficiency, efficiency of harmonic generation, and stability.

Performance of Some Radio Systems in the Presence of Thermal and Atmospheric Noise (Watt, *et al.*, p. 1914)—This paper presents a wealth of practical communications data that will be of value to engineers concerned with radio systems design and performance specification. The authors examine a large amount of experimental data, both their own and data reported by other workers, for the purpose of comparing the performance of several basic types of communication systems under various typical conditions of fading and noise. The systems studied are aural Morse, frequency shift keying teletype, and voice. From the results of this analysis it now appears possible to predict with a good degree of accuracy the performance of many types of radio systems under a wide range of typical noise conditions. This study should be valuable as a reference in considering the choice of various types of systems, as well as the operating parameters of the system finally selected.

Structure-Determined Gain-Band Product of Junction Triode Transistors (Early, p. 1924)—Ever since the transistor was first developed there has been a good deal of interest in the maximum frequency that could be achieved for amplification and oscillation. The early transistors operated at only a few megacycles. We now have all-transistor equipment that operates at 100 megacycles, and transistors that have been made to oscillate at above 1000 megacycles in the laboratory. This paper describes the upper frequency limit of a diffused base triode transistor in terms of a gain-bandwidth figure of merit that is approximately equal to the maximum frequency of oscillation, and examines what effect the structure of the transistor and the operating biases have on this merit figure. The analysis shows that the diffused base transistor has an upper frequency limit that is an order of magnitude higher than either the field effect or analog transistor, and points an encouraging finger at the possible use of transistors for some microwave applications.

IRE Standards on Audio Techniques: Definitions of Terms, 1958 (p. 1928)—This Standard updates and supersedes a like named Standard issued by the IRE in 1954, covering a subject which represents one of the largest fields of interest (in terms of number of members) within the IRE. It is encouraging to note that despite the fact that radioelectronics is rapidly changing from an empirical art to a highly sophisticated science, its practitioners are still talking in down-to-earth language. Among the 170 terms defined herein one will find such unpretentious and vividly descriptive words as babble, hiss, hum, singing, and thump. In fact, the only verbal atrocity we could find in its half-dozen pages was one in which radio engineers had no hand in inflicting on a defenseless society: onomatopoeic.

Frequency Variations in Short-Wave Propagation (Ogawa, p. 1934)—If a short-wave transmitter could be built having perfect frequency stability, the signal would nevertheless vary in frequency at the receiving end. The variations would be caused by the up-and-down movement of the reflecting layer of the ionosphere, creating a Doppler effect, and by variations of electron density in the atmosphere, causing changes in propagation velocity. This paper explores the nature and magnitude of these variations and describes experiments in which they were accurately measured. The results are of quite broad interest. For one thing, they emphasize that frequency variations in the short-wave band, where most of the world's standard frequency signals are transmitted, are surprisingly worse than in the VLF band. The magnitude of the variations will also interest communications people, especially those concerned with single sideband systems, where small frequency deviations can cause distortion of the received signal. Finally, the observations provide further insight into the short and long term instabilities and disturbances in the ionosphere itself.

IRE Standards on Recording and Reproducing: Methods of Calibration of Mechanically-Recorded Lateral Frequency Records, 1958 (p. 1940)—It is not unlikely that quite a number of PROCEEDINGS readers automatically skip over an IRE Standard when it appears, figuring that it will be about as exciting to read as the dictionary. Actually, these documents, covering as they do the measurement and description of almost every phenomenon and concept in the realm of radio engineering, are very much alive with a rich technical lore that is not only highly instructional but often interesting and unusual as well. This Standard deals with frequency records—records on which various significant frequencies have been recorded in order to test phonograph pickups and recording systems. The purpose of this document is to describe ways of measuring and calibrating the recorded amplitude of the signals impressed in the record. The front cover of this issue hints at the unexpected and ingenious nature of the methods employed. For further details see page 1940.

Annual Indexes to IRE Publications (following p. 1994)—The final 40 pages of the editorial section of this issue provide a key to a major share of the technical developments reported in our field during 1958. In these pages will be found indexes to the titles, authors, and subjects of nearly 1000 papers, letters, and book reviews which appeared in the pages of the PROCEEDINGS, the IRE NATIONAL CONVENTION RECORD, and the IRE WESCON CONVENTION RECORD this year. The 1958 index to the Professional Group TRANSACTIONS covering another 800 papers will be published early next year.

An important change has been made this year in the form of the indexes. The author and subject listings, instead of giving a cumulative index number which then has to be looked up in a table of contents to be further identified, refer directly to the month and page number where the item was published.

It might be noted in passing that these final 40 pages bring the number of PROCEEDINGS editorial pages published in 1958 to a grand total of 2200, an 18 per cent increase over 1957.

Scanning the TRANSACTIONS starts on page 1972.

General Power Relationships for Positive and Negative Nonlinear Resistive Elements*

RICHARD H. PANTELL†, ASSOCIATE MEMBER, IRE

Summary—The method developed by Manley and Rowe for the treatment of nonlinear reactive elements is extended to include nonlinear resistors. General power relationships are derived which yield modulation efficiency, efficiency of harmonic generation, and stability criterion.

Introduction

Manley and Rowe [1] developed some general power relationships for nonlinear reactive elements, and Page [2] considered power relationships for positive nonlinear resistors. The term "positive" implies that $\partial i/\partial v \geq 0$, where i = current, v = voltage, for all values of current and voltage. By means of an approach analogous to the procedure used by Manley and Rowe, it is possible to derive power relationships for positive and negative nonlinear resistors, and to obtain criteria for instability resulting from the presence of a negative nonlinear resistor.

Energy Relationships

It is assumed that voltage is a single-valued function of current, and that both the voltage and current associated with the nonlinear resistor of Fig. 1 can be expanded in Fourier series.

Each parallel branch in Fig. 1 is tuned to a different frequency. From left to right, the first branch is the nonlinear resistance, the second branch is tuned to dc, the third branch is tuned to ω_1, the fourth to ω_0, and the remaining branches resonate at sum and different frequencies of ω_1 and ω_0. The Fourier expansions for voltage and current are:

$$v = \sum_{m=-\infty}^{\infty} \sum_{n=-\infty}^{\infty} V_{mn} e^{j(mx+ny)} \tag{1}$$

$$i = \sum_{m=-\infty}^{\infty} \sum_{n=-\infty}^{\infty} I_{mn} e^{j(mx+ny)} \tag{2}$$

$$x = \omega_1 t$$

$$y = \omega_0 t.$$

The dc term is included by letting $m = 0 = n$.

Since i and v represent real quantities,

$$V_{mn} = V_{-m-n}^*$$

$$I_{mn} = I_{-m-n}^* \tag{3}$$

where the asterisk denotes the complex conjugate. The average real power associated with the mn term is

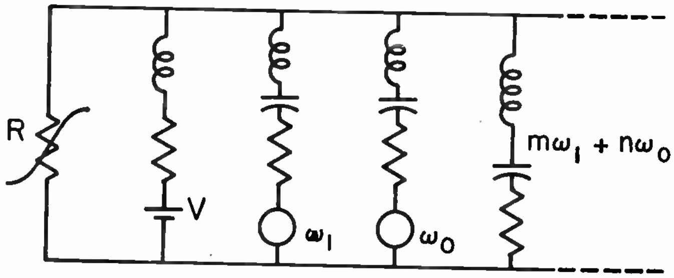

Fig. 1—The multitank nonlinear resistance circuit.

$$W_{mn} = 2Re[V_{mn}I_{mn}^*] = V_{mn}I_{mn}^* + V_{mn}^*I_{mn}. \tag{4}$$

The reactive power is

$$X_{mn} = 2\,\mathrm{Im}\,[V_{mn}I_{mn}^*] = j\left[V_{mn}^*I_{mn} - V_{mn}I_{mn}^*\right]. \tag{5}$$

The relationships expressed thus far are the same as those used by Manley and Rowe. In their treatment of the nonlinear resistive element, they proceeded in the following manner. Since

$$V_{mn} = \frac{1}{4\pi^2}\int_0^{2\pi} dy \int_0^{2\pi} dx\, v e^{-j(mx+ny)} \tag{6}$$

therefore,

$$\sum_{m=-\infty}^{\infty} \sum_{n=-\infty}^{\infty} jmV_{mn}I_{mn}^* = \frac{1}{4\pi^2}\int_0^{2\pi} dy \int_0^{2\pi} dx\, v \sum_{m=-\infty}^{\infty} \sum_{n=-\infty}^{\infty} jmI_{mn}^* e^{-j(mx+ny)}. \tag{7}$$

The double summation on the right-hand side of (7) can be expressed in a more convenient form by noting that from (2),

$$\frac{\partial i}{\partial x} = \sum_{m=-\infty}^{\infty} \sum_{n=-\infty}^{\infty} I_{mn} jm e^{j(mx+ny)} = -\sum_{m=-\infty}^{\infty} \sum_{n=-\infty}^{\infty} I_{mn}^* jm e^{-j(mx+ny)}. \tag{8}$$

Eq. (9) is obtained by the substitution of (8) in (7):

$$\sum_{m=-\infty}^{\infty} \sum_{n=-\infty}^{\infty} jmV_{mn}I_{mn}^* = -\frac{1}{4\pi^2}\int_0^{2\pi} dy \int_0^{2\pi} dx\, v \frac{\partial i}{\partial x} = -\frac{1}{4\pi^2}\int_0^{2\pi} dy \int_{i(0,y)}^{i(2\pi,y)} v\, di. \tag{9}$$

* Original manuscript received by the IRE, June 23, 1958; revised manuscript received, September 8, 1958.

† Microwave Lab., W. W. Hansen Labs. of Physics, Stanford Univ., Stanford, Calif.

Since v is a single valued function of i, and $i(0, y) = i(2\pi, y)$, the right-hand side of (9) is zero. Thus,

$$\sum_{m=-\infty}^{\infty} \sum_{n=-\infty}^{\infty} jmV_{mn}I_{mn}^* = \sum_{m=0}^{\infty} \sum_{n=-\infty}^{\infty} jm(V_{mn}I_{mn}^* - V_{mn}^*I_{mn})$$

$$= \sum_{m=0}^{\infty} \sum_{n=-\infty}^{\infty} mX_{mn} = 0. \qquad (10)$$

Similarly, (11) can be obtained by reversing the order of integration in (6),

$$\sum_{m=-\infty}^{\infty} \sum_{n=0}^{\infty} nX_{mn} = 0. \qquad (11)$$

Eqs. (10) and (11) are valid, but yield little useful information regarding the behavior of nonlinear resistors.

The procedure that follows gives relationships involving real power rather than reactive power. First, both sides of (6) are multiplied by $-m^2I_{mn}^*$ and summed over m and n, as expressed by (12):

$$\sum_{m=-\infty}^{\infty} \sum_{n=-\infty}^{\infty} -m^2V_{mn}I_{mn}^*$$

$$= \frac{1}{4\pi^2}\int_0^{2\pi} dy \int_0^{2\pi} dx\, v \sum_{m=-\infty}^{\infty} \sum_{n=-\infty}^{\infty} -m^2I_{mn}^*e^{-j(mx+ny)}. \qquad (12)$$

Since

$$\frac{\partial^2 i}{\partial x^2} = \sum_{m=-\infty}^{\infty} \sum_{n=-\infty}^{\infty} -m^2I_{mn}e^{j(mx+ny)}$$

$$= \sum_{m=-\infty}^{\infty} \sum_{n=-\infty}^{\infty} -m^2I_{mn}^*e^{-j(mx+ny)}, \qquad (13)$$

(12) can be rewritten in the form given by (14):

$$-\sum_{m=-\infty}^{\infty} \sum_{n=-\infty}^{\infty} m^2V_{mn}I_{mn}^* = \frac{1}{4\pi^2}\int_0^{2\pi} dy \int_0^{2\pi} dx\, v \frac{\partial^2 i}{\partial x^2}. \qquad (14)$$

The right-hand side of (14) can be integrated by parts:

$$\frac{1}{4\pi^2}\int_0^{2\pi} dy \int_0^{2\pi} dx\, v \frac{\partial^2 i}{\partial x^2}$$

$$= \frac{1}{4\pi^2}\int_0^{2\pi} dy \left[v \frac{\partial i}{\partial x}\bigg|_0^{2\pi} - \int_0^{2\pi} dx \frac{\partial v}{\partial x}\frac{\partial i}{\partial x} \right]. \qquad (15)$$

Because of the periodicity of v and i,

$$v \frac{\partial i}{\partial x}\bigg|_0^{2\pi} = 0.$$

Also,

$$\int_0^{2\pi} dx \frac{\partial v}{\partial x}\frac{\partial i}{\partial x} = \int_0^{2\pi} dx \frac{\partial i}{\partial v}\left(\frac{\partial v}{\partial x}\right)^2.$$

With the above equalities substituted for the right-hand side of (14), (16) is obtained:

$$\sum_{m=-\infty}^{\infty} \sum_{n=-\infty}^{\infty} m^2V_{mn}I_{mn}^*$$

$$= \frac{1}{4\pi^2}\int_0^{2\pi} dy \int_0^{2\pi} dx \frac{\partial i}{\partial v}\left(\frac{\partial v}{\partial x}\right)^2. \qquad (16)$$

Since

$$\sum_{m=-\infty}^{\infty} \sum_{n=-\infty}^{\infty} m^2V_{mn}I_{mn}^* = \sum_{m=0}^{\infty} \sum_{n=-\infty}^{\infty} m^2[V_{mn}I_{mn}^* + V_{mn}^*I_{mn}]$$

$$= \sum_{m=0}^{\infty} \sum_{n=-\infty}^{\infty} m^2W_{mn},$$

the desired power relationship is:

$$\sum_{m=0}^{\infty} \sum_{n=-\infty}^{\infty} m^2W_{mn} = h_m, \qquad (17)$$

where

$$h_m = \frac{1}{4\pi^2}\int_0^{2\pi} dy \int_0^{2\pi} dx \frac{\partial i}{\partial v}\left(\frac{\partial v}{\partial x}\right)^2. \qquad (18)$$

If the order of integration is reversed in (6), (19) may be obtained by the same procedure used to derive (17):

$$\sum_{m=-\infty}^{\infty} \sum_{n=0}^{\infty} n^2W_{mn} = h_n, \qquad (19)$$

where

$$h_n = \frac{1}{4\pi^2}\int_0^{2\pi} dx \int_0^{2\pi} dy \frac{\partial i}{\partial v}\left(\frac{\partial v}{\partial y}\right)^2. \qquad (20)$$

The power relationships expressed by (17) and (19) define the characteristics of the nonlinear resistive element.

The Positive Nonlinear Resistor

The positive resistor has the characteristic that $\partial i/\partial v \geq 0$, which means the integrands in (18) and (20) are never negative. Therefore the power relationships can be written as

$$\sum_{m=0}^{\infty} \sum_{n=-\infty}^{\infty} m^2W_{mn} \geqq 0 \qquad (21)$$

$$\sum_{m=-\infty}^{\infty} \sum_{n=0}^{\infty} n^2W_{mn} \geqq 0. \qquad (22)$$

For the case of harmonic generation this means that

$$\frac{W_{m0}}{W_{10}} \leqq \frac{1}{m^2}$$

where

W_{10} = power associated with the local oscillator frequency

W_{m0} = power associated with the mth harmonic.

This result is the same as that obtained by Page [2]. For the case where modulation is involved (23) and (24) are obtained:

$$W_{10} + m^2 W_{mn} \geqq 0 \tag{23}$$

$$W_{01} + n^2 W_{mn} \geqq 0 \tag{24}$$

where

W_{10} = power associated with the local oscillator frequency
W_{01} = power associated with the signal frequency
W_{mn} = power associated with the modulation frequency.

Since the coefficient of W_{mn} is positive in both (23) and (24), instability is not possible in the manner that instability might result for the nonlinear reactive element. In addition, power is not conserved. Since

$$P_{\text{in}} = W_{10} + W_{01}$$

$$P_{\text{out}} = |W_{mn}|,$$

the conversion efficiency is

$$\eta = \frac{P_{\text{out}}}{P_{\text{in}}} \leq \frac{1}{m^2 + n^2}.$$

For $m = n = 1$, the maximum conversion efficiency is 50 per cent. For frequency doubling by means of harmonic generation the maximum efficiency is 25 per cent.

Eqs. (17) and (19) are valid for a linear resistor. For this case

$$\frac{\partial i}{\partial v} = G = \text{constant},$$

and h_m and h_n become

$$h_m = 2G \sum_{m=0}^{\infty} \sum_{n=-\infty}^{\infty} m^2 V_{mn} V_{mn}^*$$

$$h_n = 2G \sum_{m=-\infty}^{\infty} \sum_{n=0}^{\infty} n^2 V_{mn} V_{mn}^*.$$

Since $W_{mn} = 2G V_{mn} V_{mn}^*$, this means that all the power into the resistor at each frequency is dissipated as loss and there can be no harmonic generation or modulation.

Small-Signal Analysis

If the local oscillator voltage is much larger than the signal and modulation voltages, then $\partial i/\partial v$ is a periodic function of x only:

$$\frac{\partial i}{\partial v} = \sum_{r=-\infty}^{\infty} G_r e^{jrx}. \tag{25}$$

Since $\partial i/\partial v$ is a real quantity,

$$G_{-r} = G_r^*.$$

The expression for h_n is

$$h_n = \frac{1}{4\pi^2} \int_0^{2\pi} dx \sum_{r=-\infty}^{\infty} G_r e^{jrx} \int_0^{2\pi} dy \left(\frac{\partial v}{\partial y}\right)^2, \tag{26}$$

where

$$\left(\frac{\partial v}{\partial y}\right)^2 = \sum_{q=-\infty}^{\infty} \sum_{s=-\infty}^{\infty} \sum_{m=-\infty}^{\infty} \sum_{n=-\infty}^{\infty} V_{qs} V_{mn} (-sn) e^{j[(m+q)x+(n+s)y]}.$$

Because of the orthogonality of the exponential functions over the period 2π,

$$\int_0^{2\pi} \left(\frac{\partial v}{\partial y}\right)^2 dy = 2\pi \sum_{q=-\infty}^{\infty} \sum_{m=-\infty}^{\infty} \sum_{n=-\infty}^{\infty} n^2 V_{qn}^* V_{mn} e^{j(m-q)x}.$$

Therefore h_n becomes

$$h_n = \frac{1}{2\pi} \int_0^{2\pi} dx \sum_{r=-\infty}^{\infty} \sum_{q=-\infty}^{\infty} \sum_{m=-\infty}^{\infty} \sum_{n=-\infty}^{\infty} n^2 G_r V_{qn}^* V_{mn} e^{j(m-q+r)x}$$

$$= \sum_{q=-\infty}^{\infty} \sum_{m=-\infty}^{\infty} \sum_{n=-\infty}^{\infty} n^2 G_{(q-m)} V_{qn}^* V_{mn}. \tag{27}$$

The notation $G_{(q-m)}$ does not mean a double index on G, but rather that the G_r appearing in Eq. (27) corresponds to $r = q - m$. The small-signal power relationship is

$$\sum_{m=-\infty}^{\infty} \sum_{n=0}^{\infty} n^2 W_{mn} = \sum_{q=-\infty}^{\infty} \sum_{m=-\infty}^{\infty} \sum_{n=-\infty}^{\infty} n^2 G_{(q-m)} V_{qn}^* V_{mn}$$

$$G_{(q-m)} = \frac{1}{2\pi} \int_0^{2\pi} dx \frac{\partial i}{\partial v} e^{-j(q-m)x}. \tag{28}$$

If the external circuit is adjusted so that only the signal frequency and the modulation frequency corresponding to $m = 1 = n$ face an appreciable impedance, (28) becomes

$$W_{01} + W_{11} = 2G_0[V_{01}^* V_{01} + V_{11}^* V_{11}] + 2G_{-1} V_{11} V_{01}^* + 2G_1 V_{01} V_{11}^*. \tag{29}$$

By an appropriate choice for the $x = 0$ axis for the function $\partial i/\partial v$, it is possible to make

$$G_{-1} = G_1^* = G_1 = \text{a real constant.}$$

For this choice, (29) may be written as

$$W_{01} + W_{11} = 2G_0[|V_{01}|^2 + |V_{11}|^2] + 2G_1[V_{11} V_{01}^* + V_{01} V_{11}^*]. \tag{30}$$

If instability is to occur it is necessary that

$$2G_0[|V_{01}|^2 + |V_{11}|^2] + 2G_1[V_{11} V_{01}^* + V_{01} V_{11}^*] < 0.$$

Since

$$|V_{01}|^2 + |V_{11}|^2 \geqq V_{11} V_{01}^* + V_{01} V_{11}^*,$$

the necessary conditions for instability are [3]

$$\left.\begin{array}{c} G_0 < 0 \\ \text{or} \\ G_0^2 - G_1^2 < 0. \end{array}\right\} \tag{31}$$

Equivalent Circuit

Eq. (28), which applies for the small-signal condition [4], may be derived in a somewhat different manner by noting that

$$\Delta i = \frac{\partial i}{\partial v} \Delta v = \sum_{r=-\infty}^{\infty} G_r e^{jrx} \Delta v, \tag{32}$$

where

$$\left.\begin{aligned} \Delta i &= \sum_{m=-\infty}^{\infty} \sum_{n=-\infty}^{\infty}{}' I_{mn} e^{j(mx+ny)} \\ \Delta v &= \sum_{m=-\infty}^{\infty} \sum_{n=-\infty}^{\infty}{}' V_{mn} e^{j(mx+ny)} \end{aligned}\right\}. \tag{33}$$

The prime on the summation over n indicates that the $n=0$ term is not included, and therefore Δi and Δv involve only the signal frequency and the modulation terms. Combining (32) and (33), I_{mn} may be written as

$$I_{mn} = \sum_{q=-\infty}^{\infty} G_{m-q} V_{qn}. \tag{34}$$

By taking the complex conjugate of (34), multiplying by $n^2 V_{mn}$, and then summing over m and n, (28) results. Assuming only the presence of the signal and one modulation frequency corresponding to $m=n=1$, (35) and (36) result:

$$I_{01} = G_0 V_{01} + G_1 V_{11} \tag{35}$$

$$I_{11} = G_1 V_{01} + G_0 V_{11}. \tag{36}$$

In terms of usual network notation, G_0 and G_1 correspond to the short-circuit admittance parameters, and (31) specifies the condition for non-physical realizability by means of passive elements. A π-network may be used for realization as illustrated in Fig. 2. It is interesting to note that reciprocity holds for the nonlinear resistance, whereas this is not true for the nonlinear reactance. For any specified problem where the driving sources and associated impedances are given, gain and bandwidth may be determined by ordinary network calculations by connecting the sources and impedances to the appropriate terminals of Fig. 2 [4].

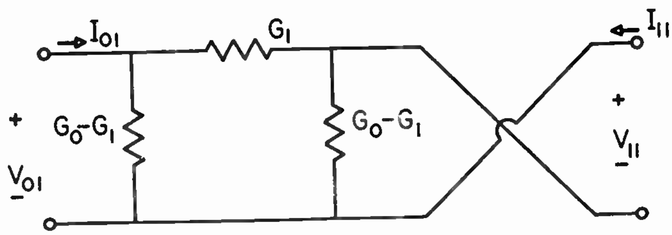

Fig. 2—Small signal equivalent circuit for the nonlinear resistance.

Bibliography

[1] J. M. Manley and H. E. Rowe, "Some general properties of nonlinear elements, pt. I, general energy relations," Proc. IRE, vol. 44, pp. 904–913; July, 1956.

[2] C. H. Page, "Frequency conversion with positive nonlinear resistors," *J. Res. Natl. Bur. Stand.*, vol. 56, pp. 179–182; April, 1956.

[3] H. C. Torrey and C. A. Whitmer, "Crystal Rectifiers," M.I.T. Rad. Lab. Ser. McGraw-Hill Book Co., Inc., New York, N. Y., vol. 15, pp. 406–415; 1948.

[4] H. E. Rowe, "Some general properties of nonlinear elements. II, Small signal theory," Proc. IRE, vol. 46, pp. 850–860; May, 1958.

[5] C. F. Edwards, "Frequency conversion by means of a nonlinear admittance," *Bell Sys. Tech. J.*, vol. 35, pp. 1403–1416; November, 1950.

[6] F. Dacos, "Energy considerations in nonlinear oscillatory circuits," *BPI Symposium Proc.*, vol. 6, pp. 447–454; 1956.

[7] W. Millar, "Some general theorems for nonlinear systems possessing resistance," *Phil. Mag.*, vol. 42, pp. 1150–1160; October, 1951.

[8] C. Cherry, "Some general theorems for nonlinear systems possessing reactance," *Phil. Mag.*, vol. 42, pp. 1161–1177; October, 1951.

Correction

G. L. Turin, author of "Error Probabilities for Binary Symmetric Ideal Reception through Nonselective Slow Fading and Noise," which appeared on pages 1603–1619 of the September, 1958, issue of Proceedings, has requested that the following corrections be made to his paper.

The first line of (12) on page 1606 should read:

$$\rho_m(u) = \frac{1}{2} \int \zeta^*(t) \xi_m(t-u) dt.$$

A factor of t should be inserted in the integrand of (17) on page 1607.

In the first column of page 1609, the thirteenth line from the top should begin: Since $\gamma = 2$ . . . .

The line immediately following (54b) on page 1612 should read: and similar expressions hold for $\hat{v}(t)$ and $\tilde{v}(t)$. On the following page, the right-hand sides of (56) and (57) should be $\tilde{\mu}(t)$ and $\tilde{v}(t)$, respectively.

On page 1614, on the next to last line of section B, the m should be a subscript to the x.

In (84), on page 1615, the right-hand side of the last equation should be $2\lambda E N_0$.

In some copies, (103) and (106) on page 1617 were printed incorrectly. The first factor on the right-hand side of (103) should read $e^{(x^2+y^2)/2}$. The first factor in the second line of (106) should be $e^{-\beta a^2/4\sigma^2}$.

The second equation of (118) should read:

$$K_2 = \frac{B}{1-B^2}.$$

Performance of Some Radio Systems in the Presence of Thermal and Atmospheric Noise*

A. D. WATT†, SENIOR MEMBER, IRE, R. M. COON†, MEMBER, IRE,
E. L. MAXWELL†, AND R. W. PLUSH†

Summary—**The performance of several basic types of communication systems are determined experimentally, and in some cases theoretically, under typical conditions with steady or fading carriers, and in the presence of thermal or atmospheric noise. The relative efficiency of various carriers and the interference factor of various types of noise are found to be dependent upon the characteristics of the particular communication system as well as the characteristics of the carrier and noise themselves.**

Methods are considered for calculating errors expected from a given system, based upon the amplitude distribution of the noise envelope.

Introduction

A COMPLETE radio communication system can be considered as consisting of a large number of independent circuit elements arranged in a manner similar to that shown in Fig. 1. In general, the objectives are to have a system capable of reproducing a given class or type of message at a given rate of transmission with maximum reliability. At the same time, it is essential that the system require a minimum amount of transmitter power and produce a minimum amount of interference to services in adjacent channels. The accomplishment of these ends requires a careful consideration of the characteristics of all parts of the system and their interrelated effects.

Fig. 1 illustrates the interesting fact that there are two system elements, the propagation path and the atmospheric noise, whose characteristics are beyond our control. In view of this, it is readily apparent that the characteristics of these two system elements must be determined as thoroughly as possible so that the other elements can be designed for optimum operation under the conditions established by the propagation path and the limiting noise.

Carrier Characteristics

The carrier characteristics are functions of many parameters, including path distance, terrain, frequency, and antennas. In general, VLF and LF carriers are nonfading, *i.e.*, have a steady amplitude for normal message periods. HF carriers as a rule, are steady for ranges where propagation is by ground wave but are subject to ionospheric fading and multipath conditions at other ranges. VHF and UHF carriers also are relatively steady for short ranges, but have appreciable fading for beyond-horizon circuits.

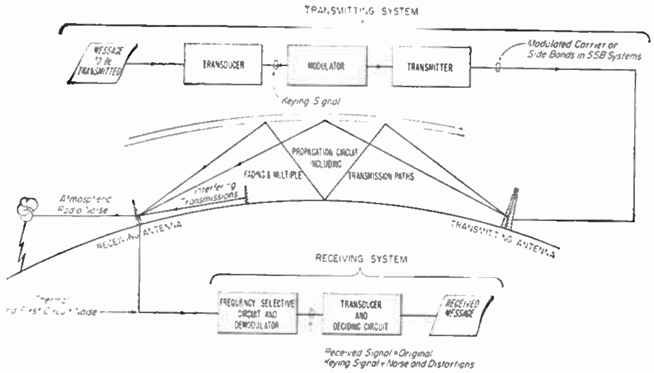

Fig. 1—Diagram of a typical radio communication system.

Long-range HF carriers frequently have a variation in amplitude which can be considered as resulting from the combination of a specularly reflected component and a number of scattered contributions. McNicol[1] has shown how the resulting envelope amplitude distribution may vary from a primarily Rayleigh distribution to that of a Guassian distribution depending, of course, on the relative amount of specular and scattered components. The actual shape of the distribution at a particular time naturally will influence the efficiency of the carrier in transferring information. The rate of variation is also an important factor in determining the errors which will be introduced by fading on specific radio systems. The average fade rate varies considerably with propagation conditions and usually is within the range of 1/10 to 10 fades per second.

Norton, *et al.*[2], Bullington, *et al.*,[3] and Chisholm, *et al.*,[4] have shown that the carriers received over typical beyond-horizon UHF paths have instantaneous envelope amplitude distributions which at times approximate the Rayleigh distribution, but also are seen to depart appreciably from this distribution.

Recent measurements of the 1046-mc radiation from Cheyenne Mountain, Colo., to Garden City, Kan., have been made with equipment which determines directly

* Original manuscript received by the IRE, January 31, 1958; revised manuscript received, August 20, 1958.
† National Bureau of Standards, Boulder, Colo.

[1] R. W. E. McNicol, "The fading of radio waves of medium and high frequencies," *Proc. IEE*, vol. 96, pt. III, pp. 517–524; November, 1946. (See also footnote 18.)

[2] K. A. Norton, P. L. Rice, H. B. Janes, and A. P. Barsis, "The rate of fading in propagation through a turbulent atmosphere," Proc. IRE, vol. 43, pp. 1341–1353; October, 1955.

[3] K. Bullington, W. J. Inkster, and A. L. Durkee, "Results of propagation tests at 505 mc and 4,090 mc on beyond-horizon paths," Proc. IRE, vol. 43, pp. 1306–1316; October, 1955.

[4] J. H. Chisholm, P. A. Portman, J. T. deBettencourt, and J. F. Roche, "Investigations of angular scattering and multipath properties of tropospheric propagation of short radio waves beyond the horizon," Proc. IRE, vol. 43, pp. 1317–1335; October, 1955.

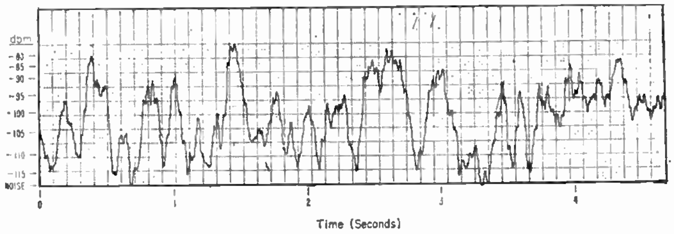

Fig. 2—Forward scatter tropospheric signal envelope, Cheyenne Mountain, Colo., to Garden City, Kan., 226 miles. Carrier frequency 1046 mc, recorder response dc to 40 cps (3 db down), 0619 MST, March 7, 1957.

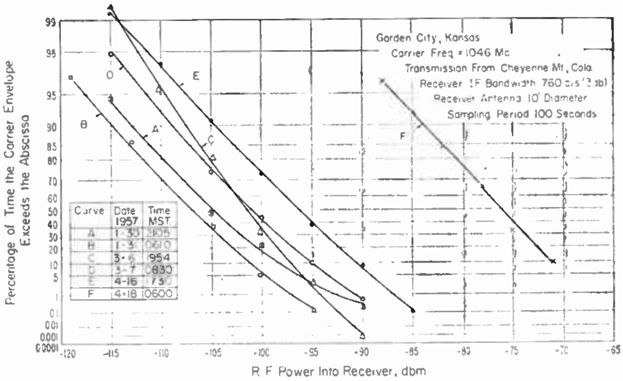

Fig. 3—Cumulative distribution of carrier envelope amplitudes.

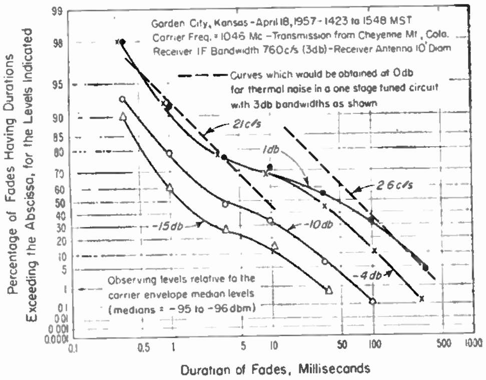

Fig. 4—Cumulative distribution of carrier fade lengths at various levels.

the cumulative distribution of the instantaneous envelope of the receiver IF output. In addition to these direct measurements of the amplitude and time distributions with equipment similar to that described elsewhere[5,6] recordings were made simultaneously with a high-speed recorder whose frequency response is from dc to 3 db down at 40 cps. A short portion of the record is shown in Fig. 2, which gives some indication of the type of field fluctuation encountered. The amplitude distributions seen in Fig. 3 were obtained directly with electronic cumulative distribution circuitry with a resolving capability of less than 0.1 millisecond where it can be seen that the instantaneous envelope amplitude is not always Rayleigh distributed. The sampling period for the simultaneously obtained data points of Fig. 3 was 100 seconds, while the data for each of the time distribution curves of Fig. 4 required approximately 10 minutes. It should be mentioned that other observations of time distributions indicate that appreciable changes in the rate of fading do occur over such paths.

Observation of the fade durations of thermal noise through a narrow-band filter has yielded results similar to that shown in Fig. 4 except with essentially straight lines having a slope of -1. The two dashed lines indicate that the fading carrier may consist of a primary fading component with effective frequency components whose 3-db bandwidth is approximately 2.6 cps,[7] and an additional component with approximately a 21-cps bandwidth. There is always the possibility in observations of this type that the transition may have been caused by a small amount of high-frequency components contributed by the thermal noise in the 760-cps bandpass of the receiver. In view of this, it would appear more desirable in the future to obtain carrier fade data directly in terms of the percentage of time the carrier envelope fades to and remains below a given level for specified time durations as shown later in Fig. 19 and also in terms of the effective frequency spectrum.

Noise Characteristics

Recent studies and measurements of the statistical characteristics of atmospheric radio noise by Hoff and Sullivan,[8] Horner,[9,10] Hoff and Johnson,[11] Yuhara, Ishida, and Higashimura,[12] and Watt and Maxwell[6,13] combined with studies of thermal noise by Landon,[14] Rice,[15–17] Norton[18] and other workers in both fields, have

[5] E. F. Florman, R. W. Plush, A. D. Watt, C. F. Peterson, and A. F. Barghausen, "Some measured statistical characteristics of a 1046mc carrier over a tropospheric scatter radio link," in preparation.

[6] A. D. Watt and E. L. Maxwell, "Measured statistical characteristics of VLF atmospheric radio noise," Proc. IRE, vol. 45, pp. 55–62; January, 1957.

[7] Frequency spectrum analysis by H. Janes on records similar to Fig. 2 yielded 3-db response bandwidths in the order of 2 to 5 cps.

[8] R. S. Hoff and A. W. Sullivan, "A survey of the atmospheric noise problem," *Proc. URSI X Gen. Assembly*, vol. 8, pt. 2, pp. 297–302; September, 1950.

[9] F. Horner, "Notes on the significant characteristics of atmospheric noise," *Proc. URSI XI Gen. Assembly*, vol. 10, pt. 4, p. 32; September, 1954.

[10] F. Horner and J. Harwood, "An investigation of atmospheric radio noise at very low frequencies," *Proc. IEE*, vol. 103, pt. B, pp. 743–751; November, 1956.

[11] R. S. Hoff and R. C. Johnson, "A statistical approach to the measurement of atmospheric noise," Proc. IRE, vol. 40, pp. 185–187; February, 1952.

[12] H. Yuhara, T. Ishida, and M. Higashimura, "Measurement of the amplitude probability distribution of atmospheric noise," *J. Radio Res. Labs.*, vol. 3, pp. 101–108; January, 1956.

[13] A. D. Watt and E. L. Maxwell, "Characteristics of atmospheric noise from 1 to 100 kc," Proc. IRE, vol. 45, pp. 787–794; June, 1957.

[14] V. D. Landon, "The distribution of amplitude with time in fluctuation noise," Proc. IRE, vol. 30, pp. 425–429; September, 1942.

[15] S. O. Rice, "Filtered thermal noise, fluctuation of energy as a function of interval length," *J. Acoust. Soc. Amer.*, vol. 14, pp. 216–227; April, 1943.

[16] S. O. Rice, "Mathematical analysis of random noise," *Bell Sys. Tech. J.*, vol. 23, pp. 282–332, July, 1944, and vol. 24, pp. 46–156; January, 1945.

[17] S. O. Rice, "Statistical properties of a sine wave plus random noise," *Bell Sys. Tech. J.*, vol. 27, pp. 109–157; January, 1948.

[18] K. A. Norton, L. E. Vogler, W. V. Mansfield, and P. J. Short, "The probability distribution of the amplitude of a constant vector plus a Rayleigh distributed vector," Proc. IRE, vol. 43, pp. 1354–1361; October, 1955.

TABLE I

COMMUNICATION SYSTEM PERFORMANCE COMPARISON

Fig.	System	wpm	Noise Dynamic Range		Carrier	$C/N_{1\ kc}$ rms Carrier to rms Noise in a 1-kc Band (db)†			SPF‡		
			Type	db*		10%	1%	0.1%	10%	1%	0.1%
6	A CW good operator	15	T	21	S	−1	1	(4)	12.8	10.8	7.8
7	B CW good operator	12	A	68	S	−11.5	−2	(4)	22.3	12.8	6.8
7	C CW fair operator	12	A	68	S	−3	—	—	13.8	—	—
8	D CW good operator	12	A	69	S	−10	(−2)	—	20.8	12.8	—
8	E CW good operator	16	A	69	S	−8	(0)	—	20	12	—
8	F CW good operator	20	A	69	S	−6	(1)	—	19	12	—
9	G FSK ±17 cps	40	T	21	S	−2.3	0	1.6	18.3	16	14.4
9	H FSK ±50 cps	60	T	21	S	0	2	3	17.8	15.8	14.8
10	I FSK ±25 cps	60	A	68	S	0	10	17	17.8	7.8	0.8
11	J FSK ±50 cps	60	A	69	S	3	11	15	14.8	6.8	2.8
12	K FSK ±425 cps	60	A	50	S	10	18	21	7.8	−0.2	−3.2
13	L FSK ±425 cps	60	A	40	ionospheric fading	12	25	34	5.8	−7.2	−16.2
14	M FM-FSK 576 TTY channels	60/ch	T	21	tropospheric fading	43	48	53	2.4	−2.6	−7.6
14	N FM 36 voice channels	100/ch	T	21	tropospheric fading	[49]	[80]		[−13.4]	[−44.4]	

* 0.001 to 90 per cent in a 1-kc band.
† For system performance as indicated. TTY and CW: character errors; voice: word errors. 1-kc effective noise band.
‡ System Performance Factor = 10 log (wpm) − $C/N_{1\ kc}$.
( ) Extrapolated or based upon extrapolated data.
[ ] Based upon random word errors. Note 10 per cent word errors ≈2 per cent character errors and 1 per cent word errors ≈0.2 per cent character errors.

placed us in a position where we can analyze with considerable detail the interfering effects of noise.

A recent paper by Crichlow[19] shows how the predictions of world-wide noise levels are being expanded to include detailed information about the character of noise to be expected at various locations, so that its interfering effect can be predicted with greater accuracy than has been possible in the past.

The cumulative envelope amplitude distributions of the noise, which are included as a basis for comparing the performance of the various radio systems in the next section, were obtained as described earlier.[6] Since the manner in which the observed amplitude distributions vary with the bandwidth of the receiving circuit is important in interpreting system performance, Fig. 5, opposite, is included to show typical atmospheric noise characteristics.

In general, the dynamic range of the noise becomes smaller and the level is reduced as the bandwidth is reduced. The actual rms value is directly proportional to the square root of the bandwidth.[6] This relation is true for all types of noise and bandwidths where the input frequency spectra are flat over the regions of interest. It also should be pointed out that the dynamic range only reduces to that of thermal noise and once this point is reached where the envelope distribution becomes Rayleigh, any further reductions in bandwidth only result in a change of level and not shape.[14]

In view of these changes in shape and level with bandwidth, and the knowledge that postdetection filtering produces an additional change in the distribution, we do not expect our system performance or error curves to exactly follow a particular noise amplitude distribution curve. However, we can anticipate a systematic and reproducible departure which can be used as a basis for future performance prediction.

In addition to the amplitude distributions, we find it necessary to have some knowledge of the statistics of the pulse spacing of the noise envelope. Information of this type is presented in an earlier paper[6] for a large number of times and at several locations. In general, the results indicate a noticeable departure from purely random pulse spacing for noise outside the tropics; however, since the general shape of the curves is quite similar for most of the observations, it is expected that for many systems the amplitude distribution will furnish the information necessary for prediction of system errors.

EXPERIMENTAL RESULTS

The performance of three frequently used types of radio systems—aural Morse code, frequency shift keying teletype, and voice—has been examined under various combinations of typical carrier and noise conditions.

A comparison of the performance of the various systems is given in Table I where the systems considered are divided into three primary groups—CW, frequency shift keying, and voice. These primary types of systems are next grouped into those operating against thermal noise or atmospheric noise as well as those operating with steady carriers or fading carriers. The factor C/N_{1kc} is defined as the rms carrier into the receiver, to rms noise in a 1-kc effective power bandwidth expressed

[19] W. Q. Crichlow, "Noise investigation at VLF by the National Bureau of Standards," PROC. IRE, vol. 45, pp. 778–782; June, 1957.

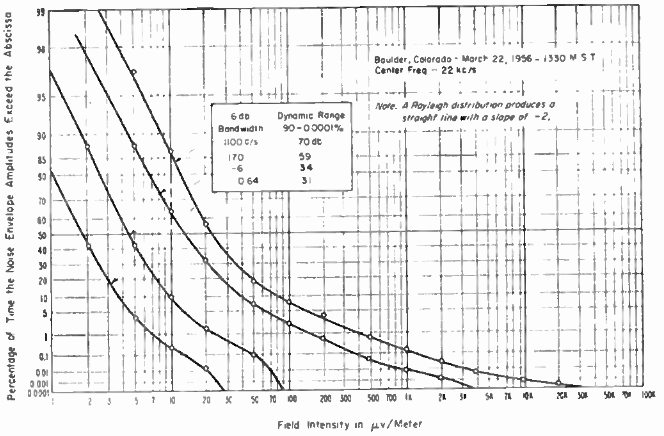

Fig. 5—Measured amplitude distributions of atmospheric noise envelopes.

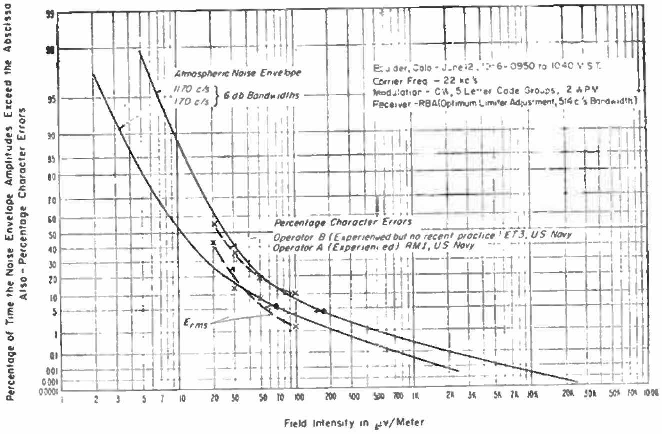

Fig. 7—Communication system performance in the presence of atmospheric noise.

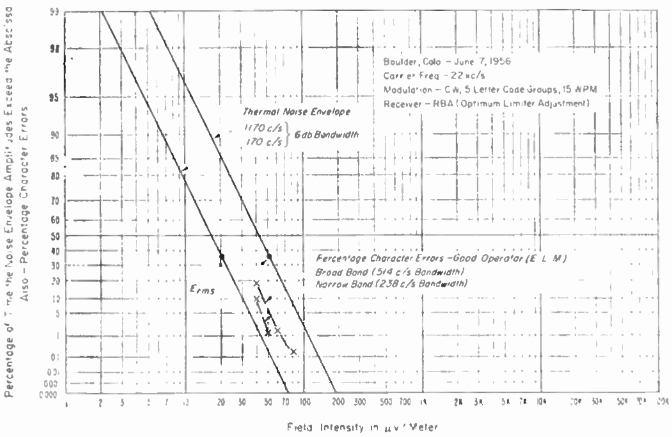

Fig. 6—Communication system performance in the presence of thermal noise.

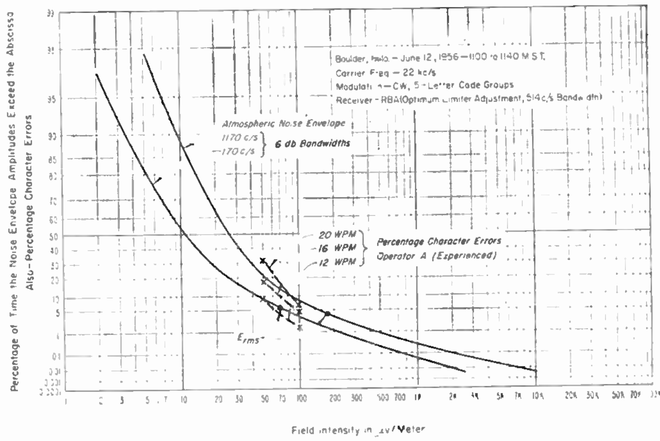

Fig. 8—Communication system performance in the presence of atmospheric noise.

in db.[20] In this paper lower case ratios are employed for voltage ratios and upper case for these ratios given in decibels. C/N_{1kc} is obtained readily from the data shown by observing that $C/N_{1kc} = C/N_y + 10 \log(y/1000)$, where y is the effective power bandwidth in which the noise is observed. Specifically, $y = 1170 \times 0.82$ and $10 \log(y/1000) = -0.2$ db. The system performance factor (SPF) is defined as 10 $\log_{10}$ (words per minute) $- C/N_{1kc}$ at the error percentages indicated which are 10 per cent, 1 per cent, and 0.1 per cent.

CW Aural Systems—Steady Carriers

The CW transmissions all consisted of five letter code groups. When comparing the SPF for systems A and B, Figs. 6 and 7, it is observed that at 10 per cent errors a good operator can perform more efficiently in the presence of atmospheric noise while at 0.1 per cent errors his efficiency is greater with thermal noise.

From systems B and C it is evident that the level of performance obtained under typical VLF atmospheric noise conditions is very dependent upon the skill of the individual operator; however, it also has been found that under similar noise conditions the level of performance for skilled operators exhibited a much smaller spread than anticipated.

Fig. 8, systems, D, E, and F, shows the effect of varying the rate of information transmission with the same skilled operator. In general, a reduction of keying rate for a fixed carrier level results in a reduction of errors. This effect is not expected to be linear over all keying rates since the human ear has a limited effective integration length.[21] It is interesting to note that the SPF change is rather small for the keying rates considered. Before passing to the automatic systems, it should be mentioned that, in our experience, human operators find it very difficult to perform at character error rates of 0.1 per cent or less.

[20] It should be noted that c/n_{1kc} is based upon the rms noise in a 1-kc effective power band rather than upon the rms noise in the receiver IF filter. The usual C/N based on the carrier and noise out of the receiver bandwidth can be obtained readily since the rms value of noise is directly related to the square root of bandwidth, and the carrier attenuation also can be obtained. It should be mentioned that in our noise measuring equipment the ratio of 3-db to 6-db bandwidths is 0.60 for the 170-cps narrow band and 0.64 for the 1170-cps wide band. The effective noise power bandwidth is approximately 0.82 times the 6-db bandwidth in both cases.

[21] W. R. Garner, "Auditory thresholds of short tones as a function of repetition rates," *J. Acoust. Soc. Amer.*, vol. 19, pp. 600–608; July, 1947.

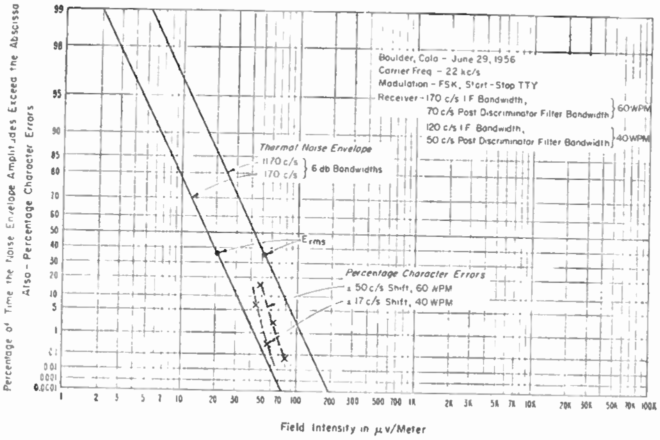

Fig. 9—Communication system performance in the presence of thermal noise.

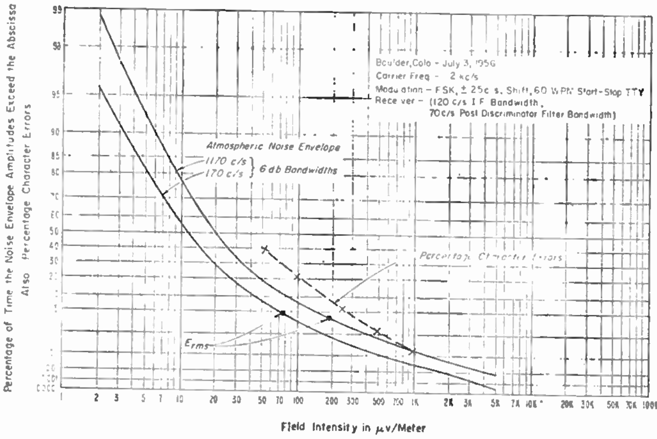

Fig. 10—Communication system performance in the presence of atmospheric noise.

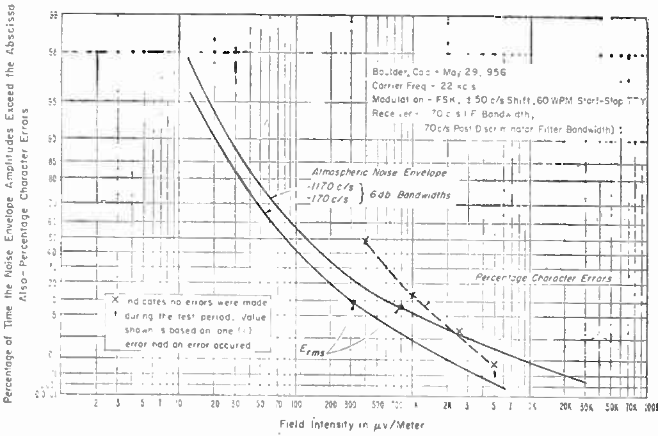

Fig. 11—Communication system performance in the presence of atmospheric noise.

FSK Systems—Steady Carrier

Frequency shift keying systems G and H, Fig. 9, illustrate operation under thermal noise and steady carrier conditions. These 60-wpm start-stop teletype systems were operated with a shift of ± 50 cps, a receiver 6-db IF bandwidth of 170 cps, and a postdiscriminator filter with a 70-cps 6-db cutoff. The 40-wpm system was operated with a shift of ± 17 cps, a receiver 6-db IF bandwidth of 120 cps, and a postdiscriminator filter with a 50-cps 6-db cutoff. As would be expected, the 40-wpm system operated at a lower carrier level for equivalent performance than was required by the 60-wpm system. In addition, it should be noted that the slope of the error curves is greater than that of the noise envelope. This is typical of FSK systems and is caused by the ability of FSK receivers to reject high amplitude impulses because of limiting and postdiscriminator filtering.

Fig. 10 shows the performance of a 60-wpm teletype system employing ± 25 cps shift in the presence of atmospheric noise. It can be noted that the radio system error curve lies considerably to the right of the atmospheric noise envelope curves rather than between them as was true in the thermal noise case. Fig. 11 illustrates the performance of a similar system except that ± 50 cps shift is employed. The character error curve now is considerably steeper than was the case in Fig. 10. In addition, it can be noticed that the high error portion of the error curve lies further to the right of the noise envelope curves than was true in Fig. 9, while at the low error rates the error curve lies between the two noise envelope curves. This difference in performance characteristics is typical of FM or FSK systems as the frequency deviation is increased.[22,23]

When the SPF of systems A and G (thermal noise) are compared at 0.1 per cent errors, the frequency shift automatic teletype systems performance is seen to be 6.6 db higher than was possible for even the best CW operator. This results from at least two factors. First, the CW Morse code is basically less efficient than the teletype code, and second, the human operator suffers from fatigue under long periods of operation and is unable to perform well at very low error rates.

An interesting fact which can be observed is that it is essential to know the maximum allowable errors for a given communication circuit if an optimum choice of system factors is to be made. As an example, we can compare the relative performance of the frequency shift teletype systems I and J employing ± 25 cps shift and ± 50 cps shift. For these two systems it is noted that the ± 25-cps shift system has the higher SPF at 10 to 1 per cent error rates. On the other hand, if a very high quality system is required, such as 0.1 per cent errors or less, it is readily apparent that the SPF is greater now for the ± 50-cps shift system. If we still further increase our frequency shift to ± 425 cps, Fig. 12, a shift frequently employed on high-frequency radio teletype circuits, it is observed that the SPF is considerably lower at all error rates with the greatest difference at the 10 per cent values.

[22] M. G. Crosby, "Frequency modulation noise characteristics," Proc. IRE, vol. 25, pp. 472–514; April, 1937.

[23] A. D. Watt, "Statistical Characteristics of Sampled and Integrated A-M and F-M Noise," Naval Res. Lab., Washington, D. C., Rep. No. 3856; October 22, 1951.

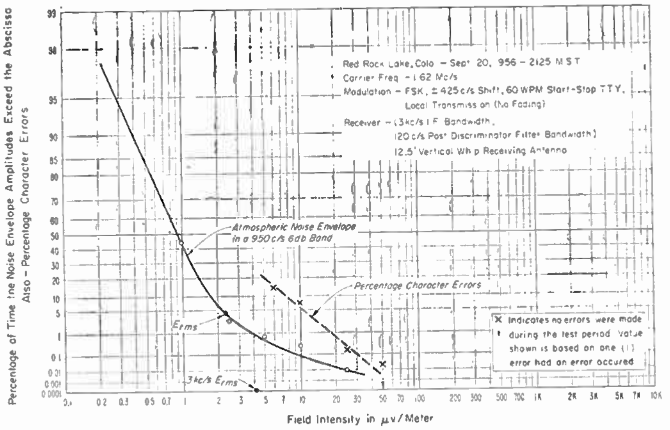

Fig. 12—Communication system performance in the presence of atmospheric noise.

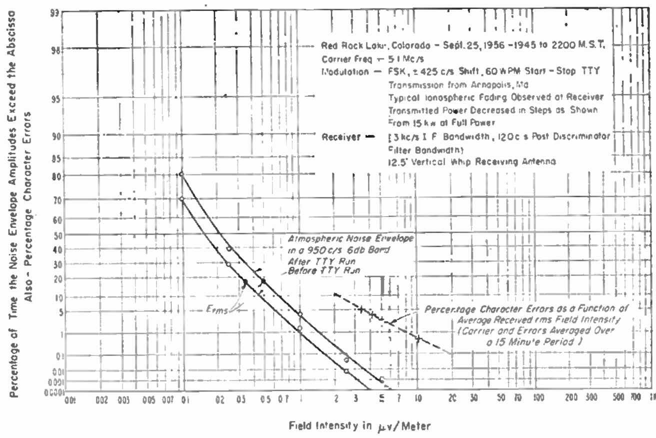

Fig. 13—Communication system performance in the presence of atmospheric noise.

FSK and FM Systems—Fading Carrier

When a fading carrier is employed, it is seen that the SPF is reduced considerably at all error rates with the greatest reduction occurring in the low percentage error region.

Fig. 13, system L, shows a typical frequency shift teletype transmission employing a 5.1-mc carrier with normal ionospheric fading. Each of the data points shown corresponds to a message approximately 15 minutes in length and the field intensity indicated is the average field intensity for each of these periods. The low error points are seen to be considerably to the right of the noise envelope curve. In practice, diversity systems are frequently employed to recover some of the carrier efficiency.

When systems K and L are compared, the SPF at 0.1 per cent errors is found to be reduced by 14 db. It should be noted also that the dynamic range of the atmospheric noise was less on the ionospheric fading, system L, than was true of the steady carrier, system K. Had the atmospheric noise dynamic ranges been the same, it is very likely that the SPF would have been reduced by an even greater amount.

System M, Fig. 14, employed a carrier frequency of 581 mc on a beyond-the-horizon path. The receiver noise in the 4.5-mc, 6-db, 3.7-mc effective IF band was the limiting factor so far as the production of errors was concerned. The basic transmitter was frequency modulated and employed 36 normal voice channels with a modulation index of 1 as subcarriers on the main carrier. Each of these voice channels could be subdivided into 16 frequency shift teletype channels although only 3 subcarrier units were available on the channel employed, which was No. 24 with a center frequency of 60 kc. The transmitter modulator gain was set so that an input sine wave of -1.4 dbm yielded ± 60-kc shift, *i.e.*, $m=1$. During the voice tests the level was set at the recommended level of -13 dbm which is 11.6 db below the maximum allowable swing per channel or ± 15.8 kc. For the 60-wpm start-stop teletype tests, an audio subcarrier employing a shift of ± 35 cps was set at the recommended level of -29 dbm which yielded a carrier swing of ± 2.5 kc. Since the subcarrier receiving equipment employed a low-pass filter with an estimated (6-db) cutoff of 50 cps and a 120-cps (6-db), 100-cps (3-db) bandwidth IF filter, the teletype channels could be spaced every 200 cps. In the 200 to 3400-cps voice band available, this would permit 16 teletype circuits, and it would appear that even if all 16 channels were operating, a level of -25.6 dbm could have been employed without exceeding the allotted swing per primary channel. If this level had been employed, it is expected that slightly improved performance would have resulted. In order to obtain the system performance curves, an attenuator was inserted in the antenna circuit and the average received voltage was reduced as shown. For the voice performance curves, random words were read slowly and distinctly while the operator at the receiving end recorded what he thought he had heard. The speaking rate was in the order of 100 words per minute although the pauses between words to permit writing reduced the actual rate to 15 words per minute. For the teletype performance curves, character errors were counted from a standard "quick brown fox" message.

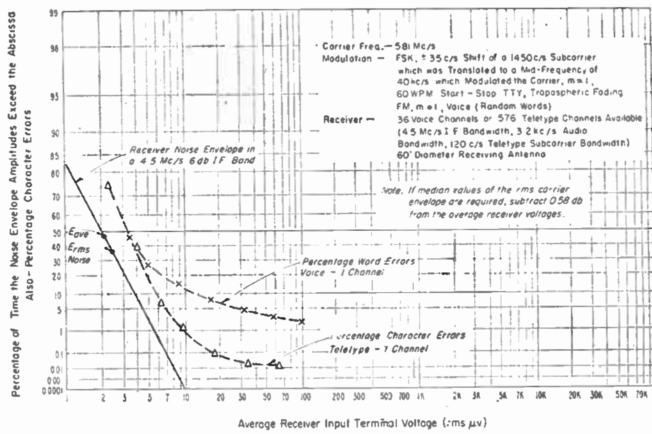

Fig. 14—Forward scatter tropospheric propagation circuit performance tests.

Since it was possible to employ up to 16 different teletype channels for each voice channel, a total of 576 teletype channels were available in this system. Here is a practical case where a fading carrier was operating in the presence of thermal noise. The teletype SPF at the 10 per cent error rate is found to be 15.4 db below the single channel 60-wpm teletype systems operating under thermal noise conditions and steady carrier, and at the 0.1 per cent error level the performance is 23.4 db lower.

System N, employing frequency modulation with a voice signal, is shown on the last line of Table I. The existing carrier and noise conditions were the same as for the preceding teletype example. When voice signals are used, it is found that the SPF decreases very markedly. It should be emphasized that these SPF's are based on word errors for the voice communication system and that they would actually correspond to approximately 2 per cent and 0.2 per cent character errors. However, this still results in a considerably lower performance factor for the voice communication system.

Comparison with the Experimental Results of Others

It may be of interest to compare our results with those obtained by others for automatic teletype systems operating in the presence of thermal noise. Fig. 15 shows the thermal noise envelope in a 1-kc band, which is used as a reference for all the system performance curves indicated. Two sets of data, the dots adapted from Jordan, *et al.*,[24] and the triangles adapted from Doelz,[25] were used to plot the ± 425-cps shift start-stop curve. The curve lying just to the left of the noise envelope is for a start-stop system employing ± 50-cps shift and is the data from Fig. 9. The curve with the square data points was adapted from Jordan[24] and indicates the experimental performance of a multiple frequency shift system. This particular system employed seven different possible frequency levels spaced by approximately 80 cps per frequency interval. Actually, only six frequencies were employed in transmitting information while the seventh was used for synchronizing purposes. It can be seen that this system is more efficient than the optimumly designed ± 50-cps binary FSK start-stop system. In addition, the curve on the left has been included with the circular experimental data points adapted from Doelz,[25] which indicated the performance of his predicted wave radio teleprinter system.

Comparison of Experimental Results with Theoretical Calculations of Errors

When the many factors involved in accurately calculating expected errors for typical systems are considered, it soon becomes apparent that a detailed analysis of all the systems described in this paper is beyond the scope of our present analysis.

[24] D. B. Jordan, H. Greenberg, E. E. Eldredge, and W. Serniuk, "Multiple frequency shift teletype systems," Proc. IRE, vol. 43, pp. 1647–1655; November, 1955.

[25] M. L. Doelz, "Predicted-wave radio teleprinter," *Electronics*, vol. 27, pp. 166–169; December, 1954.

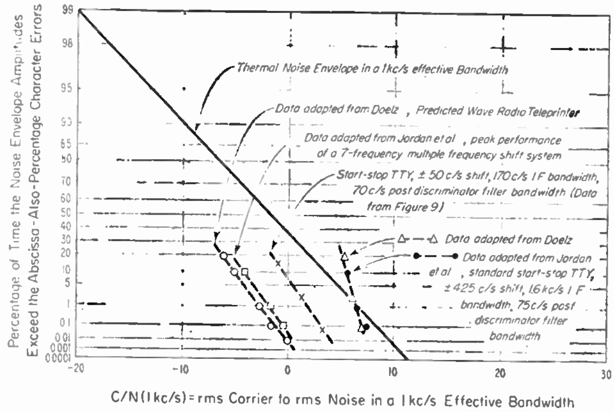

Fig. 15—Comparison of performance in thermal noise of 60-wpm teletype systems.

Montgomery[26] has shown that the errors in a binary narrow-band frequency modulation system can be considered as being one half the probability of the noise envelope exceeding the carrier envelope. The basis for this error calculation was pointed out by Corrington[27] when he showed that the average frequency of two components in a given circuit is exactly equal to that of the stronger of the two frequency components. When a sequential communication system such as the standard five-unit teletype is considered, the probability of teletype symbol error is readily obtained by the expression $P_e = 1-(1-p)^5$ when each of the binary elements is independent and has a probability of error p. The actual relationship between the errors in a practical start-stop system will depend to some extent upon the characteristics of the circuits in the receiving equipment as well as those of the start-stop teletype equipment. In general, assuming a teletype system where the probability of a binary error in a given element is largely independent of other elements (since the teletype employed in these tests had automatic line feed and carriage return), the probability of obtaining a correct character in a start-stop system can be estimated by

$$P_c \approx (1 - p)^5[(1 - p)^2]^6 = (1 - p)^{17} \qquad (1)$$

where p is the probability of an error in each binary element. The first term $(1-p)^5$ is the probability of having the five information carrying elements correct. The next term $(1-p)^2$ results since the preceding character's stop element and the start element of the particular character under consideration must also be correct. Once the receiving teletype loses synchronism with the transmitter there will be a series of errors whose length, based on observation, will average approximately six characters. We then can assume that for our given character to be correct, we must have, on the average, the pre-

[26] G. F. Montgomery, "A comparison of amplitude and angle modulation for narrow-band communication of binary-coded messages in fluctuation noise," Proc. IRE, vol. 42, pp. 447–454; February, 1954.

[27] M. S. Corrington, "Frequency modulation distortion caused by common- and adjacent-channel interference," *RCA Rev.*, vol. 7, pp. 522–560; December, 1946.

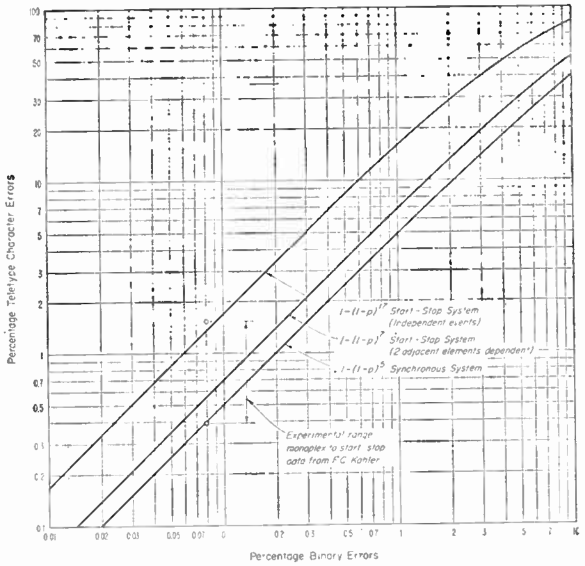

Fig. 16—Teletype character errors expected for various binary signal element errors.

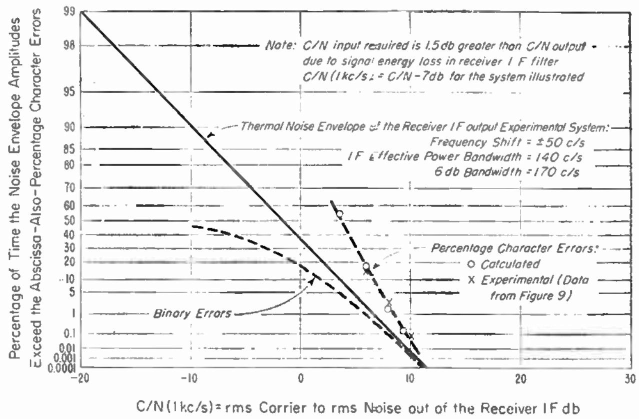

Fig. 17—Comparison of calculated and experimental FSK teletype system performance in the presence of thermal noise.

ceding six characters' start and stop elements correct, and for this reason the last expression is raised to the sixth power. The time out of synchronism can vary with printers, and it is possible that in some cases four or five characters could be employed. Eq. (1) is a rough approximation since there are numerous combinations for obtaining a correct character; however, it is expected to be sufficiently accurate for most applications.

In view of the preceding considerations, it is evident that the probability of a given start-stop character being in error is

$$P_e \approx 1 - (1 - p)^{17} \approx 17\,p \text{ for small values of } p. \qquad (2)$$

This particular start-stop teletype character error is plotted as a function of binary errors in Fig. 16. Also plotted are the character errors to be expected from a synchronous five-element system.

It is interesting to note that experimental comparisons by Kahler[28] of character errors in start-stop and synchronous systems in the 1 per cent character error range yield a difference in errors very close to that predicted (2).

When the errors in a given binary element are not independent, such as may be caused by fading or noise variations which are correlated over at least two binary elements, the resulting character errors are considerably less than when the errors are independent. If it is assumed that two adjacent elements are dependent, the expected teletype character errors can be approximated by

$$P_e \approx 1 - (1 - p)^7. \qquad (3)$$

Now we are in a position to calculate the start-stop system errors expected, and system H, which has a steady carrier and thermal noise, shall be considered first. Fig. 17 plots the expected thermal noise envelope in the 140-cps effective IF band. The binary error curve is obtained by simply dividing the envelope probability values by 2. From this binary error curve, we now apply the corrections obtained from Fig. 16 for the five-unit synchronous system error curve and start-stop curve. It should be noted that the experimental errors have been plotted 1.5 db lower than would be expected from a simple bandwidth conversion from Fig. 9. This allows for the 1.5-db loss in carrier power in the receiver IF due to the ± 50-cps frequency shift. When converting to receiver input requirements relative to a 1-kc effective noise band, we must use the relation $C/N_{1\mathrm{kc}} = C/N + \mathrm{db\ loss}$ due to shift $+10\log(y/1000)$ where y is the receiver IF effective power bandwidth.

An attempt is made now to calculate the errors expected with a steady carrier and typical atmospheric noise as would be found in the VLF region. Fig. 18 plots the atmospheric noise envelope that would be expected in a 120-cps band. This curve has been reconstructed based on a method described by Fulton.[29] The binary error curve is obtained again by dividing the noise envelope probability by 2, and the start-stop errors are obtained with the aid of Fig. 16. The experimental points are plotted directly from Fig. 10 since the shift in this case reduces the carrier out of the IF by less than 0.2 db. Before going on to the next example, it should be noted that in system J (Fig. 11), where a shift of ± 50 cps is employed, the resulting errors cannot be calculated in the manner that they were for system I of Fig. 10.

The last system to be considered is that represented by system M, which has a tropospheric forward scatter carrier in the presence of thermal noise. As pointed out

[28] F. C. Kahler, "The Effect of Fluctuations in Signal Strength on the Relative Performance of Start-Stop and Synchronous Teleprinter Systems," Naval Res. Lab., Washington, D. C., Rep. No. 4554; August 5, 1955.

[29] F. F. Fulton, Jr., "The effect of receiver bandwidth on amplitude distribution of VLF atmospheric noise," *Symp. Propagation of VLF Radio Waves*, Boulder, Colo., vol. 3, pp. 37-1 to 37-19; January 23–25, 1957.

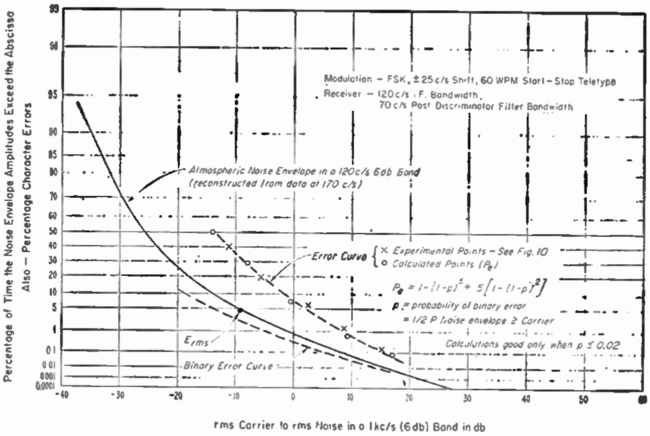

Fig. 18—Comparison of calculated and experimentally determined errors.

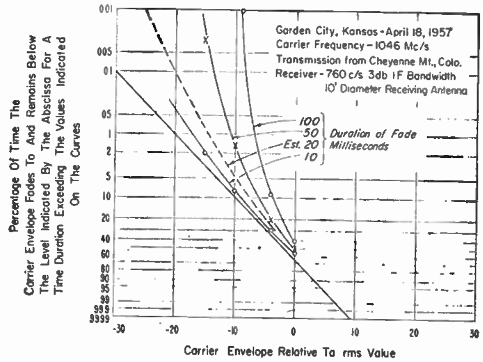

Fig. 19—Tropospheric scatter carrier fade length characteristics.

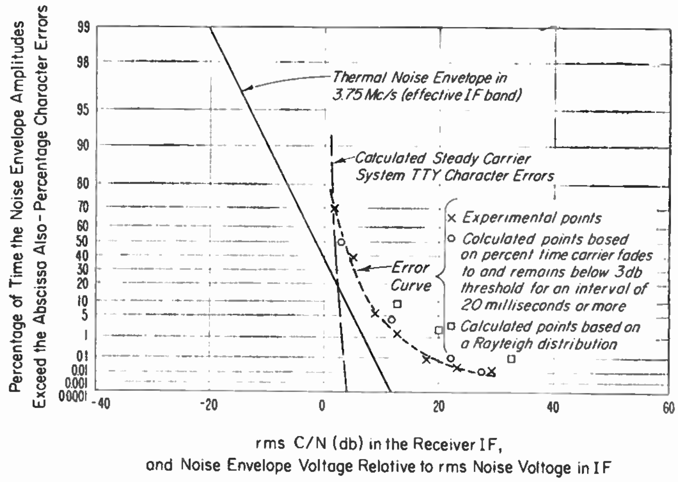

Fig. 20—Comparison of calculated and experimentally determined errors for FM, FSK forward scatter link, start-stop 60-wpm teletype system M.

by Montgomery,[26,30] the binary error rate can be calculated as one half the per cent of time that the carrier envelope is less than or equal to the noise envelope, provided the carrier envelope and the noise envelope amplitude distributions are not modified in shape or position by postdetection or signal selection filtering. It is rather evident from the description of system M that it does not meet these criteria. It can be seen from Fig. 19 that assuming a sampling period τ, which is short compared with the reciprocal of the carrier energy spectrum, the carrier envelope voltage is Rayleigh distributed as expected. When τ is increased, the distribution departs from Rayleigh, as shown.

For slowly fading carriers and narrow-band systems such as the single sideband system described by Morrow, *et al.*,[31] we could expect to calculate binary errors from the cumulative distribution of the percentage of time that the instantaneous noise envelope exceeds the carrier envelope. For Rayleigh distributions this is

$$P\left(\frac{n}{c} \geqq 1\right) = \frac{1}{1 + (C/N)^2} \tag{4}$$

where C and N are the rms values of the carrier and noise.

Since the curves of Fig. 19 are expected to vary from the Rayleigh distribution with time and the various propagation path parameters, it may be necessary to obtain the cumulative distribution of the per cent of time that the carrier fades to and remains below the noise envelope for at least τ seconds by a method described by Huntington,[32] which can be done graphically if desired.

For the wide-band FM-FSK system M, the method attempted for calculating errors is to first estimate performance under steady carrier conditions. This is done by calculating the FM noise improvement which can be shown from Stumpers[33] to be

$$\frac{C/N \text{ (subcarrier)}}{C/N \text{ (first IF)}} \sim \frac{\Delta f}{f} \times \sqrt{\frac{B_{if}}{2B_{sc}}} \tag{5}$$

where Δf is the subcarrier shift, f is the subcarrier frequency, B_{if} is the first IF bandwidth, and B_{sc} is the subcarrier IF bandwidth. For system M this is a gain of 15 db. The gain in the subcarrier FSK system is[23,33]

$$\frac{C/N \text{ (to keying circuit)}}{C/N \text{ (subcarrier)}} \sim \frac{f_D\sqrt{3B_{sc}}}{f_A{}^{3/2}} \tag{6}$$

where f_D is one half the total audio subcarrier frequency shift, and f_A is the cutoff frequency of the low-pass filter following the discriminator. For system M this is a gain of 5.4 db. The total gain of about 20 db is valid only when the input $C/N \geq 10$ db. It can be shown using this FM noise improvement and the threshold effect at $C/N \leq 6$ db, that our teletype character error curve must lie very close to the dashed curve in Fig. 20. The actual

[30] G. F. Montgomery, "Message error in diversity frequency-shift reception," Proc. IRE, vol. 42, pp. 1184–1187; July, 1954.

[31] W. E. Morrow, Jr., C. L. Mack, Jr., B. E. Nichols, and J. Leonard, "Single-sideband techniques in UHF long-range communications," Proc. IRE, vol. 44, pp. 1854–1873; December, 1956.

[32] E. V. Huntington, "Frequency distribution of product and quotient," *Ann. Math. Stat.*, vol. 10, no. 2, pp. 195–198; June, 1939.

[33] F. L. H. M. Stumpers, "Theory of frequency-modulation noise," Proc. IRE, vol. 36, pp. 1081–1092; September, 1948.

errors with a fading carrier should not be obtained by combining the distributions of this dashed curve and the appropriate carrier fade characteristic. Since the system steady-state character error curve in Fig. 20 is approximately a vertical line at $C/N=3$ db in Fig. 17, we can assume this and directly obtain an estimate of teletype character errors from Fig. 19. If the Rayleigh curve is used, the squares are obtained which do not agree very well with the observed errors. While, if it is assumed that to be certain of a teletype character error the carrier must fade to and remain below $C/N=3$ db for at least 20 msec (a binary element length), the circles are obtained.

Although the agreement appears to be good, caution should be exercised in using this type of calculation until further comparisons can be made with experimental results where the actual path statistics can be employed.

Application of Results to Calculation of Required Transmitter Power

A relatively simple expression described by Norton[34,35] for calculating the transmitter power required for a specified grade of service on a given radio transmission path can be written

$$P_t = L_t + L_{bm} - G_p + C/N_{1\text{ kc}} + F_m + T_x - 174 \text{ db.} \quad (7)$$

Each of the terms in (7) is expressed in decibels: P_t is the transmitter power in decibels above 1 watt; L_t is the loss in the transmitting antenna circuit and the transmitting antenna transmission line; L_{bm} is the median value of basic transmission loss; G_p is the path antenna gain; $C/N_{1\text{kc}}$ is the rms signal to rms noise in a 1-kc effective power band required for the specified grade of service (see Table I); F_m is the effective total noise figure[36] and includes the effects of the antenna, external noise as well as the receiver noise, together with the receiving antenna circuit and transmission line loss (it is assumed that the receiver incorporates gain adequate to ensure that the first circuit noise is detectable). When we assume a given median value of basic transmission loss L_{bm}, and median noise F_m, we can readily calculate the power required for 50 per cent of the time to yield 10, 1 and 0.1 per cent errors with the systems indicated in Table I for the types of carrier and noise shown. If it now is necessary to calculate the power required to assure this given quality of message for a given percentage x of all hours, it is necessary to include the additional factor T_x described in greater detail by Crichlow, *et al.*[36] which allows for expected variations in transmission loss and received noise about the above median predicted values. For uncorrelated normally distributed hourly medians of L_b and F, T_x can be found from the combined distribution, which is also a normal distribution whose deviation is equal to the root-sum-square of the individual deviations of L_b and F. The last term, -174, is the thermal noise power in a 1-kc band in db relative to 1 watt.

It should be noted that the only factor in (7) under the control of the terminal system designer is $C/N_{1\text{kc}}$, and for a given type and rate of transmitting information $C/N_{1\text{kc}}$ provides an index for comparing similar systems.

[34] K. A. Norton, "Transmission loss in radio propagation," Proc. IRE, vol. 41, pp. 146–152; January, 1953.

[35] K. A. Norton, "Point-to-point radio relaying via the scatter mode of tropospheric propagation," IRE Trans. on Communications Systems, vol. CS-4, pp. 39–49; March, 1956.

[36] W. Q. Crichlow, D. F. Smith, R. N. Morton, and W. R. Corliss, "World-Wide Radio Noise Levels Expected in the Frequency Band from 10 Kilocycles to 100 Megacycles," Natl. Bur. of Standards Circular 557, August 25, 1955. Available from the Supt. of Documents, U. S. Govt. Printing Office, Washington 25, D. C., price 30 cents.

Acknowledgment

The assistance of numerous personnel at the National Bureau of Standards is acknowledged gratefully. In particular, the authors wish to mention K. A. Norton, V. J. Zurich, E. F. Florman, W. Q. Crichlow, G. F. Montgomery, R. C. Kirby and F. F. Fulton for helpful discussions; R. S. Kirby who assisted in obtaining the material on scatter system performance; C. F. Peterson and A. F. Barghausen, for their cooperation and assistance which made the statistical measurements of the scatter carriers possible; E. L. Crow, for assistance with the statistical analysis, and Mrs. W. M. Mau for help in preparing the manuscript. In addition, the authors are indebted to J. A. Krcek, Office of Naval Research, for encouragement during this study and assistance with the high-frequency circuits, and R. S. Haines, L. S. Cruess, and B. Read, Northeast Air Command, for assistance in connection with the forward scatter tropospheric propagation circuits.

Structure-Determined Gain-Band Product of Junction Triode Transistors*

J. M. EARLY†, SENIOR MEMBER, IRE

Summary—This paper discusses some fundamental frequency limitations of the junction triode. It also describes briefly practical accomplishments with germanium diffused base transistors of the type reported by Lee. Finally, the frequency limitations of the junction triode are compared with those of the field effect transistor and the analog transistor.

For transistors of the mesa type with linear emitter and base electrodes (*i.e.*, an emitter stripe with parallel base contact stripes a fraction of the emitter width distant on each side), the (power gain)$^{1/2}$(bandwidth) product is found to be about $7.5 \times 10^6/s$ cps where s is emitter stripe width in centimeters. This is an order of magnitude better than the corresponding figures for field effect and analog transistors. For operation at or below the alpha cutoff frequency, the gain-band product is shown to be nearly independent of the particular alpha cutoff frequency selected. This independence arises from the reciprocity between collector depletion layer capacitance per unit area and collector depletion layer transit time. This transit time effectively determines alpha cutoff frequency in optimum gain-band designs.

Introduction

All transistors made or analyzed to date have shown finite upper frequency limits for amplification or oscillation. In this paper, frequency limits of junction triode transistors are examined in terms of the dependence of (power-gain)$^{1/2}$(bandwidth) product K on device structure and operating biases. This gain-band figure is in principle equal to the maximum frequency of oscillation.

The gain-band theory developed is then compared with experimental results on p-n-p germanium diffused base transistors. A final section summarizes results and compares theoretical performance with that reported previously for the field effect transistor[1,2] and the analog transistor.[3,4]

The structure analyzed is a somewhat idealized diffused base transistor of the mesa type,[5] as shown in Fig. 1. The width s of the emitter electrode, together with the spaces of width $s/2$ separating this electrode from the highly conducting base contacts parallel to it on both sides, will be found to be a key high frequency parameter. Thicknesses w of the base layer and x_m of the reverse biased collector depletion layer (Fig. 2) substantially determine alpha cutoff frequency.

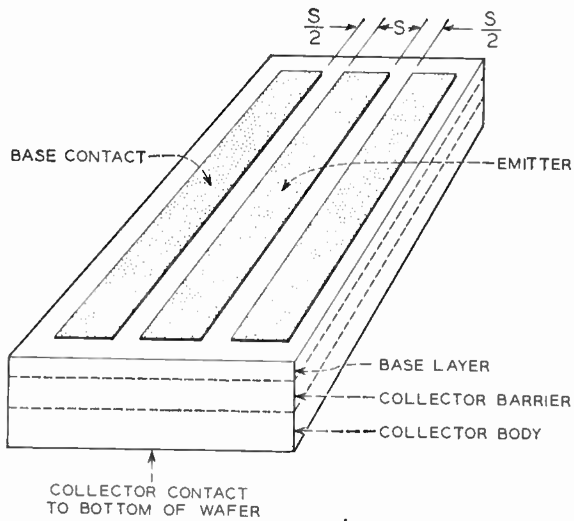

Fig. 1—Idealized transistor with linear emitter electrode and base contacts.

The analysis is simplified considerably by the assumption that collector body resistance is negligible. For this to be true, the collector contact plane at the bottom of the wafer (Fig. 1) must be close to the collector face of the collector depletion layer.

Gain-Band and Structure

The frequency performance of most junction triodes is quite fully characterized by a gain-band figure of merit which includes 3 parameters.[6] These are the alpha cutoff frequency (f_α), the ohmic base resistance (r_b'), and the collector barrier capacitance (C_c). A convenient form of the gain-band expression is:

$$K \equiv (\text{Power Gain})^{1/2}(\text{Bandwidth}) \simeq f_{\max\ \text{osc}}$$

$$= \frac{1}{4\pi}\left(\frac{1}{r_b' C_c \tau_{ec}}\right)^{1/2} \tag{1}$$

in which τ_{ec} is the emitter-to-collector signal delay time and is approximately $1/(2\pi f_{\alpha b})$.

The parameters r_b' and C_c can be related to emitter stripe width s, base layer sheet resistance $R_\square$, and collector capacitance per cm² C_{ca}. Considering only the part of the transistor from the center line of the emitter

* Original manuscript received by the IRE, June 18, 1958; revised manuscript received, September 26, 1958.

† Bell Telephone Labs., Murray Hill, N. J.

[1] W. Shockley, "A unipolar 'field-effect' transistor," Proc. IRE, vol. 40, pp. 1365–1376; November, 1952.

[2] G. C. Dacey and I. M. Ross, "The field effect transistor," *Bell Sys. Tech. J.*, vol. 34, p. 1149; November, 1955.

[3] W. Shockley, "Transistor electronics: imperfections, unipolar and analog transistors," Proc. IRE, vol. 40, pp. 1289–1313; November, 1952.

[4] W. Shockley, U. S. Patent No. 2,790,037; filed March 14, 1952, granted April 23, 1957.

[5] C. A. Lee, "High frequency diffused base germanium transistor," *Bell Sys. Tech. J.*, vol. 35, p. 23; January, 1956.

[6] R. L. Pritchard, "Frequency response of grounded-base and grounded-emitter transistors," given at the AIEE Winter Meeting, New York, N. Y.; January, 1954. The gain-band expression:

$$(\text{Power Gain})^{1/2}(\text{Bandwidth}) = \frac{f_\alpha}{8\Pi r_b' C_c}$$

is now widely accepted for junction triodes except those of the grown junction type.

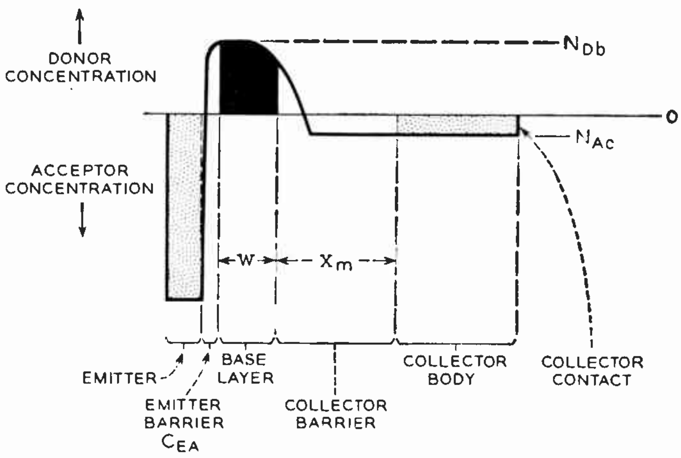

Fig. 2—Diffused base transistor—one-dimensional impurity density profile.

stripe to the near edge of one base contact,[7] and assuming the electrode stripes are one cm long, we find:

$$C_c = sC_{ca} \tag{2}$$

$$r_b' = \frac{2sR_\square}{3}. \tag{3}$$

In deriving (3), it was assumed that $R_\square$ was the same under the emitter and between the emitter and the base contact. The result derived by Pritchard[8] for base resistance of rectangular areas was used in the analysis.[9]

Putting (2) and (3) into (1) gives:

$$K = \frac{1}{4\pi s}\left(\frac{3}{2R_\square C_{ca}\tau_{ec}}\right)^{1/2} \tag{4}$$

which shows that, for fixed ratios of stripe spacing to stripe width, emitter stripe width directly determines the (power gain)$^{1/2}$(bandwidth) product of a junction triode. The result is not surprising, because the $r_b'C_c$ time constant of this structure varies as s^2. The frequency response is also determined by the factor $R_\square C_{ca}\tau_{ec}$ which should be made as small as possible for maximum response.

The One-Dimensional Factor $R_\square C_{ca}\tau_{ec}$

The factor $R_\square C_{ca}\tau_{ec}$ depends on applied biases and on the one-dimensional distribution of impurities between the emitter and the collector contact, such as is shown in Fig. 2. Minimum values of $R_\square C_{ca}\tau_{ec}$ for particular assumptions will be found by examining first the individual dependences of $R_\square$, C_{ca}, and τ_{ec} on device structure and then the joint dependence of their product.

[7] The capacitance of the portions of the collector barrier opposite to and outside of the base contacts has substantially no resistance in series with it. Since it contributes no RF power losses, it does not affect maximum frequency of oscillation. Since it causes feedback from collector to base, it reduces the gain-band product for base band applications. The effect on bandwidth is of the order $\sqrt{2}$ and is neglected here.

[8] R. L. Pritchard, "Advances in the understanding of the *p-n* junction triode," Proc. IRE, vol. 46, pp. 1130–1141; June, 1958.

[9] The approximation for r_b' in (3) is reasonable when most of the base resistance is contributed by the portion between emitter edge and base contact stripe. Eqs. (3) and (1) are greatly modified when this contribution is negligible (see footnote 8).

Collector capacitance per cm^2(C_{ca}) is simply the parallel plate capacitance of the collector depletion layer:

$$C_{ca} = \frac{\epsilon}{x_m} \tag{5}$$

where ϵ is the dielectric constant of the semiconductor and x_m is the depletion layer thickness (Fig. 2).

The principal components of the emitter-collector delay time (τ_{ec}) are the emitter charging time

$$\left(\frac{kT}{qJ_E}C_{EA}\right),$$

the base transit time (w^2/nD_{pb}), and the collector depletion layer drift delay time ($x_m/2v_{sc\,lim}$):

$$\tau_{ec} = \left(\frac{kT}{qJ_E}C_{ea} + \frac{w^2}{nD_{pb}} + \frac{x_m}{2v_{sc\,lim}}\right). \tag{6}$$

In (6), J_E is dc emitter current density, C_{ea} is emitter barrier capacitance per cm^2, n is a constant between 1 and 6 depending on the form of the base layer impurity distribution,[10–12] D_{pb} is minority carrier diffusion constant in the base layer, $v_{sc\,lim}$ is the lattice-scattering-limited maximum drift velocity for carriers passing through the reverse biased collector barrier region, and w and x_m are given in Fig. 2. For minimum τ_{ec}, J_E should be as large as possible. However, the maximum current which can reasonably be carried through the collector body is:[13]

$$J_{max} = qv_{sc\,lim}N_{Ac} \tag{7}$$

where N_{Ac} is collector body impurity concentration (Fig. 2). N_{Ac} also affects x_m because collector-to-base breakdown voltage (BV_{CB}) decreases as N_{Ac} increases.[14] Collector depletion layer thickness at breakdown also decreases with increase of N_{Ac}.[15]

C_{ea} varies as $N_{Db}^{1/2}$ and also increases somewhat as J_E increases because of the reduction in emitter barrier potential needed to pass larger current densities. These trends suggest that, for fixed x_m and fixed impurity density per unit area of base layer, there is a definite minimum in τ_{ec}.

[10] H. Krömer, "Zur theorie des Diffusions und des drifttransistors," Parts I–III, *Arch. elektr. Übertr.*, vol. 8, pp. 223–228; May, 1954; pp. 363–369; August, 1954; pp. 499–504; November, 1954.
———. "Der drifttransistor," *Naturwiss.*, vol. 40, pp. 578–579; November, 1953.
———. "The drift transistor," in "Transistors I," RCA Labs., Princeton, N. J., pp. 202–220; 1956.

[11] J. L. Moll and I. M. Ross, "The dependence of transistor parameters on the distribution of base layer resistivity," Proc. IRE, vol. 44, pp. 72–78; January, 1956.

[12] L. J. Varnerin, "Stored charge method of base transit analysis," to be submitted to the IRE.

[13] E. J. Ryder, "Mobilities of holes and electrons in high electric fields," *Phys. Rev.*, vol. 90, p. 766; June, 1953.

[14] S. L. Miller, "Avalanche breakdown in germanium," *Phys. Rev.*, vol. 99, p. 1234; August 15, 1955.

[15] It is assumed that the collector-to-base junction is essentially a step junction between material of high conductivity on the base side and material of low conductivity on the collector side. The reciprocal dependence of maximum current density and breakdown voltage can be demonstrated for graded and intrinsic barriers as well. Power density limitations implicit in this reciprocity will be the subject of a later paper.

The product $C_{ca}\tau_{ec}$ can be written:

$$C_{ca}\tau_{ec} = \frac{\epsilon}{2v_{sc\ \lim}}\left[1 + \frac{2v_{sc\ \lim}}{x_m}\left(\frac{kT}{qJ_E}C_{ea} + \frac{w^2}{nD_{pb}}\right)\right]. \qquad (8)$$

Since the second term in the bracket is inherently positive, $C_{ca}\tau_{ec}$ cannot be less than $\epsilon/2v_{sc\ \lim}$. The physical sense of (8) is that, on a fixed area (one-dimensional) basis, collector capacitance can be reduced only by thickening the collector depletion layer, thus increasing carrier transit time and therefore emitter to collector signal delay time. Detailed calculation finds actual minima about twice this big for a wide range of x_m values. In short, in optimum gain-band designs, C_{ca} and τ_{ec} have a nearly constant product (C_c and f_α in constant ratio).

The remaining one-dimensional parameter, base layer sheet resistance $R_\square$ depends on the total number of impurity centers per cm² of base layer area ($N_{Db}w$) and on majority carrier mobility μ_{nb} in the base layer

$$R_\square = \frac{1}{q\mu_{nb}N_{Db}w}. \qquad (9)$$

Increase of N_{Db} usually decreases μ_{nb} (and also D_{pb}) because of increased coulomb scattering of carriers.

Minimum $R_\square C_{ca}\tau_{ec}$

Minimum values for the parameter $R_\square C_{ca}\tau_{ec}$ have been found, assuming:

1) given values of N_{Ac};
2) $J_E = 0.5$ of $J_{\max}$ given by (7);
3) collector-to-base junction is a step junction lying largely on the collector side of the p-n transition;
4) x_m is that for $V_C = 0.3BV_{CB}$ (BV_{CB} from Miller[14]);
5) $N_{Db}w = 10^{13}$ donors/cm² of base;
6) μ_{nb} and D_{pb} vary as $N_{Db}^{-1/3}$;
7) mobilities from the work of Prince and others;[16]
8) impurity density in the base layer is constant rather than graded;
9) the emitter to base barrier is a step with very high concentration on the emitter side and a lower concentration on the base side, uniform in the barrier region.

If, under these assumptions, the $R_\square C_{ca}\tau_{ec}$ product obtained by multiplying (8) by (9) is differentiated with respect to base thickness w, a minimum is found when base transit time is:

$$\frac{w^2}{nD_b} \simeq \frac{1}{4}\left(\frac{x_m}{2v_{sc\ \lim}}\right) + \frac{5}{8}\left(\frac{kT}{qJ_E}C_{EA}\right). \qquad (10)$$

The numerical constants in (10) are quite sensitive to the assumed mobility variation with N_{Db}. The minima in $R_\square C_{ca}\tau_{ec}$ are only slightly sensitive to this assumption.

Table I shows variation of $R_\square C_{ca}\tau_{ec}$ with assumed N_{Ac}. The effect on (power gain)$^{1/2}$ (bandwidth) is given by:

TABLE I

Dependence of $R_\square C_{ca}\tau_{ec}$ and Gain-Band on Collector Impurity Concentration

N_{Ac} Acc/cm³	$R_\square C_{ca}\tau_{ect}$ sec²/cm²	$K \equiv$ (P.G.)$^{1/2}$(B.W.) cps
10^{14}	$.654\times10^{-16}$	12×10^6/s
10^{15}	1.11×10^{-16}	9.26×10^6/s
10^{16}	2.2×10^{-16}	6.56×10^6/s
10^{17}	3.88×10^{-16}	5×10^6/s

TABLE II

Calculated Transistor Design

Collector Design				Performance		
s	N_{Ac}	x_m	BV_{CB}	f_T	(P.G.)$^{1/2}$ (B.W.)	Impedance Ratio (Com. Em.)
microns	10^{16}/cm³	10^{-4} cm	volts	kmc	kmc	R_{out}/R_{in}
25	0.1	8.36	140	1.0	3.7	~55
25	0.39	2.62	52	3.0	3.0	4.0
25	0.72	1.52	33	5.0	2.72	1.2
7.5	0.39	2.62	52	3.0	10.0	38
7.5	1.72	0.72	17	10.0	7.95	2.2
2.5	1.72	0.72	17	10.0	23.8	22.7
2.5	10.6	0.15	4.5	40.0	20.0	1.0

$$K \equiv (\text{power gain})^{1/2}(\text{bandwidth}) \simeq \frac{(5\text{–}12)\times 10^6}{s}\ \text{cps} \qquad (11)$$

where s is stripe width in cm.

Particular Designs

Table II shows critical parameters of some theoretical transistor designs calculated by interpolation in Table I and related computations. Note that transformers are required to utilize the gain-band product unless the characteristic frequency $f_T \equiv 1/(2\pi\tau_{ec})$ is set at about twice the (power gain)$^{1/2}$(bandwidth) product.[17]

The decrease in (power gain)$^{1/2}$(bandwidth) with increase of f_T (therefore increase of f_α) is caused by the decrease in base region carrier mobility resulting from coulomb scattering in thin, heavily doped layers. It should be noted that reverse emitter breakdown voltage also decreases as base layer impurity concentration is increased. For the design with f_T of 40 kmc, the residual emitter barrier voltage is little over 0.1 volt and the emitter barrier capacitance is computed to be greater than 1 μf/cm². These theoretical calculations suggest that transistors usable in the microwave range may be feasible. Fabrication of 2.5 micron wide electrodes will pose some interesting mechanical and electrical problems. It should be noted that the impurity density per square centimeter of base layer which was assumed is moderate rather than very high and that experimental work may possibly yield somewhat better

[16] M. B. Prince, "Drift mobilities in germanium," *Phys. Rev.*, vol. 92, pp. 681–687; November 1, 1953.

[17] Note that for this condition $r_{b'}C_c$ is $\simeq\tau_{ec}$. This makes common emitter input impedance ($r_{b'}$) equal to output impedance τ_{ec}/C_c. Conversely note that when τ_{ec} is $> r_{b'}C_c$ output impedance is higher than input impedance, but that breakdown voltage is higher and the gain-band product slightly larger.

gain-band figures of merit. The concentration of ac emission in the portions of the emitter nearest the base contacts may also increase the gain-band product.[18]

Experimental

Experience has shown that germanium *p-n-p* diffused base transistors with a 25 micron wide emitter stripe and a base contact stripe of equal width 12 to 20 microns away from one edge frequently can be made to oscillate at above 1000 mc. In terms of the model studied, this emitter stripe is 50 microns wide and the stripe-to-stripe spacing is a little below the 1 to 2 ratio assumed in the analysis. Base layer impurity concentrations were probably somewhat higher than those assumed in the analysis. On the other hand, the ratio of collector barrier width to base layer thickness was nowhere near optimum and the collector body is usually about 75 microns thick rather than the less than 10 microns assumed in analysis. Fig. 3 shows emitter and base electrodes of such a transistor and the 10 micron diameter contact wires to the electrodes.

The feasibility of 7.5 microns wide electrodes may, of course, be questioned. Experimental electrodes of this width are shown in Fig. 4. Whether the 2.5 micron wide electrodes are more than a designer's dream remains to be seen.

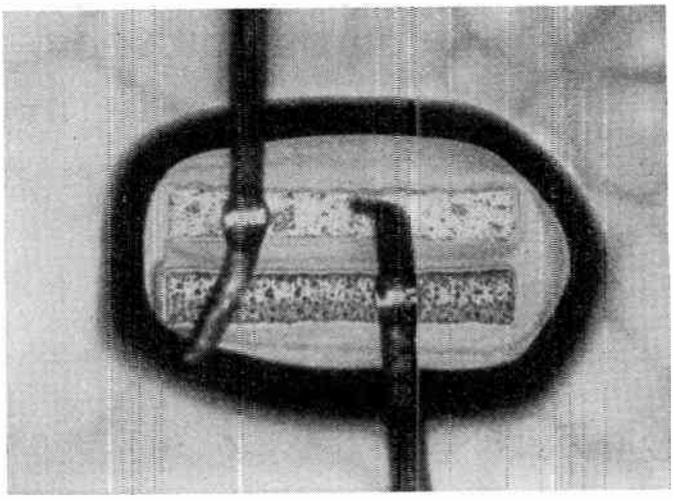

Fig. 3—Top view of experimental diffused base germanium transistor showing 1×6 mil electrodes and 0.4 mil connecting wires.

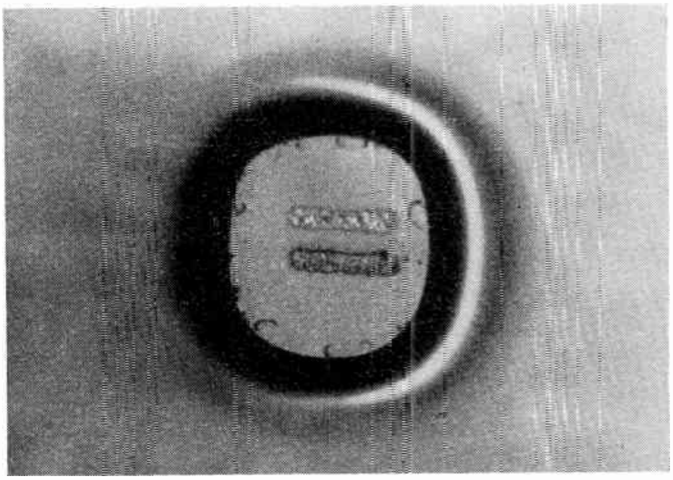

Fig. 4—Top view of experimental diffused base germanium transistor showing 0.3×1.5 mil emitter electrode and base contact.

Summary and Comparison

Analysis shows that the (power gain)$^{1/2}$ (bandwidth) product of a junction triode transistor with linear emitter and base electrodes is inversely proportional to emitter stripe width s (which includes emitter to base spacing). For *p-n-p* germanium devices, the optimum gain-band product is about $7.5 \times 10^6/s$ cps, where s is in centimeters. In addition, this gain-band product, which is approximately the same as the maximum frequency of oscillation, is reciprocal to the square root of the product of base layer sheet resistance, collector capacitance per unit area, and emitter-to-collector delay time. The reciprocity of collector capacitance per unit area and carrier drift time through the collector depletion layer make this product nearly independent of the alpha cutoff frequency of the transistor. An essentially similar value of gain-band product is expected for *n-p-n* germanium transistors, while that for silicon devices is probably a factor of two or more smaller.

The field effect transistor structure analyzed by Dacey and Ross resembles the junction triode structure of Fig. 1 in several ways.[2] The most important of the similarities is that the electrode which determines the gain-band product in the field effect unit is also a long narrow stripe with ohmic contacts closely spaced on either side. Dacey and Ross derived for the field effect unit a gain-band equation fully comparable to (11):

$$f_{\max} = 5.7 \times 10^5/L \text{ cps} \tag{12}$$

where L is the width of this gate electrode in centimeters. Although improved impurity distributions might raise this figure of merit for the field effect transistor, it seems doubtful that a factor of 10 could be achieved. The most detailed available theory of the analog transistor[4] does not contain an expression as fully worked out as that of Dacey and Ross, but there seems no obvious reason for supposing that this device has a better figure of merit than the field effect transistor. Like the junction triode, the field effect has the advantage of operating with most of the active carriers in a space charge neutral region.

Of the three major high frequency three-terminal semiconductor devices, the junction triode appears to have the best inherent gainband product and may well be suitable for some microwave applications.

Acknowledgment

The suggestions and assistance of many co-workers were very helpful in preparation of this paper. I am particularly grateful to L. J. Varnerin, D. F. Ciccolella, and R. J. Gnaedinger, and J. R. Flegal.

[18] R. L. Pritchard, "High-frequency power gain of junction transistors," Proc. IRE, vol. 43, pp. 1075–1085; September, 1955.

IRE Standards on Audio Techniques: Definitions of Terms, 1958*

58 IRE 3. S1

COMMITTEE PERSONNEL

Subcommittee on Audio Definitions

D. S. DEWIRE, *Chairman* 1956–1958
L. D. RUNKLE, *Chairman* 1955–1956

W. E. Darnell 1955–1958
D. S. Dewire 1955–1956
W. F. Dunklee 1955–1958
C. W. Frank 1955–1958
G. H. Grenier 1955–1956
A. A. McGee 1956–1958
L. D. Runkle 1956–1958
R. E. Yaeger 1955–1958

Committee on Audio Techniques‡

D. S. DEWIRE, *Chairman* 1958
IDEN KERNEY, *Chairman* 1955–1958
A. P. EVANS, *Vice-Chairman* 1958
D. S. DEWIRE, *Vice-Chairman* 1956–1958

A. A. Alexander 1956–1958
B. B. Bauer 1957–1958
C. A. Cady 1955–1958
R. H. Edmondson 1956–1958
A. P. Evans 1956–1958
L. H. Good 1955–1957
G. H. Grenier 1955–1957
F. K. Harvey 1955–1958
F. L. Hopper 1955–1958
A. H. Lind 1956–1958
D. E. Maxwell 1955–1957
A. A. McGee 1957–1958
R. C. Moody 1955–1958
R. W. Ralston 1955–1956
F. W. Roberts 1955–1958
L. D. Runkle 1955–1958
H. O. Saunders 1955–1956
F. H. Slaymaker 1955–1957
W. E. Stewart 1955–1956
R. E. Yaeger 1955–1958

Committee on Audio and Electroacoustics

1958–1959

IDEN KERNEY, *Chairman*
D. S. DEWIRE, *Vice-Chairman*
A. P. EVANS, *Vice-Chairman*
H. C. HARDY, *Vice-Chairman*

Standards Committee

1958–1959

R. F. SHEA, *Chairman*
J. G. KREER, JR., *Vice-Chairman*
C. H. PAGE, *Vice-Chairman*
L. G. CUMMING, *Vice-Chairman*

J. Avins
W. F. Bailey
M. W. Baldwin, Jr.
J. T. Bangert
W. R. Bennett
J. G. Brainerd
D. R. Brown
T. J. Carroll
P. S. Carter
A. G. Clavier
G. A. Deschamps
D. S. Dewire
S. Doba, Jr.
P. Elias
G. A. Espersen
D. Frezzolini
E. A. Gerber
A. B. Glenn
V. M. Graham
R. A. Hackbusch
H. C. Hardy
R. T. Haviland
A. G. Jensen
Iden Kerney
A. E. Kerwien
G. S. Ley
W. Mason
D. E. Maxwell
H. R. Mimno
E. Mittelmann
L. H. Montgomery
G. A. Morton
R. C. Moyer
J. H. Mulligan
W. Palmer
R. L. Pritchard
P. A. Redhead
R. Serrell
W. A. Shipman
H. R. Terhune
E. Weber
R. B. Wilcox
W. T. Wintringham

Definitions Coordinator

C. H. PAGE

* Approved by the IRE Standards Committee, September 3, 1958. Reprints of this standard, 58 IRE 3. S1, may be purchased while available from the Institute of Radio Engineers, 1 East 79th Street, New York, N. Y., at $0.60 per copy. A 20 per cent discount will be allowed for 100 or more copies mailed to one address.

‡ Deactivated September 10, 1958. Replaced by Committee 30: Audio and Electroacoustics.

I. Introduction

THIS standard is issued to supersede 54 IRE 3. S1, "IRE Standards on Audio Techniques: Definitions of Terms, 1954," to include the definitions in the 1954 standard and to add definitions of other terms for which it was felt a need exists for establishment of precise and concise meanings. Some of the previous standard definitions have been modified slightly to bring them into uniformity with the added definitions.

The definitions included in this standard all refer specifically to the use of the terms in audio techniques. Many of these terms are used in other fields with different meanings, and it is assumed that definitions for these terms in those fields are or will be included in standards issued by other technical committees. Therefore, in general, the modifying phrase "In Audio Techniques" has been omitted except in certain special cases where it appears to be particularly necessary to avoid confusion.

Terms used within definitions and shown in italics are defined elsewhere in this standard.

II. Definitions

Active Transducer. See *Transducer, Active.*

Amplification. General transmission term used to denote an increase of *Signal* magnitude.

Amplifier. A device which enables an input *Signal* to control a *Source* of power, and thus is capable of delivering at its output an enlarged reproduction of the essential characteristics of the *Signal.*

Note: Typical amplifying elements are electron tubes, transistors, and magnetic circuits.

Amplifier, Bridging. An *Amplifier* with an *Input Impedance* sufficiently high that its input may be bridged across a circuit without substantially affecting the *Signal Level* of the circuit across which it is bridged.

Amplifier, Clipper. An *Amplifier* designed to limit the instantaneous value of its output to a predetermined maximum.

Amplifier, Distribution. A *Power Amplifier* designed to energize a speech or music distribution system and having sufficiently low *Output Impedance* so that changes in *Load* do not appreciably affect the output voltage.

Amplifier, Isolation. An *Amplifier* employed to minimize the effects of a following circuit on the preceding circuit.

Amplifier, Line. An *Amplifier* which supplies a *Program* transmission line or a system with a *Signal* at a specified *Level.*

Amplifier, Monitoring. A *Power Amplifier* used primarily for evaluation and supervision of a *Program.*

Amplifier, Peak Limiting. See *Peak Limiter.*

Amplifier, Power. An *Amplifier* which drives a utilization device, such as a loudspeaker.

Amplifier, Program. See *Amplifier, Line.*

Amplitude Distortion. See *Distortion, Harmonic* and *Distortion, Intermodulation.*

Amplitude-Frequency Distortion. See *Distortion, Amplitude-Frequency.*

Amplitude-Frequency Response. The variation of *Gain, Loss, Amplification,* or *Attenuation* as a function of frequency.

Note: This response is usually measured in the region of operation in which the transfer characteristic of the system or component is essentially linear.

Amplitude Range. The ratio, usually expressed in decibels, between the upper and lower limits of *Program* amplitudes which contain all significant energy contributions.

Attack Time. The interval required, after a sudden increase in input *Signal* amplitude to a system or component, to attain a specified percentage (usually 63 per cent) of the ultimate change in *Amplification* or *Attenuation* due to this increase.

Attenuation. General transmission term used to denote a decrease of *Signal* magnitude.

Attenuator. An adjustable passive device for reducing the amplitude of a *Signal* without introducing appreciable distortion.

Audio Frequency. Any frequency corresponding to a normally audible sound wave.

Audio-Frequency Noise. Any electrical disturbance in the *Audio-Frequency* range introduced from a source extraneous to the *Signal.*

Audio-Frequency Response. See *Amplitude-Frequency Response.*

Audio Oscillator. A nonrotating device for producing *Audio-Frequency* alternating current, the frequency of which is determined by the characteristics of the device.

Audio Spectrum. The continuous range of frequencies extending from the lowest to the highest *Audio Frequency.*

Automatic Gain Control (AGC). A process by which *Gain* is automatically adjusted as a function of input or other specified parameter.

Automatic Volume Control (AVC). A process by which a substantially constant output *Volume* is automatically maintained in a system or component.

Available Power (of a Linear Source of Electric Energy). The power which a *Source* is capable of delivering into its *Conjugate Impedance.*

Note: Available Power is equal to the quotient of the mean square of the open-circuit terminal voltage of the *Source* divided by four times the resistive component of the impedance of the *Source.*

Babble. The aggregate *Crosstalk* from a large number of channels.

Balanced Amplifier Circuit. An *Amplifier* circuit in which there are two identical transmission paths usually connected so as to operate with the waves in the two paths in phase opposition.

Balanced Circuit. A circuit, the two sides of which are electrically alike and symmetrical with respect to a common reference point, usually ground.

Band-Elimination Filter. See *Filter, Band-Elimination.*

Band-Pass Filter. See *Filter, Band-Pass.*

Bass Boost. A deliberate adjustment of the *Amplitude-Frequency Response* of a system or component to accentuate the lower *Audio Frequencies.*

Bridging. The shunting of one electrical circuit by another.

Bridging Amplifier. See *Amplifier, Bridging.*

Bridging Gain. The ratio of the power a *Transducer* delivers to a specified *Load Impedance* under specified operating conditions, to the power dissipated in the reference impedance across which the input of the *Transducer* is bridged.

Note 1: If the input and/or *Output Power* consist of more than one component, such as multifrequency *Signal* or *Noise*, then the particular components used and their weighting must be specified.

Note 2: This *Gain* is usually expressed in decibels.

Bridging Loss. The ratio of the power dissipated in the reference impedance across which the input of a *Transducer* is bridged, to the power the *Transducer* delivers to a specified *Load Impedance* under specified operating conditions.

Note 1: If the input and/or *Output Power* consist of more than one component, such as multifrequency *Signal* or *Noise*, then the particular components used and their weighting must be specified.

Note 2: This *Loss* is usually expressed in decibels.

Note 3: In telephone practice this term is synonymous with the *Insertion Loss* resulting from bridging an impedance across a circuit.

Clipper Amplifier. See *Amplifier, Clipper.*

Compandor. The combination, in a transmission system of a *Compressor*, for transmitted *Signals* and an *Expander* for received *Signals.*

Note: The purpose of a *Compandor* is to improve the ratio of *Signal* to the interference entering the transmission path between *Compressor* and *Expander.*

Compressor. A *Transducer* which, for a given input *Amplitude Range*, produces a smaller output range.

Note: One type of *Compressor* reduces the *Amplitude Range* as a linear function of the envelope of speech waves.

Conjugate Impedances. See *Impedances, Conjugate.*

Crossover Network. A selective *Network* which divides its audio input into two or more frequency bands for distribution to loudspeakers.

Crosstalk. Electrical disturbances in a communication channel as a result of coupling with other communication channels.

Cue Circuit. A one-way communication circuit used to convey *Program* control information.

Current Amplification. The ratio of the magnitude of the current in a specified *Load Impedance* connected to a *Transducer*, to the magnitude of the current in the input circuit of the *Transducer.*

Note 1: If the input and/or output current consist of more than one component, such as multifrequency *Signal* or *Noise*, then the particular components used and their weighting must be specified.

Note 2: By custom this *Amplification* is often expressed in decibels by multiplying its common logarithm by 20.

Current Attenuation. The ratio of the magnitude of the current in the input circuit of a *Transducer*, to the magnitude of the current in a specified *Load Impedance* connected to the *Transducer.*

Note 1: If the input and/or output current consist of more than one component, such as multifrequency *Signal* or *Noise*, then the particular components used and their weighting must be specified.

Note 2: By custom this *Attenuation* is often expressed in decibels by multiplying its common logarithm by 20.

Cutoff Frequency. The frequency which delineates a pass band from an adjacent *Attenuation* band of a system or component.

dbm. A symbol for *Power Level* in decibels with reference to a power of 1 milliwatt (0.001 watt).

Decade. The interval between any two quantities having the ratio of 10:1.

De-Emphasis. A process complementary to *Pre-Emphasis.*

Delay Distortion. See *Distortion, Delay.*

Distortion. An undesired change in waveform.

Distortion, Amplitude. See *Distortion, Harmonic* and *Distortion, Intermodulation.*

Distortion, Amplitude-Frequency. *Distortion* due to an undesired *Amplitude-Frequency Response* characteristic.

Distortion, Delay. That form of *Distortion* which occurs when the rate of change of phase shift with frequency of a circuit or system is not constant over the frequency range required for transmission.

Distortion, Frequency. See *Distortion, Amplitude-Frequency.*

Distortion, Harmonic. *Nonlinear Distortion* characterized by the appearance in the output of harmonics of the fundamental frequency when the input wave is sinusoidal.

Distortion, Intermodulation. *Nonlinear Distortion* characterized by the appearance of frequencies in the output, equal to the sums and differences of integral multiples of the component frequencies present in the input wave.

Note: Harmonic components also present in the output are usually not included as part of the *Intermodulation Distortion.* When harmonics are included, a statement to that effect should be made.

Distortion, Nonlinear. *Distortion* caused by a deviation from a linear relationship between the input and output of a system or component.

Distortion, Per Cent Harmonic. A measure of the *Harmonic Distortion* in a system or component, numerically equal to 100 times the ratio of the square root of the sum of the squares of the root-mean-square voltages (or currents) of each of the individual harmonic frequencies, to the root-mean-square voltage (or current) of the fundamental.

Note: It is practical to measure the ratio of the root-mean-square amplitude of the residual harmonic voltages (or currents), after elimination of the fundamental, to the root-mean-square amplitude of the fundamental and harmonic voltages (or currents) combined. This measurement will indicate *Per Cent Harmonic*

Distortion with an error of less than 5 per cent if the magnitude of the *Distortion* does not exceed 30 per cent.

Distortion, Phase. See *Distortion, Phase-Frequency.*

Distortion, Phase-Frequency. *Distortion* due to a lack of direct proportionality of phase shift to frequency over the frequency range required for transmission.

Note 1: Delay Distortion is a special case.

Note 2: This definition includes the case of a linear phase-frequency relation with zero-frequency intercept differing from an integral multiple of π.

Distribution Amplifier. See *Amplifier, Distribution.*

Dividing Network (Loudspeaker Dividing Network). See *Crossover Network.*

Dynamic Range. The ratio of the specified maximum *Signal Level* capability of a system or component to its *Noise Level*, usually expressed in decibels.

Echo. A wave which has been reflected or otherwise returned with sufficient magnitude and delay to be perceived in some manner as a wave distinct from that directly transmitted.

Equalizer. A passive device designed to compensate for an undesired amplitude-frequency and/or phase-frequency characteristic of a system or component.

Expander. A *Transducer* which, for a given input *Amplitude Range*, produces a larger output range.

Note: One type of *Expander* increases the *Amplitude Range* as a linear function of the envelope of speech waves.

Filter. A selective *Network* which transmits alternating currents of desired frequencies and substantially attenuates all others.

Filter, Band-Elimination. A *Filter* which attenuates alternating currents between given upper and lower *Cutoff Frequencies* and transmits substantially all others.

Filter, Band-Pass. A *Filter* which transmits alternating currents between given upper and lower *Cutoff Frequencies* and substantially attenuates all others.

Filter, High-Pass. A *Filter* which transmits alternating currents above a given *Cutoff Frequency* and substantially attenuates all others.

Filter, Low-Pass. A *Filter* which transmits alternating currents below a given *Cutoff Frequency* and substantially attenuates all others.

Filter, Sound Effects. A *Filter*, usually adjustable, designed to reduce the pass band of a system at low and/or high frequencies in order to produce special effects.

Frequency Distortion. See *Distortion, Amplitude-Frequency.*

Frequency Response. See *Amplitude-Frequency Response.*

Gain (Transmission Gain). General term used to denote an increase in *Signal* power in transmission from one point to another. *Gain* is usually expressed in decibels and is widely used to denote *Transducer Gain.*

Gain Control. A device for adjusting the *Gain* of a system or component.

Harmonic Distortion. See *Distortion, Harmonic.*

High-Pass Filter. See *Filter, High-Pass.*

Hiss. Random *Noise* in the *Audio-Frequency* range, having subjective characteristics analogous to prolonged sibilant sounds.

Hybrid Coil. A single transformer which performs the essential function of a *Hybrid Set.*

Hybrid Set. Two or more transformers interconnected to form a *Network* having four pairs of accessible terminals to which may be connected four impedances so that electrical energy introduced into the *Network* at any one pair of terminals ideally divides between two of the other pairs with no transfer of energy to the fourth.

Hum. Electrical disturbance at the power supply frequency or harmonics thereof.

Ideal Transducer. See *Transducer, Ideal.*

Ideal Transformer. See *Transformer, Ideal.*

Image Impedances. See *Impedances, Image.*

Impedance, Input. The impedance presented by the *Transducer* to a *Source.*

Impedance, Iterative. That impedance which, when connected to one pair of terminals of a *Transducer*, produces an identical impedance at the other pair of terminals.

Note 1: It follows that the *Iterative Impedance* of a *Transducer* is the same as the impedance measured at the input terminals when an infinite number of identically similar *Transducers* are formed into an iterative or recurrent structure of infinite length by connecting the output terminals of the first *Transducer* to the input terminals of the second, the output terminals of the second to the input terminals of the third, etc.

Note 2: The *Iterative Impedances* of a four-terminal *Transducer*, are, in general, not equal to each other but for any symmetrical *Transducer* the *Iterative Impedances* are equal and are the same as the *Image Impedances*. The *Iterative Impedance* of a uniform line is the same as its characteristic impedance.

Impedance, Load. The impedance presented by the *Load* to a *Transducer.*

Impedance, Output. The impedance presented by the *Transducer* to a *Load.*

Impedance, Source. The impedance presented by the *Source* to a *Transducer.*

Impedances, Conjugate. Impedances having resistive components which are equal, and reactive components which are equal in magnitude but opposite in sign.

Impedances, Image. The impedances which will simultaneously terminate all inputs and outputs of a *Transducer* in such a way that at each of its inputs and outputs the impedances in both directions are equal.

Note: The *Image Impedances* of a four-terminal *Transducer* are, in general, not equal to each other, but for any symmetrical *Transducer*, the *Image Impedances* are equal, and are the same as the *Iterative Impedances.*

Input Impedance. See *Impedance, Input.*

Insertion Gain. Resulting from the insertion of a *Transducer* in a transmission system, the ratio of the power delivered to that part of the system following the *Transducer* to the power delivered to that same part before insertion of the *Transducer*.

Note 1: If the input and/or *Output Power* consist of more than one component, such as multifrequency *Signal* or *Noise*, then the particular components used and their weighting must be specified.

Note 2: This *Gain* is usually expressed in decibels.

Note 3: The "insertion of a *Transducer*" includes bridging of an impedance across the transmission system.

Insertion Loss. Resulting from the insertion of a *Transducer* in a transmission system, the ratio of the power delivered to that part of the system following the *Transducer*, before insertion of the *Transducer*, to the power delivered to that same part of the system after insertion of the *Transducer*.

Note 1: If the input and/or *Output Power* consist of more than one component, such as multifrequency *Signal* or *Noise*, then the particular components used and their weighting must be specified.

Note 2: This *Loss* is usually expressed in decibels.

Note 3: The "insertion of a *Transducer*" includes bridging of an impedance across the transmission system.

Intermodulation Distortion. See *Distortion, Intermodulation.*

Isolation Amplifier. See *Amplifier, Isolation.*

Isolation Transformer. See *Transformer, Isolation.*

Iterative Impedance. See *Impedance, Iterative.*

Level. The difference of a quantity from an arbitrarily specified reference quantity.

Note: The quantities of interest are often expressed in decibels, thus their difference is conveniently expressed as a ratio. Hence, *Level* is widely regarded as the ratio of the magnitude of a quantity to an arbitrary reference magnitude.

Line Amplifier. See *Amplifier, Line.*

Line Transformer. See *Transformer, Line.*

Load. 1) The device which receives *Signal* power from a *Transducer*.

2) The *Signal* power delivered by a *Transducer* (deprecated).

Load Impedance. See *Impedance, Load.*

Loss (Transmission Loss). General term used to denote a decrease in *Signal* power in transmission from one point to another. *Loss* is usually expressed in decibels.

Low-Pass Filter. See *Filter, Low-Pass.*

Microphonics. *Audio-Frequency Noise* caused by mechanical vibration of elements in a system or component.

Mixer (in Audio Techniques). A device, having two or more inputs and a common output, which operates to combine linearly in a desired proportion the separate input *Signals* to produce an output *Signal*.

Monitoring Amplifier. See *Amplifier, Monitoring.*

Motorboating. Oscillation in a system or component, usually manifested by a succession of pulses occurring at a sub-audio or low-audio repetition frequency.

Network. A combination of electrical elements.

Noise. See *Audio-Frequency Noise.*

Nonlinear Distortion. See *Distortion, Nonlinear.*

Octave. The interval between any two frequencies having a ratio of 2:1.

Output Impedance. See *Impedance, Output.*

Output Power. The power delivered by a system or component to its *Load*.

Pad. A nonadjustable passive device for reducing the amplitude of a *Signal* without introducing appreciable *Distortion*.

Passive Transducer. See *Transducer, Passive.*

Peak Limiter. A device which automatically limits the magnitude of a *Signal* to a predetermined maximum value in accordance with a specified *Attack Time* and a specified *Recovery Time*.

Peak Limiting Amplifier. See *Peak Limiter.*

Per Cent Harmonic Distortion. See *Distortion, Per Cent Harmonic.*

Phase Distortion. See *Distortion, Phase-Frequency.*

Phase-Frequency Distortion. See *Distortion, Phase-Frequency.*

Power Amplifier. See *Amplifier, Power.*

Power Gain. The ratio of the power that a *Transducer* delivers to a specified *Load*, under specified operating conditions, to the power absorbed by its input circuit.

Note 1: If the input and/or *Output Power* consist of more than one component, such as multifrequency *Signal* or *Noise*, then the particular components used and their weighting must be specified.

Note 2: This *Gain* is usually expressed in decibels.

Power Level. At any point in a transmission system, the difference of the measure of the steady-state power at that point from the measure of an arbitrarily specified amount of power chosen as a reference.

Note: The measures are often expressed in decibels, thus their difference is conveniently expressed as a ratio. Hence, *Power Level* is widely regarded as the ratio of the steady-state power at some point in a system to an arbitrary amount of power chosen as a reference.

Power Loss. The ratio of the power absorbed by the input circuit of a *Transducer* to the power delivered to a specified *Load* under specified operating conditions.

Note 1: If the input and/or *Output Power* consist of more than one component, such as multifrequency *Signal* or *Noise*, then the particular components used and their weighting must be specified.

Note 2: This *Loss* is usually expressed in decibels.

Preamplifier. An *Amplifier*, the primary function of which is to raise the output of a low-level source to an intermediate *Level* so that the *Signal* may be further processed without appreciable degradation in the signal-to-noise ratio of the system.

Note: A *Preamplifier* may include provision for equalizing and/or mixing.

Pre-Emphasis. A process in a system designed to emphasize the magnitude of some frequency components with respect to the magnitude of others.

Note: Pre-Emphasis at the transmitting end of a system, in conjunction with *De-Emphasis* at the receiving end, is applied for the purpose of improving signal-to-noise ratio.

Program. A sequence of audio signals transmitted for entertainment or information.

Program Amplifier. See *Amplifier, Line.*

Program Level. The measure of the *Program Signal* in an audio system expressed in *vu.*

Push-Pull Amplifier Circuit. See *Balanced Amplifier Circuit.*

Recovery Time. The interval required, after a sudden decrease in *Input Signal* amplitude to a system or component, to attain a specified percentage (usually 63 per cent) of the ultimate change in *Amplification* or *Attenuation* due to this decrease.

Reference Volume. The *Volume* which gives a reading of 0 *vu* on a *Standard Volume Indicator.*

Remote Line. A *Program* transmission line between a remote-pickup point and the studio or transmitter site.

Roll-Off. A gradually increasing *Loss* or *Attenuation* with increase or decrease of frequency beyond the flat portion of the *Amplitude-Frequency Response* characteristic of a system or component.

Signal. 1) A visual, audible, or other indication used to convey information.

2) The intelligence, message, or effect to be conveyed over a communication system.

3) A *Signal* wave.

Signal Level. At any point in a transmission system, the difference of the measure of the *Signal* at that point from the measure of an arbitrarily specified *Signal* chosen as a reference.

Note: The measures of the *Signal* are often expressed in decibels, thus their difference is conveniently expressed as a ratio.

Singing. An undesired self-sustained oscillation in a system or component.

Note: This term implies oscillation at a frequency in or above the pass band of the system or component.

Singing Margin. The difference in *Level,* usually expressed in decibels, between the *Singing Point* and the operating *Gain* of a system or component.

Singing Point. The minimum value of *Gain* of a system or component that will result in *Singing.*

Single-Ended Push-Pull Amplifier Circuit. An *Amplifier* circuit having two transmission paths designed to operate in a complementary manner and connected so so as to provide a single unbalanced output.

Note: This circuit provides push-pull operation without the use of a transformer.

Sound Effects Filter. See *Filter, Sound Effects.*

Source. The device which supplies *Signal* power to a *Transducer.*

Source Impedance. See *Impedance, Source.*

Standard Volume Indicator. A device for the indication of *Volume* having the characteristics prescribed in ASA-C16.5.

Thump. A low-frequency transient disturbance in a system or component characterized audibly by the onomatopoeic connotation of the word.

Transducer. A device capable of being actuated by waves from one or more transmission systems or media and of supplying related waves to one or more other transmission systems or media.

Transducer, Active. A *Transducer* whose output waves are dependent upon sources of power, apart from that supplied by any of the actuating waves, which power is controlled by one or more of these waves.

Transducer, Ideal (for Connecting a Specified Source to a Specified Load). A hypothetical passive *Transducer* which transfers the maximum possible power from the source to the *Load.*

Note: In linear *Transducers* having only one input and one output, and for which the impedance concept applies, this is equivalent to a *Transducer* which a) dissipates no energy and b) when connected to the specified *Source* and *Load* presents to each its *Conjugate Impedance.*

Transducer, Passive. A *Transducer* whose output waves are independent of any sources of power which are controlled by the actuating waves.

Transducer Gain. The ratio of the power that the *Transducer* delivers to a specified *Load* under specified operating conditions to the *Available Power* of a specified *Source.*

Note 1: If the input and/or *Output Power* consist of more than one component, such as multifrequency *Signal* or *Noise,* then the particular components used and their weighting must be specified.

Note 2: This *Gain* is usually expressed in decibels.

Transducer Loss. The ratio of the available power of a specified *Source* to the power that the *Transducer* delivers to a specified *Load* under specified operating conditions.

Note 1: If the input and/or *Output Power* consist of more than one component, such as multifrequency *Signal* or *Noise,* then the particular components used and their weighting must be specified.

Note 2: This *Loss* is usually expressed in decibels.

Transformer, Ideal. A hypothetical transformer which neither stores nor dissipates energy. Its self-inductances have a finite ratio and unity coefficient of coupling. Its self and mutual impedances are pure inductances of infinitely great value.

Transformer, Isolation. A transformer inserted in a system to separate one section of the system from undesired influences of other sections.

Transformer, Line. A transformer inserted in a system for such purposes as isolation, impedance matching or additional circuit derivation.

Transformer Loss. The ratio of the power that would be delivered to a specified *Load Impedance* if an *Ideal*

Transformer were substituted for the actual transformer, to the power delivered to the specified *Load Impedance* by the actual transformer, under the condition that the impedance ratio of the *Ideal Transformer* is equal to that specified for the actual transformer.

Note 1: If the input and/or *Output Power* consist of more than one component, such as multifrequency *Signal* or *Noise*, then the particular components used and their weighting must be specified.

Note 2: This *Loss* is usually expressed in decibels.

Transformer Loss (Deprecated). The *Loss* which would be eliminated by the insertion, at any point in a transmission system, of an *Ideal Transformer* having an impedance ratio equal to the absolute value of the ratio of the impedances facing the actual transformer.

Note: This *Loss* is usually expressed in decibels.

Transition Loss. At any point in a transmission system, the ratio of the *Available Power* from that part of the system ahead of the point under consideration to the power delivered to that part of the system beyond the point under consideration.

Note 1: If the input and/or *Output Power* consist of more than one component, such as multifrequency *Signal* or *Noise*, then the particular components used and their weighting must be specified.

Note 2: This *Loss* is usually expressed in decibels.

Treble Boost. A deliberate adjustment of the *Amplitude-Frequency Response* of a system or component to accentuate the higher *Audio Frequencies*.

Unbalanced Circuit. A circuit, the two sides of which are electrically unlike.

Voltage Amplification. The ratio of the magnitude of the voltage across a specified *Load Impedance* connected to a *Transducer* to the magnitude of the voltage across the input of the *Transducer*.

Note 1: If the input and/or output voltage consist of more than one component, such as multifrequency *Signal* or *Noise*, then the particular components used and their weighting must be specified.

Note 2: By custom this *Amplification* is often expressed in decibels by multiplying its common logarithm by 20.

Voltage Attenuation. The ratio of the magnitude of the voltage across the input of the *Transducer* to the magnitude of the voltage delivered to a specified *Load Impedance* connected to the *Transducer*.

Note 1: If the input and/or output voltage consist of more than one component, such as multifrequency *Signal* or *Noise*, then the particular components used and their weighting must be specified.

Note 2: By custom this *Attenuation* is often expressed in decibels by multiplying its common logarithm by 20.

Volume. The magnitude of a complex *Audio-Frequency* wave in an electric circuit as measured on a *Standard Volume Indicator*. The *Volume* is expressed in *vu*. In addition, the term *Volume* is used loosely to signify either the intensity of a sound or the magnitude of an *Audio-Frequency* wave.

Volume Control. See *Gain Control*.

Volume Indicator. See *Standard Volume Indicator*.

Volume Limiter (Deprecated). See *Peak Limiter*.

vu. A quantitative expression for *Volume* in an electric circuit.

Note 1: vu is pronounced "vee-you" and customarily written with lower case letters.

Note 2: The *Volume* in *vu* is numerically equal to the number of decibels which expresses the ratio of the magnitude of the waves to the magnitude of *Reference Volume*.

Note 3: The term *vu* should not be used to express results of measurements of complex waves made with devices having characteristics differing from those of the *Standard Volume Indicator*.

Frequency Variations in Short-Wave Propagation*

TORU OGAWA†, MEMBER, IRE

Summary—Frequency variations in the propagation of short-wave signals were observed at frequencies of 5 mc and 10 mc for about six months, beginning in August, 1957, utilizing the standard frequency transmission of station JJY in Tokyo. The distance from the station to the receiving point was about 360 km, and the propagation path was nearly parallel to the latitude. It was found that during the six to ten-hour period centered at noon the *E*-layer reflection of 5 mc was most suitable for utilizing the standard frequency, although the field intensity was very weak and the accuracy of the frequency comparison was only 5×10^{-9}, which was inferior by about a factor of ten to that possible with the VLF standard signals.

The propagation of signals (at 5 mc at night and 10 mc throughout 24 hours) which are widely used for communication service was accompanied by considerably large frequency variations, up to 3×10^{-7}. However, most variations are not large enough to disturb the communication quality even for those communication systems which require the severest limitation of frequency variations.

The diurnal and seasonal variations of the 5-mc signals, whose reflection point was in the *E* layer in the daytime and in the F_2 layer

* Original manuscript received by the IRE, March 3, 1958.
† Dept. of Elec. Eng., Doshisha Univ., Kyoto, Japan.

at night, were observed, and the differences between the F_2- to E-layer exchange in the morning and the E- to F_2-layer exchange at evening were also observed and discussed.

It was found by simultaneous observations of 5-mc and 10-mc signals that the long period movements at local points in the F_2 layer seemed to be nearly always correlated with each other.

The apparatus used is described and its limitations are discussed.

Introduction

THE information obtained from the observation of frequency variations in short-wave propagation is divided principally into three classes. The first class considers the utility of the standard frequency transmissions, since the observed variations of up to 3×10^{-7} caused in the propagation path were so large compared with the variations of the standard frequency itself. (These latter variations are small multiples of 10^{-9} at the transmitter.)[1] The second class of information is related to the distortion in special communication systems. In the rather serious case of the SSB system, the variations could be large enough to disturb the transmission quality, since the allowable value of the variation without considerable distortion has been measured as 2 cycles, *i.e.*, 2×10^{-7} at 10 mc.[2] In the future this effect will become more serious in the problem of communication quality, because it will be necessary to reduce the bandwidth more and more in order to avoid congestion in communications. As to the transmission of standard frequency signals, those in the VLF band were surprisingly superior to the ones in the HF band,[3] in which most standard frequency stations are now operated; therefore the VLF band may be used increasingly. However, it is impractical for commercial communications to change to the VLF band, since its usable frequency bandwidth is very narrow. The third class of information concerns the instability of the ionosphere. The vertical velocity of position of the same electron density can be directly and continuously observed by measuring the frequency variations in the propagation, and the velocity can be measured to an accuracy of 1 m/s or smaller. Therefore, the fine and sudden disturbances in the ionosphere can also be observed.

Frequency variations in short-wave propagation have been observed by several authors for rather short periods,[4–6] and many of these observers placed the emphasis on the standard frequency transmission. The present author has constructed an apparatus suitable for the continuous observation and study of the character of frequency variations in relation to the three areas mentioned above.

The frequency variations in propagation are caused by two factors, the Doppler effect at the reflection point and the variations of the group velocity in the ionosphere. The Doppler effect is proportional to the vertical component of the velocity of the point which has enough electron density to reflect the radio wave being considered, and the variations of the group velocity are caused by the variations of electron density from the wave entrance point to the exit point of the ionosphere. These two effects may be summarized in equations. The frequency variation in the total propagation path is expressed as

$$\delta f = f \frac{d}{dt} \int_0^l \frac{dl}{u}, \tag{1}$$

where l is the distance from the transmitting point to the receiving point measured along the propagation path, and u is the group velocity of the radio wave. Neglecting the earth's magnetic field and collision friction, u is given for short waves by

$$u = c\left(1 - \frac{e^2 N}{m\pi f^2}\right)^{1/2}, \tag{2}$$

where c is the velocity of light in free space, e and m are the charge and mass of an electron, respectively, and N is the electron density of the ionosphere. Therefore, assuming the propagation path to be symmetric about the vertical line through the reflection point,

$$\delta f = 2\frac{f}{c}\frac{d}{dt}\int_0^h \left(1 + \frac{e^2 N}{2\pi m f^2}\right) \cos i dh, \tag{3}$$

where h is the real height of the reflection point and i is the angle between dl and a line normal to the boundary of the ionosphere. Since (1) can be transformed into an equation involving the familiar variable h', the virtual height of the reflection point, that is,

$$\delta f = \frac{2f \cos i_0}{c} \frac{dh'}{dt}, \tag{4}$$

where i_0 is the incident angle to the ionosphere, then the frequency variation can also be expressed in terms of the time derivative of the virtual height.

Apparatus

A block diagram of the apparatus is shown in Fig. 1. The incoming standard frequency from the antenna is mixed at the receiver input with a harmonic frequency of the auxiliary crystal oscillator and then amplified. The auxiliary crystal oscillator is adjusted to a frequency slightly different from a subharmonic of the standard frequency. The output signal of the receiver is again amplified by a selective amplifier, which is fol-

[1] See, *e.g.*, National Bureau of Standards, Boulder Labs., Colo., "Standard frequencies and time signals WWV and WWVH," Proc. IRE, vol. 44, pp. 1470–1473; October, 1956.

[2] See, *e.g.*, N. Koomans, "Single-sideband telephony applied to the radio link between the Netherlands and the Netherlands East Indies," Proc. IRE, vol. 26, pp. 182–206; February, 1938.

[3] J. A. Pierce, "Intercontinental frequency comparison by very-low-frequency radio transmission," Proc. IRE, vol. 45, pp. 794–803; June, 1957.

[4] L. Essen, "Standard frequency transmission," *Proc. IEE*, vol. 101, pt. 3, pp. 249–255; July, 1954.

[5] J. M. Steele, "The standard frequency monitor at the National Physical Laboratory," *Proc. IEE*, vol. 102, pt. 2, pp. 155–165; March, 1955.

[6] I. Takahashi, T. Ogawa, M. Yamano, A. Hirai, and M. Takiuchi, "Doppler shift of the received frequency from the standard station reflected by the ionosphere," Proc. IRE, vol. 45, p. 1408; October, 1957.

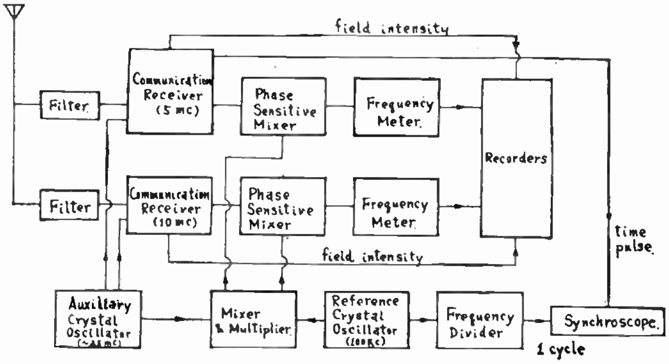

Fig. 1—Block diagram of apparatus.

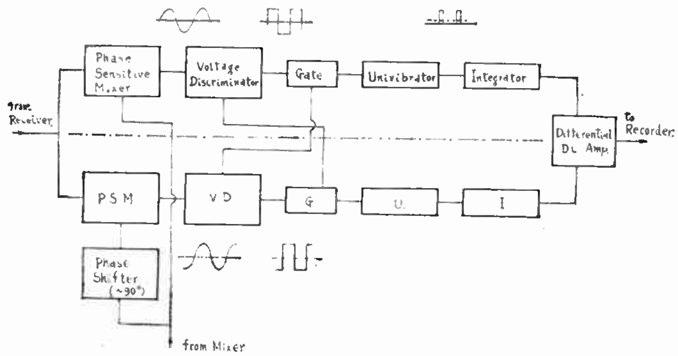

Fig. 2—Block diagram of phase sensitive mixer and frequency meter.

lowed by the phase sensitive mixer. The output of the auxiliary crystal oscillator is also introduced into the mixer and multiplier in which its harmonics are mixed with a harmonic of a 100-kc reference crystal oscillator. The two beat frequencies are fed into a phase sensitive mixer, producing a frequency which is the difference between the incoming frequency and the harmonics of the reference crystal oscillator. The effect of the variations in the frequency of the auxiliary crystal oscillator is canceled out by this last mixer. The output of the last phase sensitive mixer is introduced into a frequency meter having a high-frequency sensitivity, which can be operated at a frequency of 0.02 cps or lower at a sufficiently large amplitude, and whose output current is proportional to the frequency of the input signal.

The frequency meter is similar in principle to the counting-rate meter,[7] and its block diagram and waveforms for each stage are shown in Fig. 2. The beat signal is transformed into a rectangular signal by a voltage discriminator, and after differentiation, it drives the univibrator, which produces a constant width pulse per each cycle of the beat frequency. By integrating these pulses, the output direct current becomes proportional to the beat frequency. The frequency sensitivity may be increased by adjusting the width of these pulses.

In the present apparatus, a second channel was added, as shown below the broken line in Fig. 2. The phase of the reference signal fed to the second phase sensitive mixer is shifted about 90° from that of the first mixer. The gate of one channel is opened when that channel is operating, but closed when the other channel is being used. Therefore, when the incoming signal frequency is higher than the harmonics of the reference frequency, only the upper channel is in action while the lower channel is stopped, and vice versa. Therefore, the deflection in the recorder is to the right or to the left according to whether the incoming standard frequency is higher or lower than the harmonics of the reference frequency, respectively; in other words the frequency meter becomes sign sensitive. As a result, it is not necessary for the reference oscillator to be offset from its nominal frequency so that the pulses generated at the last stage of the frequency divider can be compared with the time signals modulating the standard frequency; also, it is available for other uses. In the comparison of the time signals, the variations caused by the propagation path are integrated over a long time interval—*e.g.*, for 24 hours—and the measuring error becomes very small. However, there are several disadvantages to this method. First, the action threshold voltage of the two discriminators must be adjusted to the same amount when the signal is weak, and second, the closer the beat frequency is to zero, the smaller becomes the voltage-sensitivity of the discriminators. Therefore, in the case of weak signals, it is better that the reference oscillator be offset; in practice the lower channel of the frequency meter was only used in simultaneous operation with the time signal comparison.

The over-all accuracy of the complete apparatus is limited by several factors. The most important one is the accuracy of the reference crystal oscillator, and other ones are the variations of the pulse height and width at the univibrator and the balancing of the direct current amplifier in the frequency meter. The drift of the reference crystal oscillator is measured to be about 1×10^{-8} per day by means of the time comparison between the output pulse of the frequency divider and the standard time signal employing a synchroscope, and by the frequency comparison method utilizing the 5-mc signal received via *E*-layer reflection. As the errors arising from other factors are much smaller than that of the reference oscillator, the total accuracy is estimated to be about 1×10^{-8} per day, *i.e.*, the error in measurement of the vertical velocity of the reflection point is estimated to be about 1.5 m/s per day in the case of vertical incidence. Of course the total error for a short period is less than this value and is smaller than one meter per second per day.

Such a method, utilizing the frequency meter, is superior to the ordinary beat method[8,9] in the direct read-

[7] W. C. Elmore and M. Sands, "Electronics, Experimental Techniques," McGraw-Hill Book Co., Inc., New York, N. Y., pp. 249–256; 1949.

[8] A. H. Allan, D. D. Crombie, and W. A. Penton, "Frequency variations in New Zealand of 16 kc/s transmission from GBR Rugby," *Nature*, vol. 177, pp. 178–179; January 28, 1956.

[9] I. Takahashi, T. Ogawa, M. Yamano, A. Hirai, and M. Takeyama, "Stark modulation atomic clock," *Rev. Sci. Instr.*, vol. 27, pp. 739–745; September, 1956.

ing of frequency variations. However, the disadvantage is that when the beat frequency becomes very low, the errors of the frequency meter are relatively not negligible. Generally, in frequency comparison it is preferable to employ the frequency meter method when the frequency difference is 0.1 cps or higher, and the ordinary beat method when it is 0.1 cps or lower.

Finally, the field intensity of the received signal can be recorded for assistance in analysis by a calibrated bridge circuit in the receiver.

Observed Results and Discussion

Observations were made beginning August, 1957, and the frequencies observed were at 5 mc and 10 mc. The observation point was at Doshisha University in Kyoto, Japan, at long. 135.8° E and lat. 35.0° N, which is about 360 km distance from the standard frequency station JJY of the Radio Research Laboratories in Tokyo, Japan, at long. 139.5° E and lat. 35.7° N. As the propagation path was nearly parallel to the latitude, the effects of the extraordinary wave could be neglected.

The frequency variations were almost continuously observed except for the periods of improvement of apparatus, and the field intensity was sometimes observed.

These two frequencies were selected for the following reasons. To use a radio wave signal as the frequency standard, it is important in many cases that the frequency variations caused by the propagation medium be as small as possible even when the field intensity is at its lowest detectable level. Earlier observations have shown that the variations are much smaller in the case of the *E*-layer reflection than in that of the other layers. In the present case, the incident angle to the *E* layer is about 60°; therefore, the radio waves with frequencies higher than about 7 mc cannot be received by *E*-layer reflection during the whole year, except during periods of extraordinary disturbances in the ionosphere. Even if a frequency less than this value is selected, the period of *E*-layer reflection is limited. However, as the frequency is lowered, this time interval increases. From this point of view, the 2.5-mc standard frequency is more suitable than the 5-mc one. However, the field intensity of the former is much smaller than that of the latter due to the increased attenuation of the ionosphere. Also, the standard station JJY is not always on the air at 2.5 mc. The 5-mc signal was selected not only to measure its utility as a standard frequency in the daytime but also as a communication frequency at night, when the frequency variation usually is very large due to the F_2-layer disturbances.

The frequency range of 10-mc signals is suitable for long-distance communication in the daytime and also at night. Most domestic radio communication systems whose range is larger than several hundred kilometers are operated in the neighborhood of this frequency, especially in the daytime. Thus, by measuring the frequency variation at 10 mc, the signal distortion of domestic service in the daytime and of intercontinental service at night may be explained. The 15-mc standard signal might also have been observed as well as the 10 mc, but the analysis of the data was very complex because at this frequency, even in the daytime, the signal intensity of the radio wave from Hawaii (WWVH) becomes stronger than the one from Tokyo (JJY) more frequently than at 10 mc.

Typical examples of the diurnal variations of frequency variation are shown in Fig. 3(a) and (b). The frequency variation record at 5 mc in Fig. 3(a) can be roughly separated into four time intervals. Period I is the six to ten hours centered at about noon, when the received signal is assumed to be the result of *E*-layer reflection, because in this time interval the electron density of the *E* layer is great enough to reflect a 5-mc signal which approaches at an incident angle of about 60°. The good quality of the 5-mc signal in this period is of great interest: it is most suitable as a frequency and time standard transmission, because the frequency variations are very small compared with the other periods of the 5-mc record and the whole part of the 10 mc, as shown in Fig. 3(b). On the days in which the ionosphere disturbances were small, it was possible to compare the standard frequency to the local stable oscillator with a precision up to 5×10^{-9} by a two to three hours frequency comparison. These days were about 75 per cent of the total period of observation. Fig. 4 shows the seasonal variation of such usable time intervals for standard frequency comparison. The two solid lines show the theoretical curves indicating the limiting times for *E*-layer reflection based upon the law that the critical frequency of the *E* layer is proportional to $(\cos\chi)^{1/4}$, where χ is the solar zenith angle. The limiting points observed are almost all located inside but near the theoretical curves. Some of the larger intervals between the theoretical curves and the observed points indicate that the movements of the *E* layer near the beginning and the end of the reflection period became irregular. In Period I the field intensity was so weak, as shown in Fig. 5(a), that it will be difficult to use the radio signals for communication service, even if the frequency variations were small. In Period II most of the frequency variations were of the order of 5×10^{-8}, but were sometimes accompanied by sudden variations of 2×10^{7}. Because the electron density of the *E* layer at night decreases to about one tenth of the value in the daytime,[10] the propagation of the 5-mc wave at that time was obviously via the F_2 layer. The frequency variations are assumed to depend both upon the variations in the height of the reflection point in the F_2 layer and upon the variations of group velocity in the ionosphere. However, the variations of the group velocity cannot possibly cause such large frequency variations for such long time intervals. For example, let us imagine an extreme case in which the height of the reflection point is not changing and the electron density in

[10] A. P. Mitra, "Night-time ionization in the lower ionosphere," *J. Atmos. Terr. Phys.*, vol. 10, pp. 140–162; March, 1957.

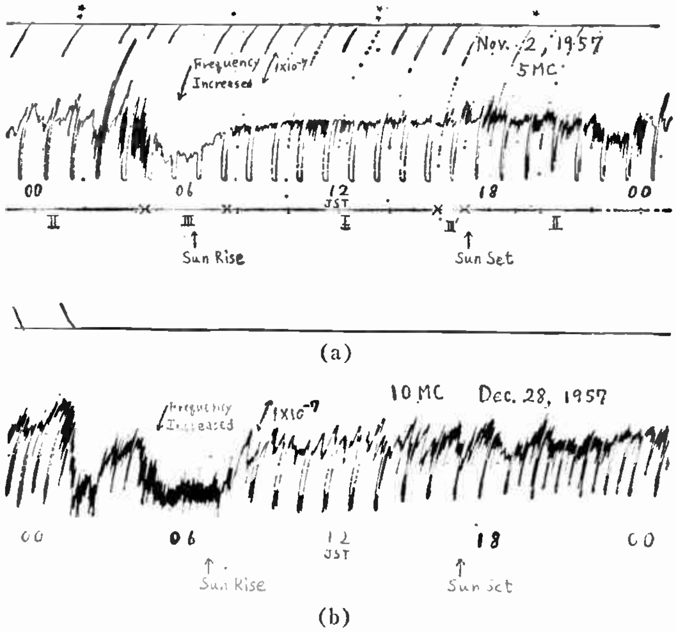

Fig. 3—Typical example of diurnal variation. (a) 5 mc. (b) 10 mc.

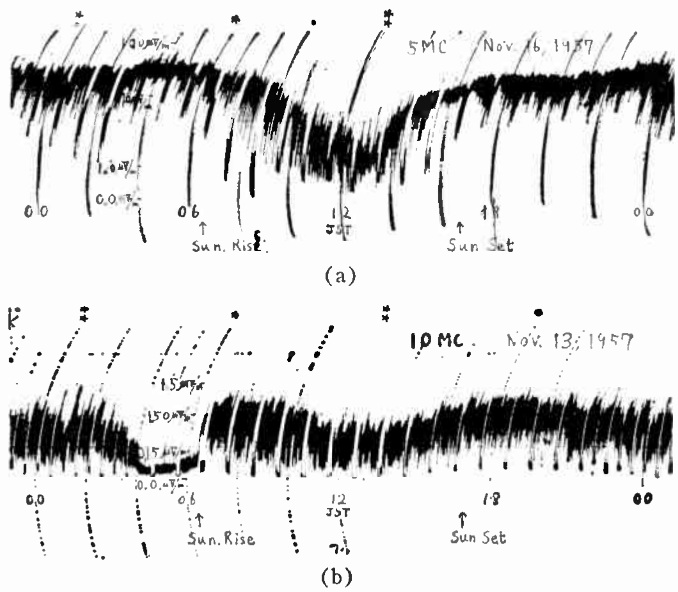

Fig. 5—Typical example of field intensity variations. (a) 5 mc. (b) 10 mc.

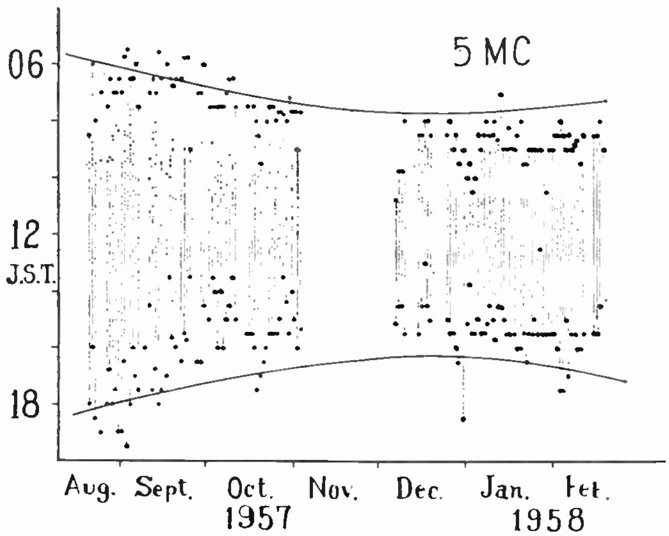

Fig. 4—Seasonal variation of usable time intervals for standard frequency comparison at 5 mc.

the ionosphere below the reflection point, a distance of 10 km, varies uniformly with time from zero to 5×10^4 per cubic centimeter in 5 seconds. For that extreme case, the frequency variation is estimated from (3) to be only about 4×10^{-9} at 5 mc. Consequently, the frequency variations will mainly depend upon the effect of the variations of the reflection point itself. Remarkable variations up to the order of -3×10^{-7} appeared for about one hour between 1 A.M. and 4 A.M. on most days. Although these variations accompany reception of the radio wave from WWVH, the mechanism of their origin is not clear.

In Period III, centered around sunrise, the variations appeared to increase the frequency; the cause of this increase is believed to be the movement of the reflection point from the F_2 layer to the E layer. The frequency change was gradual and reached a value up to about $+1\times10^{-7}$. In Period III′, which was at sunset, the variations tended to decrease the frequency, although not so much as in Period III; but they were accompanied by sudden variations of short duration. Such variations are believed to be caused by the inverse of the process in Period III, that is, by the reflection point moving from the E layer to the F_2 layer. In the F_2- to E-layer change, the reflection point appeared to be coming down at a mean velocity of about 20 m/s, whereas in the E- to F_2-layer change the reflection occurs simultaneously at both layers, which are moving up at a velocity somewhat smaller than that mentioned above. In the latter case, the relative field intensities of the waves from the different layers are rapidly alternating in their relative intensities. It is interesting to note that the processes were different for the F_2- to E-layer and the E- to F_2-layer exchanges.

Except during Period I, the field intensity was sufficient for use in communication service, and was between 10 μv/m and 10 mv/m. Fig. 6(a) shows an example of the distribution of the frequency variations at 5 mc, measured at hourly intervals from midnight throughout the day. Although the maximum frequency variations amount to 3×10^{-7}, even those communication systems that allow a variation of only 2 cps may be successfully operated.

The standard frequency station JJY is off the air from 29 minutes to 39 minutes past each hour, and the hourly interruption of the recordings during the daytime due to this are plainly visible. These interruptions on the records were shortened at night by the WWVH transmission, which is off the air for the period between 30 minutes to 34 minutes past each hour, and in some cases by the WWV transmission, which is continuous

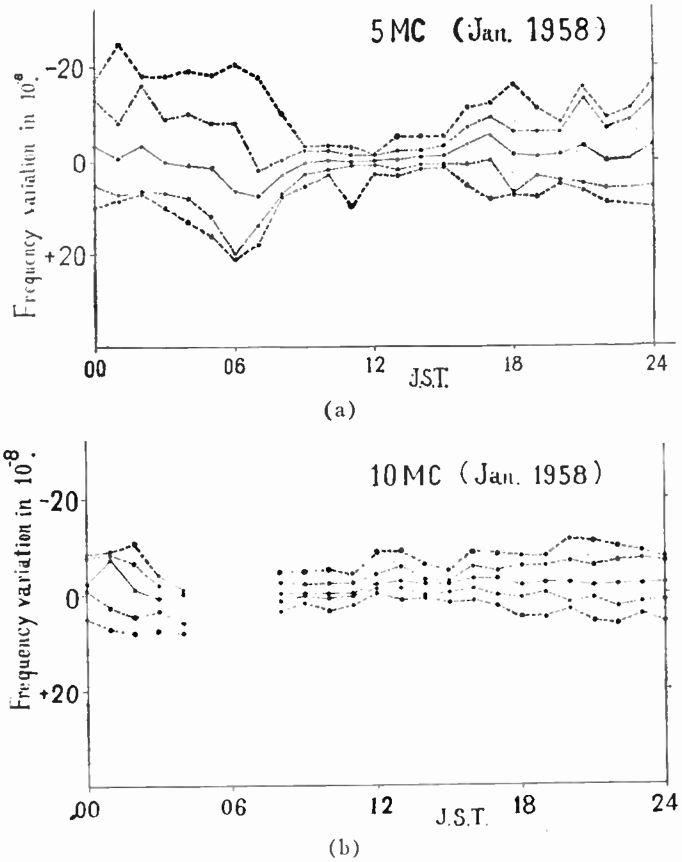

Fig. 6—Distribution of frequency variations. (a) 5 mc. (b) 10 mc. Dotted line, maximum variation; broken line, 90 per cent variation; and solid line, mean variation. (Distributions of 10 mc from 5:00 to 7:00 A.M. could not be obtained according to the penetration of signal.)

during the JJY interruption. It is interesting to observe that the frequency variations of the radio signals from WWVH were of the same order as those from JJY, although the distance of WWVH is about twenty times that of JJY; however the observation period was very much shorter than that for JJY.

Typical examples of frequency variations at 10 mc are shown in Fig. 3(b). At this frequency the changes on the record are not so distinct as at 5 mc, because the reflection of the 10-mc radio wave from JJY and WWVH is always via the F_2 layer, except in the cases of the appearance of a layer having a much larger electron density at or below the height of the F_2 layer. The field intensity dropped to almost zero because of the deep penetration of the signals into the F_2 layer from about 4 A.M. to 6 A.M., as shown in Fig. 5(b); this time interval was, of course, slightly different from day to day. The distribution of frequency variations at 10 mc for each hour is shown in Fig. 6(b); the variations are normally less than 2 cps, although sudden variations amounting to 3 cps do occur at times.

Fig. 7 shows a typical example of simultaneous observation of frequency variations at 5 mc and 10 mc at night. The two almost correlate with each other not only in the amount of variation but also in the length of duration, except for those of short duration. Hence it may be concluded that in the F_2 layer at night independent variations of the electron density within small volumes are not very pronounced, but that the variations of the layer as a whole are the dominant phenomena.

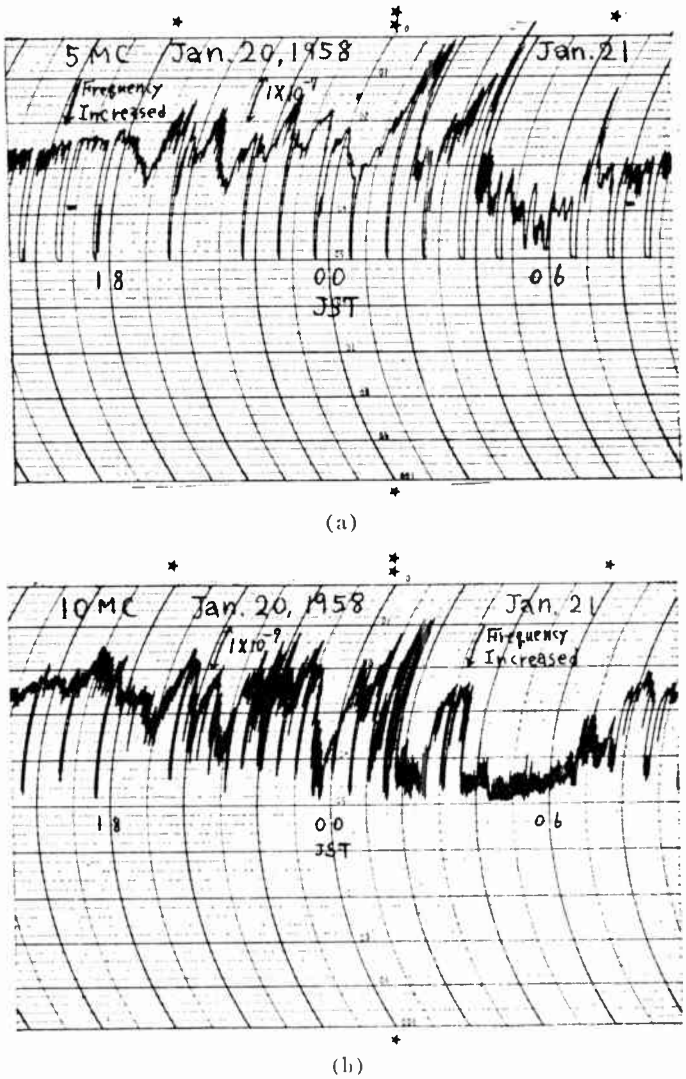

Fig. 7—An example of simultaneous observation of 5-mc and 10-mc signals reflected from the F_2 layer.

It was not completely evident whether any of the frequency variations corresponded closely to the appearance of the sporadic E layer or not. However, several observations around the time of appearance of the sporadic E layer at night showed the frequency variations were of the order 4×10^{-8} and that vertical velocity of the reflection point seemed unexpectedly small at 5 mc. Also, the signal from Hawaii was not received; therefore the signal recordings were similar to those in the daytime.

Acknowledgment

The author expresses his thanks to Prof. I. Takahashi of Kyoto University for his encouragement, and K. Takeuchi and E. Kuroda for their assistance.

IRE Standards on Recording and Reproducing: Methods of Calibration of Mechanically-Recorded Lateral Frequency Records, 1958*

58 IRE 19. S1

COMMITTEE PERSONNEL

Subcommittee on Mechanical Recording

LINCOLN THOMPSON, *Chairman* 1954–1958

W. S. Bachman 1954–1958
B. B. Bauer 1957–1958
S. M. Fairchild 1954–1958
T. A. Lindenberg 1954–1955
A. R. Morgan 1954–1958
R. C. Moyer 1954–1958
F. W. Roberts 1954–1958
M. F. Royston 1954–1957
R. A. Schlegel 1954–1957
A. S. R. Tobey 1954–1958
B. J. White, Jr., 1958

Committee on Recording and Reproducing

R. C. MOYER, *Chairman* 1958
D. E. MAXWELL, *Chairman* 1956–1958
A. W. FRIEND, *Chairman* 1954–1956
R. C. MOYER, *Vice-Chairman* 1956–1958
M. S. CORRINGTON, *Vice Chairman* 1954–1956

S. J. Begun 1955–1957
M. Camras 1955–1958
W. R. Chynoweth 1956–1958
F. A. Comerci 1955–1958
E. W. D'Arcy 1955–1958
S. M. Fairchild 1955–1957
R. M. Fraser 1955–1957
A. W. Friend 1956–1958
C. J. LeBel 1955–1958
R. C. Moyer 1955–1956
C. B. Pear, Jr. 1955–1957
A. P. G. Peterson 1955–1956
H. E. Roys 1955–1957
W. E. Stewart 1956–1958
L. Thompson 1955–1958
T. G. Veal 1955–1958
R. A. VonBehren 1955–1957
C. F. West 1955–1957

Standards Committee 1958–1959

R. F. SHEA, *Chairman*
J. G. KREER, JR., *Vice-Chairman*
C. H. PAGE, *Vice-Chairman*
L. G. CUMMING, *Vice-Chairman*

J. Avins
W. F. Bailey
M. W. Baldwin, Jr.
J. T. Bangert
W. R. Bennett
J. G. Brainerd
D. R. Brown
T. J. Carroll
P. S. Carter
A. G. Clavier
G. A. Deschamps
D. S. Dewire
S. Doba, Jr.
P. Elias
G. A. Espersen
D. Frezzolini
E. A. Gerber
A. B. Glenn
V. M. Graham
R. A. Hackbusch
H. C. Hardy
R. T. Haviland
A. G. Jensen
A. E. Kerwien
G. S. Ley
Wayne Mason
D. E. Maxwell
H. R. Mimno
E. Mittelmann
L. H. Montgomery
G. A. Morton
R. C. Moyer
J. H. Mulligan
W. Palmer
R. L. Pritchard
P. A. Redhead
R. Serrell
W. A. Shipman
H. R. Terhune
E. Weber
R. B. Wilcox
W. T. Wintringham

Measurements Coordinator

J. G. KREER, JR

* Approved by the IRE Standards Committee, February 13, 1958. Reprints of this standard, 58 IRE 19. S1, may be purchased while available from the Institute of Radio Engineers, 1 East 79th Street, New York, N. Y., at $0.60 per copy. A 20 per cent discount will be allowed for 100 or more copies mailed to one address.

I. Introduction

MECHANICALLY-RECORDED frequency records are made for the purpose of calibrating recording systems and recording heads. Such records are available commercially for testing phonograph pickups and reproducing systems. Usually, a frequency record contains a number of sinusoidal signals of various significant frequencies recorded in separate short bands on the record.

Three basic methods are described in this standard for calibrating laterally-modulated frequency records. The same general techniques also are applicable to vertically-modulated frequency records. The oldest of these is the "Microscope Method," in which the recorded amplitude is measured directly by use of a microscope. The second method is the "Light-Pattern Method," in which the recorded amplitude is determined by use of the principle that, under specified conditions, the reflected light from a band of recorded grooves forms a pattern the width of which is related to the recorded velocity. The main body of the Standard covers the Light-Pattern Method due to Buchmann-Meyer, while in the Appendix are given two approved refinements for improving accuracy of observation, particularly at short-recorded wavelengths.

In the third method, the "Variable-Speed Method," a pickup stylus is engaged with the record groove and the record is rotated at different speeds. Thus, the pickup stylus is driven at a constant amplitude for a given recorded groove band, and the pickup output frequency is proportional to groove speed. By providing several bands with different recorded wavelengths on the record, and by operating over a sufficient speed range, an overlapping of the pickup output frequency from one band to another will result, and the response-frequency characteristics of the pickup itself can be factored out of the measurement of recorded amplitude.

No single standard method for calibrating mechanically-recorded frequency records yet devised gives completely accurate results under all conditions, particularly at high recorded frequencies. Accordingly, in recording and reproducing practice, all three basic methods described in this Standard are used in order to cross-check results and average out errors in measurement. The Microscope Method is limited in precision by the optical and mechanical properties of the available microscope and accessory equipment. Under optimum conditions recorded amplitudes as small as 50 microinches can be measured with less than 10 per cent error. This sets a practical upper frequency limit on the Microscope Method of about 10,000 cps for a recorded level of 5 cm per second. The basic Light-Pattern Method is limited in accuracy at both very low and very high frequencies, due to the diffuse nature of the pattern edges. Nevertheless, under proper conditions this method can provide reasonable accuracy at recorded frequencies as high as 15,000 cps, particularly with the refinements in technique described in the Appendix. The Variable-Speed Method is accurate through the lower and middle ranges of frequencies, but suffers increasingly serious errors at high frequencies where the recorded wavelength is less than about 3 times the stylus radius.

2. Microscope Method of Measurement

In the Microscope Method of Calibration the recorded grooves of a frequency record are viewed directly with a microscope having a magnifying power range between 25× and 500×, and arranged to provide vertical illumination of the grooves. Each frequency to be measured need be recorded for only a few cycles with suitable identification breaks between frequencies.

2.1 Measuring Equipment for Microscope Method

2.1.1 Apparatus: Any conventional microscope having a vertical illuminator may be used with the following typical apparatus:

Filar micrometer eyepiece having a magnification of about 12.5×.

Achromatic dry microscope objectives—48 mm, 32 mm, 16 mm, 8 mm, 4 mm, corrected for use without cover glass, and designed for tube lengths which match the microscope barrel lengths with the vertical illuminator in place. Ease of observation is materially increased if the glass surfaces of the objectives are treated with a reflection-reducing coating.

Mechanical stage.

Collimated light source with adjustable iris diaphragm.

Record fixture which will support the frequency record to be measured beneath the microscope objective.

Glass stage micrometer for calibrating the setup.

2.1.2 Arrangement of Apparatus: It is desirable that the measuring equipment be set up on a sturdy bench. The filar micrometer eyepiece is used to replace the regular microscope eyepiece and the vertical illuminator is mounted on the barrel of the microscope. The objective is fastened to the vertical illuminator and a source of collimated light placed opposite the light aperture of the illuminator at a distance of from 2 to 3 inches. The arrangement of this apparatus is shown in Fig. 1. It is essential that the iris diaphragm on the light source be closed down until optimum contrast and resolution of the image are obtained. The light source and the position of the mirror in the vertical illuminator should be adjusted until a small circular spot of light is projected onto the record.

2.2 Measuring Procedure for Microscope Method

2.2.1 Calibration of Microscope: The divisions of the filar micrometer eyepiece may be calibrated for each objective lens by placing the glass stage micrometer beneath each objective lens. In order to minimize measurement errors arising from the limiting accuracy of

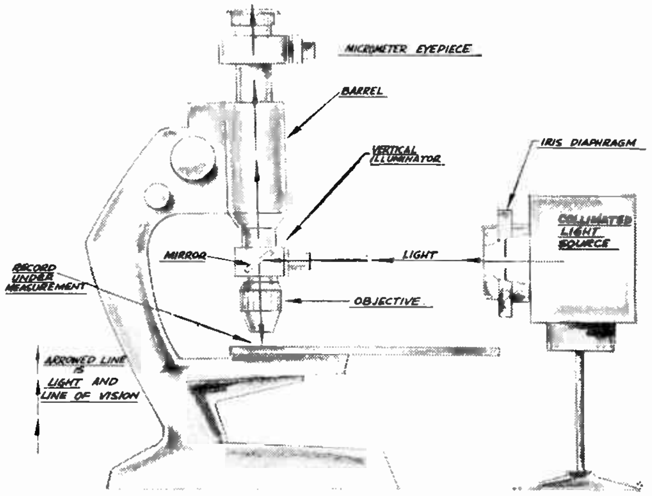

Fig. 1—Arrangement of apparatus for Microscope Method of calibrating mechanically-recorded frequency records.

calibration of the micrometer screw, it is important, particularly at high recorded frequencies, that the filar eyepiece be calibrated at that portion of the screw where the amplitude measurement is to be made. In use, that objective is chosen which will give a measurable image of the recorded groove modulation in the microscope eyepiece.

2.2.2 *Measuring Technique:* The record to be calibrated is supported on the fixture under the microscope as shown in Fig. 1. An objective should be chosen which gives a magnification sufficient to observe several wavelengths of the frequency band being measured. With the vertical illuminator adjusted as above, the groove edges or bottom will be defined by the reflected light, as shown in Fig. 2. The maximum excursions can be measured with the micrometer eyepiece. When high power objectives are used, it becomes apparent that the grooves are not perfectly smooth. Fine lines parallel to the groove bottom caused by stylus imperfections are frequently clearly visible and may also be used for the measurement of amplitude.

2.3 Results with Microscope Method

2.3.1 *Limits of Accuracy:* With this method it is possible, if the groove wall is sufficiently well defined and if the precision of the optical equipment is adequate, to make useful measurements of recorded frequencies as high as 10,000 cps. A 10,000-cps signal recorded with normal stylus velocity of 5 centimeters per second rms will have an amplitude of 88.7 micro-inches peak to peak.

2.3.2 *Method of Presentation:* The individual measured amplitudes may be tabulated or plotted directly as a function of the recorded frequency. It is customary in recording practice to use the term "decibel" to express the relative amplitude of each of the recorded frequencies. This is accomplished by multiplying by 20 the common logarithm of the ratio of each amplitude to the amplitude of a recorded reference frequency. For some work, stylus velocity may be desired, and this can be

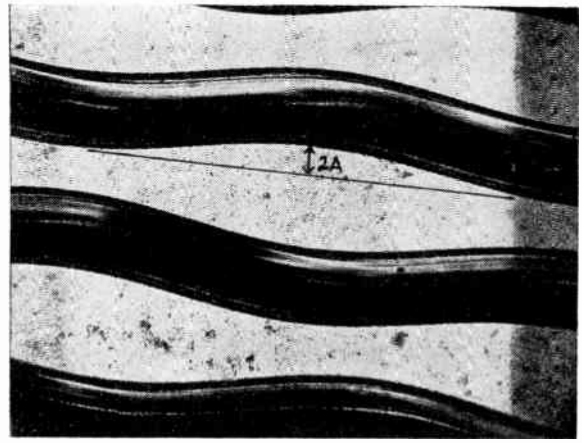

Fig. 2—Photograph showing typical recorded-groove section as observed by Microscope Method. Recorded frequency is 1000 cps, and magnification is 250×. Peak-to-peak recorded amplitude 2A is 0.00056 inch, corresponding to a velocity of 8.9 cm/sec.

readily calculated from the amplitude, by the relations

$$V_{\max} = 2\pi f A$$

or

$$V_{\text{rms}} = \sqrt{2}\pi f A,$$

where A is one half the peak-to-peak amplitude as measured, and f is the recorded frequency. The calculated velocity data may be tabulated or plotted either directly as a function of the recorded frequency, or as relative recorded velocity with respect to the velocity at a reference frequency. Relative recorded velocity is customarily expressed in decibels by multiplying by 20 the common logarithm of the ratio of the calculated velocity to the velocity of a recorded reference frequency.

3. Light-Pattern Method of Measurement

A frequency record intended for calibration by the light-pattern method[1] is prepared by recording each frequency for a sufficiently long time to produce a band of at least ten modulated grooves. A similar number of unmodulated grooves is left between the modulated bands. The higher frequencies are usually recorded at the outside of the record, with frequencies decreasing toward the center.

3.1 Apparatus and Measuring Setup for Light-Pattern Method

A light approximating a collimated source is required. A point source may be used at sufficient distance. A clear-glass incandescent lamp with one straight-coil filament is adequate. A turntable support for the record is also needed, together with a scale graduated in centimeters. A suggested arrangement for making measurements by this method is shown in Fig. 3.

Also shown in Fig. 3 are detail sections illustrating the reflection of the light from the inner and outer groove walls to the viewing positions for taking bandwidth measurements. An optional refinement in technique

[1] G. Buchmann and E. Meyer, "Eine neue optische Messmethode für Grammophon platten," *Elek. Nachr.-Tech.*, vol. 7, p. 147; 1930. Translated in *J. Acoust. Soc. Amer.*, vol. 12, p. 303; 1940.

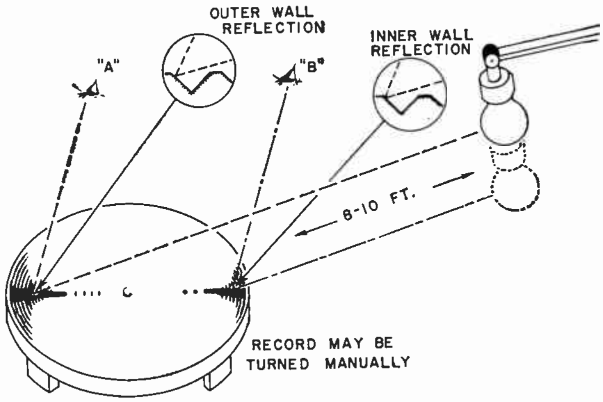

Fig. 3—Suggested arrangement of apparatus for Light-Pattern Method of calibrating disc records.

would substitute a telescope measurement for direct measurement with the scale. Still further refinements are obtained by the use of color filters and photography.

3.2 Measuring Procedure for Light-Pattern Method

The type of light pattern resulting from use of this method is indicated in Fig. 3. The widths of both inner and outer reflected light bands for each frequency are measured directly while observing from the position which gives the most brilliant pattern reflection. For low frequencies it is necessary to rotate the disk so that reflections at the outermost edges appear. Continuous rotation gives the best results at all frequencies.

The recorded velocities may be obtained by application of the following formula:[2]

$$V = 2\pi(N/60)(B_oB_i)/(B_o + B_i)$$

where

V = the maximum recorded velocity of modulation, cm. per sec.

N = revolutions per minute at which the record was recorded.

B_o = width of outer pattern in centimeters (pattern farther away from the light source).

B_i = width of inner pattern in centimeters (pattern nearer the light source).

3.3 Limitation of Light-Pattern Method

Measurements made by the light-pattern method described above are subject to the major limitation that the light pattern does not end abruptly at its sides, but rather exhibits a slow drop-off, providing a degree of uncertainty in the measurement of pattern width, especially at short recorded wavelengths. At long recorded wavelengths the pattern width is small, and accurate results are increasingly difficult to obtain. In addition, cyclic shifting of the pattern results from geometric inaccuracies in the disc, such as groove eccentricity and lack of disc flatness.

Two methods are described in the Appendix for improving the accuracy of measurements at short recorded wavelengths. The first method[3] uses the principle of the sextant to provide improved accuracy of measurement. The second method[4] makes use of interference patterns from which the theoretically correct pattern width can be calculated.

4. Variable-Speed Method of Measurement

This method consists of reproducing the several frequency bands of the frequency test record under measurement with a conventional pickup and a variable-speed turntable. One of the recorded frequency bands on the frequency record is selected as a reference frequency band. The turntable speed is adjusted for each of the other frequency bands in turn, so that the reproduced frequency in each case is the same as that of the reference band.[5] The pickup output voltage for each band is then compared with the reference frequency band pickup output voltage. By taking into account the relative output voltages and normal recorded frequencies, simple calculations can be made which give the relative recorded velocity of each band compared to the velocity level of the reference frequency band. When a wide range of frequencies is to be measured, more than one reference frequency band usually must be used to cover the entire range.

4.1 Measuring Equipment for Variable-Speed Method

A turntable, the speed of which is continuously variable over a range of the order of 10 or 15 to one, is required. The low-speed limit may typically be 5 to 10 rpm; the high-speed limit 80 to 100 rpm. A conventional tone arm and a high-compliance pickup with suitable stylus for the type of record to be calibrated is also required. Measuring equipment consists of a suitable vacuum-tube-voltmeter capable of measuring the pickup output voltage and, where necessary, suitable band-pass filters for attenuating record noise.

4.2 Measuring Procedure for Variable-Speed Method

Selection of the reference frequency bands will depend to some extent on the normal speed of the record to be calibrated and the speed range of the turntable. The first, or lowest, reference frequency band should be selected so that all of the low-frequency bands on the record up to approximately 200 cycles may be reproduced at this lowest reference frequency by either increasing or decreasing the turntable speed. The pickup output from each band when reproduced at the reference frequency should be noted and compared with the output from the reference frequency band when reproduced at normal speed for the record.

The above procedure should be repeated, using one or more higher reference frequencies selected so the group

[2] B. B. Bauer, "Measurement of recording characteristics by means of light patterns," *J. Acoust. Soc. Amer.*, vol. 8, p. 387; 1946.

[3] P. E. Axon and W. K. E. Geddes, "The calibration of disc recordings by light-pattern measurements," *Proc. IEE*, vol. 100, pt. III, pp. 217–227; July, 1953.

[4] B. B. Bauer, "Calibration of test records by interference patterns," *J. Acoust. Soc. Amer.*, vol. 27, pp. 586–594; May, 1955.

[5] R. C. Moyer, D. R. Andrews, and H. E. Roys, "Methods of calibrating frequency records," Proc. IRE, vol. 38, pp. 1306–1313; November, 1950.

of bands measured at each reference frequency will overlap by one or more bands those measured at the next lower reference frequency.

4.3 Results with Variable-Speed Method

The relative recorded velocity of each test frequency band in a group, compared to the recorded velocity of the reference frequency band, may be expressed as follows:

$$\text{Relative recorded velocity in db} = 20 \log \left[\frac{E_r f_x}{E_x f_r} \right]$$

where

E_r = voltage output from reference band.
E_x = voltage output from test band when reproduced at reference band frequency.
f_r = recorded frequency of reference band.
f_x = recorded frequency of test band.

Similar calculations may be made for each group of bands where a different reference band frequency is selected. Since overlapping groups of frequency bands have been selected, the various portions of the calibration curve thus arrived at may be arbitrarily connected at common frequency points, thereby producing a continuous calibration curve for the bands measured. Absolute velocity calibration in centimeters per second may then be obtained by determining the velocity of one band by either of the two preceding methods.

4.3.1 Limitations of Variable-Speed Method: For accurate results with the variable-speed method the stylus of the calibrating pickup must track the record grooves perfectly, and the record material must not yield either under the downward pressure of the stylus tip or as the groove walls apply vibratory movement to the stylus. However, at high velocities the resulting stylus accelerations cause forces of a sufficient degree to cause appreciable yielding of the material. (A correction formula[6] has been developed to take such yielding into account.) The lower the mass of the pickup elements set in vibration by the stylus, the lower such forces will be. The higher the compliance of the pickup mechanism, the more perfect the tracking will be. Accordingly, the closer the approach to a zero-mass, zero-stiffness pickup, the more accurate the above results will be. Additionally, as velocities are reached which produce curvatures of the groove which are comparable to the stylus tip radius, the poorer the tracking will be. Thus, this method has limitations which generally become more marked, the higher the recorded frequency.

Appendix

The limitations of the basic Light-Pattern Method indicated in Part 3.3 may be reduced by the refinements in techniques presented in this Appendix.

[6] O. Kornei, "On the playback loss in the reproduction of phonograph records," *J. Soc. Mot. Pict. & Telev. Engs.*, vol. 37, pp. 569–590; December, 1941.

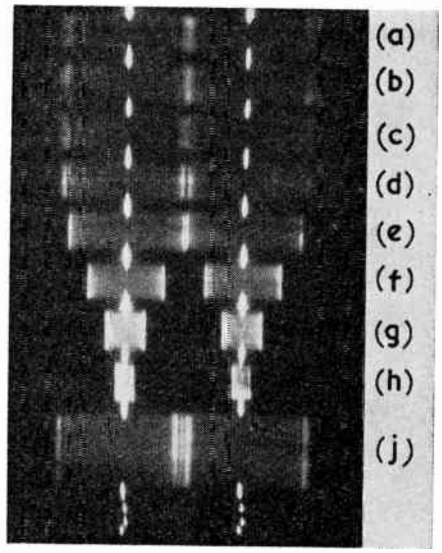

Fig. 4—Photograph of twin images formed by the sextant technique for making light-pattern measurements of disc records. Images are adjusted for coincidence of the 500-cps tone patterns.

Tone-Pattern Frequencies

(a) 4 kc	(d) 1 kc	(g) 100 cps
(b) 3 kc	(e) 500 cps	(h) 50 cps
(c) 2 kc	(f) 200 cps	(j) 1 kc

(Reprinted with permission from reference 3.)

A. Sextant Technique for Making Light-Pattern Measurements

This method of measuring the light pattern width uses the principle of the sextant. Two identical images of the light pattern are produced, and these images are moveable with respect to each other in a horizontal direction. The width of a light pattern corresponding to a given recorded frequency is measured by the relative displacement of the two images necessary to cause the right-hand edge of one to coincide with the left-hand edge of the other. This type of alignment is relatively unaffected by oscillation of the pattern, such as would result from groove eccentricity and lack of disc flatness, since both images move together in an identical manner. The type of pattern resulting from application of this technique is shown in Fig. 4, where the 500-cps patterns have been adjusted for edge-to-edge coincidence. Pattern width is measured by the center-to-center distance between the images for the coincident condition.

A.1 Apparatus and Measuring Procedure

A diagram of the measuring apparatus is shown in Fig. 5. Light from the lamp L_1 is reflected by the inclined plane mirror M_1 to the collimating mirror C. The collimated beam of light is limited in vertical extent by the slit S and passes above the prisms P_1 and P_2, and between the mirrors M_1 and M_2, to the disc. It can be shown that when the light source is at infinity (a condition approximated by the collimated light source), the focal plane of the light reflected from either the near-side or far-side grooves coincides with the vertical plane through the center of the disc. In the sextant method the reflected light pattern is viewed at its focal plane

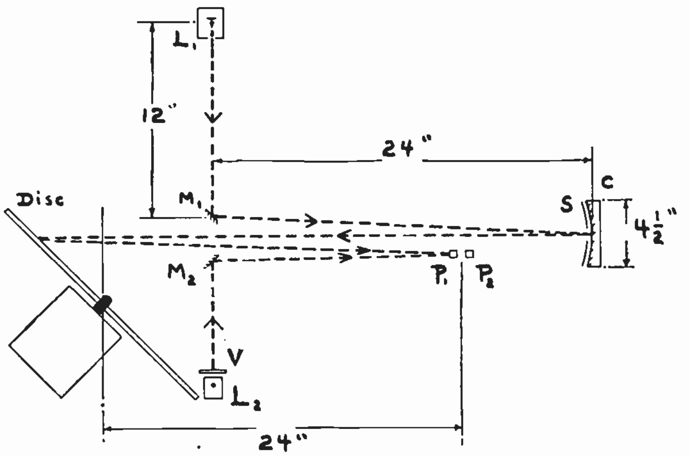

Fig. 5—Functional diagram showing arrangement of optical elements with the sextant technique for making light-pattern measurements. (Reprinted with permission from reference 3.)

rather than at the surface of the disc, so that by moving the disc vertically all patterns, whether near side or far side, are brought to the same point for observation.

The turntable is rotated at about 20 rpm, which is just sufficient to merge the luminous elements of a 50-cps band of tone into a continuous pattern.

The two separable images are produced respectively by the prisms P_1 and P_2, which reflect the light from the disc through a right angle, in a direction normal to the plane of the diagram. When the prisms are parallel, as in the plan view shown in Fig. 6, coincident images of the light pattern are observed in the telescope, while counter-rotation of the prisms about a vertical axis causes the two images to separate horizontally. The linear movements of the images can be made equal and opposite if the prism P_1, which is nearer to the pattern, is arranged to rotate slightly more rapidly than P_2.

When a correct edge-to-edge adjustment has been made, the separation of the two images is equal to the width of the light pattern and is measured by observation of a vernier scale system, V (Fig. 5). To read the scale the lamp L_2 is switched on and an image of the scale is formed by the mirror M_2 in the focal plane below the light pattern but still within the field of view of the telescope. Twin images of both the scale and the light patterns will then be seen and their separation may be read off directly. The vernier is illuminated by light of one color and the main scale by another, appropriate color filters being inserted into the respective image paths via P_1 and P_2. This allows the vernier to be seen moving across the scale without redundant and confusing duplicate images.

The vertical spread of the collimated beam due to the length of the filament of L_1 allows some latitude in the inclination of the disk necessary to secure adequate reflection into the viewing system. The width of the collimated beam is the limiting width of patterns which may be measured.

A.2 Results with Sextant Method

Results with the sextant technique show good correspondence of velocity ratios determined from near-side pattern measurements with those from far-side measurements. The edge-to-edge adjustment is not affected by oscillation of the pattern which may result from lack of perfect flatness in the disc surface or by eccentricity and wobble of the disc during rotation. The sextant principle provides an improved means of gauging the edges of the reflected light pattern and increases the accuracy and repeatability of the measurements at all frequencies.

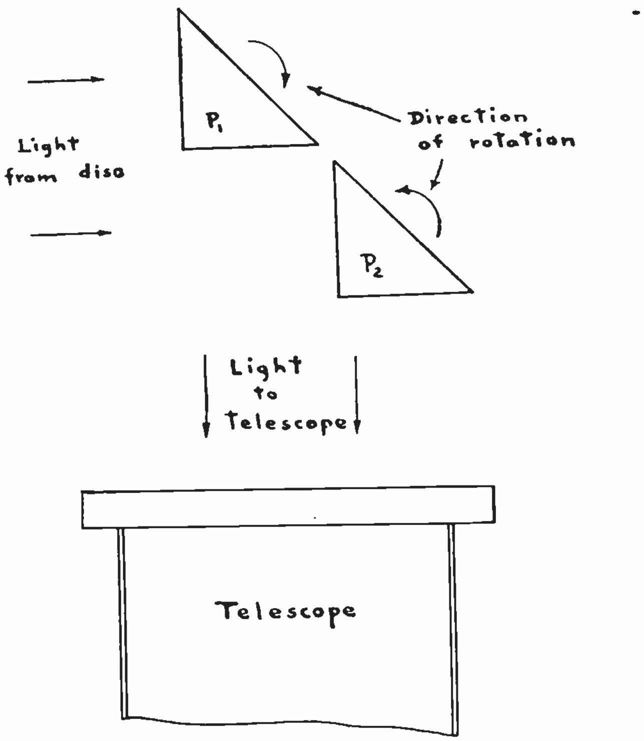

Fig. 6—Plan view showing arrangement of prism and telescope in the sextant technique for making light-pattern measurements. (Reprinted with permission from reference 3.)

B. *B*-Line Light Pattern Method of Measurement

When a reflected light pattern from a test record is examined through appropriate color filters, two distinct interference patterns of lines appear. These lines have been designated by Bauer[4] as *A* lines and *B* lines. The *A* lines are identified with the frequency and the *B* lines with the amplitude of the signal recorded on the test record. The *B*-line method is most suited for measuring recorded frequencies above 1000 cps.

B.1 Measuring Equipment and Setup

In addition to the apparatus required for the basic Light-Pattern Method, a color filter is required. In most instances a type "A" red photographic filter will be satisfactory. The arrangement of apparatus is shown in Fig. 7. An intense source of light is recommended, and this can conveniently take the form of a slide projector. Measurements may be performed visually by means of a ruler or a scale, as in Part 3.2. For maximum accuracy,

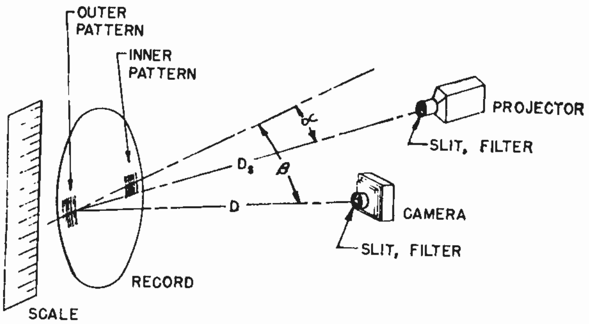

Fig. 7—Arrangement of apparatus for making light-pattern measurements by the B-line technique.

however, it is best to photograph the patterns. The camera lens should be provided with a slit having a width approximately $f/100$, where f is the focal length of the lens, to produce a sharp, well-defined pattern of the interference lines. The slit may be cut from opaque paper and inserted into the camera filter holder. If the light source is a projector, it should preferably also be provided with a slit having a width of approximately $D_s/100$, where D_s is the distance from the light source to the record. A scale should be placed near the pattern so that it will appear in the photograph and allow for ease of measurements.

B.2 Measuring Procedure for B-Line Method

It is recommended that the projector be placed at 6 feet or more from the record with the projector slit so oriented that it will be in the plane passing through the camera, the projector, and the pattern. The camera should be placed at about 2 feet or more from the record; the distance being determined by ability to focus clearly upon the grooves and the scale divisions. The angle α of Fig. 7 is preferably about 20° and the angle β will then be approximately $90° - \alpha$, or 70°. With the filter and slit removed from the camera, angles α and β should be adjusted until a clear and bright pattern is reflected into the camera. After focusing, the slit and filter are installed in the camera and the camera slit is oriented so that it will be in the plane passing through the camera, the projector, and the pattern. The camera lens iris is preferably adjusted to f:4.5 or slower. It is recommended that a series of exposures variously timed be made to insure a properly exposed image. After one side of the pattern has been thus photographed, the record is moved in its own plane until the second pattern is in view and the above procedure is repeated.

B.3 Results with B-Line Method

Two types of interference patterns can be observed in the typical photograph of Fig. 8.

a) A set of evenly-spaced dark lines, independent of the amplitude of modulation, are dependent only upon frequency of modulation, the color of light, and the rotational speed at which the disc was recorded. These

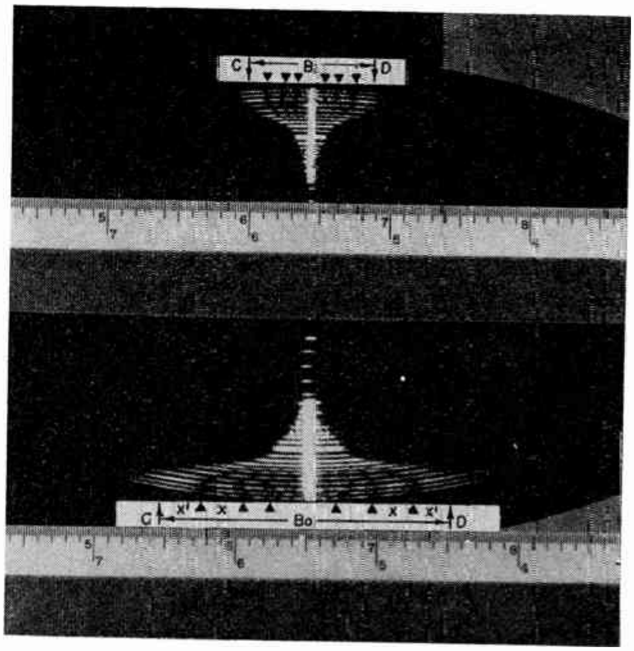

Fig. 8—Photograph of typical light pattern resulting with the B-line technique. B-lines are denoted by the black arrowheads, and the theoretical lengths of the light pattern for both the inner and outer reflections are shown by B_i and B_o, respectively.

are called the A lines and they are of no interest in record calibration.

b) The set of lines most clearly visible toward the sides of the pattern which are broader than A lines, are unevenly spaced and are dependent upon the amplitude of modulation. These are called B lines and they are useful in calibrating records. B lines are "modulated" by the A lines.

In accordance with the B-line pattern theory, the correct width of the pattern is obtained by adding to the outer B lines a measure equal to the distance between the first and second B lines. In Fig. 8 the distance between the first and second B lines, B_1 and B_2, is labeled x. This distance is added on both sides as x' establishing the theoretical ends of the pattern at points C and D. The distance between these points, B_o, is the B-line width of the pattern. The solid triangles denote the positions of the B lines. B_o is the B-line pattern width for the outer pattern; B_i is the B-line pattern width for the inner pattern. The modulation velocity is found by the following equation:

$$V = 2\pi(N/60)(B_oB_i)/(B_o + B_i)$$

where

V = maximum velocity of modulation, cm per sec.
N = record speed, rpm.
B_o = B-line pattern width of the outer pattern, cm.
B_i = B-line pattern width of the inner pattern, cm.

This method is useful only for frequencies above 1000 cycles. Above this frequency it provides more sharply defined measuring points than the normally-viewed pattern edges with a resultant improvement in accuracy.

Correspondence

D-Day in Engineering Education*

At the risk of being called an old fogey (I am a 34-year-old graduate student), I should like to take issue with part of the editorial in "Poles and Zeros."[1]

For the past several years I have observed young engineering graduates reporting for work in a government lab. These young men, of widely varying degrees of ability, all seem to have one trait in common. They are reluctant to work with their hands. The drawings they turn out are smudges. They approach a drill press with trepidation, and will go to any lengths to avoid a lathe. Few can wire a chassis with any dexterity.

But far more serious than lack of manual skills (which, after all, can be learned on the job) is the common attitude that manual work is "for technicians," and therefore is somehow beneath their dignity. As one of them proudly put it: "An engineer should only do theoretical work."

If, as I suspect, this attitude springs from the elimination of drafting and shop courses from the curricula of some schools, then I seriously question the wisdom of such removal. I submit that an engineer who avoids the practical aspects of his profession is less than half an engineer—he cannot command the respect of the technicians and artisans he will eventually be supervising, nor can he really appreciate the problems of construction and production of hardware; which, after all, is the ultimate purpose of engineering.

I am in no way trying to question the value of theory. By all means, let us have as much of basic physics and mathematics as we can cram into the curricula. But let us not forget that the mind is often at its best when the hands are occupied!

Charles E. Hendrix
6466 West 84th Place
Los Angeles 45, Calif.

Although I have many gray hairs, I am still struggling toward getting an education. I have some strong feelings about our education system, and the editorial in "Poles and Zeros" hits on my gripe. However, after reading it several times, I'm not sure how its writer stands.

My complaint about the education system is that too many redundant subjects are required to obtain an EE degree. For instance, I would like to take technical writing. The prerequisite for this course is 7 semesters (Georgia Tech) of "English." My investigations show that these "English" courses are not composition and rhetoric, but literature. I fail to see the bearing that literature has on technical writing. Likewise most colleges require languages and history. Granted, these subjects would be nice to take if we had the time or desire to take them.

In my 20 years of work in industry I find many who agree with my stand. Many professional educators disagree. Aren't we being influenced too much by the "polished" white shirt educator and engineers and overlooking what we really need to know to beat Russia?

George W. Hann
Motorola Inc.
P. O. Box 10134
Fort Worth, Tex.

* Received by the IRE, September 18, 1958; and September 22, 1958.

[1] Proc. IRE, vol. 46, p. 1571; September, 1958.

Current Build-Up in Semiconductor Devices*

Introduction

The purpose of this letter is to lay a mathematical foundation for the switching action of devices in which carrier multiplication at a collector junction plays an important role in the switching process. The physical source of this multiplication may be an avalanche effect, hook-collector action, or a similar multiplicative mechanism. The mathematical formulation of the general problem will, of course, depend on device geometry as well as on operating conditions, so that in addition to predicting the functional dependence of switching time on multiplication, we may expect the results to provide important information concerning the efficacy of various possible design procedures whose aim is improved switching speed.

The analytical technique to be used is one that finds frequent use in the solution of partial differential equations and can be used to advantage in treating minority carriers in a semiconductor. We assume that during the switching action, minority carrier densities and the currents associated with them are increasing at an exponential rate in time. We then attempt to find a self-consistent solution to the equations governing the behavior of currents and carrier densities in the device.

Although the assumption of exponential build-up does not require mathematical justification, a physical interpretation may be helpful. Consider the three-layer diode shown in Fig. 1, and suppose one injects a delta function containing P holes across junction 1. These holes move across the n base layer and enter the depletion region at junction 2. We suppose for simplicity that the form and amplitude of the delta function are maintained throughout its motion across the base. Suppose further that in the depletion region each hole experiences an instantaneous multiplication, so that each hole from the base results in M holes at the collector layer. Now each ionizing collision produces a hole-electron pair, and the direction of the depletion-layer field is such that the electrons so produced move into the base. Thus, a transfer of qMP units of charge across the depletion layer occurs.

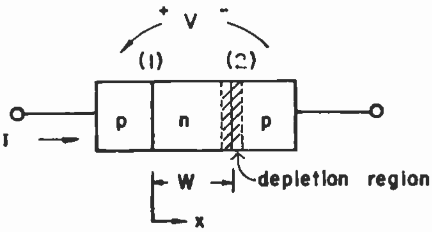

Fig. 1—Three-layer diode, or transistor with base bias lead not shown.

This charge is carried to the base by qP units of charge, which were brought in to neutralize the originally injected holes, and $q(M-1)P$ units due to secondary electrons. The effect of this increase of electrons into the base is to draw an additional charge of holes into the base at junction 1 to maintain space-charge neutrality. This added hole density is in the form of a delta function, its magnitude being M times the original delta function.

On a time scale, the amplified replica of the originally injected holes appears τ_0 seconds after the first one, where τ_0 is the transit time for holes across the base. The cycle of operations just described now repeats itself with this amplified input to form a geometrically increasing series.[1] The result of three such cycles is shown graphically in Fig. 2. The envelope of the injected hole density at junction 1 is seen to be exponential; the time constant is evidently a function of M and the device construction parameters. We anticipate this time dependence mathematically by assuming at the outset that $p(x, t) = p(x)e^{\lambda t}$, and expect to find a functional relationship between λ and the device parameters.

Before proceeding with the program outlined, however, we note that the assumptions above would accurately depict the exponential build-up if the injected holes had an infinite lifetime and moved across the base by drift only in a constant field. For this slightly artificial but very instructive case, we may quickly arrive at the time constant as follows.

We note that

$$p(t + n\tau_0) = M^n p(t). \tag{1}$$

Therefore,

$$\ln [p(t + n\tau_0)/p(t)] = n \log M. \tag{2}$$

Now the value of $n\tau_0$ for which $p(t+n\tau_0)$ is just equal to e times $p(t)$ is by definition the time constant.

* Received by the IRE, May 26, 1958. This work was supported by Signal Corps contract. It was presented at the Congrès International de l'État Solid et ses Applications a l'Electronique et aux Telecommunications, Brussels, Belgium, June, 1958, and should appear in the report of the conference.

[1] Reasoning of this type has been previously employed by H. Statz and R. A. Pucel, "The spacistor, a new class of high-frequency semiconductor devices," Proc. IRE, vol. 45, pp. 317–324; March, 1957. See p. 322.

Using (2), the value of n required is

$$n = [\log M]^{-1}$$

and therefore the time constant for the build-up is

$$\tau = n\tau_0 = \tau_0/[\log M]. \quad (3)$$

We return to this formula later for comparison purposes.

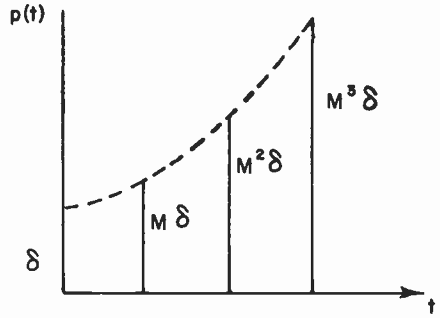

Fig. 2—Illustrating the build-up mechanism.

Solution of the Differential Equations for Minority Carrier Continuity

Proceeding now as outlined above, we write first the partial differential equation for hole continuity in the n base layer for the general case of hole motion by drift and diffusion:

$$\partial p/\partial t = -(p - p_n)/\tau_p - p\mu_p\partial E/\partial x - \mu_p E\partial p/\partial x + D_p\partial^2 p/\partial x^2. \quad (4)$$

We will first assume that holes move only by diffusion, so that (4) simplifies to

$$\partial p/\partial t = -(p - p_n)/\tau_p + D_p\partial^2 p/\partial x^2. \quad (5)$$

We now suppose that p consists of a dc part and an ac part

$$p = p_0(x) + e^{\lambda t}p_1(x)$$

so that the ac part of (5) becomes

$$\lambda p_1(x)e^{\lambda t} = -[p_1(x)/\tau_p]e^{\lambda t} + D_p e^{\lambda t}d^2p_1(x)/dx^2. \quad (6)$$

Using the definitions

$$1/\tau_p = \nu_p$$
$$\xi = [(\lambda + \nu_p)/D_p]^{1/2} \quad (7)$$

the solution to (6) can be written as

$$p_1(x) = A_1e^{\xi x} + A_2e^{-\xi x}. \quad (8)$$

We now assume that the switching is proceeding with a sufficiently large voltage across the device (this voltage appears as a back bias across junction 2) so that the hole density at $x = W$ can be set equal to zero. Mathematically,

$$p_1 = 0 \text{ at } x = W. \quad (9)$$

Using this in (8), we find the ratio of A_2 to A_1 and conclude

$$p_1(x) = 2A_1 \exp(\xi W)\sinh \xi(x - W). \quad (10)$$

Now the ratio of current carried by holes at $x = W$ and $x = 0$ is

$$(\partial p/\partial x)_W/(\partial p/\partial x)_0 = 1/\cosh[W(\lambda + \nu_p)/D_p]^{1/2} \equiv \beta(\lambda) \quad (11)$$

where β is the transport factor for hole flow for the exponentially rising solution.

If γ is the injection efficiency at the emitter and $I \exp(\lambda t)$ is the total ac current through the device, then we may write

$$I \exp(\lambda t) = M\beta(\lambda)\gamma I \exp(\lambda t). \quad (12)$$

The right side of this equation is the total current crossing the collector junction. This current is M times the hole current arriving at the depletion layer, which in turn is $\beta(\lambda)\gamma$ times the total current at the emitter junction. Evidently $M\beta(\lambda)\gamma$ is the effective value of α for this case:

$$\alpha(\lambda) = M\beta(\lambda)\gamma. \quad (13)$$

Now, combining (11) and (12), we find

$$\gamma M = \cosh \xi W = \cosh W[(\lambda + \nu_p)/D_p]^{1/2}. \quad (14)$$

This equation contains only one unknown, λ. It therefore contains the functional relationship sought between λ and the device parameters. To obtain this relationship in a useful form, we first assume that $\nu_p = 0$ (infinite lifetime), and that $\gamma M > 3$. Then the error in approximating the cosh by a single exponential is less than 10 per cent and (14) becomes

$$\exp[W^2(\lambda/D_p)]^{1/2} = 2\gamma M.$$

Taking logarithms, we have

$$W[\lambda/D_p]^{1/2} = \log 2\gamma M. \quad (15)$$

Eq. (15) may be rewritten as

$$\lambda = D_p[\log 2\gamma M]^2/W^2 \quad (16)$$

and the time constant associated with the build-up is thus

$$\tau = [\lambda]^{-1} = W^2/D_p[\log 2\gamma M]^2 = \tau_d/[\log 2\gamma M]^2 \quad (17)$$

where τ_d is the diffusion time across the base layer.

Several interesting conclusions can be drawn with the aid of (17). Before doing this, however, we first make two observations.

First, by a process entirely similar to that just carried out, one may solve (4) under the assumptions that $D_p = 0$ and $\partial E/\partial x = 0$; *i.e.*, carriers move only by drift in a constant field. Such a situation does not give a boundary condition of $p = 0$ at $x = W$ and the appropriate solution is

$$p_1(x) = A \exp(\lambda + \nu)(W - x)/\mu_p E. \quad (18)$$

Eq. (13) still applies and gives

$$\gamma M = \exp(\lambda + \nu_p)W/\mu_p E. \quad (19)$$

Taking logarithms again and letting $\nu_p = 0$, find

$$\tau = \tau_0/\log \gamma M$$

which reproduces (3) obtained earlier if we let $\gamma = 1$, as we did implicitly in the earlier derivation. τ_0 is once again the transit time, this time defined by $\tau_0 = W/\mu_p E$.

Our second observation is that if we let $M = 1$ and $\lambda = j\omega$, (13) is identical to the expression normally obtained for alpha, which is a result that one might anticipate. It is interesting to note this agreement, since no statement of boundary conditions on hole density at junction 1, the emitter, has been made. This of course points up the fact that the evaluation of β is a transport problem, not a junction effect.

We now return to (17) to see what suggestions it contains for the design of high-speed devices. As we should expect, τ depends directly on τ_d, and hence directly on W^2. Therefore, other things being equal, decreasing the base width makes for a faster switching device. However, (17) also indicates that τ is a rather sensitive function of M, and may be decreased appreciably if M is great enough. This basic dependence of build-up speed on M is responsible in part for the generation of "millimicrosecond" pulses in transistors where the alpha cut-off frequency is much lower than the frequencies corresponding to $[\lambda]^{-1}$. [It also frequently happens that "punch-through" plays an important role in the pulse generators mentioned. This may be simply accounted for in (17) by noting that the base width modulation which finally produces the punch-through merely decreases the transit time τ_d.]

An instructive way to visualize the effects of multiplication in increasing build-up speed is to calculate the effective base width W^*, during the switching, where W^* is defined by

$$W^* = W/\ln 2M\gamma = W/[0.7 + \ln \gamma + \ln M]. \quad (20)$$

Eq. (17) then becomes

$$\tau = (W^*)^2/D_p \quad (21)$$

so that W^* is seen to be the base width which the device seems to have on a strictly diffusion basis. For most cases, γ will be nearly unity and $\ln\gamma$ will be negligible. Thus, for the following values of M, the reduction of W and increase of λ are given by the factors indicated in Table I. It should be noted that λ increases most rapidly for the smaller M's.

TABLE I

M	10	100	1000	10,000
W^*/W	0.33	0.19	0.132	0.101
increase of λ	9	28	57	98

These values once again show the advantage of obtaining speed by using multiplication. Alternately, Table I indicates that a 100-mc transistor with no collector multiplication is roughly equivalent to a 3-mc transistor with a multiplication of 100 as far as build-up speed is concerned.

As a concluding observation, we note that there is a rather appreciable difference in the dependence of (3) and (17) on M. Eq. (3), which is the time constant for our hypothetical device where minority carriers move by drift only in a constant field, shows a $[\log M]^{-1}$ dependence, while (17), the time constant for the device in which minority carriers move only by diffusion, shows a $[\log 2M\gamma]^{-2}$ dependence. To explain this difference, we recall that when the minority carriers do move by diffusion, even though the *average* particle takes a time τ_d to diffuse across the base, some of the particles arrive at the collector much faster than this. If the multiplication is high, these "early" particles may in fact entirely determine the resulting time constant. For motion in a field, however, there is no "spreading" of this sort; the form of the injected charge distribution is maintained throughout the transit and the average base transit time is the significant one. The conclusion to be drawn from these remarks is that if M is high, the time constant in the build-up will be determined predominantly by diffusion effects, even in graded-base devices.

The problem of voltage build-up is more complicated than that of current build-up considered here, because the variation of M with voltage and time leads to nonlinear integral equations rather than linear differential equations. The authors plan to submit results of a study of this problem in the near future.

An important generalization of (14) may be made by assuming that an admittance $A(\lambda)$ rather than constant voltage is applied between emitter and collector. We let $A_c(\lambda)$ represent the internal admittance of the collector junction where

$$A_c(\lambda) = \lambda C_c + r_c^{-1} \tag{22}$$

where C_c is the collector depletion layer capacity and

$$r_c^{-1} = (M - 1)nI_c/V_c \tag{23}$$

where I_c is the dc collector current and M is approximated by the conventional expression

$$M = [1 - (V_c/V_B)^n]^{-1}. \tag{24}$$

Assuming that the admittance of the emitter junction is much larger than that of the collector, *i.e.*, $qV_c/kT \gg (M-1)n$, we obtain in place of (14)

$$A(\lambda)[A(\lambda) + A_c(\lambda)]^{-1}\gamma(\lambda)\beta(\lambda)M = 1 \tag{25}$$

where the dependence of $\gamma(\lambda)$ allows for the variation of emitter efficiency with λ due to effective thinning [as in (20)] of the base layer for rapidly rising currents. If only capacitative terms are important, (25) shows that the larger the external capacitance, the faster the build-up, a result also obtained from the large signal theory.

W. Shockley
J. Gibbons
Shockley Semiconductor Lab.
Beckman Instruments, Inc.
Mountain View, Calif.

On the Need for Revision in Transistor Terminology and Notation*

Recently the writer has been conducting a course in transistor electronics. Whatever effect it may have had on the student, the experience has convinced him that the terminology and notation need revision in order to get more nearly in step with things as they are, and that such a revision could make life a little easier, for the student at least.

Consider first the matter of configuration. It seems certain that most transistors are and will be used in the common-emitter configuration. Accordingly, that configuration should be taken as the standard, just as the common cathode is for vacuum tubes. Then the current gain figure, for example, should be the beta figure, and the alpha figure would not call for separate mention, any more than does the $\mu+1$ figure for the gain of a common-grid triode. The impression, incidentally, which one sometimes encounters, that the common-base configuration of a transistor is somehow more "fundamental" than the others, is, of course, without foundation. It is sometimes said, for instance, that the common-emitter transistor shows a larger current gain (and lower frequency possibilities) than does the common-base because it has positive feedback, as expressed by $\beta=\alpha/(1-\alpha)$. But it is just as correct, and just as "fundamental," to say that the common base transistor has lower current gain and better frequency response because of *negative* feedback, as expressed by $\alpha=\beta/(1+\beta)$. This latter way of looking at the matter, incidentally, might make the analogy between transistor and vacuum triode clearer. The high-frequency cutoff, of course, should refer to the common-emitter connection.

Thus the common-emitter current gain is of great importance. It has been designated β, or h_{21}, or h_{21e}, or h_{fe}, or in various other ways. The writer recommends that one symbol, not needing any subscripts, be used for it. Then subscripts could be reserved to indicate various stages, conditions, etc. Since the symbol β has already had some use, it would seem to be a logical choice.

Other quantities of interest are the input and output impedances. The common way of designating these, the output impedance for open input and the input impedance for shorted output, is desirable, since this corresponds most closely to the way in which the transistor will be actually used. Whether impedance or admittance values are quoted is rather unimportant. Thus the parameters h_{11} and h_{22} are suitable; perhaps, in order to use as few subscripts as possible, the symbols h_i and h_o, which are used sometimes, might be desirable. Another possibility would be to use the symbols y_i (input admittance with output shorted) and z_o (output impedance with input open); these definitions would agree with those which the symbols would have as elements of Y and Z matrices.

The symbol μ for the collector-to-base voltage feedback factor is diametrically opposite to the usage for the vacuum triode. Actually, this collector-to-base feedback factor should be considered as a "Durchgriff" or reciprocal of an amplification factor.[1] In many circuits, however, this quantity is of small importance anyway.

In the writer's opinion, the utility of the h parameters, considered as matrix elements, and h matrix, in transistor circuitry, is greatly overrated. Often the statement is made that, because of the reaction of output on input, simple methods of analysis are unsuitable, and a matrix treatment should be used. Then, once that is granted, that is the last seen of matrix analysis, and the design proceeds by individual stages, the effects of reaction of output on input being taken into account through successive approximations, if necessary. Actually, if matrix methods are to be used in dealing with cascaded structures, the useful matrix is not the "hybrid" but rather the transmission matrix[2] (or transfer, or "chain," or "Kettenmatrix"). It is true that the hybrid matrix can have some utility in treating neutralization. From this viewpoint, if a matrix is to be quoted for the transistor, the transmission matrix would seem to be the useful one. The argument that the h matrix is used because its elements are readily measured is surely not valid; it is worthwhile to measure that set of values, but then, for quotation, to convert them to whatever set will be most immediately useful to the user.

Another quantity which seems rather illogical is the quantity I_{bco}, the collector to base leakage current with open emitter. This quantity, or something related to it, is of great interest, especially as a function of temperature; but it is suggested that the collector leakage current with open base, possibly designated I_{co}, is a more immediately useful representation.

In the representation of characteristic curves, one still occasionally sees the voltage axis vertical and the current horizontal. It would seem worthwhile always to have the voltage axis horizontal and the current vertical, and, moreover, always to use the first quadrant; negative values, when required by the type of transistor concerned, would be indicated merely by signs. Incidentally, it would sometimes be very helpful if, in a plot of transistor output characteristics, *e.g.*, an enlarged inset of the region within, say, 100 μamp and 0.5 volt or so, of the origin, could be included, since this region of operation may be desirable for low noise.[3]

It is apparent that many of these anomalies in the terminology and notation are legacies from the point-contact transistor. In retrospect, one might say that the terminology and notation tried to develop more quickly than the device, and, accordingly, now find themselves not entirely suitable. Similar arguments have been presented concerning the graphical symbols,[4] but it is not desirable to discuss that matter here. This should be an illustration, though, of the fact that it may be undesirable to try to standardize these things too quickly in a new field, lest the field later find itself saddled with a fossil notation and terminology.

* Received by the IRE, May 12, 1958.

[1] E. Benz, "Einführung in die Funktechnik," Springer Verlag, Vienna, Austria, 4th ed., p. 209; 1950.

[2] H. L. Armstrong, "A treatment of cascaded active four-terminal networks, with application to transistor circuits," IRE Trans. on Circuit Theory, vol. CT-3, pp. 138–140; June, 1956.

[3] W. K. Volkers and N. E. Pedersen, "The hushed transistor amplifier," *Tele-Tech and Electronic Indus.*, vol. 14, p. 82; December, 1955; vol. 15, p. 70; January, 1956; and p. 72; February, 1956.

[4] H. E. Tompkins, "Foreword to transistor papers," IRE Trans. on Circuit Theory, vol. CT-4, p. 173; September, 1957.

In conclusion, this calls to mind one more point, which is connected with semiconductors, if not directly with transistors. When, oh when, will someone, in a definition, etc., dealing with Hall and related magnetic effects, admit that the field involved is the B field, not the H?

H. L. ARMSTRONG
Pacific Semiconductors, Inc.
Culver City, Calif.

Antipodal Reception of Sputnik III*

The reception of radio signals from an orbiting earth satellite near the antipodes has been reported by Wells.[1] His observations have indicated that "in all respects, the image signals appeared to originate in a point source similar to the actual satellite."

The 20-mc radio transmissions from Sputnik III have been monitored by members of the Stanford University Radio Propagation Laboratory in an attempt to confirm this phenomenon. The signals were received on a standard communications receiver connected either to a fixed "turnstile" antenna $\frac{3}{8}\lambda$ above the ground, or to a three-element horizontal Yagi $\frac{5}{8}\lambda$ above the ground. The Yagi antenna can be rotated to determine the approximate direction of arrival of the signals. During most of the period means were available to determine the absolute frequency of the signals, and (when they were sufficiently strong to record them on magnetic tape.

Between May 16 and June 13, 1958, the high passages of Sputnik III near Stanford occurred in the afternoon or evening. On 13 occasions during this period signals from the satellite were observed at a time midway between two direct afternoon passes. In this same interval five attempts to receive these signals were unsuccessful, and two have been classified as questionable. The height of the satellite was approximately 1100 km when at the antipodes, and 800 km when at the receiving location. A plot of the afternoon data, similar to that given by Wells, is shown in Fig. 1.

The low passages of the satellite took place during the morning hours in this period. Antipodal signals were detected only twice, while 13 attempts were unsuccessful and two questionable. The antipodal height was near the apogee value of approximately 1800 km, and the height when executing a direct pass was about 220 km during these observations.

When the antipodal signals were observed in the afternoon on the Yagi antenna, the directions of arrival on all occasions were estimated to lie between southeast and southwest. On the assumption of normal earth-ionosphere multi-hop propagation, it

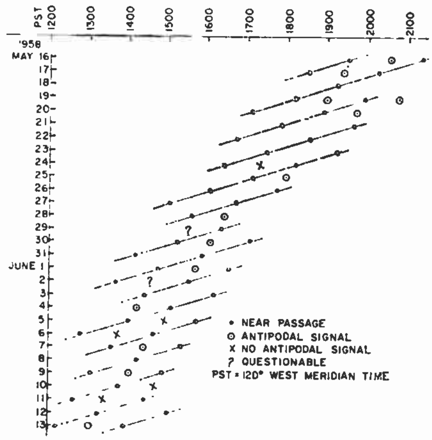

Fig. 1—Afternoon observations of the 20-mc transmissions from Sputnik III between May 16 and June 13, 1958.

is possible to estimate the direction of arrival of a signal by noting the amount of Doppler shift which has been imparted to it. Maximum positive shift should be observed in the direction in which the satellite will next approach for a direct passage. Maximum negative shift should be found in the direction in which the satellite last departed; intermediate shifts should be found in the intermediate directions. The absolute frequencies of the afternoon antipodal signals indicated Doppler shifts which were consistent with azimuths of arrival between southeast and south. The directions of arrival for the morning observations are not certain.

Perhaps the most significant signal characteristic was a nearly *constant frequency* throughout each antipodal passage. *This requires that the arriving energy be confined to a relatively narrow cone in some unchanging direction.* Fig. 2 is a spectrograph of the recorded signals during one of the strongest antipodal passages observed. If the signals had arrived simultaneously from several directions or throughout a wide cone, the observed spectrum would have consisted of several traces at different frequencies, or a single broad trace. If the direction of arrival had changed appreciably during the course of a passage, a corresponding variation in Doppler shift would have been observed.

On 53 occasions between June 14 and August 27 attempts to receive antipodal signals were unsuccessful. By the end of August the high passes of Sputnik III again occurred in the early evening and on August 28, signals were received from the southeast when the satellite was near the antipodes. A spectrum analysis of these signals shows several traces indicative of multipath propagation (Fig. 3). The presence of these components gives the signal a "rough" tone quality when monitored aurally, an effect which had not been noted previously. Antipodal signals have been observed on four occasions since then, up to the time of this writing (September 20, 1958).

The mode of propagation appears to involve penetration of the F layer followed by internal ionospheric reflection. The direction of arrival remains unchanged throughout each antipodal passage. The times of the observations suggest that the ionospheric tilt

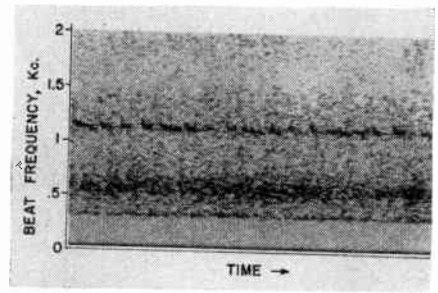

Fig. 2—Spectrum analysis of the signals received from Sputnik III while it was in the vicinity of the antipodes. This 5.6 second sample was recorded at 2046 PST, May 19, 1958, and the characteristic keying pattern is clearly visible a little above 1.1 kc. The absolute frequency was not determined on this passage.

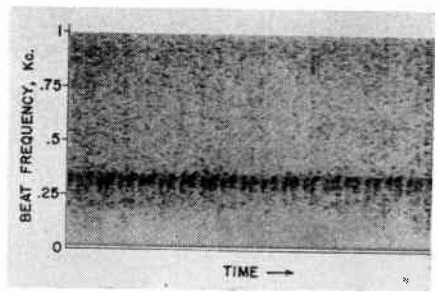

Fig. 3—Spectrum analysis of the signals from Sputnik III when it was close to the antipodes. This 11.2 second sample was recorded at 1815 PST, August 28, 1958. The detected signals are seen to be composed of several frequency components all near 300 cps. Absolute frequency = 20.004660 ± beat frequency (mc). Knowledge of the direction of arrival (SE) and the approximate satellite oscillator frequency suggests the choice of the negative sign in this case.

to the southeast of the receiving location which occurs prior to local sunset is important in providing a propagation path and for selecting a narrow azimuth of arrival.

The assistance of D. M. Annett, whose efforts are responsible for much of the construction and operation of the receiving installation, is gratefully acknowledged.

O. K. GARRIOTT
O. G. VILLARD, JR.
Radio Propagation Lab.
Stanford University
Stanford, Calif.

* Received by the IRE, September 29, 1958. This work has been supported by grant no Y/32.43/268 from the National Science Foundation.

[1] H. W. Wells, "Unusual propagation at 40 mc from the USSR satellite," PROC. IRE, vol. 46, p. 610; March, 1958.

WWV Standard Frequency Transmissions*

Since October 9, 1957, the National Bureau of Standards radio stations WWV and WWVH have been maintained as constant as possible with respect to atomic frequency standards maintained and operated by the Boulder Laboratories, National Bureau of Standards. On October 9, 1957, the USA Frequency Standard was 1.4 parts in 10^9 high with respect to the frequency derived from the UT 2 second (provisional value) as determined by the U. S. Naval Observatory. The atomic frequency standards remain con-

* Received by the IRE, October 14, 1958.

stant and are known to be constant to 1 part in 10^9 or better. The broadcast frequency can be further corrected with respect to the USA Frequency Standard as indicated in the table below. This correction is *not* with respect to the current value of frequency based on UT 2. A minus sign indicates that the broadcast frequency was low.

The WWV and WWVH time signals are synchronized; however, they may gradually depart from UT 2 (mean solar time corrected for polar variation and annual fluctuation in the rotation of the earth). Corrections are determined and published by the U. S. Naval Observatory.

WWV and WWVH time signals are maintained in close agreement with UT 2 by making step adjustments in time of precisely plus or minus 20 milliseconds on Wednesdays at 1900 UT when necessary; no step adjustment was made at WWV and WWVH during this month.

WWV FREQUENCY*

September, 1958 1500 UT	Parts in 10^9
1	−2.6
2	−2.7
3	−2.7
4	−2.7
5	−2.7
6	−2.8
7	−2.8
8	−2.8
9	−2.9
10	−3.0
11	−3.0
12	−3.0
13	−3.0
14	−3.0
15	−3.0
16	−2.9
17	−2.9
18	−2.8
19	−2.8
20	−2.6
21	−2.5
22	−2.4
23	−2.4
24	−2.4
25	−2.4
26	−2.4
27	−2.4
28	−2.4
29	−2.4
30	−2.4

* WWVH frequency is synchronized with that of WWV.

W. D. George
Radio Standards Lab.
Natl. Bur. of Standards
Boulder, Colo.

Compound Interferometers*

The very interesting article by Covington and Broten[1] on a "compound interferometer" prompts the suggestion of another way of tackling the design of such systems. For simplicity, suppose that the system is a combination of a large number of elementary detectors, all similar and having little or no directionality as individuals. The arguments can readily be extended to include continuous systems.

With this simplification, the system described by Covington and Broten resembles in form the system shown in Fig. 1. The over-all length contains $4n$ equally spaced positions. The unoccupied positions are marked with dots. Full circles show the two antennas of the simple interferometer. Asterisks show the numerous equally-spaced elements representing the continuous slotted-waveguide array. The distances of these elements from that on the extreme left are shown in the diagram as multiples of the basic interval D.

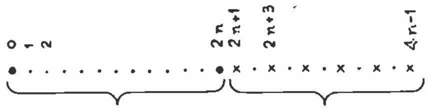

Fig. 1.

If u_r denotes the fluctuating electrical signal obtained from the detector that lies at a distance rD from the left, the signal from the simple interferometer is

$$U_1 = u_0 + u_{2n}$$

and the signal from the long array is

$$U_2 = u_{2n+1} + u_{2n+3} + \cdots u_{4n-1}.$$

Covington and Broten measure, in effect, the mean product of the signals U_1 and U_2 and this may be written, through the above equations, as the sum of many mean products of pairs of signals, one signal from a detector in the interferometer and one signal from a detector in the long array.

$$\overline{U_1U_2} = \overline{u_0u_{2n+1}} + \overline{u_0u_{2n+3}} + \cdots \overline{u_{2n}u_{2n+1}} + \cdots.$$

The reception pattern appropriate to $\overline{U_1U_2}$ is therefore the sum of reception patterns appropriate to these various pairs of elementary detectors. It can be shown that these elementary reception patterns are in fact sinusoids whose "space frequencies" are proportional to the distances separating the detectors in each pair. Thus, if the radio wavelength is L and the distance separating the detectors is $(2r-1)D$, then the reception pattern corresponding to the mean product of the signals of the two detectors is

$$\cos 2\pi(2r-1)D\theta/L \tag{1}$$

where θ is the angle of incidence (understood to be small).

It will be observed that in the arrangement of Fig. 1 the various pairs of detectors present every odd multiple of the basic distance, from D to $(4n-1)D$ and that each multiple appears only once. Thus the detector at $2n$ combined with the various detectors of the long array gives intervals $1, 3, 5 \cdots (2n-1)$, times the basic distance. The detector at position 0 combined with the various detectors of the long array gives intervals of $(2n+1)$ to $(4n-1)$ times the basic distance D. Thus the reception pattern corresponding to $\overline{U_1/U_2}$ is

$$A(\theta) = \sum_{1}^{r=2n} \cos 2\pi(2r-1)D\theta/L$$
$$= \frac{\sin 4n(2\pi D\theta/L)}{2 \sin (2\pi D\theta/L)}. \tag{2}$$

This pattern has the optimum form discussed by Covington and Broten.

The same pattern could be obtained with other arrangements. Some of them are pictured in Fig. 2.

Fig. 2(a) and 2(b) have been described by Covington and Broten. In Fig. 2(c) and 2(d) the long array is reduced to one-third or to one-fourth of the over-all length of the system, and the simple interferometer is replaced by an array of three or of four detectors.

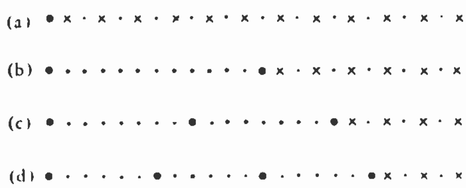

Fig. 2.

These systems all have the same reception pattern (2) because they all show the same set of space intervals between members of the two arrays.

It will be noted that Fig. 2(c) and 2(d) comprise only seven detectors while Fig. 2(b) needs eight and Fig. 2(a) needs thirteen. This economy in detectors could be of use in experiments where the individual detectors are costly. A system with a given over-all length uses the fewest detectors when the number of detectors in the two arrays are equal, or differ by unity.

The same test can be extended to two-dimensional arrays.[2,3] Thus it is shown[4] that the Mills cross has an optimum reception pattern in two dimensions, but that one of the four arms of the cross is redundant and can be omitted without affecting the performance.

N. F. Barber
Dominion Physical Lab.
Dept. of Sci. and Indus. Res.
Lower Hutt, N. Z.

Authors' Comment[5]

We are pleased to see the interesting exposition and design for compound interferometers proposed by Barber, and would like to report that the original 300-foot compound interferometer in operation at the National Research Council's laboratories in Ottawa has now been doubled in length. This newer system may be explained readily with reference to the configurations shown in

* Received by the IRE, May 16, 1958.

[1] A. E. Covington and N. W. Broten, "An interferometer for radio astronomy with a single-lobed radiation pattern," IRE Trans. on Antennas and Propagation, vol. AP-5, pp. 247–255; July, 1957.

[2] B. Y. Mills, A. G. Little, K. V. Sheridan, and O. B. Slee, "A high resolution radio telescope for use at 3.5 m," Proc. IRE, vol. 46, pp. 67–84; January, 1958.

[3] W. N. Christiansen and D. S. Mathewson, "Scanning the sun with a highly directional array," Proc. IRE, vol. 46, pp. 127–131; January, 1958.

[4] N. F. Barber, "Optimum arrays for direction finding," *N.Z.J. Sci.*, vol. 1, pp. 35–51; March, 1958.

[5] Received by the IRE, July 7, 1958.

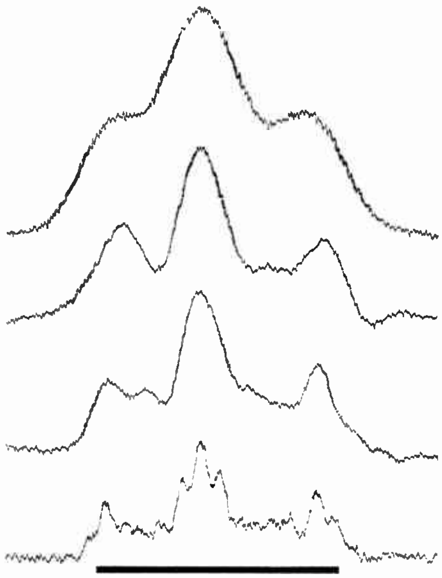

Fig. 3.

Barber's Fig. 2—as a transformation from Fig. 2(b) to 2(d)—keeping in mind, however, that the array length corresponding to the asterisks is fixed at 150 feet. Appropriate switches have been provided in the feeder system so that the various combinations of the array and each of the four interferometer elements may be used. The various antenna beams scan the solar disk in North-South strips and the complete system of array and four elements has recently been tested. Four drift curves for June 28, 1958, are shown in Fig. 3; these were obtained with the array alone, with the array and one interferometer element, with the array and two elements, and with the array and four elements. The approximate East-West beamwidths are, respectively: 8, 4, 2, and 1 minutes of arc. With these increases in resolution, the separation of the three radio emissive sunspot regions from the solar background becomes successively more prominent. The extent of the visible disk, 31′32″, is shown as a line.

A. E. Covington
N. W. Broten
Radio and Elec. Eng. Div.
Natl. Res. Council
Ottawa, Canada

Potential Well Theory of Velocity Modulation*

The behavior of an electron beam in transit through an accelerating aperture of such velocity modulation devices as klystrons has been described by a bunching theory. It is the purpose of this communication to present another way of viewing the interaction which is based upon a potential well model.

* Received by the IRE, May 8, 1958.

A simple, one-dimensional analysis may be made by representing the potential as

$$V(x) = \frac{zq^2}{\sqrt{x^2 + a^2}}, \qquad a = \frac{L}{2} \tag{1}$$

where zq is the net capacitative charge of the aperture with L its cross-sectional dimension. Thus the barrier height is $2zq^2/L$. A critical trapping velocity v_c given by

$$v_c^2 = \frac{2zq^2}{m\sqrt{x_0^2 + a^2}} \tag{2}$$

defines the injection velocity v_0 for which an oscillatory motion arises; for $v_0 < v_c$, the potential barrier prevents the escape of the entering electron. In (2), m is the electron mass and x_0 the accelerative path length from cathode to aperture.

The amplitude and period of the oscillating, trapped electron have been characterized. The former has the values

$$x^* = \frac{\pm\sqrt{\dfrac{4z^2q^2}{m^2} - a^2\left(v_0^2 - \dfrac{2zq^2}{m}\cdot\dfrac{1}{\sqrt{x_0^2+a^2}}\right)^2}}{v_0^2 - \dfrac{2zq^2}{m}\cdot\dfrac{1}{\sqrt{x_0^2+a^2}}}. \tag{3}$$

The oscillation turns out to be nonlinear with the resultant power series development for the period T:

$$T = \frac{4(x_0^2 + a^2)^{3/4}}{\left(\dfrac{zq^2}{2m}\right)^{1/2}} \cdot \left\{ 1 + \frac{1}{12} - \frac{1}{4\left(1 + \dfrac{a^2}{x_0^2}\right)} + \cdots \right\}. \tag{4}$$

Eq. (4) actually holds for the limit of $v_0 \to 0$; the general expression has been derived, but will be dealt with when a fuller discussion is presented at a later time. Nevertheless, it is clear from (4) that high-frequency oscillations associate with small dimensions and high voltages.

The classical, nonrelativistic theory pursued so far is adhered to in the determination of the radiated power per electron. The accelerative relation

$$\alpha(x) = \frac{zq^2}{m} \cdot \frac{x}{(x^2 + a^2)^{3/2}} \tag{5}$$

employed in the power equation $P = dE/dt = (2q^2/3c^3)\alpha^2$ leads to the average radiated power

$$P_{av} = \frac{z^2q^6}{6c^3m^2}\left\{\frac{1}{x^*}\cdot\frac{1}{2a^3}\tan^{-1}\frac{x^*}{a} + \frac{1}{2a^2}\cdot\frac{1}{x^{*2} + a^2} - \frac{1}{(x^{*2} + a^2)^2}\right\}. \tag{6}$$

A complete understanding of the theoretical implications of the potential well theory of velocity modulation necessitates numerical evaluation of (3), (4), and (6). The interrelation of radiated power and frequency with dimensions and applied voltages will be quite interesting to elucidate in some detail. It is hoped that a deeper understanding of klystron operation may result from further study.

Louis Gold
Edgerton, Germeshausen and Grier, Inc.
Boston 15, Mass.

Parallel Plane Waveguide Partially Filled with a Dielectric*

In a recent letter, Duncan *et al.*,[1] gave a qualitative description for a field configuration in a parallel plane waveguide partially filled with a dielectric. A more exact analysis, however, yields results which partially contradict the field structure picture presented in their letter.

Some of the principal points in the solution of this propagation problem and the final results for TE modes on this line are presented below. The geometry and coordinate systems are shown in Fig. 1.

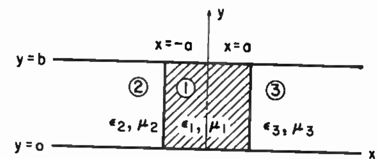

Fig. 1—Cross section of the parallel plane waveguide partially filled with a dielectric. The positive z axis is out of the paper.

The general solution of the scalar wave equation for TE modes is that

$$H_z = (Ae^{k_x x} + Be^{-k_x x})(Ce^{k_y y} + De^{-k_y y})e^{-j\beta z} \tag{1}$$

where

- A, B, C, and D are arbitrary constants,
- β = propagation constant,
- k_x and k_y are separation constants which come from the solution of the wave equation.

The separation constants k_x and k_y are related to the propagation constant, frequency, and properties of the medium by

$$k_x^2 + k_y^2 = \beta^2 - \omega^2\mu\epsilon. \tag{2}$$

The other field quantities can be obtained from the expression for H_z, and they are of similar form. Equations which are identical to (1) and (2) can be written for each of the three regions. Subscripts 1, 2, and 3 must be attached to each of the field quantities, arbitrary constants, material constants, and k's to denote their respective regions. Of course, β must be the same for all three regions. Upon applying the boundary conditions at the conducting planes ($y=0$ and $y=b$), it is determined that

$$k_y = j\frac{n\pi}{b} \qquad n = 0, 1, 2, \cdots. \tag{3}$$

It is assumed that $\mu_1 = \mu_2 = \mu_3 = \mu_0$, and $\epsilon_2 = \epsilon_3$. This symmetry of the structure causes all solutions to fall into two groups, even and odd modes. The distinction is based upon whether

$$E_y(x) = E_y(-x) \text{ or } E_y(x) = -E_y(-x). \tag{4}$$

When the proper boundary conditions are applied at one of the dielectric-air interfaces, it is found that if $n \neq 0$, a TE mode can propagate only if the entire space between the conducting planes is filled with a

* Received by the IRE, April 28, 1958.
[1] B. J. Duncan, L. Swern, and K. Tomiyasu, "Microwave magnetic field in dielectric-loaded coaxial line," Proc. IRE, vol. 46, pp. 500–502; February, 1958.

homogeneous dielectric. Therefore, only the $n=0$ case is of interest for TE modes. Applying the boundary conditions for the $n=0$ case results in the following conditional equations for the even and odd TE modes respectively:

$$k_{x_{2e}} = -k_{x_{1e}} \tanh k_{x_{1e}} a, \tag{5}$$

$$k_{x_{2o}} = -k_{x_{1o}} \coth k_{x_{1o}} a. \tag{6}$$

The subscripts e and o refer to the even and odd modes. In order to have physically realizable propagation in the z direction, it can be shown that $k_{x_{2e}}$ and $k_{x_{2o}}$ must be positive real numbers. Eqs. (5) and (6) show, therefore, that $k_{x_{1e}}$ and $k_{x_{1o}}$ must be pure imaginary numbers and that $(k_{x_{1e}}a)$ and $(k_{x_{1o}}a)$ must be restricted to certain intervals. If we let $k_{x_{1e}} = jk_{x_{de}}$ and $k_{x_{1o}} = jk_{x_{do}}$, where the subscript d refers to the dielectric or region 1, the conditional equations are changed to

$$k_{x_{2e}} = k_{x_{de}} \tan k_{x_{de}} a, \tag{7}$$

$$k_{x_{2o}} = -k_{x_{do}} \cot k_{x_{do}} a. \tag{8}$$

Since the propagation constant (β) must be the same in all regions, the following equations must also be satisfied:

$$k_{x_{de}}^2 - \omega^2\mu\epsilon_1 = -k_{x_{2e}}^2 - \omega^2\mu\epsilon_2, \tag{9}$$

$$k_{x_{do}}^2 - \omega^2\mu\epsilon_1 = -k_{x_{2o}}^2 - \omega^2\mu\epsilon_2. \tag{10}$$

Substituting (7) into (9) (eliminating $k_{x_{2e}}$), and substituting (8) into (10) (eliminating $k_{x_{2o}}$), we have

$$\pi^2\left(\frac{2a}{\lambda_0}\right)^2(K_1 - K_2) = \left[\frac{k_{x_{de}}a}{\cos k_{x_{de}}}\right]^2 \tag{11}$$

$$\pi^2\left(\frac{2a}{\lambda_0}\right)^2(K_1 - K_2) = \left[\frac{k_{x_{do}}a}{\sin k_{x_{do}}a}\right]^2 \tag{12}$$

where $K_1 = \epsilon_1/\epsilon_0$ and $K_2 = \epsilon_2/\epsilon_0$.

Graphical techniques can be used to obtain the distribution constants $k_{x_{do}}$ and $k_{x_{de}}$ after $(2a/\lambda_0)$ and $(K_1 - K_2)$ have been specified.

The final field equations for the symmetric TE modes are given below.

Region 1

$$H_{x_1} = A_{1e}\frac{\beta}{k_{x_{de}}}\cos(k_{x_{de}}x)e^{-j\beta z} \tag{13}$$

$$H_{z_1} = jA_{1e}\sin(k_{x_{de}}x)e^{-j\beta z} \tag{14}$$

$$E_{y_1} = A_{1e}\frac{\omega\mu}{k_{x_{de}}}\cos(k_{x_{de}}x)e^{-j\beta z} \tag{15}$$

Region 2

$$H_{x_2} = A_{1e}\frac{\beta}{k_{x_{2e}}}\sin(k_{x_{de}}a)e^{k_{x_{2e}}(a+x)}e^{-j\beta z} \tag{16}$$

$$H_{z_2} = -jA_{1e}\sin(k_{x_{de}}a)e^{k_{x_{2e}}(a+x)}e^{-j\beta z} \tag{17}$$

$$E_{y_2} = -A_{1e}\frac{\omega\mu}{k_{x_{2e}}}\sin(k_{x_{de}}a)e^{k_{x_{2e}}(a+x)}e^{-j\beta z} \tag{18}$$

Region 3

The field quantities in Region 3 are the same as in Region 2 except that $e^{k_{x_{2e}}(a+x)}$ is replaced by $e^{k_{x_{2e}}(a-x)}$. The antisymmetric modes are the same as the above except that the roles of the sines and cosines are reversed. The fact that $n=0$ means that there is no variation of the fields in the y direction; that is also shown in (13) through (18).

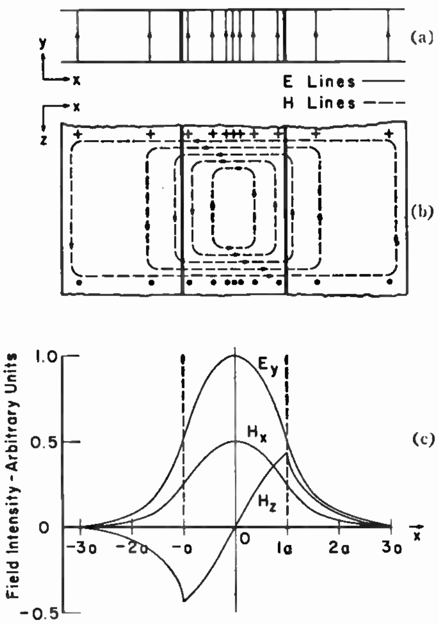

Fig. 2—Field configuration for the dominant mode in parallel plane waveguide partially filled with a dielectric; (a) cross-sectional view, (b) top view, (c) graph of field intensities in a transverse plane.

The mode which is most similar to that shown in Duncan *et al.*[1] is the lowest order even mode (dominant mode) in which

$$0 \le (k_{x_{de}}a) \le \frac{\pi}{2}.$$

The field configuration as well as a graph of the field magnitudes are shown in Fig. 2. The magnetic lines are closed loops lying in planes of y = constant as in Duncan *et al.* The E lines, however, do not have kinks but rather are parallel to the y axis in all three regions. The field distributions in the x direction are sinusoidal or cosinusoidal in the dielectric region, and decay exponentially in the air region. The discrepancy between the two analyses is due to the previously made first-order approximation[1] that the potential difference between the top and bottom plates is a constant in the region of the dielectric.

A similar analysis has been made on TM waves in this structure and, contrary to the previous correspondence,[1] it was found that TM waves could not propagate therein. The propagation of hybrid modes on this type of line has been analyzed by Tischer.[2,3] It has recently come to the writer's attention that this structure has also been analyzed by Moore and Beam.[4] This complete paper, however, has not been referenced by the principal indexes in the field. This work appears to have some errors in the equations concerning metallic and dielectric losses.

M. Cohn
Radiation Lab.
The Johns Hopkins University
Baltimore, Md

[2] F. J. Tischer, "Microwellenleitung mit geringen verlusten," (Waveguides with small losses). *Arch. Elekt. Übertr.*, vol. 7, pp. 592–596; December, 1953.

[3] F. J. Tischer, "The *H*-guide, a waveguide for microwaves," 1956 IRE Convention Record, pt. 5, pp. 44–47.

[4] R. A. Moore and R. E. Beam, "A duo-dielectric parallel plane waveguide," *Proc. NEC*, vol. 12, pp. 689–705; April, 1957

An Effect of Pulse Type Radiation on Transistors Packaged in a Moist Atmosphere*

In a recent series of experiments on the effects of high-dose rate radiation on transistors, using the Godiva[1] critical assembly of the Los Alamos Scientific Laboratory, an interesting phenomenon was observed.

The investigation of interest consisted of monitoring the transistor collector-to-base leakage current (I_{co}) along a 3-volt, 75-ohm load line, while simultaneously subjecting the transistor to a pulse of neutron plus gamma-ray radiation.

During the pulse of radiation, transistors received a total neutron dose in the order $10^{12}n/\text{cm}^2$, and a total gamma dose 10^3 rad in a period of 200 μsec, at rates which varied with time up to a maximum of $10^{17}n/\text{cm}^2$-sec and 10^7 rad/sec for the neutrons and gamma rays, respectively.

Transistors of several types, including *n-p-n* and *p-n-p* units of both germanium and silicon were tested in this manner. In all cases the I_{co} vs time characteristic of the form shown in curve A of Fig. 1 was obtained. With one germanium *p-n-p* type, however, an additional peak was observed as in curve B of Fig. 1. This peak occurred at a much later time and was one to two orders of magnitude smaller than the initial I_{co} transient.

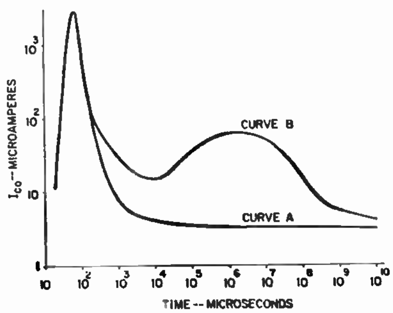

Fig. 1—I_{co} vs time.

All units of this transistor type demonstrated this characteristic behavior (curve B) under test.

Examination of the variations in transistor type, packaging, etc., between this type and all others lead us to believe that the second peak is caused by the presence of water vapor in the transistor case.

This conclusion is based on: 1) the only transistor type to show a second peak was the only transistor packaged in a moist atmosphere and 2) the second peak was not observed in a transistor which differed from the "second peak" type only in that a desiccant was added inside the case.

Work on this phenomenon is continuing in order to arrive at a completely satisfactory mechanism to explain this effect. A possible explanation may be that a partial dehydration of the transistor surface due to

* Received by the IRE, May 19, 1958. This work was performed under AF Contract No. 33 (600) 31315.

[1] R. E. Peterson and G. A. Newby, "An unreflected U-235 critical assembly," *Nuclear Sci. Eng.*, vol. 1, pp. 112–125; May 1956.

radiolysis takes place with a subsequent diffusion outward of the radiolysis products. This is followed by a rehydration of the surface by diffusion of water into the semiconductor. The initial increasing portion of the second peak seems to fit a film diffusion controlled mechanism while the decreasing portion appears compatible with slow first or pseudo-first order kinetics.

We wish to express our thanks to C. H. Zierdt of the General Electric Company for providing us with several specially prepared transistors.

W. A. Bohan
M. G. Chasanov
E. N. Schroeder
IBM Corp.
Military Products Div.
Oswego, N. Y.

Theory of the *P-N* Junction Device Using Avalanche Multiplication*

Several devices have been developed which utilize the avalanche multiplication in a reverse-biased junction,[1-3] since the nature of the phenomenon was clarified by McKay, *et al.*[4,5] Among them the three-terminal *p-n-p-n* switch is most versatile in its application.

Avalanche multiplication has been usually understood, after McKay, as the phenomenon that the electron or hole current is *multiplied by a constant factor* upon passing through a reverse-biased junction. This note points out that this is the case only when the current is composed purely of the electron or hole current on either side of the junction, and proposes a more general, but simple formulation of the phenomenon. This point is important in the central junction of the *p-n-p-n* switch.

According to the atomic theory of the avalanche multiplication,[6,7] the number of electron-hole pairs created per unit time by an electron or a hole is a complicated function of the electric field acting on it and usually expressed as $\alpha\mu_n E$ or $\beta\mu_p E$, where α and β are the ionization rates of electron and hole, respectively, the μ's represent mobilities, and E, the field strength. The continuity equation for electrons reads

$$-\frac{1}{q}\frac{dI_n}{dx} = \alpha\mu_n En + \beta\mu_p Ep, \qquad (1)$$

where recombination of carriers is neglected. If we can consider that the current in the space-charge region is mainly composed of drift component[8] and $\alpha \cong \beta$, (1) becomes

$$(dI_n/dx) = \alpha I, \qquad (2)$$

where I is the total current through the junction and is constant. By integration the increment ΔI_n in the electron curent upon passing through the junction is shown

$$\Delta I_n = I \int_{\text{depletion layer}} \alpha dx \equiv IA. \qquad (3a)$$

Similarly for the hole current

$$\Delta I_p = IA. \qquad (3b)$$

Thus, the increments are proportional to *total* current. If, on either side of the junction, the electron or hole component is nearly equal to the total current

$$\Delta I = I_f - I_i = IA = I_f A,$$

or

$$1 - (1/M) = A = (V/V_B)^n,$$

where V is the applied voltage and V_B the breakdown voltage of the junction. Hitherto this form has been used in the literature. This equation is convenient indeed when applied to the collector junction in an avalanche transistor where the current on the collector side of the collector junction is mainly composed of the carrier of minority to the base region. But when we consider both electron and hole components, it is apt to lead to an incorrect result because of the ambiguous nature of the old formulation.

For example, in the *p-n-p-n* switch in Fig. 1(a), it is shown in the literature[3] that the total current at J_2 is

$$I = IM_p\alpha_{1N} + IM_n\alpha_{2N} + I_{CO}. \qquad (4)$$

At first sight this seems incorrect. If we evaluate the right side of (4) on the N_B side of J_2, we must drop M_p in the first term because the hole current emitted at J_1 is not yet multiplied before passing through J_2, or if we evaluate on the P_B side of J_2, M_n in the second term must be dropped for the same reason. Fig. 1(b) shows the change of the composition of current according to location in the device.

In our scheme the situation becomes clearer. Consider the N_B side of J_2. The hole current, which is collected there, is $\alpha_{1N}I$ and the electron current, which is collected and multiplied, is $\alpha_{2N}I + IA$ according to (3a). Therefore the total current is

$$I = I\alpha_{1N} + I\alpha_{2N} + IA + I_{CO}. \qquad (5)$$

It is easily shown that the same expression is obtained if we consider the P_B side of J_2. The condition for breakover is now

$$1 - \alpha_{1N} - \alpha_{2N} = A. \qquad (6)$$

This leads to the same expression for breakover voltage V_O as is obtained from (4):

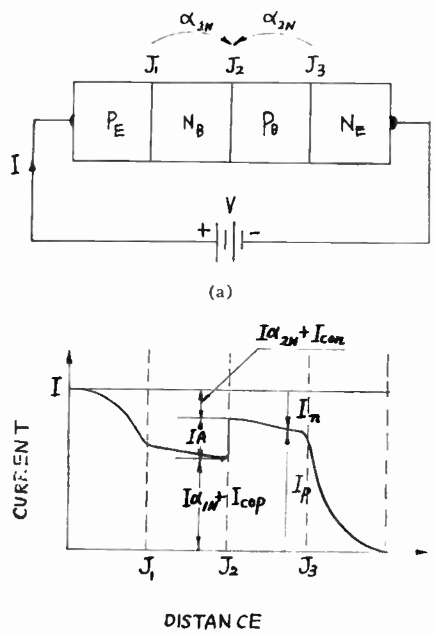

(a)

(b)

Fig. 1—(a) The structure of *p-n-p-n* switch. (b) composition of current when a small multiplication occurs in the center junction.

$$V_O/V_B = (1 - \alpha_{1N} - \alpha_{2N})^{1/n}.$$

Thus the new formulation is suitable to the case where both electron and hole components are important. It, of course, reduces to the old one if the current on either side of the junction is composed only of electron or hole current.

Toshio Misawa
Semiconductor Div.
Sony Corp.
Shinagawa, Tokyo, Japan

* Received by the IRE, May 15, 1958.

[1] M. C. Kidd, W. Hasenberg, and W. M. Webster, "Delayed collector conduction, a new effect in junction transistors," *RCA Rev.*, vol. 16, pp. 16–33; March, 1955.

[2] S. L. Miller and J. J. Ebers, "Alloyed junction avalanche transistors," *Bell Sys. Tech. J.*, vol. 34, pp. 883–902; September, 1955.

[3] J. L. Moll, M. Tanenbaum, J. M. Goldey, and N. Holonyak, "*P-N-P-N* transistor switches," Proc. IRE, vol. 44, pp. 1174–1182; September, 1956.

[4] K. G. McKay, "Avalanche breakdown in silicon," *Phys. Rev.*, vol. 94, pp. 877–884; May 15, 1954.

[5] S. L. Miller, "Avalanche breakdown in germanium," *Phys. Rev.*, vol. 99, pp. 1234–1241; August 15, 1955, and "Ionization rates for holes and electrons in silicon," *Phys. Rev.*, vol. 105, pp. 1246–1249; February 15, 1957.

[6] P. A. Wolff, "Theory of electron multiplication in Si and Ge," *Phys. Rev.*, vol. 95, pp. 1415–1420; September 15, 1954.

[7] J. Yamashita, "Theory of electron multiplication in silicon," *Prog. Theor. Phys.*, vol. 15, pp. 95–110; February, 1956.

[8] This problem was discussed by the writer at the 1956 Annual Meeting of the Physical Society of Japan, July 17, 1956. See also, F. W. G. Rose, "On the impact ionization in the space-charge region of *p-n* junctions," *J. Electronics*, vol. 3, pp. 396–400; October, 1957.

Number of Trees in a Graph*

An important property of a linear graph is its number of distinct trees. Trent[1] and Lantieri,[2] among other authors, have shown how to calculate this number by use of a symmetrical determinant T, and Weinberg[3] has used this determinant in applying Kirchhoff's topological laws. If we let n_t represent the total number of nodes of a graph and define $n \equiv n_t - 1$, then n is the order of the determinant T and its elements are given by

t_{ii} = number of branches connected to node i

t_{ik} = −(number of branches connected between nodes i and k) $(i \neq k)$.

* Received by the IRE, May 12, 1958.

[1] H. M. Trent, "A note on the enumeration and listing of all possible trees in a connected linear graph," *Proc. Natl. Acad. Sci.*, vol. 40, pp. 1004–1007; October, 1954.

[2] J. Lantieri, "Méthode de Détermination des Arbres d'un Réseau," *Ann. Télécommun.*, vol. 5, pp. 204–208; May, 1950.

[3] L. Weinberg, "Kirchhoff's 'third and fourth laws,'" IRE Trans. on Circuit Theory, vol. CT-5, pp. 8–30; March, 1958.

It is thus clear that the elements of the determinant may be found by inspection of the graph. The only problem that remains is the evaluation of the determinant.

When the number of nodes is large, it would appear that evaluation of the determinant is cumbersome. A simple method for evaluating the determinant would therefore be useful. It is the purpose of this note to point out that straightforward evaluation of the determinant is probably never necessary. To illustrate this we show that a formula for the determinant of a complete polygon (or complete graph) is readily found, and then show that formulas for two other special graphs may also be derived.

We define a complete polygon in the usual way as one in which each node is connected to every other node by exactly one branch; examples for $n=3$ and $n=4$ are shown in Fig. 1(a) and 1(b), respectively, where the nodes have been numbered in a clockwise order. It is evident that n branches are connected to each node.

One of the special types of graphs we consider is derived from a complete graph by removing p branches from a single node; thus it is required that $p \leq n$. Without loss of generality the p branches are removed from node 1 and one branch from each of the other nodes 2, 3, $\cdots$, $p+1$. An example is shown in Fig. 2 for $n=5$ and $p=2$; the missing branches are shown dashed. The other type of graph is derived from a complete graph by removing a branch from different pairs of nodes, with r being equal to the number of different pairs of nodes with missing branches. Since we permit only one branch to be missing from a node, it is clear that $n_t \geq 2r$. The graph for which $n=5$ and $r=3$ is given in Fig. 3, where again the missing branches are shown dashed.

For the complete polygon it is found that

$$T = (n+1)^{n-1}. \tag{1}$$

Thus for the graphs in Fig. 1(a) and 1(b) there are 16 and 1296 trees, respectively. For $n=3$ the determinant is

$$T = \begin{vmatrix} 3 & -1 & -1 \\ -1 & 3 & -1 \\ -1 & -1 & 3 \end{vmatrix} \tag{2}$$

and in general the determinant is given by

$$T = \begin{vmatrix} n & -1 & -1 & \cdots & -1 \\ -1 & n & -1 & \cdots & -1 \\ \cdot & \cdot & \cdot & \cdots & \cdot \\ -1 & -1 & -1 & \cdots & n \end{vmatrix}. \tag{3}$$

Such a special form of determinant is evaluated simply by writing it as the determinant of the sum of a matrix, each of whose elements is -1, and a diagonal matrix, each of whose elements is $n+1$, and then expanding this determinant about the elements of the diagonal matrix.[4] However, it is useful in deriving formulas for the other two special types of graphs to make use of the properties of this determinant in another form of evaluation.

Inspection of (2) shows that the sum of the elements in each column is equal to

[4] A. C. Aitken, "Determinants and Matrices," Oliver and Boyd Ltd., Edinburgh and London, p. 87 and ex. 2, p. 133; 1956.

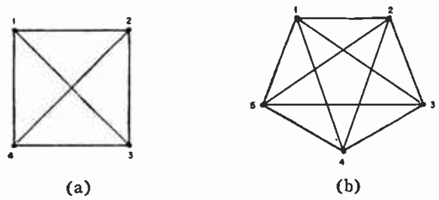

Fig. 1—Complete polygons for $n=3$ and $n=4$.

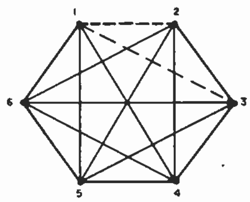

Fig. 2—Graph for $n=5$ and $p=2$.

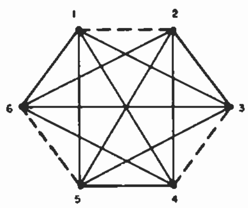

Fig. 3—Graph for $n=5$ and $r=3$.

unity. This property, it is clear, is true for all n. Therefore, if all of the succeeding rows are added to the first, the latter becomes a row of ones, and

$$T = \begin{vmatrix} 1 & 1 & 1 \\ -1 & 3 & -1 \\ -1 & -1 & 3 \end{vmatrix}. \tag{4}$$

Then the first row is added successively to each of the other rows to give

$$T = \begin{vmatrix} 1 & 1 & 1 \\ 0 & 4 & 0 \\ 0 & 0 & 4 \end{vmatrix} \tag{5}$$

whose value is now obtained by inspection. By the same reasoning we can show that in general $T=(n+1)^{n-1}$.

Making use of these properties allows the other formulas to be derived. For example, for the graph in Fig. 3 we have

$$T = \begin{vmatrix} 4 & 0 & -1 & -1 & -1 \\ 0 & 4 & -1 & -1 & -1 \\ -1 & -1 & 4 & 0 & -1 \\ -1 & -1 & 0 & 4 & -1 \\ -1 & -1 & -1 & -1 & 4 \end{vmatrix} \tag{6}$$

which is transformed to

$$T = \begin{vmatrix} 1 & 1 & 1 & 1 & 0 \\ 0 & 4 & -1 & -1 & -1 \\ 0 & 0 & 5 & 1 & -1 \\ 0 & 0 & 1 & 5 & -1 \\ 0 & 0 & 0 & 0 & 4 \end{vmatrix}. \tag{7}$$

To obtain (7) from (6) we added all the succeeding rows to the first row, and then added the new first row successively to the 3rd, 4th, and 5th rows. The determinant is now readily evaluated as

$$\begin{aligned} T &= 4\begin{vmatrix} 5 & 1 & -1 \\ 1 & 5 & -1 \\ 0 & 0 & 4 \end{vmatrix} \\ &= 4^2(5^2-1) \\ &= 4^3(61) \\ &= 384. \end{aligned} \tag{8}$$

By performing the same types of operations on the T for a graph in which $n=7$ and $r=4$, we find

$$\begin{aligned} T &= 6^4 8^2 \\ &= 16{,}384. \end{aligned} \tag{9}$$

The answers are given in the form of the next to the last equation of (8) and (9) because this form suggests the general formula. In fact, we find that the number of trees in a graph in which there are r pairs of nodes with missing branches is given by

$$T = (n-1)^r (n+1)^{n-1-r}. \tag{10}$$

Here $n \geq 1$ and $n+1 \geq 2r$.

Similarly, for a graph in which there are p branches missing from one node we derive that the number of trees is

$$T = n^{p-1}(n-p)(n+1)^{n-1-p}. \tag{11}$$

Here $n \geq 1$ and $p \leq n$.

We thus conclude that because of the special form of the determinant its evaluation is not computationally difficult. To eliminate the necessity of evaluating the determinant for three special types of graphs, formulas have been derived for these cases.

Louis Weinberg
Hughes Research Labs.
Culver City, Calif.

Algebraic Approach to Signal Flow Graphs*

Much has been written about networks consisting of unilateral elements exclusively, *i.e.*, signal flow graphs, in particular by Mason[1,2] who has provided us with a complete set of topological rules for the analysis of such networks (and of others[3]). The usefulness of these rules cannot be doubted, but everyone cannot spend the time required for their mastery especially when the usual tools of matrix analysis are readily available. Therefore, this note indicates an orderly, *i.e.*, matrix, method of analyzing signal flow graphs. Incidentally, this approach could serve as a convenient starting point for the proof of some of the topological rules.

Let $T_{\alpha\beta}$ denote the transmittance pointing from node α to node β, and put $T_{\alpha\alpha}=1$ for all input nodes; let v_α be the node to

* Received by the IRE, May 19, 1958.
[1] S. J. Mason, "Feedback theory—some properties of signal flow graphs," Proc. IRE, vol. 41, pp. 1144–1156; September, 1953.
[2] S. J. Mason, "Feedback theory—further properties of signal flow graphs," Proc. IRE, vol. 44, pp. 920–926; July, 1956.
[3] S. J. Mason, "Topological analysis of linear nonreciprocal networks," Proc. IRE, vol. 45, pp. 829–838; June, 1957.

datum voltage of node α, then

$$v_\beta = \sum_\alpha T_{\alpha\beta} v_\alpha. \tag{1}$$

Forming voltages into vector v and transmittances into the square matrix T, we write for (1)

$$v = T_t v, \tag{2}$$

T_t being the transpose of T. Equivalently, denoting by I the unit matrix,

$$(T_t - I)v = 0. \tag{3}$$

This equation solves the network. Note that v contains the inputs as well as the driven voltages.

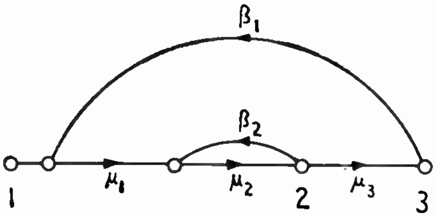

Fig. 1.

As a specific example consider Fig. 1, where the hollow circles denote mixing points. In order to analyze this situation without the use of additional rules, a sufficient number of nodes to break all loops must be identified. In our example one node is required in addition to the input terminal. By inspection,

$$T - I = \begin{Vmatrix} 0 & \mu_1\mu_2 \\ 0 & \beta_2\mu_2 + \mu_3\beta_1\mu_1\mu_2 - 1 \end{Vmatrix}.$$

Denoting cofactors by superscripts we find for the through transmittance H_{13},

$$\begin{aligned} -\mu_3 H_{12} &= \mu_3 \frac{V_2}{V_1} = \mu_3 \frac{(T_t - I)^{12}}{(T_t - I)^{11}} \\ &= \mu_3 \frac{(T - I)^{21}}{(T - I)^{11}} \\ &= \frac{\mu_1\mu_2\mu_3}{1 - \mu_2\beta_2 - \mu_1\mu_2\mu_3\beta_1}. \end{aligned}$$

Amos Nathan
Faculty of Elec. Eng.
Technion, Israel Inst. Tech.
Haifa, Israel

On the Coupling Coefficients in the "Coupled-Mode" Theory*

The "coupled-mode" theory has proved itself to be an important tool in the analysis of energy exchange phenomena between traveling waves. In its original form[1] it is capable of yielding important qualitative results. To extend its range of usefulness into the quantitative domain, one needs to evaluate the coupling coefficients which govern the energy exchange. This is done in this paper where we treat the "small coupling" case. We assume that in obtaining the coupling coefficients for the small coupling case we may use for the different physical observables their values in the absence of coupling. This procedure is analogous to that used in evaluating the Q of a cavity or the attenuation constant of a waveguide, for the small loss case, where the loss-free field solutions are used instead of the actual solutions in the presence of losses, and is a type of perturbation theory formulated on physical grounds.

Using Haus'[2] formulation of Pierce's coupled-mode theory we write for the system of differential equations obeyed by the mode amplitudes

$$\frac{d[A]}{dz} = [C][A]. \tag{1}$$

$[A]$ is a column matrix, whose individual components $A_i(z)$ are normalized such that $\pm A_iA_i^*$ is the power carried by the ith mode in the $+z$ direction, the z direction being taken as the direction of propagation. $[c]$ is a square matrix whose determination is the subject of this paper.

The condition of power conservation yields:

$$C_{ki}^* = \mp C_{ik} \qquad k \neq i \tag{2}$$

where the upper and lower signs apply when modes i and k carry power in the same or opposite directions, respectively. Using (1) and (2) we get:

$$C_{mn} = \frac{\frac{d}{dz}(A_mA_m^*)}{2\,\mathrm{Re}\,(A_m^*A_n)} \tag{3}$$

for C_{mn} real.

$$C_{mn} = j\frac{\frac{d}{dz}(A_mA_m^*)}{\mathrm{Im}\,(A_mA_n^*)} \tag{4}$$

for C_{mn} imaginary.

A_m and A_n have to be defined in terms of the physical observables (fields, current, etc.) in such a way that either $Re(A_mA_n^*)$ is proportional to the distance rate of change of power in mode m (or n), in which case (3) applies or $\mathrm{Im}\,(A_mA_n^*)$ is proportional to the power rate of change, in which case (4) applies. The proportionality constant is real in both cases.

To illustrate the application of the theory we treat the cases of the traveling-wave tube and the double stream amplifier.

Traveling-Wave Tube

The coupled-modes are the "fast" and "slow" space-charge waves and the circuit-forward wave (the circuit-backward wave is assumed matched out).

Let:

$$A_nA_n^* = \frac{VV^*}{2K} = \frac{E_zE_z^*}{2\beta_c^2K} \tag{5}$$

where

K = field-normalized circuit impedance,[3]
E_z = effective axial field,
β_c = free (uncoupled) propagation constant of the circuit. In its free state the beam carries RF kinetic power P_K

$$P_K = -\frac{Au_0}{2\eta}\,\mathrm{Re}\,(v_zi_z^*) \tag{6}$$

where

A = beam cross-section area,
u_0 = beam dc velocity,
$\eta = |e/m|$ = charge to mass ratio of the electron,
v_z, i_z are the beam ac velocity and current density, respectively.

For a single space-charge wave (6) can be rewritten as:

$$P_K = A_mA_m^* = \frac{\omega_qV_0}{\omega I_0}I_zI_z^* \tag{7}$$

where:

ω_q, ω = beam reduced plasma frequency and frequency, respectively,
V_0, I_0 = beam dc voltage and current, respectively,
I_z = beam ac current.

In view of (6) and (7) we can write

$$A_m = \left(\frac{\omega_qV_0}{\omega I_0}\right)^{1/2} I_z \tag{8}$$

$$A_n = \frac{1}{(2K)^{1/2}\beta_c}E_z. \tag{9}$$

Employing Poynting's theorem we can show that the rate of change of circuit power is given by:

$$\frac{d}{dz}(A_nA_n^*) = -\frac{1}{2}\,\mathrm{Re}\,(E_zI_z^*)$$

using (8)–(10) and assuming

$$\beta_c \simeq \frac{\omega}{u_0} = \beta_e, \tag{10}$$

we get:

$$C_{mn}^2 = S^2 = \frac{\beta_e^3C^3}{2\beta_q} \tag{11}$$

S being defined by (11).

Taking A_1 as the forward-circuit mode, A_2 and A_3 as the "fast" and "slow" space-charge wave, and assuming $C_{23} = 0$ and $e^{-\Gamma z}$ propagation, (1) becomes

$$\begin{aligned} (-j\beta_c + \Gamma)A_1 + SA_2 + SA_3 &= 0 \\ -SA_1 + [-j(\beta_e - \beta_q) + \Gamma]A_2 &= 0 \\ SA_1 + [-j(\beta_e + \beta_q) + \Gamma]A_3 &= 0 \end{aligned} \tag{12}$$

resulting in the determinantal equation:

$$\begin{aligned} j\beta_e^2\beta_c - \beta_e^2\Gamma - j\beta_q^2\beta_c + \beta_q^2\Gamma - 2\beta_e\beta_c\Gamma \\ -j\beta_e\Gamma^2 - 2j\beta_e\Gamma^2 + \Gamma^3 - 2j\beta_qS^2 = 0. \end{aligned} \tag{13}$$

Eq. (13) can be solved directly for Γ. To cast the result in a more familiar form we adopt the convention:

$$\begin{aligned} -\Gamma &= -j\beta_e + \beta_eC\delta \\ \beta_c &= \beta_e(1 + cb) \\ \beta_q &= \beta_e(4QC^3)^{1/2}. \end{aligned}$$

Eq. (13) becomes the well-known equation for the traveling-wave tube[3]

$$(\delta^2 + 4QC)(-b + j\delta) = +1. \tag{14}$$

* Received by the IRE, May 26, 1958.

[1] J. R. Pierce, "Coupling of modes of propagation," *J. Appl. Phys.*, vol. 25, pp. 179–183; February, 1954.

[2] H. Haus, "Coupled Mode Theory," M.I.T., Cambridge, Mass., unpublished report.

[3] J. R. Pierce, "Traveling-Wave Tubes," D. Van Nostrand Co., Inc., New York, N. Y.; 1950.

It should be noted that in no place have we used results from other traveling-wave tube theories. We have merely adopted some of Pierce's conventional symbols in order to arrive at (14).

Double Stream Amplifier

The interaction is assumed to take place between the "slow" space-charge wave of the fast electron beam, called A_2, and the "fast" space-charge wave of the slow beam, denoted as A_1. The slow and fast electron beams have equal charge densities and have dc velocities u_{01} and u_{02}, respectively.

Using results of the kinetic power theorem in a way analogous to that leading to (8) we get:

$$A_1 = \left(\frac{u_{01}\omega_q}{2\eta\omega\,|\,\rho_0\,|\,A}\right)^{1/2} I_1, \qquad (15)$$

$$A_2 = \left(\frac{u_{02}\omega_q}{2\eta\omega\,|\,\rho_0\,|\,A}\right)^{1/2} I_2. \qquad (16)$$

In analogy with (10) we get:

$$\frac{d}{dz}(A_1A_1^*) = -\operatorname{Re}(E_1I_2^*). \qquad (17)$$

Using (15)–(17) in (4) plus the result:

$$E_1 = \frac{jI_1}{\omega\epsilon A}$$

leads to

$$C_{12} = -j\,\frac{\omega_p^2}{\omega_q(u_{01}u_{02})^{1/2}} \qquad (18)$$

and a determinantal equation whose solution, assuming $e^{-j\beta Z}$ propagation, is:

$$\beta_{1,2} = \frac{\beta_{01}+\beta_{02}}{2} \pm \left[\left(\frac{\beta_{01}-\beta_{02}}{\sqrt{2}}\right)^2 - |\,C_{12}\,|^2\right]^{1/2} \qquad (19)$$

where:

$$\beta_{01} = \frac{\omega}{u_{01}} - \frac{\omega_q}{u_0} = \frac{\omega}{u_{01}} - \beta_q$$

$$\beta_{02} = \frac{\omega}{u_{02}} + \frac{\omega_q}{u_0} = \frac{\omega}{u_{02}} + \beta_q.$$

Defining:

$$u_{01} = u_0(1-b)$$

$$u_{02} = u_0(1+b)$$

$$\beta_{1,2} = \beta_e(1+\delta_{1,2}), \qquad x = \frac{b\beta_e}{\beta_q}$$

and assuming

$$b^2 \ll 1, \qquad \frac{\beta_p}{\beta_e} < 1, \qquad \beta_p = \beta_q$$

leads to:

$$\delta_{1,2} = \pm\frac{\beta_p}{\beta_e}\,[(1+x^2) - (1+4x^2+4x)^{1/2}]^{1/2}. \qquad (20)$$

The "classical" small signal analysis yields:[4]

$$\delta_{1,2} = \pm\frac{\beta_p}{\beta_e}\,[(1+x^2) - (1+4x^2)^{1/2}]^{1/2}. \qquad (21)$$

[4] A. B. Haeff, "The electron-wave tube—a novel method of generation and amplification of microwave energy," Proc. IRE, vol. 37, pp. 4–10; January, 1949.

The difference between the two results is believed to be due to the failure of our two-mode picture to take into account the two extreme modes. Some of the differences are shown in Table I.

TABLE I

Feature	Small Signal (Haeff)	Coupled Modes (Two-Modes Approximation)
Maximum Gain at	$x = \frac{1}{2}\sqrt{3}$	$x = 1.0$
Maximum Gain of	$\frac{1}{2}(\omega_p/\omega)$ nepers	ω_p/ω nepers
Gain Obtained for	$0 < x < \sqrt{2}$	$0 < x < 2$

We are aware of the fact that this problem has been recently solved in a more formal manner by Haus of M.I.T. We believe that the approximate perturbation solution given here may still prove useful.

Acknowledgment

The author takes pleasure in acknowledging many helpful suggestions and discussions with Prof. J. R. Whinnery.

Amnon Yariv
Electronics Res. Lab.
University of California
Berkeley, Calif.

Effect of Beam Coupling Coefficient on Broad-Band Operation of Multicavity Klystrons*

To meet some of the requirements of present-day electronic systems, attention has recently been focused on the problem of broad-band operation of multicavity klystrons.[1-7] The major advantages of using broad-band multicavity klystrons at high-power levels (in comparison with a TWT operating over the same bandwidth) presumably are 1) no backward wave is present (as the multicavity-klystron structure is not bilateral) and the attenuator problem (which is present in a TWT) may be eliminated, and 2) possible better efficiency in the case of a multicavity klystron than in a TWT. This statement is based on the fact that under synchronously tuned conditions, a typical high-power klystron can have an efficiency in the neighborhood of 40 per cent.

In a discussion of broad-band operation of multicavity klystrons, one comes across the question: "Under what conditions is the broad-band operation of multicavity klystrons profitable?"

A suitable starting point for a discussion of the above problem is the relation

$$V^{(0)} = MZ^{(0)}i \qquad (1)$$

where M and $Z^{(0)}$ are the beam coupling coefficient and shunt impedance of the output cavity, respectively, and i is the ac current in the beam at the entrance to the output cavity. We note that the maximum voltage across the output gap $V_{\max}^{(0)}$ which we can best use is the dc voltage of the beam V_0; this is so because, for any value of $V^{(0)}$ larger than the dc beam voltage V_0, electrons would be reflected at the output gap and they will travel toward the input. It is also known that $i_{\max}$ (the maximum ac current in the beam at the output gap) is approximately equal to the dc current (for instance under ballistic assumptions $i_{\max} = 1.16I$).

Hence, under the optimum conditions for power transfer from the output cavity, we may write

$$V^{(0)} \approx V_0 \approx MZ^{(0)}I \qquad (2)$$

or

$$Z^{(0)} \approx Z_0 \qquad (2a)$$

when

$$M \approx 1$$

$$Z_0 = \frac{V_0}{I}.$$

Z_0 being the dc beam impedance, and I the dc current of the beam at input.

We may also write

$$Z^{(0)} = (R/Q)_0 Q_L^{(0)} \qquad (3)$$

where $(R/Q)_0$ and $Q_L^{(0)}$ are the values of R/Q and Q of the output cavity under loaded conditions. From (3) we note that for optimum performance $Q_L^{(0)}$ is specified when once the beam voltage V_0 and dc beam current I are specified. In practice, however, the relation $Z^{(0)} \approx Z_0$ is not always satisfied. Many klystron engineers choose values of $Q_L^{(0)}$ based on experience which are at variance with the above simple relation. Actually the shunt impedance across the output gap is made several times the value of beam impedance Z_0 at higher frequencies. We note that as $Z^{(0)}$ goes up the value of $Q_L^{(0)}$ goes up or equivalently $Q_E^{(0)}$ goes up ($Q_E^{(0)}$ being the external Q of the output cavity).

Since RF power is extracted from the output cavity, it is clear that the same (the output cavity) determines the bandwidth over which efficient power transfer can be effected.

We will now discuss the problem as follows. The bunched beam as it enters the output gap exhibits a velocity distribution which in turn alters the value of the beam coupling coefficient considerably. The usual value of beam coupling coefficient M for a *gridless gap* is given by

* Received by the IRE, May 19, 1958.

[1] K. H. Kreuchen, B. A. Auld, and N. E. Dixon, "A study of the broadband frequency response of the multicavity klystron amplifier," *J. Electronics*, vol. 2, p. 529; May, 1957.

[2] L. D. Smullin and A. Bers, "Stagger Tuned Multicavity Klystron," Conference on Electron Tube Res., Berkeley, Calif.; 1957.

[3] S. V. Yadavalli, "Application of the potential analog in multicavity klystron design and operation," Proc. IRE, vol. 45, pp. 1286–1287; September, 1957. Also presented in collaboration with C. A. Arnold and J. P. Lindley at the Conference on Electron Tube Res., 1957.

[4] W. J. Dodds, T. Moreno, and W. J. McBride, Jr., "Methods of increasing bandwidth of high power microwave amplifiers," 1957 WESCON Convention Record, pt. 3, pp. 101–110.

[5] W. L. Beaver, R. L. Jepsen, and R. L. Walter, "Wide band klystron amplifiers," 1957 WESCON Convention Record, pt. 3, pp. 111–113.

[6] P. G. R. King, "A five per cent bandwidth 2.5 mw s-band klystron," *SERL Tech. J.*, vol. 8, p. 29; January, 1958.

[7] H. T. Curnow, "Factors influencing the design of multicavity klystrons," *SERL Tech. J.*, vol. 8, p. 42; January, 1958.

$$M = \frac{I_0(\gamma_0 r_0)}{I_0(\gamma_0 b_0)} \frac{\sin \omega d g/2u_0}{\omega d g/2u_0} \tag{4}$$

where:

I_0 denotes a Bessel function

γ_0 = the radial propagation constant

$$\left(\gamma_0 = \frac{\omega}{u_0}\sqrt{1 - u_0^2/c^2}\right)$$

u_0 = dc beam velocity corresponding to the dc voltage V_0

ω = the operating frequency, c the velocity of light

d_g = the gap length,

r_0 and b_0 = the radii of the beam and drift tube, respectively.

In calculating the loaded $Q(Q_L^{(0)})$ of the output cavity for optimum performance, we need to use the average value of the beam coupling coefficient. If the velocity distribution of the bunched beam is specified by a probability distribution $P(u)$, assuming the velocity distribution is uniform over the beam cross section, we can write the average beam coupling coefficient as

$$\langle M\rangle_{av} = \frac{1}{N+1}\sum_{n=0}^{N}\left\{\int_{u_1}^{u_2} \frac{I_0(\gamma R_n)}{I_0(\gamma b_0)} \frac{\sin \omega d g/2u}{\omega d g/2u}\cdot P(u)du\right\} \tag{5}$$

where N is the number of equal parts into where r_0 is divided $R_n = nr_0/N$, n is a dummy index, d_g is the output gap length, u is the beam velocity and

$$\gamma = \frac{\omega}{u}\sqrt{1 - u^2/c^2}.$$

We also have $\int_{u_1}^{u_2} P(u)du = 1$, where u_1 and u_2 are the lowest and highest velocities of the electrons in the beam. Employing the velocity distributions near saturation obtained by Webber[8] recently, the above value of $\langle M\rangle_{av}$ has been computed for several cases. One should remember that there are two types of velocity distributions of interest here, 1) as the beam enters and 2) as the beam leaves the output gap. That is, we can calculate two types of average beam coupling coefficients $\langle M\rangle_{av}{}^i$ and $\langle M\rangle_{av}{}^o$ where the superscripts i and o denote the corresponding velocity distributions employed whether at *input* or *output* of the output gap. Wherever Webber's distributions were not available, estimates have been made regarding the velocity distribution.

As the power output is proportional to $\langle M\rangle^2 i^2$, one is essentially interested in a plot of $\langle M\rangle^{-2} i^{-2}$. All the computations have been reduced to a plot of $Z^{(0)}/Z_0$ vs $\gamma_0 r_0$. In Fig. 1 it is assumed that the gap transit angle is

$$60^\circ \left(= \frac{\omega d g}{u_0}\right),$$

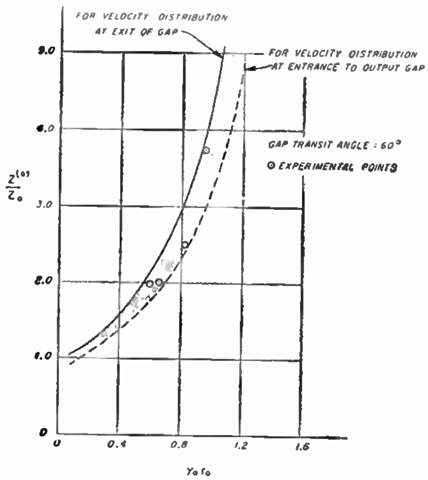

Fig. 1—Plot of normalized output gap impedance vs $\gamma_0 r_0$.

and the RF current in the beam is $1\cdot 1I$. Two curves are shown corresponding to the two limiting velocity distributions in Fig. 1; some experimental points observed in this laboratory and elsewhere are also shown here for comparison. We may indicate here that if one uses the velocity distribution at the middle of the gap in the calculation of $\langle M\rangle_{av}$ we should be able to predict the value of shunt impedance (across the output cavity) very close to the actual value which in turn determines $Q_L^{(0)}$ and $Q_E^{(0)}$ when the unloaded Q of the cavity is known.

In practice the beam radii that are chosen in klystrons operating at different frequencies are such that $\gamma_0 r_0$ goes up with frequency. As mentioned before $Z^{(0)} = kZ_0$ where k is usually greater than unity. We conclude then that it is better to build broad-band klystrons with small $\gamma_0 r_0$. To state differently, this means that for a given value of Γ_0 1) it is better to build broadband multicavity klystrons at lower frequencies (that is, a broad-band multicavity klystron at L band would be more profitable than the one at S band as far as bandwidth and efficiency are concerned) and 2) it is better to operate broadband multicavity klystrons at higher voltages (also higher perveances) than the synchronously tuned klystrons.

S. V. Yadavalli
General Electric Microwave Lab.
Palo Alto, Calif.

[8] S. E. Webber, "Ballistic Analysis of a Two-Cavity Ferrite Beam Klystron," G. E. Res. Lab., Palo Alto, Calif., Rep. No. 57-RL-1721; April, 1957. Also see. "Large Signal Analysis of the Multi-cavity Klystron," G. E. Res. Lab., Palo Alto, Calif., Memo Rep. No. EE-39; June, 1957. There is additional unpublished work. These calculations were carried out on electronic computers IBM 704 and 650.

Improvements in Some Bounds on Transient Responses*

Consider a system function $Z(s)$ of a lumped, linear, fixed, finite, and stable network, all of whose poles have negative (nonzero) real parts. Moreover, assuming that the number of poles of $Z(s)$ is equal to or greater than the number of zeros of $Z(s)$, this rational system function may be expanded into the following infinite series, for s is sufficiently large.

$$Z(s) = K + \frac{1}{Cs} + \frac{K_2}{s^2} + \cdots.$$

In the neighborhood of $s=0$, $Z(s)$ may be represented by

$$Z(s) = r + k_1 s + k_2 s^2 + \cdots.$$

It has been shown recently that when the real frequency responses ($s=j\omega$) of $Z(s)$ are restricted in various ways, the corresponding transient responses are bounded. The purpose of this note is to report improvements on some of these results. In particular, denoting the real part of the system function at real frequencies by $R(\omega)$ and the corresponding response to a unit impulse of current applied at $t=0$ by $W(t)$, these two functions may be related by the following Fourier cosine transform:

$$W(t) = \frac{2}{\pi}\int_0^\infty R(\omega)\cos\omega t d\omega, \qquad t \geq 0.$$

In this case, the specific result which is to be improved is given by theorem 2 of Zemanian[1] wherein bounds on $W(t)$ are given when $R(\omega)$ is monotonic decreasing for $\omega \geq 0$. The improved result is stated by the following theorem. Both the upper and lower bounds are now best possible so that no further improvement can be made.

Theorem: If $Z(s)$ is a system function satisfying the aforementioned restrictions, if the number of poles of $Z(s)$ is one greater than the number of its zeros, and if $R(\omega)$ is monotonic decreasing for $\omega \geq 0$, then the lowest possible upper bound on all unit impulses corresponding to such $Z(s)$ is

$$W(t) \leq \frac{1}{C}\cdot\frac{\sin\dfrac{\pi t}{2rC}}{\dfrac{\pi t}{2rC}} \qquad for\ 0 \leq t \leq rC$$

and

$$W(t) \leq \frac{2r}{\pi t} \qquad for\ rC \leq t$$

and the greatest possible lower is

$$W(t) \geq \frac{1}{C}\cdot\frac{\sin\theta_1}{\theta_1} \qquad for\ 0 < t \leq \frac{2rC\theta_1}{\pi},$$

$$W(t) \geq \frac{1}{C}\cdot\frac{\sin\dfrac{\pi t}{2rC}}{\dfrac{\pi t}{2rC}} \qquad for\ \frac{2rC\theta_1}{\pi} \leq t \leq 3rC.$$

and

$$W(t) \geq -\frac{2r}{\pi t} \qquad for\ 3rC \leq t$$

where θ_1 is the number satisfying $\theta_1 = \tan\theta_1$ and $\pi < \theta_1 < 3\pi/2$ (that is, $\theta_1 = 4.49 \cdots$).

Proof of this theorem has been published elsewhere[2] and will not be repeated here.

It should be pointed out that this result applies to any two variables that are related by the Fourier cosine transform. For in-

* Received by the IRE, May 19, 1958.

[1] A. H. Zemanian, "Further bounds existing on the transient responses of various types of networks," Proc. IRE, vol. 43, pp. 322–326; March, 1955.

[2] A. H. Zemanian, "Bounds on the Fourier transforms of monotonic functions," *Duke Math. J.*, vol. 24, pp. 499–504; December, 1957.

stance, if the symbol $R(\omega)$ represents the power-density function of a random signal, then $W(t)/4$ will represent the corresponding autocorrelation function.

This property of the Fourier cosine transform may be applied to the response $A(t)$ of a network to a unit step of current applied at $t=0$, since $A(t)$ is related to the imaginary part $I(\omega)$ of the system impedance at real frequencies by the following expression.

$$A(t) = r + \frac{2}{\pi}\int_0^\infty \frac{I(\omega)}{\omega}\cos \omega t d\omega, \quad t \geq 0.$$

This leads to the following theorem whose proof is practically the same. The stated bounds are, once again, best possible.

Theorem: If $Z(s)$ is a system function satisfying the aforementioned restrictions and if $I(\omega)/\omega$ is monotonic increasing for $\omega \geq 0$, then the lowest possible upper bound on all unit step responses corresponding to such $Z(s)$ is

$$A(t) \leq r - (r-K)\frac{\sin \theta_1}{\theta_1}$$

$$\text{for } 0 < t \leq \frac{2\theta_1 k_1}{\pi(r-K)},$$

$$A(t) \leq r - (r-K)\frac{\sin \dfrac{\pi(r-K)t}{2k_1}}{\dfrac{\pi(r-K)t}{2k_1}}$$

$$\text{for } \frac{2\theta_1 k_1}{\pi(r-K)} \leq t \leq \frac{3k_1}{(r-K)},$$

and

$$A(t) \leq r + \frac{2k_1}{\pi t} \qquad \text{for } \frac{3k_1}{(r-K)} \leq t$$

and the greatest possible lower bound is

$$A(t) \geq r - (r-K)\frac{\sin \dfrac{\pi(r-K)t}{2k_1}}{\dfrac{\pi(r-K)t}{2k_1}}$$

$$\text{for } 0 \leq t \leq \frac{k_1}{(r-K)}$$

and

$$A(t) \geq r - \frac{2k_1}{\pi t} \qquad \text{for } \frac{k_1}{(r-K)} \leq t$$

where θ_1 is defined in the first theorem.

An immediate consequence of this theorem is that, for system functions of the stated type, the overshoot of the unit step response—defined as the greatest value of $[A(t)-r]/r$—is never greater than $|\sin \theta_1/\theta_1| = 0.2172$ and the rise time from $t=0$ to the time when the unit step response first equals r has no positive lower bound.

Finally, a similar result is shown to hold on any two variables that are related by the Fourier sine transforms.[2] However, this result is not readily applicable to the unit impulse response since it assumes that the imaginary part of the system function is monotonic decreasing for positive ω. This is impossible for the networks considered here.

ARMEN H. ZEMANIAN
Dept. of Elec. Eng.
New York University
New York, N.Y.

Geometric-Analytic Theory of Noisy Two-Port Networks*

In two recent notes in this journal[1,2] an outline on the manner in which the Cayley-Klein model of three-dimensional hyperbolic space can be used in studying problems dealing with bilateral two-port networks was presented. By a stereographic transformation, points in the complex impedance plane were mapped on the surface of the unit sphere constituting the absolute surface of the Cayley-Klein model. Now a natural question is: "What physical interpretation can we give to points *inside* the surface of the unit sphere?" The answer is that these points may be thought of as corresponding to noise-power ratios. Thus, noise-power ratio transformations through noise-free bilateral two-port networks can be geometrically represented by non-Euclidean transformations in models of three-dimensional hyperbolic space. The special case of impedance transformations through noise-free bilateral two-port networks is obtained as non-Euclidean transformations of points on the absolute surfaces of the different models.

The input voltage V' and the input current I' of a noise-free bilateral two-port network are linearly related to the output voltage V and the output current I:

$$\psi' = \begin{pmatrix} V' \\ I' \end{pmatrix} = \begin{pmatrix} a & b \\ c & d \end{pmatrix}\begin{pmatrix} V \\ I \end{pmatrix} = T\psi,$$

$$ad - bc = 1. \tag{1}$$

The input impedance $Z' = V'/I'$ is expressed in terms of the output impedance $Z = V/I$ by the linear fractional transformation:

$$Z' = \frac{aZ+b}{cZ+d}. \tag{2}$$

For a noise process, transformed by a noise-free two-port network, (1) and (2) are exchanged for

$$Q' = \begin{pmatrix} Q_1' \\ Q_2' \\ Q_3' \\ Q_4' \end{pmatrix} = \begin{pmatrix} \overline{V'V'^*} \\ \overline{V'I'^*} \\ \overline{V'^*I'} \\ \overline{I'I'^*} \end{pmatrix} = \begin{pmatrix} aa^* & ab^* & ba^* & bb^* \\ ac^* & ad^* & bc^* & bd^* \\ ca^* & cb^* & da^* & db^* \\ cc^* & cd^* & dc^* & dd^* \end{pmatrix}\begin{pmatrix} \overline{VV^*} \\ \overline{VI^*} \\ \overline{V^*I} \\ \overline{II^*} \end{pmatrix} \tag{3}$$

and

$$s'^2 = \frac{Q_1'}{Q_4'} = \frac{aa^*s^2 + ab^*Z_{cor} + ba^*Z^*_{cor} + bb^*}{cc^*s^2 + cd^*Z_{cor} + dc^*Z^*_{cor} + dd^*} \tag{4a}$$

$$Z'_{cor} = \frac{Q_2'}{Q_4'} = \frac{ac^*s^2 + ad^*Z_{cor} + bc^*Z^*_{cor} + bd^*}{cc^*s^2 + cd^*Z_{cor} + dc^*Z^*_{cor} + dd^*} \tag{4b}$$

$$Z'^*_{cor} = \frac{Q_3'}{Q_4'} = \frac{ca^*s^2 + cb^*Z_{cor} + da^*Z^*_{cor} + db^*}{cc^*s^2 + cd^*Z_{cor} + dc^*Z^*_{cor} + dd^*}. \tag{4c}$$

Asterisks indicate the complex conjugate of the designated quantities and bars indicate averages over an ensemble of noise processes with identical statistical properties.

In the case of complete correlation, $s^2 = ZZ^*$, with $Z_{cor} = Z$, and (4a) reduces to $s'^2 = Z'Z'^*$, with $Z'_{cor} = Z'$; (4b) reduces to (2), and (4c) reduces to the complex conjugate of (2).

The four-vector Q in (3) is analogous to the "Stokes vector" used by Stokes in 1852 in characterizing partially polarized light. The 4×4 matrix in (3) has been used in optics by Soleillet, Perrin, Chandrasekhar, Mueller, Parke, and others. It is the Kronecker product, $T\times T^*$, of the 2×2 matrix T in (1). The components of the Q vector are the components of a 2×2 Hermitian coherency matrix analogous to the "density matrix" introduced in quantum mechanics by von Neumann, and the "coherency matrix" introduced in optics by Wiener.

The conformal transformation (4) can be considered to be a non-Euclidean transformation in a Poincaré model of three-dimensional hyperbolic space having the Z_{cor} plane as the absolute surface. The transformation has been thoroughly studied by Poincaré,[3] Picard,[4] Fricke and Klein,[5] and others.

Eqs. (3) and (4) have been used as the basis of a general theory of noisy two-port networks.[6] Among the topics treated are a wave representation of noisy two-ports (with the introduction of a complex correlation-reflection coefficient), the equivalent noisy network of Rothe and Dahlke,[7] and a cascade of noisy two-port networks.

If the Q vector is expressed in terms of Rothe and Dalke's equivalent noise resistance r_n, equivalent noise conductance g_n, and complex correlation impedance Z_{cor}, we obtain

$$Q = 4kT_0\Delta f g_n \begin{pmatrix} \dfrac{r_n}{g_n} + |Z_{cor}|^2 \\ Z_{cor} \\ Z^*_{cor} \\ 1 \end{pmatrix} \tag{5}$$

* Received by the IRE, May 19, 1958.

[1] E. F. Bolinder, "Noisy and noise-free two-port networks treated by the isometric circle method," PROC. IRE, vol. 45, pp. 1412–1413; October, 1957.
[2] E. F. Bolinder, "Radio engineering use of the Cayley-Klein model of three-dimensional hyperbolic space," to be published.
[3] H. Poincaré, "Mémoire sur les groupes Kleinéens," *Acta Mat.*, vol. 3, pp. 49–92; 1883.
[4] E. Picard, "Sur un groupe de transformations des points de l'espace situés du même côte d'un plan," *Bull. Soc. Math. Franc*, vol. 12, pp. 43–47; 1884.
[5] R. Fricke and F. Klein, "Vorlesungen über die Theorie der automorphen Functionen," B. G. Teubner Verlag, Leipzig, Germany, vol. 1; 1897.
[6] E. F. Bolinder, "Theory of noisy two-port networks," presented at the URSI-IRE meeting, Washington, D. C.; April 23–26, 1958.
[7] H. Rothe and W. Dahlke, "Theory of noisy fourpoles," PROC. IRE, vol. 44, pp. 811–818; June, 1956; "Theorie rauschender Vierpole," *Arch. Elekt. Übertr.*, vol. 9, pp. 117–121; March, 1955.

where k is Boltzmann's constant, T_0 is the absolute temperature, and Δf is the bandwidth.

A complete presentation of the geometric-analytic theory of noisy two-port networks will be given elsewhere.

E. FOLKE BOLINDER
Electromagnetic Radiation Lab.
Air Force Cambridge Res. Center
Bedford, Mass.
Formerly at Res. Lab. of Electronics
Mass. Inst. Tech.
Cambridge, Mass.

Comparison of Phase Difference and Doppler Shift Measurements for Studying Ionospheric Fine Structure Using Earth Satellites*

In using signals from earth satellites to investigate ionospheric fine structure, it would appear that at least two approaches might be used. One is the technique of measuring continuously the phase difference of signals received over slightly different paths (spaced receiving antennas), and the second is that of examining the Doppler shift on the frequency of a single signal.

The basic differences in the two techniques can be best illustrated by neglecting terms due to gross geometrical effects (which can be eliminated in the recording process by a number of techniques). In Fig. 1, two antennas spaced by a distance Z receive signals from source S. The propagation medium is considered essentially constant except for a region whose thickness is small compared to the height H of the source.

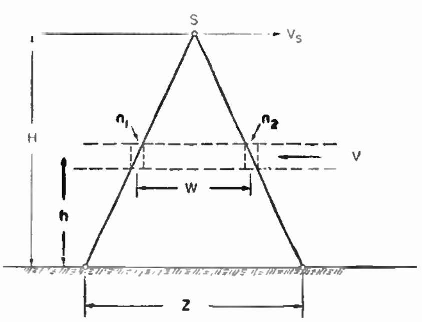

Fig. 1—Simplified geometry for phase difference measurements.

(This assumption is included mainly to permit considering the two rays as parallel during their transit through the layer.) The motion of the source is now replaced by assuming a velocity V of the layer.

The phase difference between the two signals is:

$$\alpha(n) = \phi_1 - \phi_2 = \frac{2\pi L}{\lambda_0}(n_1 - n_2).$$

* Received by the IRE, June 2, 1958.

The geometric paths, L, are considered of equal lengths, and n_1 and n_2 are the effective refractive indexes for the two rays in the layer.

If we consider one component of the index structure

$$n_i = A_i \sin k_i x, \ \left(k_i = \frac{2\pi}{\lambda_i}\right)$$

in terms of the assumed layer velocity V, the time variation of α will be

$$\alpha_i(t) = \frac{2\pi L}{\lambda_0} A_i [\sin \omega_i t - \sin \omega_i (t + \tau)]$$

where

$$\omega_i \tau = \frac{2\pi W}{\lambda_i} \quad \text{and} \quad W = Z\left(1 - \frac{h}{H}\right).$$

Removing the time function $\sin \omega_i t$, this may be written as

$$\alpha_i = \frac{2\pi L}{\lambda_0} A_i 2 \sin \frac{\omega_i \tau}{2} = \frac{2\pi L}{\lambda_0} A_i 2 \sin \frac{\pi W}{\lambda_i} \qquad (1)$$

indicating that such recordings of phase difference are insensitive to certain discrete wavelengths in the medium depending upon the antenna spacing and other geometry. That is, for any wavelength λ_p for which W/λ_p is integral, the quantity α will not contain a contribution from A_p.

To examine the similar property of the Doppler frequency shift, we differentiate, with respect to time, the phase of the signal received at one antenna. Thus

$$\Delta f = \frac{1}{2\pi} \frac{d}{dt}\left[\frac{2\pi L}{\lambda_0} n\right]$$

$$\Delta f = \frac{L}{\lambda_0} \frac{dn}{dt}.$$

Again, examining the contribution of ith component and replacing x by Vt, we obtain:

$$\Delta f = \frac{L}{\lambda_0} A_i k_i V \cos k_i V t = \frac{L}{\lambda_0} A_i \frac{2\pi V}{\lambda_i} \cos \omega_i t.$$

Removing the time function $\cos \omega_i t$, this becomes

$$\Delta f = \frac{2\pi L}{\lambda_0} A_i \frac{V}{\lambda_i} \qquad (2)$$

indicating that in the limit of very long wavelengths in the index structure (λ_i) and in the case of zero velocity of the layer (V) the Doppler produces no information concerning the amplitude A_i of the ith component. However, (2) states that the "sensitivity" is inversely proportional to the wavelength λ_i and thus becomes greater for shorter components. This, of course, is very desirable from the standpoint of fine structure experiments.

Fig. 2 plots both (1) and (2) for comparison. The added scale on the abscissa is based on an assumed physical situation to indicate the order of the effects expected in the case of a satellite.

The clearly defined minima predicted in the phase records are not seen in similar

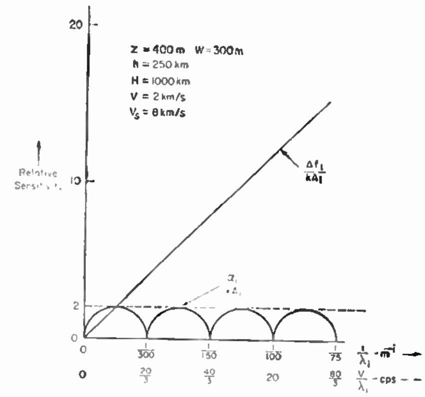

Fig. 2—Relative response of phase difference and Doppler measurements to different spatial wavelengths of ionospheric turbulence for simplified case.

measurements in the troposphere[1] and would not actually be expected for the ionosphere. This may be interpreted as indicating that the turbulence occurs throughout a sufficient range of the paths so that the superposition of many effective values of W results in smoothing out the nulls indicated for the simple case.

An important practical consideration in comparing the two approaches is the frequency stability of the satellite transmitter. In the observations of phase difference, frequency variations do not enter as a first-order effect. In contrast, since the Doppler measurements are primarily a frequency measurement, fluctuations in transmitter frequency are indistinguishable from the ionospheric effects to be measured.

The foregoing is intended only as a preliminary consideration because the final practical answer as to what technique is more desirable in a given case depends upon additional factors, such as the actual performance available in instruments for measuring phase differences and frequency differences.

M. C. THOMPSON, JR.
D. M. WATERS
Natl. Bur. of Standards
Boulder, Colo.

[1] J. W. Herbstreit and M. C. Thompson, Jr., "Measurements of the phase of radio waves received over transmission paths with electrical lengths varying as a result of atmospheric turbulence," PROC. IRE, vol. 43, pp. 1391-1401; October, 1955.

AM Transmitters As SSB Jammers*

In recent months much has been written concerning the advantages of using SSB in preference to AM for radiotelephone service. Power comparisons which have been made between these two systems have yielded a variety of decibel gain figures in favor of SSB. It is quite apparent that if one is skilled at making assumptions, decibel gain

* Received by the IRE, June 2, 1958.

figures suitable for almost any occasion may be obtained. It is pointless to debate this issue since the calculations are almost always correct leaving only the assumptions (which are a matter of personal judgment) as the subject for controversy.

While it must be conceded that a suppressed-carrier SSB system will generally show a power gain when compared with an equivalent AM system in a communications circuit, a rather dramatic change takes place when the AM transmitter is used as a jammer *against* the SSB transmitter. It is my purpose here to demonstrate that an AM transmitter, if properly used, can be quite effective as an SSB jammer.

For purposes of discussion let us assume that we are to jam a 1-kilowatt (peak envelope power output) suppressed-carrier SSB transmitter and that we are given a 125-watt (carrier output) AM transmitter with which to do the job. Antenna gains and propagation conditions for both the SSB and AM units must be chosen as identical. Now, how do we use the AM transmitter and what degree of success may we expect in our efforts to jam the SSB circuit?

The answer to the first part of this question is quite simple. Since the SSB receiver responds to RF signals in a band extending from, let us say, 300 to 3000 cycles away from the SSB carrier frequency, we must set the AM jammer frequency and choose a form of modulation for the AM transmitter which will produce the highest possible average RF power in this 2700-cycle pass band. Thus, we set the AM carrier frequency in the center of the SSB pass band (1650 cycles away from the SSB carrier frequency) and modulate with a square wave of fundamental frequency, say, 100 cycles and upper frequency limit of 1350 cycles. Such a square wave will be sufficiently "square" to yield very nearly 125 watts of average sideband power and together with the 125 watts of average carrier power we will have a total of 250 watts of average jamming power falling in the SSB pass band. (Perhaps a more direct way of arriving at this result is to visualize the jammer signal in the time domain. With square-wave modulation we have no output half of the time and twice the carrier voltage level the other half of the time. Thus, we have 500 watts being radiated with a 50 per cent duty cycle yielding 250 watts of average power.)

In order to estimate the degree of success which may be expected with our available 250 watts of average jamming power, we must determine the average sideband power which will result from speech modulation of the 1-kilowatt SSB transmitter. Admittedly, any choice for the peak-to-average power ratio for voice SSB that we may make will be subject to challenge. If one attempts to pick a mean of the figures which have been published, a four-to-one ratio would probably be a reasonable one. In other words, an SSB transmitter having one kilowatt of peak-power capability will radiate an average power of 250 watts when voice modulated. Thus, we see that the 125-watt AM transmitter can be quite effective as an SSB jammer since its use can result in a signal-to-jamming average power ratio of unity at the output terminals of the SSB receiver.

The situation outlined above is quite significant, not only because of the power ratios but also because of the cost ratios which are involved. What defensive measures does SSB then offer against this type of jamming? There are perhaps two types of action which may be taken by the SSB operators, neither of which offers an effective solution. First, the obvious (and that is the trouble) thing to do is to switch sidebands when jammed. This requires some coordination between transmitter and receiver and in addition such action will be expected and carefully watched for by the jammer. When we realize that "changing sidebands" in SSB is equivalent to changing the operating frequency we see that SSB offers no special advantage in this regard. Secondly, a narrow-band rejection or "notch" filter could be installed in the SSB receiver to take out the AM carrier heterodyne. In the case cited above, such action would cut the jammer's effectiveness by two-to-one in average power or 3 db. However, such tunable filters are seldom employed in SSB receivers outside the amateur field, probably because of the skill and attention which is required of the operator for satisfactory results. (On the other hand, without such filters the SSB system becomes quite vulnerable to straight continuous-wave jamming; a situation which makes the communications equipment-to-jamming equipment cost ratio even larger.) Although one might wish to argue the details of what is given above, the basic premise that an AM transmitter can be quite effective as a jammer against SSB seems secure.

In closing, it is somewhat interesting to observe that in the previous example a signal-to-jamming average power ratio of unity, or zero db, at the output of the receiver was obtained by using a 125-watt AM transmitter against a 1-kilowatt SSB transmitter. I shall resist the temptation of computing the AM power advantage in decibels.

JOHN P. COSTAS
209 Palmer Drive
Fayetteville, N. Y.

Taper Sections in Circular Waveguides*

Solymar[1] has discussed the determination of the TE_{0n} modes distribution produced by a conical tapered transaction between two circular waveguides.

In the writer's doctorate dissertation in electrical engineering[2] the same structure, among other problems, was considered. The problem was approached in a different manner but the results obtained were essentially the same as those obtained by Solymar.

The field in the tapered section has been represented as superposition of modes of the cylindrical guide and the generalized telegraphist's equations[3] have been derived. The TE_{01} mode is found to be coupled only with TE_{0n} modes. The coupling is expressed by the voltage and current transfer coefficients which decrease as n increases.

Assume the following:

1) structure without losses,
2) cone of small aperture,
3) diameters of the two guides to be connected not very different and much larger than the cutoff diameters for the TE_{01} and TE_{02} modes,
4) only first-order approximation considered,
5) reflections at the junctions at the tapered section neglected,
6) all the energy carried by the TE_{01} mode in the input guide.

For the excitation of the TE_{02} mode a formula practically identical to the one given by Solymar is obtained; the only difference is that in place of the factor a/λ there is the factor $(a+b)/2(\lambda_{01}\lambda_{02})^{1/2}$ where a and b are the radii of the two guides and λ_{01} and λ_{02}, the wavelengths for the TE_{01} and TE_{02} modes in a guide of radius $(a+b)/2$.

It may not be out of place here to mention that using the telegraphist's equations approach to calculate the variation of the propagation constants due to the imperfect conductivity of the walls and the mode conversion due to curves in the circular guides, the writer[2] has found results essentially identical with those obtained by Oswald[4] and Jouguet,[5] who used a different approach.

GIORGIO GEROSA
Electrotechnical Institute
University of Rome
Rome, Italy

* Received by the IRE, June 2, 1958.

[1] L. Solymar, "Design of a conical taper in circular waveguide system supporting H_{01} mode," PROC. IRE, vol. 46, pp. 618–619; March, 1958.

[2] G. Gerosa, "Study of a very long feeding system for a microwave lens aerial using a circular waveguide propagating TE_{01} mode," Electrotechnical Institute, University of Rome, Italy; March 31, 1956.

[3] S. A. Schelkunoff, "Conversion of Maxwell's equations into generalized telegraphist's equations," *Bell Sys. Tech. J.*, vol. 34, pp. 995–1043; September, 1955.

[4] J. Oswald, "Calcul des pertes par effet joule dans les guides d'ondes," *Cables & Transm.*, vol. 1, pp. 205–219; October, 1947.

[5] M. Jouguet, "Les effets de la courbure sur la propagation des ondes électromagnétiques dans les guides à section circulaire," *Cables & Transm.*, vol. 1, pp. 133–153; July, 1947.

Common Emitter Transistor Amplifiers*

The recent letter from Dion[1] pointing out the equivalence of an emitter follower and a common emitter amplifier with resistance in series with the base is interesting. There is, however, a further point that should be considered: the gain stability in the two cases.

As has been shown,[2] the gain stability of a transistor amplifier depends upon the re-

* Received by the IRE, June 16, 1958.

[1] D. F. Dion, "Common emitter transistor amplifiers," PROC. IRE, vol. 46, p. 920; May, 1958.

[2] R. F. Purton, "Transistor amplifiers: common base versus common emitter," *ATE J.*, vol. 14, pp. 157–163; April, 1958.

sistances in series with its electrodes. The most variable transistor parameter both from unit to unit and with respect to frequency and ambient variations is probably α_{fe}. The power gain stability against variation in α_{fe} is improved by resistance in series with the emitter (emitter feedback), but is worsened by resistance in series with the base. The emitter follower arrangement is, therefore, preferable on this account.

The stabilities can be calculated as follows. If it is assumed that the input resistance is arranged to match the source resistance, then the circuits for the two cases are as shown in Fig. 1, with

$$R_G = R + R'_{IN} = \alpha_{fe} R_L. \qquad (1)$$

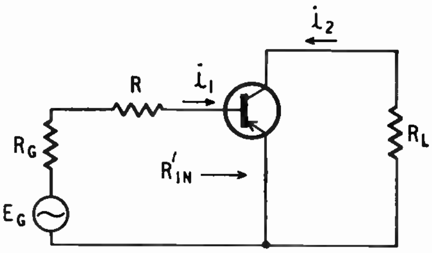

(a)

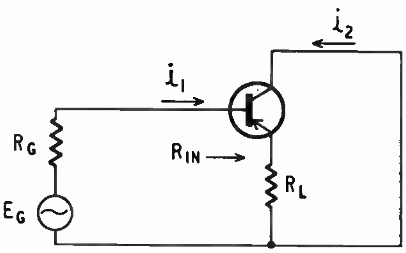

(b)

Fig. 1—(a) Common emitter amplifier with input resistance increased by addition of R. (b) Emitter follower amplifier.

For the common emitter amplifier, transducer power gain is

$$G_1 = \alpha_{fe}^2 i_1^2 R_L \cdot \frac{4R_G}{E_G^2} \cdot$$

$$= \alpha_{fe}^2 \cdot \frac{E_G^2 \cdot R_L}{(R_G + R + R_{IN}')^2} \cdot \frac{4R_G}{E_G^2}$$

$$= \frac{4R_L R_G}{(R_G + R + R_{IN}')^2} \cdot \alpha_{fe}^2. \qquad (2)$$

Therefore, from (1), $G_1 = \alpha_{fe}$ as shown by Dion. Also, from (2),

$$\frac{dG_1}{G_1} = \frac{2\alpha_{fe} d\alpha_{fe}}{\alpha_{fe}^2} = \frac{2d\alpha_{fe}}{\alpha_{fe}}, \qquad (3)$$

i.e., a given percentage change in α_{fe} will produce twice this change in G_1.

For the emitter follower

$$G_2 = \alpha_{fe}^2 \frac{E_G^2 \cdot R_L}{(R_G + \alpha_{fe} R_L)^2} \cdot \frac{4R_G}{E_G^2}$$

$$= \frac{4R_L R_G}{(R_G + \alpha_{fe} R_L)^2} \cdot \alpha_{fe}^2. \qquad (4)$$

Therefore again from (1) $G_2 = \alpha_{fe}$.

From (4)

$$\frac{dG_2}{G_2} = \frac{2R_G}{(R_G + \alpha_{fe} R_L)} \cdot \frac{d\alpha_{fe}}{\alpha_{fe}} \cdot$$

Therefore from (1)

$$\frac{dG_2}{G_2} = \frac{d\alpha_{fe}}{\alpha_{fe}} \cdot$$

That is, the gain variation is only half that of the previous case.

It should be noted that both stabilities are poor—at least as bad as α_{fe} itself. This is because of the high source resistance in series with the base.

R. F. Purton
British Telecommun. Res. Ltd.
Taplow, Berks., England

Resonance-Probability and Entropy-Evolution Relationships*

Resonance-Probability

For some time now I have had the intuitive feeling that the Q of a tuned circuit, and the σ (standard deviation) of a probability distribution are close kin. Resonance curves seem to be a special class of probability curves. If so, there should be a whole family of analogies, whereby the many probability concepts have a running mate in an ac tuned circuit arrangement. In plain words, is there a basic underlying concept that covers both resonance effects and probability response? I think so, but so far I can't prove it. If ac circuits behavior is truly analogous to probability response, then ac circuits can provide a simple solution of complex problems in probability and statistics.

I have never found anything in the literature on the similarities between ac circuit response and probability. Just what is the probability counterpart of frequency? Of inductance? Of capacitance? Of resistance? Of Q? Does any one know? Is it worth following up?

Entropy-Evolution

The second concept that has disturbed my sleep of late is, what appears to me to be the amazing "face" correlation between cybernetic *entropy*, and organic evolution. Whereas thermodynamics uses *entropy* as an index of the unavailability of heat, cybernetics uses *entropy* in a broader sense: an index of the state of disorganization in any "system," be it organic, mechanical, or even semantic. Cybernetics shows that any state of organization tends toward disorganization; there is a natural tendency for order to downgrade toward disorder, that is, *entropy*, the index of disorder, always tends to increase.

Now, natural evolution is the process by which increased organization takes place; greater specialization results in time. More or less random variations fall into specialized patterns, which continue. So evolution is anti-entropic. The trend is from the scrambled to the organized; the ordered; the specialized.

In most cases, "nature" dictates that every state of organization tends toward breakdown, whether gradually or fast. In some unique cases, this apparent universal rule has the opposite polarity. From chaos, order and system sets in. It seems to me that "normal" cybernetic entropy and "normal" organic evolution are one and the same; except that entropy works in a + direction (toward breakdown) when cybernetics is considered, and in a − direction (toward improvement) when evolution is considered.

What I want to know is, what factors determine whether a "system" (machine or living thing) tends to breakdown or to build up? If we knew, then machines could be designed that have capabilities to improve their mode of operation as they work.

George H. Amber
Amber and Amber
Detroit 35, Mich.

* Received by the IRE, April 25, 1958; revised manuscript received, June 26, 1958.

The Dependence of Minority Carrier Lifetime on Majority Carrier Density*

In a recent letter Chang[1] has derived a simple relationship between the ratio of the diffusion length of holes in an n region to that of electrons in an adjacent p region and the ratio of the conductivities of the regions. This derivation was based on the assumption that the minority carrier lifetime is inversely proportional to the majority carrier density. This is only true under certain conditions which are discussed below.

We shall confine our attention to the semiconductors for which it has been shown that the recombination process can be described by the statistics of Shockley and Read,[2] *viz.*, germanium[3] and silicon.[4,5] The low-level lifetime of the minority carriers, assuming a small density of recombination centers with a single recombination level, for the four possible cases which can arise is shown in Table I. τ_n and τ_p are the lifetimes of electrons and holes as minority carriers. τ_{no} is the lifetime of electrons injected into a highly p-type specimen; τ_{po} is the lifetime of holes injected into a highly n-type specimen. n_o and p_o are the thermal equilibrium electron and hole densities; n_1 and p_1 are the values the electron and hole densities

* Received by the IRE, June 9, 1958. This note is published by permission of the Dir. of Radio Res. of the Dept. of Sci. and Indus. Res., Eng.

[1] S. S. L. Chang, "Relation between ratio of diffusion lengths of minority carriers and ratio of conductivities," Proc. IRE, vol. 45, pp. 1019–1020; July, 1957.

[2] W. Shockley and W. T. Read, "Statistics of the recombinations of holes and electrons," *Phys. Rev.*, vol. 87, pp. 835–842; September 1, 1952.

[3] J. A. Burton, *et al.*, "Effect of nickel and copper impurities on the recombination of holes and electrons in germanium," *J. Phys. Chem.*, vol. 57, pp. 853–859; November, 1953.

[4] G. Bemski, "Lifetime of electrons in p-type silicon," *Phys. Rev.*, vol. 100, pp. 523–524; October 15, 1955.

[5] C. A. Bittmann and G. Bemski, "Lifetime in pulled silicon crystals," *J. Appl. Phys.*, vol. 28, pp. 1423–1426; December, 1957.

TABLE I

E_R in Upper Half of Energy Gap		E_R in Lower Half of Energy Gap	
Case 1: p-type	Case 2: n-type	Case 3: p-type	Case 4: n-type
$\tau_n=\tau_{no}+\tau_{po}n_1/p_o$ Provided that: for silicon $(E_F-E_V)\ge(E_c-E_R)$ or germanium $(E_F-E_V)>(E_c-E_R)$ by more than $3\frac{1}{2}\,kT$ then $\tau_n\simeq\tau_{po}n_1/p_o$*	$\tau_p=\tau_{po}(1+n_1/n_o)$ Provided that: $(E_R-E_F)>0$ by more than $1\frac{1}{2}\,kT$ for both silicon and germanium then $\tau_p\simeq\tau_{po}n_1/n_o$*	$\tau_n=\tau_{no}(1+p_1/p_o)$ Provided that: $(E_F-E_R)>0$ by more than $1\frac{1}{2}\,kT$ for both silicon and germanium then $\tau_n\simeq\tau_{no}p_1/p_o$*	$\tau_p=\tau_{po}+\tau_{no}p_1/n_o$ Provided that: for silicon $(E_c-E_F)>(E_F-E_V)$ by more than 3 kT; for germanium $(E_c-E_F)\ge(E_R-E_V)$ then $\tau_p\simeq\tau_{no}p_1/n_o$*

* The above inequalities are based on a maximum error in the approximation of about 25 per cent.

TABLE II

	Case 3: p-type		Case 4: n-type	
	(E_R-E_V) in ev	Resistivity in ohm-cm	(E_R-E_V) in ev	Resistivity in ohm-cm
Germanium	0.048[6] 0.2[7] 0.27[3]	>0.02 >6 Invalid*	0.2[7] 0.27[3]	>0.3 >5
Silicon	0.065[8]† 0.09[9]‡ 0.14[9]‡ 0.17[5] 0.2[4]‡	>0.1 >0.3 >2 >6 >20	0.055[8]†, 0.063[9]‡, 0.067[9]‡ 0.1[9]‡ 0.17[5,10]‡ 0.22[5,11]	>0.02 >0.05 >20 >125

* The expressions for the minority carrier lifetime in Table I apply only to extrinsic material.
† In transistors.
‡ In diodes.

would have if the Fermi level were located at the same position in energy as the recombination centers. The energy level of the recombination centers is denoted by E_R, the thermal equilibrium position of the Fermi level being denoted by E_F. Fig. 1 shows the position of the Fermi level, as a function of resistivity in germanium and silicon. The values for the mobilities were taken from the published literature and the densities of states were calculated using effective masses determined from cyclotron resonance data, viz., $M_e=0.55M_o$, $M_h=0.37M_o$ for germanium; $M_e=0.27M_o$, $M_h=0.39M_o$ for silicon.

Fig. 1 shows the location of the main recombination levels in germanium and silicon. These levels have been attributed to the presence of copper atoms. All the recombination levels are shown in the lower half of the energy gap since the published literature suggests that this is the case. It is assumed in Table I that τ_{no} is about ten times τ_{po} for germanium,[3] and that τ_{po} is nine times τ_{no} for silicon.[5]

It can be seen from Table I and Fig. 1 that the general requirement for the assumption that the minority carrier lifetime is inversely proportional to the majority carrier density to be valid is, in all four cases, that the recombination levels lie near the appropriate band edge and/or that the semiconductor should be only weakly extrinsic.

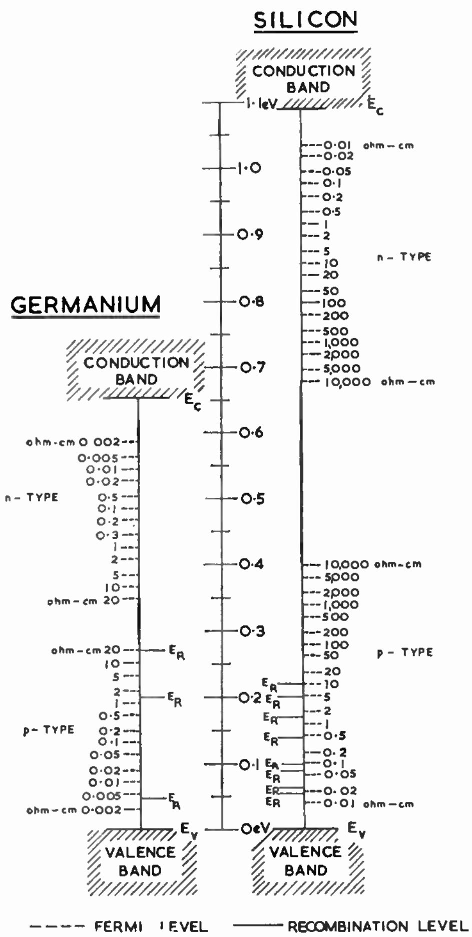

Fig. 1—Energy levels in germanium and silicon at 300°K.

Table II, relating to cases 3 and 4, which are those of interest, shows the resistivity ranges for which the assumption is valid for the main recombination levels reported for germanium and silicon.

[6] M. S. Rideout, "The Temperature Dependence of Minority Carrier Lifetime in p-Type Germanium and Silicon," Rep. of the Meeting on Semiconductors (Physical Society and B.T.H., Ltd., Rugby, England), pp. 33–37; April, 1956.
[7] R. G. Shulman and B. T. Wyluda, "Copper in germanium: recombination center and trapping center," *Phys. Rev.*, vol. 102, pp. 1455–1457; June 15, 1956.
[8] D. M. Evans, "The measurement of the temperature dependence of the mobility and effective lifetime of minority carriers in the base region of silicon transistors," to be published.
[9] B. Ross and J. R. Madigan, "Thermal generation of recombination centres in silicon," *Phys. Rev.*, vol. 108, pp. 1428–1433; December 15, 1957.
[10] D. J. Sandiford and J. Shields, "Reverse Currents and Carrier Lifetimes in Silicon p-n Junctions," Rep. of the Meeting on Semiconductors (Physical Society and B.T.H., Ltd., Rugby, England), pp. 49–54; April, 1956.
[11] D. M. Evans, unpublished.

In Table II, for the recombination levels shown in the first two lines for n-type silicon, it is assumed that τ_{no} is $2.75\tau_{po}$.[9]

D. M. Evans
Dept. of Sci. and Indus. Res.
Radio Res. Station,
Slough, Bucks, England

The Internal Current Gain of Drift Transistors*

For diffusion-type (homogeneous-base) transistors the common-base internal short-circuit current gain α_d can be specified in terms of two parameters. These are $f_{\alpha d}$, its internal cutoff frequency, and α_{do}, its zero-frequency value,[1] both of which depend on a single dimensionless parameter $\omega W^2/2D$ (for a unidimensional model). Here ω is the angular frequency, W the active base width of the transistor, and D the diffusion constant for minority carriers in the base. For drift (inhomogeneous-base) transistors this is no longer the case, because the value of α_d depends in effect on *two* dimensionless parameters $\omega W^2/2D$ and $\Delta V/kT$; the latter is the relative drift potential across the base.

Although measurements of the external complex current transmission under finite termination conditions are possible,[2,3] and from these the internal complex current gain may be determined, such measurements involve specialized and costly equipment, which is not always readily available. The purpose of the present note is to show that a complete specification of the internal current gain of a drift transistor can be obtained using a relatively simple method.

If the complex theoretical loci of α_d are calculated from Kroemer's theory,[4] in terms of $\omega W^2/2D$ and $\Delta V/kT$, which may be regarded as disposable parameters,[5] it is found that there is a direct relationship between the ratio $f_{\alpha d}/f_1$ and $\Delta V/kT$, where f_1 is the frequency at which the modulus of the common-emitter internal short-circuit current gain β has a value of unity.[6] This relationship is shown in Fig. 1 for values of $\Delta V/kT$ up to eight. It is clear, therefore, that for such practical drift transistors as conform to the theoretical model, we may determine $\Delta V/kT$

* Received by the IRE, June 4, 1958. The work described here was carried out as a part of the program of the Radio Res. Board. It is published by permission of the Dir. of Radio Res. of the Dept. of Sci. and Indus. Res.
[1] R. L. Pritchard, "Frequency variations of current amplification factor for junction transistors," Proc. IRE, vol. 40, pp. 1476–1481; November, 1952.
[2] F. J. Hyde and R. W. Smith, "An investigation of the current gain of transistors at frequencies up to 150 mc/s," *Proc. IEE*, vol. 105B, pp. 221–228; 1958.
[3] H. G. Follingstad, "Complete linear characterization of transistors from low through very high frequencies," IRE Trans. on Instrumentation, vol. I-6, pp. 49–63, March, 1957.
[4] H. Kroemer, "The drift transistor," in "Transistors I," RCA Labs., Princeton, N. J., p. 202; 1956.
[5] F. J. Hyde, "An investigation of the current gain of a drift transistor at frequencies up to 105 mc/s," *Proc. IEE*, to be published.
[6] In a private communication from L. G. Cripps, it was shown that f_1 is also the frequency at which the real part of α_d has a value of ½.

TABLE I
CURRENT GAIN DATA OF COMMERCIAL DRIFT TRANSISTORS

Transistor		2N247 No. 1	2N247 No. 2	2N247 No. 3	2N247 No. 4	2N384
Measured f_α; mc		40	35	41.5	43	92.5
Measured $f_{1\beta}$; mc		24	20	26.5	26.5	50
$f_\alpha/f_{1\beta}$		1.67	1.75	1.57	1.62	1.85
ΔV	From above value of $f_\alpha/f_{1\beta}$	5.0	5.75	4.0	4.5	6.75
kT	From analysis of complex α and α_d	5.0	5.5	4.0	4.0	7.0
Measured values of c_e; pF		100	50	80	80	35
$\omega c_e r_e'$ at $I_e=2.0$ ma		0.31	0.14	0.26	0.27	0.25

from the ratio $f_{\alpha d}/f_1$. If α_{d0}, $f_{\alpha d}$, and $\Delta V/kT$ are known, then α_d may be specified at any frequency, by fitting the data to a family of universal curves for α_d.[5]

Now in practice $f_{\alpha d}$ and f_1 cannot be measured directly because they are "internal" parameters. We may readily measure the corresponding external parameters, however, which will be designated f_α and $f_{1\beta}$, respectively. The effects of the ohmic base resistance r_{bb}' and collector depletion-layer capacitance c_c on the relationships between f_α and $f_{\alpha d}$ and between f_1 and $f_{1\beta}$ are small for the drift transistor.[5] That of the emitter depletion-layer capacitance c_e can be made small by operating at a high value of direct emitter current I_e. Too high a value of I_e, however, will give rise to high-level injection and heating effects which should be avoided.

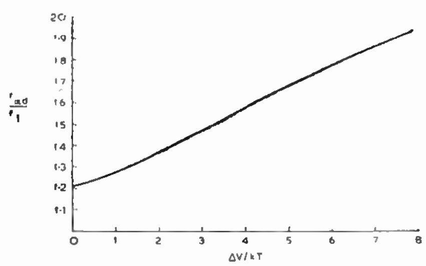

Fig. 1—Dependence of the ratio $f_{\alpha d}/f_1$ on $\Delta V/kT$.

Provided that the dc operating condition is suitably chosen, we may then use the ratio $f_\alpha/f_{1\beta}$ instead of $f_{\alpha d}/f_1$ to determine $\Delta V/kT$ from Fig. 1. The extent of the approximation involved in ignoring the effect of c_e may be estimated from (1), which shows the relationship between the measured near-short-circuit external current gain α and α_d as affected by c_e,

$$\alpha_d = \alpha(1 + j\omega c_e/y_i). \qquad (1)$$

Here y_i is the internal short-circuit emitter input admittance for the common-base connection, and is complex. It may be calculated from theory using data obtained from low-frequency measurements[5] of β, or to a first approximation it may be replaced by $1/r_e'$ where r_e' is given by $25/I_e$ ohms when I_e is in milliamperes. c_e may be measured by one of several methods to be described in a later publication. The condition required for $f_\alpha \simeq f_{\alpha d}$ and $f_{1\beta} \simeq f_1$ is that $\omega c_e r_e' \ll 1$ at the frequencies in question. The condition for $f_\alpha/f_{1\beta}$ to be approximately equal to $f_{\alpha d}/f_1$ is less stringent, because ratios are involved and the corrections to f_α and $f_{1\beta}$ to obtain $f_{\alpha d}$ and f_1, respectively, are both in the same sense. Results are presented in Table I for four 2N247-type transistors ($I_e=2.0$ ma, $V_c=-9.0$ volts) and one 2N384-type transistor ($I_e=2.0$ ma, $V_c=-12$ volts). The values of $\Delta V/kT$ in the fourth row have been determined from the ratio $f_\alpha/f_{1\beta}$ and Fig. 1. Those in the fifth row have been obtained from a detailed analysis of the loci of the complex external current gain,[5] which were measured by a twin-channel comparator method[2] in the frequency range 1–105 mc. The two sets of data are seen to be in good agreement.

In the penultimate row the values of emitter depletion-layer capacitance are shown and in the last row, the values of $\omega c_e r_e'$. From these values it may be estimated that the ratio $f_\alpha/f_{1\beta}$ should not differ greatly from $f_{\alpha d}/f_1$.

The internal consistency of the results is such as to suggest that the transistor types investigated conform to Kroemer's simple model and that the value of $\Delta V/kT$ and hence α_d at any frequency may be readily determined.

F. J. HYDE
Dept. of Sci. and Indus. Res.
Radio Res. Station,
Slough, Bucks, England

Theory of Diode and Transistor Noise*

The representation of noise in junction diodes and transistors above the $1/f$ range by superposition of a thermal noise source (Nyquist) and a current generator (Schottky noise source) has recently been used extensively.[1–3]

The theory is based upon independent carrier motion and one-dimensional diffusion process:

$$D_p \frac{\partial^2 p}{\partial x^2} = \frac{\partial p}{\partial t} - \frac{p - p_n}{\tau_p} \qquad (1)$$

with $(p-p_n)$ = excess-hole concentration (p_n = equilibrium concentration), τ_p = lifetime, and D_p = hole-diffusion constant.

Using the transmission line analogy or other formalism, the following equation for the noise current can be derived:

$$\overline{i^2} = 4kTGdf - 2eIdf \text{ (usual notations)} \qquad (2)$$

with G = junction conductance, I = junction current (positive for forward, negative for backward bias).

The assumptions in this case exclude, *e.g.*, high-current regions or a more complicated geometry as in the case of point-contact diodes.[4]

It might be interesting to note that a similar representation was used years ago for point-contact devices.[4] The difference was, roughly speaking, based on the assumption of a shot-noise current uncorrelated and additive to the Nyquist noise of the differential resistance. This leads to

$$\overline{i^2} = 4kTG\Delta f + 2e|I|df. \qquad (3)$$

$|I|$ = absolute current value in both directions.[4]

This expression can be derived on the basis of an equivalent network for a barrier with an exponential current-voltage relation of the form $I_f = kV^n + \rho V$, and was based on noise-factor measurements on many of the available point-contact diodes (Ge and Si). A law for the dynamic case was also derived which was especially useful for the mixer case;[5] the equivalent dynamic noise factor, p, which correlates the diode noise to the Nyquist noise of the differential resistance, is

$$p(\theta) = A + \frac{20}{\pi} V \left[\frac{n+1}{n} \sin\theta + \left(\pi - \frac{n+1}{n}\theta \right) \cos\theta \right] \qquad (4)$$

when V = exploration voltage, A = constant, n = exponent of characteristic, and θ = angle of current flow.

The higher noise current of point-contact diodes, and the deviations of the $I(V)$ characteristics from the Schottky-Wagner form[6]

$$I = I_0(e^{\alpha V} - 1)$$

with $\alpha = 40$ volts^{-1} are considered in the multicontact theory[7] which made it necessary to assume uncorrelated noise contributions as in (3). In this case the semiconductor noise

* Received by the IRE, May 27, 1958.

[1] A. van der Ziel and A. T. Becking, "Theory of junction diode and junction transistor noise," PROC. IRE, vol. 46, pp. 589–594; March, 1958.

[2] A. Uhlir, "High-frequency shot noise in *p-n* junctions," PROC. IRE, vol. 44, p. 557; April, 1956, correction, p. 1541; November, 1956.

[3] W. Guggenbühl and M. J. O. Strutt, "Theorie des Hochfrequenzrauschens von Transistoren bei kleinen Stromdichten," *Nachrichtentechn. Fachberichte*, vol. 5, pp. 30–33; 1956.

W. Guggenbühl and M. J. O. Strutt, "Theory and experiments on shot noise in semiconductor junction diodes and transistors," PROC. IRE, vol. 45, pp. 839–854; June, 1957.

[4] H. F. Mataré, "Das Rauschen von Dioden und Detektoren im statischen und dynamischen Zustand," *Elek. Nach. Tech.*, vol. 19, pp. 111–126; 1942. "Bruit de fond des diodes à cristal," *Onde elect.*, vol. 29, pp. 231–240; June, 1949, and "Statistische Schwankungen in Halbleitern," *Z. Naturf.*, vol. 4, pp. 275–283; 1949.

[5] H. F. Mataré, "Bruit de fond de semiconducteurs I," *J. Phys. Radium*, vol. 8, pp. 364–372; December, 1949, and "Bruit de fond de semiconducteurs II," vol. 11, pp. 130–140; March, 1950. "Empfangsprobleme im Ultrahochfrequenzgebiet," Verlag R. Oldenbourg, Munich, Ger.; 1951.

[6] H. A. Bethe, "Theory of the boundary layer of crystal rectifiers," RL Report No. 43-12; November 23, 1942.

[7] H. J. Yearian, "DC characteristics of silicon and germanium point contact crystal rectifiers," *Brit. J. Appl. Phys.*, vol. 21, pp. 187–221, and "The multicontact theory, Part II," vol. 21, pp. 283–289, 1950.

can also be calculated on the basis of an appropriate equivalent network.[4] This scheme was used later to calculate harmonics mixing and reinforcement with Ge and Si point-contact diodes.[8]

Apparently the approach used in (3) for junctions should be applied, for which the restrictive assumptions leading to (2) are not fulfilled, *e.g.*, in the case of high-current densities (power devices) and more complicated contact geometrics when the individual noise currents of parallel junctions are not correlated.

H. F. MATARÉ
Solid-State Res. Lab.
Sylvania Electric Products, Inc.
Bayside, N. Y.

[8] H. F. Mataré, "Oberwellenmischung und Verzerrung mit Kristalldioden," *Arch. elekt. Übertr.*, vol. 7, pp. 1–15; 1953.

Dispersion of High-Frequency Elastic Waves in Thin Plates*

In a recent application of the theory of elastic waves in thin plates to ultrasonic delay lines, Mapleton[1] has reviewed most of the mathematical phases of the problem.

On comparing his calculations with our own work, the following extension was derived which is of practical value. The primary problem in transmission of ultrasonic energy is to consider the effects of dispersion on the delay time and reproducibility of the pulse. It should be emphasized that the dispersion effects noted below are not intrinsic in the medium as in optical materials but are introduced by the boundary conditions.

The first solution of the shear waves discussed by Mapleton is of the most importance, and his frequency equation may be considerably simplified by suitable approximations. The first is $\Delta^2=\beta^2=k_T^2-k^2$ to yield

$$4\alpha\beta k^2 \sinh(h\beta) + (\beta^2-k^2)\tanh(\alpha h)\cos\beta h = 0. \quad (1)$$

On dividing through by k^4 and rearranging terms and eliminating β and α

$$\tan\left[\pi(2\psi\Delta-1)/2\Delta\right] = 4\left[1-\xi(1+\Delta^2)\right]^{1/2}/(1-\Delta^2)^2 \cdot \coth\pi\psi\left[1-\xi(1+\Delta^2)\right]^{1/2} \quad (2)$$

where

$$\psi=\frac{2hf}{v} \quad \text{and} \quad \xi=\left(\frac{v_t}{v_L}\right)^2$$

and $2h$ = thickness of plate, f = frequency, and v = velocity of wave.

For the large values of the argument y, coth y approaches 1.00 as a limit; and with the condition Δ is a small quantity, only relatively constant terms are on the right side of (2). For fused quartz, the constant H is 3.004, and since the tangent is a cyclic function with period π, successive values of Δ_n satisfying the transcendental equation may be had:

$$\tan\tfrac{1}{2}\pi\left[2\psi\Delta_n-(2n+1)/\Delta_n\right] = H \quad \text{where } n = 0, 1, 2, 3 \cdots. \quad (3)$$

As Δ_n is small, the tangent may be expanded: $\tan y = y + y^3/3! + \cdots$ and only the first term retained.

$$\Delta_n = (n+\tfrac{1}{2})/\psi(1-H/\psi\pi). \quad (4)$$

Now if $v/v_t=1+\delta$ from the expansion of β^2, $\delta_n=\frac{1}{2}\Delta_n^2$

$$\delta_n = \tfrac{1}{2}\left[(n+\tfrac{1}{2})/(\psi-H/\pi)\right]^2 \quad \text{and for } \psi \gg H/\pi \quad (5)$$

$$\delta_n \approx \tfrac{1}{2}\left[(n+\tfrac{1}{2})/\psi\right]^2 = \tfrac{1}{2}\left[(n+\tfrac{1}{2})v/2hf\right]^2. \quad (5a)$$

Eq. (5) will give the increment in velocity as a function of the order of the mode, frequency, and thickness of plate. The last term may be neglected in many cases as in (5a). Mapleton's frequency equation for the second solution of the shear wave has been similarly treated and gives the even modes in the plate. The compressional cases yield solutions identical in form with the shear cases. Calculations of δ_n based on (5) have agreed with Mapleton's values for the shear case, but plots on log–log papers of his other values against h do not give a straight line with -2 slope for the compressional modes in fused quartz and the single crystal calculations.

The analogy between the elastic vibrations in the plate and the electromagnetic modes in a wave guide is excellent, if more complicated, if it is recalled that Mapleton's work deals with phase velocity, and not the group velocity with which the energy of a pulse is transmitted. The latter turns out to be

$$v_g = (\partial k/\partial\omega)^{-1} = C_T(1-\delta_n). \quad (6)$$

Table I summarizes approximately the dispersion effects in a 1000-μsec line, at 15 mc, 0.636 cm thick, using (5a).

TABLE I

Freq. mc	Delay Mode	Excess—μsec		Number of Cycles Deficit		
	Mode 1	3	5	1	3	5
5	1.86	16.74	48.50	9.00	81	225
10	0.465	4.185	11.625	4.48	40.32	112
15	0.210	1.89	5.25	3.00	27.00	75.0
20	0.116	1.046	2.90	2.24	20.16	55.6
25	0.074	0.667	1.86	1.8	17.1	45.0
30	0.052	0.273	1.31	1.49	13.4	37.2
35	0.032	0.207	0.57	1.28	11.5	32.0

The practical significance of (5) or (5a) lies in the dispersion effects that will arise in thin plates used for wide band delay lines. At 15 mc, Table I shows an excess of 0.210 μsec in the lowest mode and within the band pass from 10–20 mc that may be used for short pulses, the excess varies from 0.42 to 0.12, respectively. This would result in a distorted pulse with a steeper rise than fall.

Furthermore, although no consideration has been paid to the distribution of energy in the different modes, it is evident that these can be excited and conflict with each other. A reasonable assumption might be that the amplitude in each mode after equilibrium has been reached varies as for plane wave excitation. Thus when comparable amounts of energy exist in the different modes, the differences in the cycles delayed should be evident with pass band measurements made under CW or pulsed conditions. Between 10 and 20 megacycles, the lowest two modes differ by 36 and 18 cycles, respectively, so that 18 maxima and minima between 3–8 db departure from a smooth curve in the 10-mc pass band are possible.

Effects of this type have been observed and agree well with the theory after reasonable allowances for other complicating factors are made.

The actual difference in velocity of the different modes may be observed in the longer lines at low frequency. For instance, a 2780 μsec line one half inch thick gave a difference in rise time of 0.8 μsec between 8 and 40 mc while throughout the pass band ripples spaced $\frac{1}{2}$–1 mc apart were seen amounting to 6 db because of the phase relations in the modes. Even with short lines the dispersion effect is noticeable. Several 124 μsec lines had ripples 6–8 mc wide superimposed on the band-pass of the crystal. By good design of crystal excitation and choice of line thickness as well as use of absorbing stops it is possible to suppress these ripples. Delay lines with less than $\frac{1}{4}$-db ripple have been constructed in this laboratory.

DAVID L. ARENBERG
Arenberg Ultrasonic Lab., Inc.
Boston, Mass.

* Received by the IRE, June 25, 1958. This work was supported by the USAF through the Rome Air Dev. Center.

[1] R. E. Mapleton, "Elastic wave propagation in solid media," *J. Appl. Phys.*, vol. 23, pp. 1346–1354; December, 1952.

Computer Fabrication and Circuit Techniques*

Two techniques were developed during the design and construction of a small general purpose digital computer which may be of value to others working in this field. The first is a fabrication technique which obviates the need for super-conducting paths in the plug-in connectors. The control winding of a cryotron can be placed on the stationary unit, and a gate wire which is doubled back on itself to form a hairpin is placed on the plug-in unit. The gate wire acts as the pin and the control winding as the socket of a connector. Coupling between the two is magnetic, and therefore a superconducting connection is not necessary. Information flow from the plug-in unit to the stationary unit requires that the control winding be on the plug-in unit and the gate hairpin on the stationary unit. The only ohmic contacts necessary are the power supply wires, the resistance of which is noncritical.

The second development is a circuit technique which forms a pulse on one of two

* Received by the IRE, July 3, 1958.

wires to indicate a binary ONE or ZERO from a pulse-or-no-pulse representation on a single wire. In many logical circuits the output is frequently obtained in a pulse-or-no-pulse representation, while the two-wire complementary representation may be required by the inputs of the next logical circuit. The circuit described will provide the required conversion, as well as reduce the number of inputs from outside the helium bath. The circuit takes advantage of the ability of a cryotron to switch when a full-amplitude control current occurs and not switch when a half-amplitude control current occurs. The gate wires of two cryotrons are joined, and a pulse applied at the junction. One of the two cryotrons is always resistive. The other is resistive only when an input pulse occurs. The current therefore flows through a superconducting gate wire when no input pulse occurs, and divides equally between two resistive gates when an input pulse does occur. The current can then be routed to the control winding of one cryotron of a second pair of cryotrons in such a way that the cryotron is resistive only when no input pulse occurs. The other cryotron of the second pair of cryotrons therefore contains the information in complementary form.

Fred Herzfeld
RCA Labs.
Princeton, N. J.
Formerly at Computer Comp. and Sys. Lab.
Mass. Inst. Tech.
Cambridge, Mass.

Radiometer Circuits*

In a recent letter to the editor[1] the least detectable noise for a number of radiometer circuits originally described in a previous article[2] was given as follows:

$$\sigma_{1d}^2 = 4\sigma_n^2\sqrt{\frac{\gamma}{\alpha}} \quad \text{sine wave modulation, sine wave multiplier}$$

$$\sigma_{1d}^2 = \pi\sigma_n^2\sqrt{\frac{\gamma}{\alpha}} \quad \text{square wave modulation, sine wave multiplier}$$

$$\sigma_{1d}^2 = 2\sigma_n^2\sqrt{\frac{\gamma}{\alpha}} \quad \text{two receiver cross correlation.}$$

The figure for square wave modulation and square wave multiplier was not given but would be

$$\sigma_{1d}^2 = \frac{8}{\pi}\sigma_n^2\sqrt{\frac{\gamma}{\alpha}}.$$

An alternate system shown in Fig. 1 uses two receivers but one antenna. The signals $y_1(t)$ and $y_2(t)$ both contain receiver noise, which is assumed the same for both receivers. Since there is no correlation between the receiver noises, the output noise power is the sum of the two noise powers. However, the signal due to them is four times that for the case of one receiver. The output signal-to-noise ratio is therefore improved by a factor of 2.

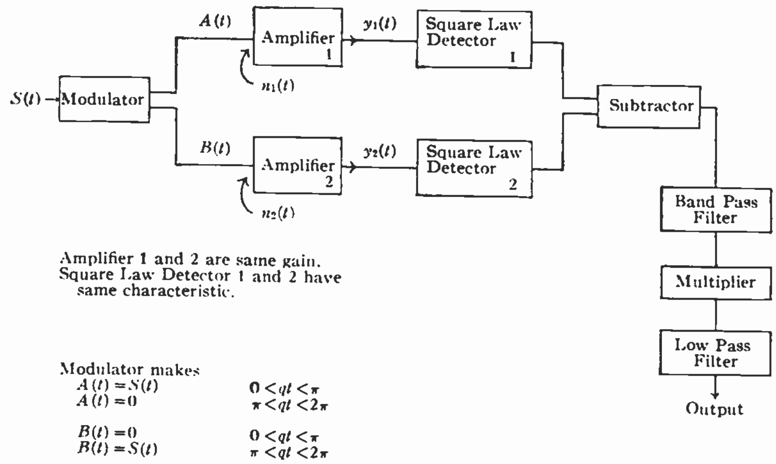

Fig. 1.

The corresponding figures are

$$\sigma_{1d}^2 = \frac{\pi}{2}\sigma_n^2\sqrt{\frac{\gamma}{\alpha}}$$

for modified square wave modulation and sine wave multiplier and

$$\sigma_{1d}^2 = \frac{4}{\pi}\sigma_n^2\sqrt{\frac{\gamma}{\alpha}}$$

for modified square wave modulation and square wave multiplier. This last case is $\pi/2$ or 1.57 times as sensitive as the two receiver cross correlator.

Martin Graham
The Rice Institute
Houston, Tex.

* Received by the IRE, June 23, 1958.

[1] D. G. Tucker, M. H. Graham, and S. J. Goldstein, Jr., "A comparison of two radiometer circuits," Proc. IRE, vol. 45, pp. 365–366; March, 1957.

[2] S. J. Goldstein, "A comparison of two radiometer circuits," Proc. IRE, vol. 43, pp. 1663–1666; November, 1955.

Application of Inductive Probability to Communications*

Inductive Probability

Although probability plays a key role in the study of radar and communication systems, engineers have, for the most part, concerned themselves with only one of its possible meanings. The consequence of this seems to be an unnecessarily restricted point of view which severely limits the usefulness of available information derived from observation. The concept of probability employed by engineers is the frequency concept of mathematical statistics: the relative frequency in the long run of one property of events or things with respect to another. Statements about frequency probability depend upon empirical procedure and the observation of facts.

Although many conceptions of probability are possible, Carnap[1] finds that these can essentially be reduced to two: the frequency concept, and the conception of probability as a certain logical relation between propositions. The latter concept has been termed logical or inductive probability, because its value is determined by logical analysis. This statement does not imply, however, that inductive probability has nothing to do with observational facts. On the contrary, inductive probability is relative to given evidence and has, in fact, two arguments, the hypothesis and the evidence, but since its statements are logically derived, each statement is logically true for each stage of the evidence. It may be interpreted as an estimate of relative frequency and as a fair betting quotient. If the relative frequency itself is known, then the relative frequency is the fair betting quotient

From the point of view of radar and communications, the primary significance of inductive probability is that it avoids the pitfall of frequency probability which results from assigning *a priori* probabilities according to the principle of indifference, *i.e.*, assuming equal *a priori* probabilities in cases of complete ignorance. For example, there are eight possible three-digit, binary sequences, each of which is called a state description. The method of frequency probability is to assign a measure $M(S_i)$ to each state description S_i such that

$$\sum_i M(S_i) = 1$$

with each state description given *a priori* equal measure. On the other hand, the eight possible three-digit, binary sequences can be considered in groups called structure descriptions such that the sequence consisting of three zeros is one structure description, the three sequences consisting of one units digit and two zero digits a second, the three sequences consisting of two units digits and one zero digit a third, and the sequence consisting of three units digits a fourth. The method of inductive probability is to assign a measure $M(S_r)$ to each structure description such that

* Received by the IRE, June 26, 1958.

[1] R. Carnap, "Logical Foundations of Probability," University of Chicago Press, Chicago, Ill.; 1950.

$$\sum_r M(S_r) = 1$$

with each structure description given *a priori* equal measure. Moreover, if the inductive probability of a structure description is p and there are m members of this description, the inductive probability of each member is p/m.

The measure function $M(S_r)$ permits account to be taken of intuitive notions about learning by experience. Thus, if x_1, x_2, x_3, represent a sequence of binary digits, then $P(Ux_3/Ux_2 \text{ and } Ux_1) > P(Ux_2/Ux_1) > P(Ux_1)$ states that the probability of the third digit x_3 being a units' digit U, given that x_2 and x_1 are units' digits is greater than the probability of x_2 being a units' digit, given that x_1 is a units' digit, is greater than the probability of x_1 being a units' digit. Such a statement expresses the notion of the confirmation of a hypothesis by accumulating evidence.

The quantitative statement of inductive probability is given by the degree of confirmation $c^*(h, e_{-}j)$ whose values are real numbers belonging to the interval 0–1. With reference to communications $c^*(h, e_{-}j)$ may be read as the degree of confirmation, based on the available evidence e, for the hypothesis h that the next observation j will be a signal. It is given by the relation

$$c^*(h, e_{-}j) = \frac{s_2 + w_2}{s_1 + w_1 + s_2 + w_2} \tag{1}$$

where s_1 is the number of times the negative attribute is observed, w_1 is the logical width (that is, number of forms of this attribute), s_2 the number of times the positive attribute is observed, and w_2 the logical width of the positive attribute. In the example of the binary sequences a units digit might be called the positive attribute and the zero digit the negative attribute. The attribute appellations could, of course, be reversed if this is desired.

Application of Inductive Probability

Errors in decision caused by use of a finite number of thresholds (usually one) and inappropriate settings of these thresholds limit detection probability, and these factors, plus, under certain conditions, an excessive number of integrations, limit information rate. Currently employed decision methods use constant threshold settings, independent of changing posterior probabilities. Inductive probability affords a means of altering threshold settings, and the consequences to probability of error and information rate will be examined.

In the discussion to follow, it will be assumed that the noise statistics are stationary, and that the signal statistics may vary with time.

A bidirectional, dual threshold communication system has been described elsewhere[2] with a capability for a significant reduction in probability of error, provided the thresholds can be set appropriately. A null zone is created between the two thresholds such that if the peak of a received waveform is within the null zone, the receiver requests the transmitter over a feedback path to repeat the message. If the received waveform is above the upper threshold a positive signal is recorded, if below the lower threshold, a negative signal. In this system there are, therefore, three attributes: the positive signal attribute, the negative signal attribute, and the null or neutral attribute, only the first two of which are recorded. The probability of error of this system can be controlled by the threshold settings. Thus, if the thresholds are widely separated the probability of error is low, but the average number of transmissions per message symbol is high. On the other hand, if the thresholds are brought close together, the probability of error is relatively high but the average transmission time is low. It is found that performance can be considerably improved by integrating successive observations before making a decision, and when integration is combined with decision feedback, the method of operation is called cumulative decision feedback. In any case, the objective is to find that condition of operation which results in maximum information rate. This is, therefore, a problem in the setting of thresholds.

The difficulty with this system is that for a given noise power, but unknown signal amplitude, the appropriate threshold settings are unknown. Hence, a way must be found to estimate what these settings should be. It is suggested that inductive probability can be used to accomplish this result, and for clarification the distinction is drawn between the method of operation just described and the proposed modifications to it. In each case a decision is made about each message symbol as it comes along, but in the first method this is done by making a decision any time the peak of the received waveform is outside the threshold limits, whereas in the new method the decision for or against a positive attribute message symbol is made only after the number of repetitions of the message is sufficient to attain the specified degree of confirmation, with neutral attribute observations unrecorded. Moreover, in the new system the rate of increase in the degree of confirmation may be used to control the separation of the thresholds, that separation being sought which results in the maximum rate of increase. This rate, it will be noted, is controlled by the number of null observations or the one hand and by the concentration in favor of one kind of signal attribute over the other on the other hand, since if the numbers of observations of each kind of attribute remain more or less balanced, the degree of confirmation will remain in the neighborhood of 0.5. In comparing the performance of these two methods, it is noted that the first method arrives at decisions more rapidly than the new method but with threshold settings which may be inappropriate. This may not be serious for large signal-to-noise ratios and, in fact, for these the inductive probability method appears to be inefficient, because it calls for repetitions when they may be unnecessary, but for small signal-to-noise ratios, inappropriate threshold settings must result in poor decisions, although made with relative rapidity.

Leonard S. Schwartz
New York University
New York 53, N. Y.

[2] B. Harris, A. Hauptschein, and L. S. Schwartz, "Optimum decision feedback systems," 1957 IRE National Convention Record, pt. 2, pp. 3–10.

A Transistor-Magnetic Core Binary Counter*

A technique for using transistor-magnetic core combinations to perform digital operations has been described by Guterman and Carey.[1] It is the purpose of this letter to describe an even simpler transistor-magnetic core binary counter that is also useful at counting rates as high as 2×10^6 pulses per second.

The counter consists of transistors and cores connected in such a manner that the count is indicated in binary form by the positive and negative residual magnetizations of the cores. The transistors are used as regenerative amplifiers to change the magnetic state of the cores when an input pulse is applied to the counter.

A single stage of the counter consists of a permalloy core having a rectangular hysteresis loop, a transistor, a silicon diode, and a resistor, all arranged as shown in Fig. 1(a).

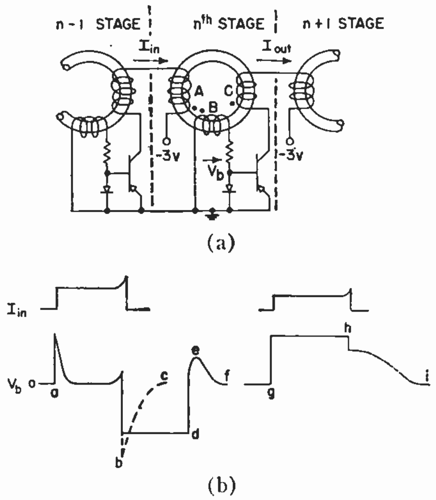

Fig. 1—(a) Circuit of binary counter. (b) Input current and base voltage waveforms.

Each stage of the counter is essentially a blocking oscillator that is triggered by alternate current pulses from the previous stage. For example, an output current pulse from stage $n-1$ [Fig. 1(a)] will trigger stage n if the core n is in the $+B_r$ state, but will not trigger this stage if the core is in the $-B_r$ state. In detail, if core n is in the $+B_r$ state, the current pulse from the previous stage will cause the core flux to change over the path $+B_r$ to $+B_m$ to $+B_r$ (Fig. 2) and produce the voltage a-b-c of Fig. 1(b). The negative voltage at point b is sufficient to trigger the transistor in stage n. The regenerative action of the transistor and core produces the waveform b-d-e-f as the flux in the core changes from $+B_r$ to $-B_m$ to $-B_r$. The next current pulse from stage $n-1$ will change the state of the core from $-B_r$ to $+B_m$ and in so doing will produce a positive voltage in winding B of sufficient duration to produce a large minority carrier storage in the diode. This carrier storage persists long enough to prevent the negative voltage

* Received by the IRE, July 21, 1958.

[1] S. S. Guterman and W. M. Carey, Jr., "A transistor-magnetic core circuit: a new device applied to digital computing techniques," 1955 IRE Convention Record, pt. 4, pp. 84–94.

in winding B (due to the turnoff of the current pulse from the previous stage) from triggering the transistor [see g-h-i of Fig. 1(b)]. The alternate outputs of stage n will trigger the $n+1$ stage in a similar manner.

The duration of the input current pulse to the nth stage can be adjusted so that it is just long enough to saturate the nth core by selecting the proper number of turns for the output winding of the core $n-1$.

An input current pulse of the proper length to operate the first stage of the counter could be obtained from a conventional blocking oscillator. However, the circuit shown in Fig. 3 has two advantages that make it superior to the blocking oscillator, namely, the circuit performs as a binary counter stage, and the duration of the output pulse is controlled by the saturation flux density of the core rather than the transistor parameters. To explain the operation of the circuit, assume that the core is in the $-B_r$ state and that the current I_1 due to the input pulse is in such a direction as to change the core in the direction of $+B_m$ (Fig. 2). The regenerative action of the transistor and core will cause I_1 to continue to flow until the core is saturated at $+B_m$. The base current of T_1 flowing through D_2 will produce sufficient hole storage in D_2 to prevent the triggering of T_2 by the regenerative turnoff of I_1, thus leaving the core in the $+B_r$ state.

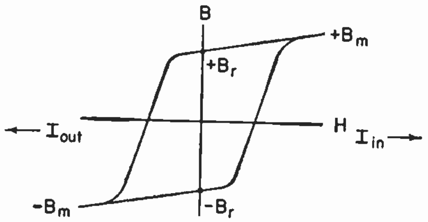

Fig. 2—Hysteresis loop of core.

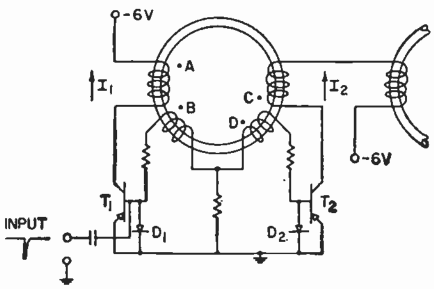

Fig. 3—Input stage for counter.

The current I_1 due to the next input signal will cause the flux to change from $+B_r$ to $+B_m$ in such a short time (approximately 0.1 μsec) that no appreciable hole storage will be developed in D_2. When I_1 turns off, T_2 will be triggered and change the flux in the core from $+B_r$ to $-B_m$. The hole storage in D_1 will prevent the triggering of T_1 by the turnoff of I_2.

If winding c of Fig. 3 is connected directly to the -6 volt supply rather than to the next core, a simple complementing flip-flop circuit is obtained which can be used in an accumulator-type adder circuit and other digital applications.

The circuits described are capable of high counting rates and yet require very little power at low counting rates. For example, a five stage binary counter has a total power consumption of 40 μw when operated at a counting rate of 100 pulses per second. Counting rates as high as 2×10^6 per second have been obtained with commercially available cores. Good reliability is indicated by the fact that the circuit of Fig. 1 has been successfully operated over a temperature range of $-65°$F to $+160°$F with a supply voltage of -2.0 to -4.5 volts.

HENRY R. IRONS
U. S. Naval Ordnance Lab.
White Oak, Silver Spring, Md.

Tropospheric Effects on 6-MC Pulses*

A test was performed at Boulder, Colo., during February, 1958, to make an independent measurement of the virtual height of echoes from a Model C-4 ionosphere recorder. The transmitted pulses from the recorder, of 50-μsec length, were observed at a temporary field site 5.2 km away, using loran equipment. The path ran in a north-south direction along the western edge of a flat plain about one mile above sea level. The land to the west of the path rises to peaks two or three thousand feet higher, and is mountainous with increasing elevation up to the Continental Divide, which has peaks twelve to fourteen thousand feet above sea level at a distance of 20 miles farther west.

In performing the test, the relative delays of the ground pulse and an ionospherically-reflected pulse were compared. For the best comparison, it was desired to adjust conditions so that the two received pulses would be of about the same height on an A-scan presentation and, of course, below receiver saturation.

The plane of the vertical delta transmitting antenna at the C-4 site was oriented normal to the direct path, as was the horizontal dipole at the receiving site. With these antennas and with the ionospheric conditions which prevailed at the time of the test, ground wave and sky wave received pulses were about equal in amplitude near 9 mc. The ground wave pulse was steady and the sky wave slowly fading.

It was desired to obtain another set of observations at 6 mc. At this frequency, and with the antennas as above, the ground pulse was steady but much larger than the sky pulse.

In order to obtain equal ground and sky wave pulse height at 6 mc, a vertical loop antenna was substituted for the dipole and rotated to reduce the ground wave pickup. When the plane of the loop was oriented to a direction almost at right angles to the path for a null in output, the ground wave amplitude suddenly dropped to where it was comparable to that of the sky wave, but at this point it became much more unstable than the sky wave, being characterized by sharp minima within the width of the pulse, which rippled and fluctuated at a rate of several times per second.

When the direct ground wave from the transmitting antenna is discriminated against by the loop antenna, the chief remaining ground wave signal is believed to be of a multipath nature having been scattered from numerous off-path scatterers. The vast mountainous area to the west is considered to be the most probable source of such scatter, with fluctuations producing variable multipath phase interference, which distorts the pulse in the described manner.

RICHARD SILBERSTEIN
Natl. Bur. of Standards
Boulder, Colo.

* Received by the IRE, July 3, 1958.

A New Type of Fading Observable on High-Frequency Radio Transmissions Propagated over Paths Crossing the Magnetic Equator*

During the course of a systematic study of the amplitude variations of the carrier-wave component of short-wave broadcasts propagated over long paths of varying orientations,[1] a type of fading has been identified which to the best of the authors' knowledge has not previously been described in the literature. Although existing data are fragmentary, the effect appears to be worth reporting at the present time in view of its evident importance in the design of high-frequency communications circuits crossing the magnetic equator.

Owing to multipath propagation, an HF carrier wave propagated over long distances via the ionosphere may be expected to fade in such a manner that its amplitude probability distribution is Rayleigh. The received energy is spread out into a spectrum, whose distribution of intensity per unit bandwidth vs frequency is roughly Gaussian. This is known to be generally true for a wide variety of path lengths and orientations.[2]

It is accordingly quite unexpected to encounter a situation in which the received carrier energy appears to be split into two independently fading components of comparable strength, separated in the frequency spectrum by several tens of cycles. The weaker of the two components beats with the stronger, closely resembling a modulation of the latter. Moreover, only two major components are found, and the fre-

* Received by the IRE, July 16, 1958. This work was supported by the AF Cambridge Res. Center, under contract AF-19-604-1830.

[1] K. C. Yeh and O. G. Villard, Jr., "On the fading and attenuation of high-frequency radio waves over a long path crossing the auroral zone," presented at URSI meeting, Washington, D. C.; April, 1958.

[2] G. L. Grisdale, J. G. Morris, and D. S. Palmer, "Fading of long-distance radio signals and a comparison of space—and polarization—diversity reception in the 6–18 mc/s range," *Proc. IEE*, vol. 104, pt. B, pp. 39–51; January, 1957.

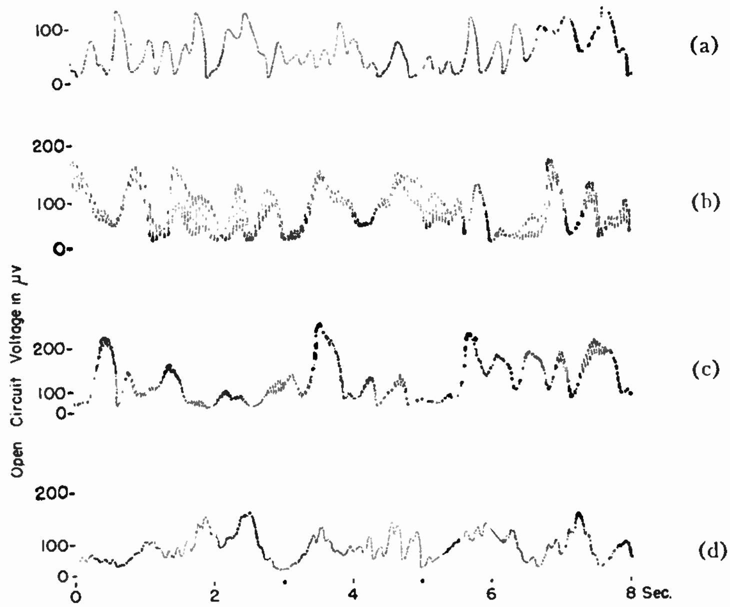

Fig. 1—Typical sequence showing the appearance and disappearance of Doppler fading on BBC's Singapore relay station on 9.690 mc, August 1, 1957. (a) 0250 PST. (b) 0300 PST. (c) 0320 PST. (d) 0335 PST.

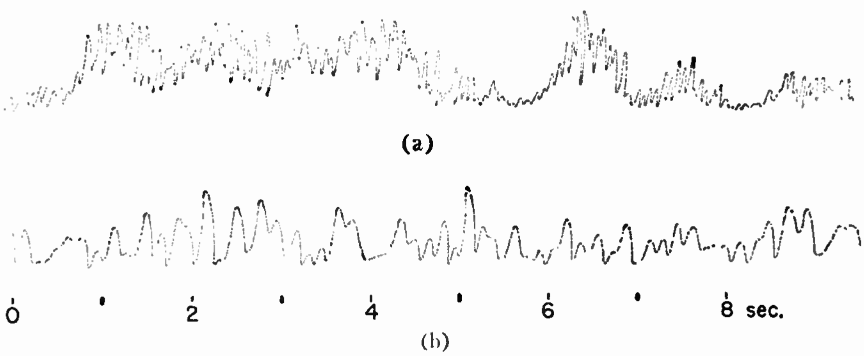

Fig. 2—Example of Doppler fading received simultaneously on two frequencies for BBC's Singapore relay station. 0735 PST, August 26, 1957. (a) 21.655 mc. (b) 9.690 mc.

quency difference between them remains roughly constant for periods of the order of tens of minutes.

This effect has thus far been observed systematically only on signals which have crossed the magnetic equator. Fig. 1 shows a recording of the 9.690-mc transmission of the British Broadcasting Company's Far Eastern Relay Station, located at Singapore, Malaya. It was received at Palo Alto, Calif., via the short great-circle path, on a receiver having an intermediate-frequency bandwidth of the order of 200 cps. The frequency response of the ink recorder extends from zero to roughly 70 cps. This degree of selectivity has been found to be sufficient to reject virtually all program modulation except for infrequently-occurring deep bass notes which are readily recognizable as such.

The fading which is the subject of this communication will be observed as the relatively high-frequency fluctuation noticeable on the records for 0300 and 0320 PST in Fig. 1. It is probable that the effect is also present in the records for 0250 and 0335 PST, but at those times the "beating" frequency—if present—is so close to the individual-component fading frequency that a clear distinction cannot readily be made.

The "beating" frequency has these interesting properties: 1) When recordings can be made of signals from the same station at two radio frequencies simultaneously, the beat frequency is found to be very nearly proportional to the radio frequency. (See Fig. 2.) (During the five occasions on which this fading was observed simultaneously on 9.690 mc and 21.655 mc, the observed beat frequency ratio varied from 2.15 to 2.29 while the radio frequency ratio was 2.23. This circumstance would appear to rule out interference and spurious modulation as a source of the effect; in addition, it would appear that time delays associated with the approach to a critical frequency are also ruled out. 2) The beat frequency remains relatively constant for considerable periods of time, changing appreciably only in intervals of the order of fifteen minutes to half an hour. Because the first of these properties suggests that the fading may be due to the combination of a strongly Doppler-shifted carrier component with an unshifted one, the effect has been tentatively named "Doppler-fading."

The heavy lines in Fig. 3 show the times that this fading was looked for and found on the 9-mc Singapore transmissions during the month of August, 1957. (The light lines indicate the times the effect was looked for but not found.) The transmissions were sampled during the periods shown, at irregular intervals 10 to 20 minutes apart. The station was on the air from 0100 to 0900 PST on 9 and 15 mc, and from 0500 to 0800 PST on 21 mc.

The higher frequencies were also sampled but since the effect was found most consistently on 9.6 mc, most of the observations were made on that frequency.

Rotatable Yagi antennas, roughly two-thirds of a wavelength high, were employed to record the 15 and 21-mc signal; at 9.6 mc a "maypole" arrangement of self-terminating sloping-Vee antennas was used. In all cases, the signal appeared to be coming from the short great-circle direction, as could readily be demonstrated by changing the beam directions.

Although the Doppler fading effect was seen during the month of August almost daily in the case of Singapore, it was found only sporadically in recordings made of Radio Australia (9 and 15 mc), Radio Peking (11 and 15 mc), and Station LRA in Buenos Aires (9 mc). It was not observed at all in a large number of recordings made of stations in England and Europe (9, 11, 15, and 21 mc).

A variation in the daily time of occurrence is suggested by the data of Fig. 3.

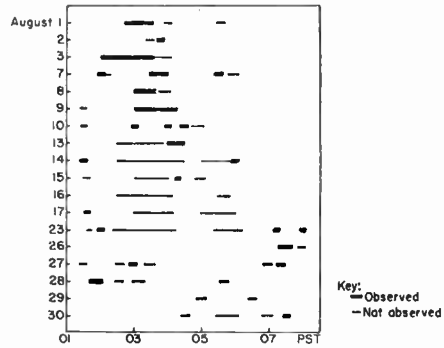

Fig. 3—Time of occurrence of Doppler fading for BBC's Singapore relay station on 9 mc in August, 1957.

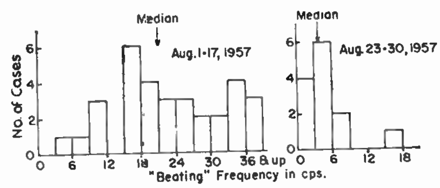

Fig. 4—To illustrate the change in "beating" frequency in August, 1957 for BBC's Singapore station on 9.690 mc.

Fig. 4 illustrates the change in median "beating" frequency which is observed if the data for August 1–17 are compared with those from August 23–30. Although the records taken on any given day are seldom continuous enough to permit a firm conclusion to be drawn, the Doppler beat is typically slow when it first appears, speeding up as time progresses, and slowing down again as the effect disappears. This trend is visible in Fig. 1.

An attempt to observe this fading during one week of observations in January, 1958, yielded only one example.

No determination has been made of the direction of the presumed Doppler shift, and it is not known whether the beating effect is also observed on modulation side frequencies of the carrier wave. However it is a curious fact that presence or absence of the Doppler beating could not readily be determined by listening to the program modulation.

Although the data are too sparse as yet to permit firm conclusions to be drawn, it is tempting to ascribe this fading to a combination of conventional and tilt-supported propagation across the evening equatorial height bulge, as has been proposed by the late Sidney Stein.[3] For example, at Singapore, Osborne[4] reports that the minimum virtual height of the F layer may rise more than 100 km at a rate of 20 to 100 km/hr between 1700 and 2100 local time, depending on the season. One effect of such a marked increase in height—a phenomenon confined to equatorial latitudes—is to make possible tilt-supported ionospheric propagation of the type which involves two or more successive reflections from the F layer without intermediate reflection from the ground.[5] Such tilt-supported propagation modes are often observed simultaneously with conventional multiple earth-ionosphere reflections. If both types of propagation have approximately equal strength, and the path of one varies in electrical length with respect to that of the other, interference effects can be expected which would be similar to those observed. (See Fig. 5.)

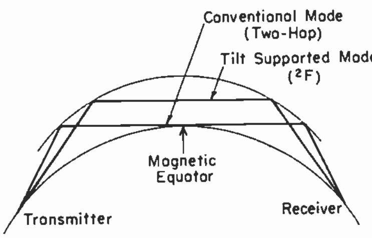

Fig. 5—To illustrate beating of two components of the same signal propagated via two differing modes. (Diagram not to scale.)

In view of the time of day at which the Doppler fading was observed (Singapore time is 9 hours earlier than Palo Alto time), and in view of the fact that paths crossing the magnetic equator are apparently favored, Stein's hypothesis is very tentatively offered in explanation of the present observations.

However, there is considerable difficulty in accounting for the high fading frequencies which have been observed, in view of their relatively long time duration. A relative path length change of roughly 2000 km/hr is required to account for a Doppler shift of 20 cps at a radio frequency of 9.7 mc; it is not easy to imagine a means whereby such a path length change could be maintained for periods of the order of one hour.

It is possible that the present observations may in some way be related to the anomalous fading observed by Subba Rao and Somayajulu.[6] However, their fading is about one order of magnitude slower, is relatively irregular, and is present all night long.

If the equatorial-bulge mode-interference hypothesis is correct, it might be possible to explain the absence of Doppler fading in the case of such stations as Radio Australia and LRA in Buenos Aires in terms of their relatively greater distance from the magnetic equator. (Their broadcasting schedules were relatively unfavorable, as well.) If reference is made to Fig. 11 of footnote 5, it can be seen that in order to excite both conventional and tilt-supported modes, it is desirable that the transmitted energy be incident on the ionospheric region containing the tilt over a wide range of angles of incidence. It is well known that signals which have traveled a long distance tend to have their energy restricted to a relatively narrow range of vertical angles. It is accordingly possible that in the case of stations far from the equator, the spread of vertical angles may not be sufficient to excite both types of modes at the tilted region.

Doppler fading of the sort described can have a major effect on the fading statistics of high-frequency signals propagated over transequatorial paths. Such rapid fading of the carrier in effect represents a spurious modulation which may become a matter for serious concern when data transmission systems utilizing the lower audio frequencies are employed.

K. C. Yeh
O. G. Villard, Jr.
Radio Propagation Lab.
Stanford University
Stanford, Calif.

[3] S. Stein, "The role of ionospheric-layer tilts in long-range high-frequency radio propagation," *J. Geophys. Res.*, vol. 63, pp. 217–241; March, 1958.

[4] B. W. Osborne, "Ionospheric behaviour in the F_2 region at Singapore," *J. Atmos. Terr. Phys.*, vol. 2, pp. 66–78; July, 1951.

[5] O. G. Villard, Jr., S. Stein, and K. C. Yeh, "Studies of transequatorial ionospheric propagation by the scatter-sounding method," *J. Geophys. Res.*, vol. 62, pp. 299–412; September, 1957.

[6] N. S. Subba Rao and Y. V. Somayajulu, "A peculiar type of rapid fading in radio reception," *Nature*, vol. 163, p. 442; March, 1949.

A Note Concerning Instantaneous Frequency*

Recent discussions of instantaneous frequency have apparently not stressed the connection between the concept of instantaneous frequency and that of complex frequency as used in steady-state circuit analysis. It is the purpose of this note to point out how the definition of instantaneous frequency[1] follows from that of steady-state complex frequency in a straightforward fashion.

To establish the basis for subsequent generalization, the following facts of steady-state analysis are recalled:

1) The complex frequency of the function $f(t)=\exp(\sigma+i\omega)t$ is given by

$$\frac{d}{dt}[\log f(t)]. \tag{1}$$

2) Two complex conjugate frequencies are associated with the function $\sin \omega t$ (or $\cos \omega t$): the frequency with positive imaginary part is obtained by deleting the negative spectrum of the function and applying (1) to twice the remainder.

These notions may be extended to an arbitrary real function $f(t)$ with Fourier spectrum $F(\omega)$ by defining an associated complex function $f_+(t)$ as the inverse transform

$$F_+(\omega) = \begin{cases} 2F(\omega), & \omega > 0 \\ 0 & \omega < 0 \end{cases}. \tag{2}$$

The complex instantaneous frequency $\Omega(t)$ of $f(t)$ is then found by applying (1):

$$\Omega(t) = \frac{d}{dt}[\log f_+(t)]. \tag{3}$$

One may write

$$F_+(\omega) = F(\omega)[1 + \operatorname{sgn} \omega]$$

and may thus identify

$$f_+(t) = [f(t) + if_H(t)], \tag{4}$$

where $f_H(t)$ is the Hilbert transform[2] of $f(t)$; *i.e.*,

$$f_H(t) = -\frac{1}{\pi}\int_{-\infty}^{+\infty}\frac{f(\tau)d\tau}{t-\tau}. \tag{5}$$

Then

$$\Omega(t) = \frac{d}{dt}\log[f^2(t) + f_H^2(t)]^{1/2} + i\frac{d}{dt}\tan^{-1}\frac{f_H(t)}{f(t)}, \tag{6}$$

and the imaginary part of this expression is the instantaneous frequency as defined by Harman.

With respect to the real part of (6), it may be of interest to consider the special case of an $f(t)$ whose spectrum is narrow as compared to its center frequency ω_0. One may then identify the real part of (6) as the logarithmic derivative of the envelope

$$r(t) = [f^2(t) + f_H^2(t)]^{1/2}.$$

It is easily shown that the spectrum of $r^2(t)$ is given by

$$\mathfrak{F}[r^2(t)] = \frac{1}{2\pi}\int_{-\infty}^{+\infty} F_+(x)F_+^*(x-\omega)dx.$$

The spectral extent of $r^2(t)$ is thus seen to be as narrow as is consistent with the spectral width of $f(t)$ about ω_0, a property which one would intuitively demand of any reasonable definition of the envelope.

The author wishes to thank Drs. N. M. Abramson and W. W. Harman for their helpful comments.

D. A. Linden
Dept. of Elec. Eng.
Stanford University
Stanford, Calif.

* Received by the IRE, August 4, 1958.

[1] W. W. Harman, "Instantaneous frequency," Proc. IRE, vol. 42, p. 599; March, 1954.

[2] Multiplication of $F(\omega)$ by $\operatorname{sgn} \omega$ is equivalent to the convolution of $f(t)$ with $\mathfrak{F}^{-1}[\operatorname{sgn} \omega] = -(i/\pi t)$ which leads to (5).

Contributors

R. Marshall Coon (M'55) was born in Anthony, Kans., on June 29, 1912. He received the B.S.E.E. degree from Kansas State College, Manhattan, Kans., in 1937. He then joined the Westinghouse Electric Corporation as a student engineer. From 1938 to 1941 he was engaged in power work with the Kansas Gas and Electric Company. For the next eight years he did research for the U. S. Naval Ordnance Laboratory, primarily on magnetism related to underwater ordnance. He spent two years with Boeing Airplane Company doing electrical design on the B-47.

R. M. Coon

Since 1951, he has been with the Modulation Systems Section of the National Bureau of Standards, Boulder, Colo.

Mr. Coon is a member of Kappa Eta Kappa and RESA.

❖

James M. Early (A'48–SM'54) was born in Syracuse, N. Y., on August 25, 1922. He received the B.S. degree in pulp and paper manufacturing from the New York College of Forestry, Syracuse, in 1943.

J. M. Early

After two and one-half years of military service, he joined the staff of the Department of Electrical Engineering at Ohio State University, Columbus, Ohio, where he received the M.S. in electrical engineering in 1948 and the Ph.D. in 1951.

Since becoming affiliated with Bell Telephone Laboratories, Murray Hill, N.J., in 1951, he has been concerned with junction transistor development, particularly high-frequency transistors.

Dr. Early is a member of the American Physical Society.

❖

E. L. Maxwell was born in Fort Collins, Colo., on December 24, 1930. He acquired his first training in electronics through work with amateur radio. In 1950 he obtained his First-Class Radiotelephone License and worked in broadcast radio for three and a half years. From 1951 to 1952 he was on active duty with the U. S. Air Force as a radio maintenance technician. During this period he attended the advanced Radio Technician School at Scott Field, Ill.

E. L. Maxwell

He has partially completed his undergraduate work toward the B.S. degree in electrical engineering at the University of Colorado, Boulder.

In 1955 he joined the National Bureau of Standards Central Radio Propagation Laboratory in Boulder, where he has been working on noise studies and radio system problems.

❖

Toru Ogawa (M'58) was born in Tokushima Prefecture, Japan, on March 9, 1924. He received the Rigakush degree in physics from Kyoto University in 1949, and remained there for four years of post-graduate study. He was appointed lecturer of electrical engineering at Doshisha University in 1953, and became an assistant professor in 1955.

T. Ogawa

From 1949 to 1957 he was engaged in research work on microwave spectroscopy, the atomic clock, and radio wave propagation at Kyoto University. Since 1957 he has continued his radio propagation work at Doshisha University.

He is a member of the Physical Society of Japan and the Institute of Electrical Communication Engineers of Japan.

❖

Richard H. Pantell (S'54–A'55) was born in New York, N. Y., on December 25, 1927. He received the B.S. and M.S. degrees from Massachusetts Institute of Technology, Cambridge, Mass., in 1950. His studies at M.I.T. were performed within the electrical engineering cooperative course, with four semesters spent at the General Electric test program. During the 1950–1951 academic year he taught electrical engineering at the Polytechnic Institute of Brooklyn, N. Y. From 1951 to 1954 he was a research assistant at the Stanford Electronics Research Laboratory, Stanford, Calif., investigating new techniques for network synthesis. In 1954 he received the Ph.D. degree in electrical engineering from Stanford University.

R. H. Pantell

From 1954 to 1956 Dr. Pantell was assistant professor of electrical engineering at Stanford University and research associate in the Microwave Laboratory. He taught a graduate course in network synthesis, and did research on the development of a high-power traveling-wave tube. He was granted a leave of absence from Stanford to become a visiting assistant professor at the University of Illinois during 1956–1957. There he worked on the generation of millimeter and submillimeter wavelengths, and taught courses in network synthesis and microwave measurements.

Dr. Pantell has resumed his position at Stanford and is continuing his research into the generation of microwave energy.

He is a member of Sigma Xi.

❖

Robert W. Plush was born in Beloit, Kans., on November 17, 1929. He received the B.S.E.E. from Purdue University, Lafayette, Ind., in 1951. He then served with the U. S. Navy.

R. W. Plush

After his release from active duty in June, 1953, he was engaged in engineering and maintenance supervision for a feed mill in Kansas.

In 1956 he joined the National Bureau of Standards Central Radio Propagation Laboratory in Boulder, Colo., where he has been engaged in measuring the short-term properties of tropospheric forward scatter carriers and studying the effects of various types and levels of noise on radio systems.

Mr. Plush has taken graduate work at both Kansas State College, Manhattan, Kans., and the University of Colorado in Boulder. He has been an amateur radio operator since 1951.

❖

Arthur D. Watt (SM'54) was born in Cedar Lake, Ind., on November 2, 1920. He received the B.S.E.E. degree from Purdue University, La fayette, Ind., in 1942. From 1942 to 1951 he was employed at the Naval Research Laboratory, where he worked on transmitters, receivers, antennas, facsimile, television, communication theory, and communication system design problems. While at NRL, he took graduate work at the University of Maryland, College Park, Md.

A. D. Watt

In 1951 he joined the National Bureau of Standards Central Radio Propagation Laboratory in Boulder, Colo., where he has been concerned with modulation and radio system problems, including studies to optimize utilization of the frequency spectrum and signal to noise studies.

Mr. Watt is a member of HKN, a charter member of the Boulder RESA branch, and is active in URSI and CCIR work.

Scanning the TRANSACTIONS

Chopped off TV pictures are no novelty to viewers, broadcasters, or advertisers. The message that shows up on a home set with the telephone number across the bottom cut off has been an annoyance to people in the business ever since TV began broadcasting commercials. WRCA-TV in New York recently decided to do something about it. They broadcast a special pattern each morning for 15 minutes before regular air time and asked viewers to report how much of the pattern was visible on their sets. The pattern consisted of a number of radial lines marked off in segments equal to 5 per cent of the picture height, as shown below. As a result of this test, NBC was able to pin down the "safe area" of a TV picture, indicated by the dotted line. It should now be possible to insure that the top of an actor's head will be fully visible in the home. This will be a great boon to followers of Westerns, where the only way you can tell the hero from the villain is by his white hat. (C. L. Townsend, "TV receiver picture area losses," IRE TRANS. ON BROADCAST TRANSMISSION SYSTEMS, September, 1958.)

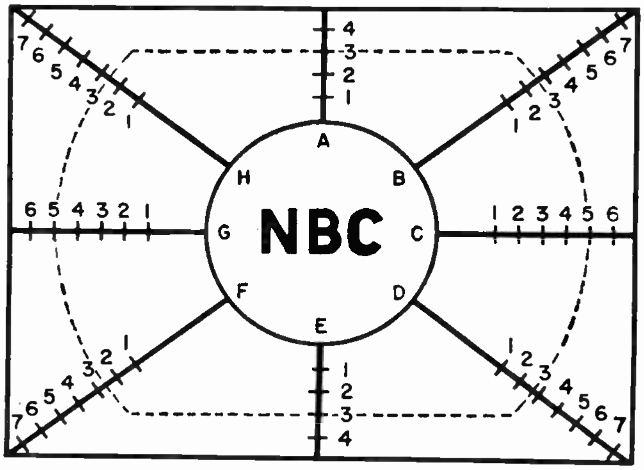

An automatic language translator that can translate scientific Russian into English is under development. The machine has a Russian-English "dictionary" capable of translating 160,000 Russian entries. The "dictionary" is on a glass disk, 10 inches in diameter, which rotates at 1200 rpm. The Russian words and their English meanings are photographically coded on the glass disk in black marks. Capacity of the disk is 60 million marks—6 million per square inch. Passage by an electronic "eye" translates the marks into electrical signals that are interpreted and translated by an electronic computer. The memory is capable of storing 30 million bits of digital information with a maximum access time to 50 milliseconds, and has a scanning rate of one million bits per second. (G. Shiner, "The USAF automatic language translator, Mark I," 1958 IRE NATIONAL CONVENTION RECORD, Part 4.)

Electronics is revolutionizing the highway building business. The usual method of selecting the best highway route calls for costly and time-consuming detailed surveys of each proposed route, followed by laborious hand plottings and calculations of elevations and the amount of digging and filling required along the entire route. During the last three to five years this time-honored method has been rapidly replaced by a new technique involving aerial photography, stereoscopy, and digital computers. Pairs of overlapping aerial photographs are first taken over the proposed route. The two photographs are then projected to form a three dimensional picture, and an observer manipulates an illuminated spot until it appears to him to rest on the ground. The position and a relative elevation of the spot are translated directly into digital data and fed to a computer which then quickly calculates from a series of such readings the highway profile and the amount of earth-moving work involved. Alternate routes can be explored in a matter of hours, instead of days or weeks. Most impressive of all, it is conservatively estimated that highway construction costs can be reduced by as much as 20 per cent, which in the next ten years might mean a saving of 20 billion dollars. (J. M. Cahn, "Automation in highway design," IRE TRANS. ON INDUSTRIAL ELECTRONICS, August, 1958.)

To aim a moon radar antenna, a punch card operated steering system has been developed that is twenty-five times more accurate than previous electronic systems. The system can be applied in modified form to tracking other celestial bodies, including satellites. Naval Observatory data regarding the orbit of the moon is punched into cards and fed to a digital computer, which then calculates where the moon will be at different instants with respect to the antenna. This information is stored on magnetic tapes and fed into an analog conversion system which provides a continuous flow of positional signals that keep the antenna aimed constantly and accurately at the moon as it moves across the sky.

Techniques for bouncing radar signals off the moon, pioneered by the Signal Corps in 1946, have recently taken on added importance in radio communications and radio astronomy. Last year the Naval Research Laboratory succeeded in receiving voice signals that were reflected by the moon, opening up the possibility of using the moon to relay long-distance radio transmissions. More recently, the same group used moon radar to measure the distance to the moon with an accuracy of within 1000 feet. (O. Guzmann, "Digital moon-radar antenna programmer with analog rate signal integrator," 1958 IRE NATIONAL CONVENTION RECORD, Part 4.)

A novel tube that tells time has been developed for measuring how long equipment or components have been operating. The tube consists of a small electrolytic cell containing a colored electrolyte, the color of which changes with the amount of dc current that has passed through it. At any time during the life of a particular piece of equipment, its "age" can be determined to within 5 per cent simply by unplugging the cell and measuring its color with a colorimeter. The device should prove particularly useful in obtaining reliability data, so that lifetimes of components and modules can be predicted and replacements made before a failure occurs. (W. Eriksen and E. Handley, "The tube that tells time," 1958 IRE NATIONAL CONVENTION RECORD, Part 3.)

Coded television pictures show promise of enabling bandwidth reductions of as much as 4 to 1. An experimental system has been developed which eliminates redundancies from the picture and takes advantage of certain properties of human vision to reduce the amount of information that has to be transmitted. A normal television camera output is fed into a small high-speed electronic computer which codes the video signal before transmission to the receiver, where a similar computer translates the code before presenting the picture on a normal television tube. An essential feature of the device is the temporary retention of the coded signal in electrostatic storage tubes to average out the information rate.

Existing methods for television transmission, such as microwave relay systems or coaxial cable, require the equivalent of 1000 telephone circuits for one video channel. As a result, such transmissions are very expensive. Furthermore, in the case of trans-Atlantic or trans-Pacific communication, television transmission is not possible at present because no circuits of adequate bandwidth are available. Therefore, commercial long-distance relaying—especially transoceanic routes—will probably be the most important application of this new system. Military applications may also be important, since the "beyond the horizon" scatter propagation communication links now under construction will generally be able to handle the coded signal. Also, since the transmission is coded, it cannot be deciphered without special receiving equipment. If a moderate reduction in picture quality is acceptable, it is possible to construct an entirely transistorized version of very narrow bandwidth for field use. A similar system could also be used to transmit facsimile or news photos more rapidly than apparatus currently in use. (W. F. Schreiber and C. F. Knapp, "TV bandwidth reduction by digital coding," 1958 IRE National Convention Record, Part 4.)

Radio engineers seem to be using telephones more and more for monitoring or controlling equipment in remote locations. The use of long distance telephone lines for gathering nuclear radiation data from unattended field stations was reported here only recently. Now a dialing circuit, costing all of $150, has been proposed for the remote control of transmitting equipment at an unattended antenna tower, so that such system parameters as frequency, polarization, and RF match can be independently adjusted over a single telephone line. (L. Young and G. M. Ward, "Telephone remote control circuit for an antenna site," IRE Trans. on Antennas and Propagation, October, 1958.)

Low-noise amplifiers are becoming of increasing interest as the number of available varieties of amplifying elements continues to grow. The circuit designer's problem is how to get the best noise performance from a composite amplifier in which individual units with specified noise properties are interconnected. General theorems on optimum possible performance were derived by H. A. Haus and R. B. Adler in Proc. IRE, August, 1958. As was promised there, the detailed proofs showing how these optimum results can actually be realized and the bases by which all amplifiers are classified and canonically represented have now been published in the appropriate Transactions. (R. B. Adler and H. A. Haus, "Network realization of optimum amplifier noise performance" and "Canonical form of linear noisy networks," IRE Trans. on Circuit Theory, September, 1958.)

Books

Feedback Theory and its Applications, by P. H. Hammond

Published (1958) by The Macmillan Co., 60 Fifth Ave., N. Y. 11, N. Y. 333 pages+10 appendix pages +4 index pages+xv pages. 204 figures. 8¾×5¾. $7.00.

"The aim of this book," according to the author, "is to present well-tried methods of linear and non-linear feedback system analysis and to illustrate their application to a variety of engineering devices which incorporate feedback in some form. The book is intended for graduate engineering and physics students and others who require an introduction to the subject and a view of its scope and future."

In line with his stated purpose, the author—the principal scientific officer of the Royal Radar Establishment, Malvern, England—has produced a concise, clearly written, well-balanced text which covers the basic theory of linear and nonlinear feedback systems together with a number of applications. Of particular value are the well-chosen examples and the many interpretive comments of the author which reflect his extensive experience in this field, and which should go far in aiding the student to bridge the gap between the theory and the art of feedback system practice.

Feedback theory is introduced in chapter one by means of the differential equations of motion of a speed governor. A linear approximation is arrived at for this system and proceeding via the Laplace transformation a flow diagram representation in operational form is developed. After a discussion of the properties of feedback in chapter two, the important question of stability is considered in chapter three. The Routh criterion is stated but the major emphasis is on the Nyquist criterion which is derived from first principles, and its application is illustrated by several clever examples. In chapter four graphical methods of representing the frequency response function and their use in stability determinations are developed. Applications of these techniques to certain electronic circuits are then described in chapters five and six, with particular emphasis being paid to the "operational amplifier" and its use as an analog computer element. The design of stabilizing networks is illustrated by the use of phase-gain characteristics.

Servomechanisms and other control systems are introduced in chapter seven, using linear theory. Examples are taken from hydraulic and electrical servomechanism practice. In chapter eight stabilization techniques are discussed, with the aid of numerous examples. Linear theory is then shown to be inadequate to explain the behavior of certain systems, and the remaining five chapters are devoted to nonlinear techniques—in particular the phase plane and the describing function. These techniques are illustrated by a study of the behavior of a positional servomechanism with inherent nonlinearities such as motor torque limitations, backlash in the gears, and coulomb friction and stiction in the load. A separate chapter is devoted to the study of on-off controlled servomechanisms; the properties of on-off elements are discussed by means of the phase plane and the describing function, and the optimization of transient performance is considered.

In the final chapter the application of electronic analog computers to the study of control systems with nonlinear elements is discussed. A design technique is illustrated by means of a marine autopilot, with a full description of the steps needed to simulate the system on the computer.

While the selection of material in any book is always open to question, it is the opinion of this reviewer that the omission of root locus techniques mars an otherwise excellent introductory book. However, in spite of this omission, the book provides an excellent introduction to practical feedback systems.

Although the book treats a specialized subject, it is written in a simple manner with only a moderate amount of mathematics. It should be particularly useful to those interested in learning something of both the theoretical and practical aspects of feedback systems.

John E. Bertram
Columbia Univ.
New York 27, N. Y.

Space Charge Waves and Slow Electromagnetic Waves, by A. H. W. Beck

Published (1958) by Pergamon Press, Inc., 122 E. 55 St., N. Y. 22, N. Y. 321 pages+3 index pages+70 appendix pages+xi pages. Illus. 8¾×5¾. $15.00.

Imagine yourself starting work in a field of practical importance, a difficult field, and one in which a great deal of work has been done, a lot of it rather involved mathematically. What would help you most?

The best thing, of course, would be a wise and patient friend—a man familiar with nearly all of the published literature, a man with a sound practical background to enable him to sort the trivial or wrong from the correct and the important, a man with limitless hours to explain matters to you.

Except for the limitless hours for personal explanation, Mr. Beck is just this man, and his new book, which seems to me even more useful than his earlier book, "Thermionic Valves," is the best written substitute for personal counsel concerning the theory of operation of microwave tubes.

This book covers a tremendous range. It starts out by describing the klystron, the traveling-wave tube and other microwave devices, and explaining space charge waves and the source of microwave energy. It then goes on to Maxwell's equations, slow-wave structures, including filter structures and helices, space-charge-wave theory, the related matter of plasma oscillations, matching boundary conditions at the input, the operation of klystrons, traveling-wave tubes and other tubes in terms of space-charge-wave theory, and noise phenomena. It includes references to nonlinear theory. A number of appendixes cover matters not treated in the main body of the text, including focusing of electron beams and coupled-mode theory.

It is hard to imagine a matter of any real importance to microwave tubes which isn't brought to the reader's attention and, best of all, sensibly evaluated. Of course, in many instances, explanations of the detail that the reader may desire can't be included, but there are very complete references to published work. The degree of the author's familiarity with the field is such that he in some instances gives references to unpublished work which has come his way. This rectitude will reassure if it does not help the reader.

Of course, the author is neither omniscient, infallible, nor gifted with second sight, and neither am I. He may very well have made errors of which I am unaware. He misses Walker's theory of the backward-wave oscillator, which antedates that of Heffner, and Walker's work on the conditions for waves in multivelocity flow. I think there is a view about the linearization of kinetic power expressions which he might well have expressed, and that a few pointed remarks about an alleged dispersion relation for plasma oscillations might not have been amiss. And, he missed by just a hair being able to include the new and important work of Siegman, Watkins and Hsieh which shows that multivelocity streams are not so irretrievably noisy as I and others had thought.

In other words, Mr. Beck is a human, not a superhuman, friend to those who work with microwave tubes. I think, however, that he may remain their best friend for some time.

J. R. PIERCE
Bell Telephone Labs.
Murray Hill, N. J.

English-Russian, Russian-English Electronics Dictionary, compiled by Department of the Army

Published (1958) by McGraw-Hill Book Co., Inc., 330 W. 42 St., N. Y. 36, N. Y. 943 pages. $6\frac{1}{4} \times 9\frac{1}{4}$. $8.00.

The excellent "Russian-English, English-Russian Electronics Dictionary" compiled by the Signal Corps in 1955 has now been republished by McGraw-Hill between hard covers, and thus made even more widely available than before.

The volume contains separate Russian-English and English-Russian sections listing over 22,000 technical words and expressions often encountered in electronic and communication engineering. Heaviest emphasis is on telecommunication engineering—radio transmitters, antennas, receivers, and wire communication apparatus and procedures. In these fields coverage is authoritative and complete. In radar, electronic navigation aids, acoustics, automatic control, electron devices, and measurements the listings are not quite so detailed, but entirely adequate for all but the most recent or specialized terms.

No volume of this size could cover all the many byways of contemporary electronic engineering in complete detail. This shows up here as a weakness in subjects with jargon which is fairly new (*e.g.*, digital computers, solid state components, and information theory) or of a theoretical rather than experimental nature (*e.g.*, some of the fringe fields of applied mathematics or physics).

Still, the book gives as good over-all coverage of electronics as is to be found in any single volume. Its worth is testified to by the fact that it was reprinted several years ago in the Soviet Union and is widely used there in preference to the available Soviet electronics dictionaries.

This reviewer can recommend the book highly to anyone who ever has occasion to look at the increasingly important Soviet electronics literature. However, he would like to point out that the original paper-bound volume is still available from the Superintendent of Documents in Washington for $3.50, less than half the price of the new hard-cover reprint.

PAUL E. GREEN, JR.
Lincoln Lab., M.I.T.
Lexington, Mass.

Magnetic Tape Recording, by H. G. M. Spratt

Published (1958) by The Macmillan Co., 60 Fifth Ave., N. Y. 11, N. Y. 288 pages+7 index pages+23 appendix pages. Illus. $8\frac{3}{4} \times 5\frac{3}{4}$. $8.50.

This book is an extremely well written story of magnetic tape recording. It is organized on a very broad basis. Indeed, it embraces on the one hand the "Ultimate Nature of Magnetism" and on the other, detailed designs and applications of complete magnetic tape recorders. One slight flaw, from an American point of view, is that the equipment shown is all British or European. The book is very well constructed with a fine use of English and an excellent format. The illustrations are carefully done and, so far as we could determine, practically error-free.

From a discussion of the principles of magnetism, electroacoustics, and magnetic recording, the book proceeds into a discussion of tape manufacture and test and then into discussions of actual recording machines and their applications.

It is difficult from an American point of view to determine for whom the book is intended. Certainly, it is not for the student, since there are no problems and no derivations given. It can hardly be for the designer, since there is no development of design principles. It does, however, give several final design equations without development and shows a number of existing circuits. This leaves as its potential audience those who wish to have a general knowledge of the practices of tape recording, primarily in the reproduction of speech and music, without expecting a detailed description of the field. For instance, in the discussion of tape manufacture, the various processes are described, including a discussion of the necessity of air conditioning, but there is very little basic chemistry.

Our main criticism of the book is that it is descriptive of a broad field but has little depth in any area.

A. MEYERHOFF
K. MCILWAIN
Burroughs Corp.
Paoli, Pa.

Television Engineering, Vol. IV: General Circuit Techniques, by S. W. Amos and D. C. Birkinshaw

Published (1958) by Iliffe and Sons Ltd., Dorset House, Stamford St., London S.E. 1, England. 260 pages+1 bibliography page+2 index pages. Illus. $8\frac{3}{4} \times 5\frac{1}{2}$. 35s.

This is the fourth and final volume in a series on "Television Engineering" written by members of the BBC Engineering Division. Volume I deals with basic principles of television, particularly optics and camera tubes. Volume II is concerned with video amplifiers, including a special section on camera-head amplifiers. Volume III is on circuits commonly used for generating special waveforms, and their use in television. The present volume treats a number of circuit techniques which are used extensively in television, but do not properly belong to the earlier volumes. The books were written primarily for instructing the BBC staff, but Volume IV is discussed below from the standpoint of its usefulness to American readers, in and out of television engineering.

Topics include counter circuits, frequency dividers, dc clamp and restorer circuits, gamma-control (nonlinear characteristic) amplifiers, delay lines, fixed and variable equalizers, shunt-regulated amplifiers and cathode followers, line and field output stages, and electrical characteristics of scanning coils.

The previous knowledge expected of the reader is best illustrated by quoting the first sentence: "In a twin-interlaced television system the various pulses required in the sync signals or for camera operation have frequencies equal to the field frequency, line frequency or twice line frequency." The pace thus set is maintained throughout; in other words, this book is not for the beginner, but for the person already familiar with all the jargon of television circuitry. The innocent will find no help. This seems unfortunate, for most of the topics dealt with also have wide applications in fields other than television, particularly in experimental nuclear physics. I think that the number of potential readers would have been doubled by the addition of a three-page glossary of television terms.

The mathematical demands made on the reader are much more modest; anyone to whom the equation $L(di/dt)=j\omega Li$ expresses an obvious truth will have no difficulty here. Complete derivations are given for most of the design equations, following the admirable custom of placing derivations in short appendixes at the end of each chapter. Of course, the American reader will have to realize that pF is the British form of $\mu\mu f$.

American engineering writers would do well to study this book for its literary quality alone. Ideas are expressed with a clarity and brevity very rare on this side of the Atlantic. One has the feeling that every single sentence has been scrutinized many times, every unnecessary word removed, and every possible ambiguity of meaning corrected. Because of this, the amount of material covered is greater than most American writers would be able to squeeze into a volume twice the size.

Another outstanding characteristic of this book is the number of illustrations. The use of circuit diagrams and diagrams showing the waveforms at various points in the circuits can only be described as lavish, and this is no small part of the reason so much can be said in so little space. Although the text proper occupies only 250 pages, it includes 175 diagrams and two pages of plates. This feature, plus the clean typography and excellent quality of paper, make the book very easy and pleasant to read.

Anyone concerned with the practical design, use, or servicing of circuits of the type mentioned above will find this book one of the most useful he can locate. That it is completely sound technically, authoritative, and up-to-date, of course goes without saying.

E. T. Jaynes
Stanford University
Stanford, Calif.

Recent Books

Bussard, R. W., and DeLauer, R. D. *Nuclear Rocket Propulsion.* McGraw-Hill Book Co., Inc., 330 W. 42 St., N. Y. 36, N. Y. $10.00.

Eckman, D. P. *Automatic Process Control.* John Wiley and Sons, Inc., 440 Fourth Ave., N. Y. 16, N. Y. $9.00.

Electron Tube Materials Compilation of ASTM Standards. American Society for Testing Materials, 1916 Race St., Philadelphia 3, Pa. $3.50.

Feldtkeller, Richard. *Theorie der Spulen und Übertrager.* S. Hirzel, Stuttgart N, Birkenwaldstrasse 185, Germany. DM 24.

Gottlieb, I. *Basic Pulses.* John F. Rider, Inc., 116 W. 14 St., N. Y. 11, N. Y. $3.50.

Krugman, Leonard. *Fundamentals of Transistors. Second Edition.* John F. Rider, Inc. 116 W. 14 St., N. Y. 11, N. Y. $3.50.

Moir, James. *High Quality Sound Reproduction.* The Macmillan Co., 60 Fifth Ave., N. Y. 11, N. Y. $14.00.

Schure, A., Ed. *Gas Tubes.* John F. Rider, Inc., 116 W. 14 St., N. Y. 11, N. Y. $1.50.

Shand, E. B. *Glass Engineering Handbook.* McGraw-Hill Book Co., Inc., 330 W. 42 St., N. Y. 36, N. Y. $10.00.

Taylor, Angus E. *Introduction to Functional Analysis.* John Wiley and Sons, Inc., 440 Fourth Ave., N. Y. 16, N. Y. $12.50.

Abstracts of IRE Transactions

The following issues of Transactions have recently been published, and are now available from the Institute of Radio Engineers, Inc., 1 East 79th Street, New York 21, N. Y. at the following prices. The contents of each issue and, where available, abstracts of technical papers are given below.

Sponsoring Group	Publication	Group Members	IRE Members	Non-Members*
Antennas and Propagation	Vol. AP-6, No. 4	$1.50	$2.25	$4.50
Broadcast and Television Receivers	Vol. BTR-4, No. 4	2.50	3.75	7.50
Broadcast Transmission Systems	PGBTS-11	0.65	0.95	1.95
Circuit Theory	Vol. CT-5, No. 3	1.35	2.05	4.05
Electronic Computers	Vol. EC-7, No. 3	1.50	2.25	4.50
Industrial Electronics	PGIE-7	1.85	2.75	5.55
Reliability and Quality Control	PGRQC-14	1.40	2.10	4.20

*** Libraries and colleges may purchase copies at IRE Member rates.**

Antennas and Propagation

Vol. AP-6, No. 4, October, 1958

Contributions—The Effect of Echo on the Operation of High-Frequency Communication Circuits—D. K. Bailey (p. 325)

Echo on high-frequency communication services is defined as the simultaneous reception of signals over both major and minor arcs of the great circle connecting a transmitter and receiver. Two distinct kinds of echo are recognized according to the illumination conditions under which they occur. Echo of the first kind is observed when the great-circle path coincides with the twilight zone surrounding the earth, whereas echo of the second kind, which can occur only on fairly long communication paths, is most severe when the short path is most intensely illuminated. Little can be done to obviate echo of the first kind and it is not, like echo of the second kind, amenable to prediction by available methods of calculating sky-wave field intensities. Radio traffic data are cited which corroborate calculations and show both that echo of the second kind is more severe at times of maximum solar activity, and is less severe on higher frequencies. Conclusions are drawn concerning mode of operation and choice of operating frequency to minimize echo interference.

Foreground Terrain Effects on Overland UHF Transmissions—L. G. Trolese and L. J. Anderson (p. 330)

This paper describes an experimental study of the influence of the shape of foreground terrain profiles near terminals of UHF links on the received field. A gently rounded shape of the foreground profile causes a marked diffraction pattern to be superimposed on the normal variation of field strength with height. The diffraction geometry shows similarity to knife-edge geometry and the rounded terrain feature appears to act geometrically as an equivalent knife edge. The amplitude of the spatial variations in signal are, however, much greater than knife-edge theory predicts. A sizeable foreground diffraction enhancement of received field can be realized by locating the antenna at the height of the first diffraction maximum. Changing refraction due to meteorological variations can change both the position in height and intensity of the diffraction pattern.

A Rapid Beam-Swinging Experiment in Transhorizon Propagation—Alan T. Waterman, Jr. (p. 338)

By using a broadside phased array for an antenna, a narrow beam can be swung rapidly and in quick succession through a limited sector by fast control of the phasing, rather than by movement of the entire antenna structure. This technique is used at the receiving end of a 101-mile beyond-the-horizon transmission path in order to probe the portion of the troposphere through which the signal is propagated. At the frequency employed of 3.12 kmc, a 0.49-degree beam is swung in azimuth through a 4.2-degree sector each tenth of a second.

A variety of phenomena are observed with this technique which have not been directly apparent in slower beam-swinging experiments. The beam-broadening effect attributed to atmospheric scattering is not always evident on any one sector scan. However, the change from scan to scan is frequently rapid enough so that a time average would show the broadening. At times the scan-to-scan changes are systematic and show a continuity indicative of a motion of the scattering or reflecting regions; in some cases this motion is too rapid to be accounted for by transport of air, thus implying a wave motion rippling through the atmosphere. At other times the atmospheric structure is too fine to be resolved by the beamwidth employed, and the time variations are too rapid to reveal a continuity from one scan to the next.

Effect of Mountains with Smooth Crests on Wave Propagation—I. P. Shkarofsky, H. E. J. Neugebauer, and M. P. Bachynski (p. 341)

A new method of solving the problem of diffraction of EM waves by the smooth crest of a perfectly reflecting cylindrical mountain has been previously reported. This paper presents the results in a form more suitable for practical applications. The theory is extended, and good agreement with model experiments is obtained for scattering angles up to 5 degrees. The procedure for including the effects of reflections from the ground on either side of the mountain is also indicated. A few examples illustrate cases encountered in practice, and exhibit effects up to 8 db compared with knife-edge diffraction.

Pattern of an Antenna on a Curved Lossy Surface—J. R. Wait and A. M. Conda (p. 348)

Extensive numerical results are presented for the radiation fields of electric and magnetic type antennas mounted on smooth curved surfaces of finite conductivity. The model chosen is a circular cylinder whose surface impedance is specified. A residue series representation is employed for the portion of space deep in the shadow while a geometrical-optical representation is used in the "lit" region. In the penumbra, the fields are expressed in terms of the "Fock functions." The results are also applicable to other smoothly varying curved surfaces such as spheres, parabolic cylinders, and paraboloids. As an application, the E-plane patterns are computed for a small loop antenna on a spherical earth for both sea and land illustrating the so-called cut-back effect.

Nonresonant Slotted Arrays—Andre Dion (p. 360)

The distribution of slot conductance of nonresonant arrays is obtained by considering the array as a continuous line source. Distributions of conductance per unit length for three Taylor aperture distributions are thus obtained. However, the discreteness of the array is retained for a discussion of second-order beams and for the development of a method leading to their suppression. The performance of an experimental array is described.

Gains of Finite-Size Corner-Reflector Antennas—H. V. Cottony and A. C. Wilson (p. 366)

An experimental corner reflector was erected at the Table Mesa antenna range near Boulder. The aperture angle of this antenna was made adjustable to any value between 20 and 180 degrees. The widths and lengths of the reflecting surfaces were each adjustable from 0.4 to 5.0 wavelengths. Measurements of gain were made for numerous combinations of lengths and widths of reflecting surfaces. These measurements were made with a half-wave dipole in the first, second and third maximum positions. The aperture angle was adjusted to maximize the gain. The principal results are presented in the form of contours of constant gain plotted for a range of widths and lengths of reflecting surfaces from 0.4 to 5.0 wavelengths. These graphs should be useful to a designer of corner-reflector antennas.

Scanning Surface Wave Antennas—Oblique Surface Waves Over a Corrugated Conductor—R. W. Hougardy and R. C. Hansen (p. 370)

The existence of a surface wave which propagates across a corrugated metallic surface at an oblique angle with the teeth is investigated both experimentally and theoretically in this paper. Expressions are derived which give the variation of the wave velocity and amplitude with the change of wave direction. Experimentally measured values of the surface velocity compare favorably with the theory.

The radiation pattern of an experimental antenna is given which demonstrates that a low sidelobe, narrow azimuth beam scannable to ± 30 degrees with a cosesant-squared elevation pattern is attainable. A method of feeding this antenna to give a low silhouette, making the corrugated scanner antenna suitable for flush mounted applications, is illustrated.

Communications—Measurements of the Bandwidth of Radio Waves Propagated by the Troposphere Beyond the Horizon—J. H. Chisholm, L. P. Rainville, J. F. Roche, and H. G. Root (p. 377)

Remarks on the Fading of Scattered Radio Waves—Richard A. Silverman (p. 378)

Phantom Radar Targets at Millimeter Radio Wavelengths—C. W. Tolbert, A. W. Straiton, and C. O. Britt (p. 380)

This paper describes the techniques and the measured radar return from "phantom targets" using 8.6 and 4.3-millimeter radars. The radar returns are compared to the measured back-scattering cross section of water drops, insects, steam and other materials at 8.6-mm wavelength as measured by a CW radar at this wavelength.

Within the limits of the conditions used in the laboratory, it was impossible to produce returns from synthesized refractive index gradients of sufficient magnitude to account for those noted on the radar. It is concluded, therefore, that for the millimeter wavelengths and the short ranges considered, the observed phantom returns were due to solid or liquid particles in the atmosphere.

Telephone Remote Control Circuit for an Antenna Test Site—L. Young and G. M. Ward (p. 385)

A circuit is described which permits the remote control of several quantities, such as transmitter frequency, direction of polarization and RF match, at an unattended antenna tower. It requires only a single telephone line, which already exists for communication purposes at many test sites. Each quantity is controlled by a separate motor. The motors are controlled separately from the control end. This is achieved by adapting and installing a dialing circuit which allows, first, any desired motor to be "dialed"; next, to be controlled; and, finally, the line cleared so that another motor can be called.

The parts for the dialing circuit were purchased at a total cost of about $150. Detailed circuit diagrams are given showing how the circuit is constructed.

Contributors (p. 387)

Annual Index 1958 (follows p. 388)

Broadcast and Television Receivers

VOL. BTR-4, NO. 4,

SEPTEMBER, 1958

Faith of the Engineer (p. 1)

Professional Groups on Broadcast and Television Receivers Administrative Committee (p. 2)

Vacuum-Tube Requirements in Vertical-Deflection Circuits—Karl W. Angel (p. 3)

This paper discusses linearity and efficiency problems which must be considered in the selection of an output tube for a vertical-deflection power amplifier. Because the purpose of the vertical-deflection power amplifier is to supply a given peak-to-peak current to the vertical yoke winding, the design problem is essentially one of matching the resistive component of the yoke to the tube characteristics in much the same manner as in audio-power amplifier design.

The Reaction of Sync Separators in Television Receivers to Impulse Noise—E. Luedicke (p. 15)

Transistor Thermal Stability—M. J. Hellstrom (p. 42)

The thermal stability of a transistor connected in a general bias circuit, with no signal applied, is analyzed. Graphical solutions are necessary to determine stability. Only cases in which the effects of temperature variations in input conductance are negligible will be considered.

Under certain conditions, frequently satisfied in practice, the solutions reduce to one which is more convenient to use. In a slightly smaller class of circuits still another simplification leads to a useful criterion which may be stated as follows.

Stability will exist when $SKEI_{c_0}|T_l < 5.3$.

$S = dI_c/dI_{c_0}$, Stability Factor
K = Thermal Resistance, °C/W
E = Average Collector to Base Voltage
$I_{c_0}|T_l$ = Leakage Current at a Temperature
$T_l = T_a + KP_0$
T_a = Ambient Temperature
P_0 = Collector Dissipation in the Absence of any Leakage Current

In this case the equilibrium junction temperature T_j will not exceed T_l by more than 14.4°C.

An illuminating interpretation of the stability factor, S, and a simple formula for calculating its value are incidental results of the analysis.

The Transistor and the Circuit Application Engineer—F. L. Abboud (p. 51)

To the engineer who has been working with vacuum tubes and vacuum-tube circuits, the transistor presents itself in many instances as a complicated electronic device. This paper presents the transistor to the engineer in the light of analogy and parallelism to the vacuum tube with which he is familiar, bearing in mind the inherent physical and operational differences between the transistor and the vacuum tube. Some of the problems met in transistor circuit design caused by the differences referred to above will be brought out where appropriate.

Transistor Circuitry Utilized in a New TV Sync Generator—L. M. Leeds (p. 60)

Receiver Video Transistor Amplifiers—R. G. Salaman (p. 68)

The problem of the common emitter video amplifier is divided into three categories according to the relative positions of device and load time constants. Optimum values of components are derived for each case. Two types of three transistor circuits are described; one of which uses a battery voltage of one half the peak to peak signal output voltage.

In general, this paper gives background to enable one to design a practical video amplifier for given output, gain and passband requirements.

Call for Papers for Spring Meeting (p. 77)

Improving the Television Horizontal Oscillator—Bill Feingold (p. 78)

Three popular methods of controlling the output amplitude of a stabilized multivibrator are discussed and their common problem of frequency variation with drive control indicated. A corrected circuit is presented along with statistical data to substantiate the improvement.

Broadcast Transmission Systems

PGBTS-1, September, 1958

TV Receiver Picture Area Losses—C. L. Townsend (p. 1)

The TV Helical Antenna Adapted to Structural Tower Shapes—R. E. Fisk (p. 4)

The side-fire helical antenna, successfully used for UHF and VHF high channel television transmission, has now been adapted for low channel VHF service. Investigation of properties of a helical radiator wound around a polygonal supporting structure has made possible the required increased bandwidth and provided directional patterns for special TV coverage applications. Through scale model work, a channel 2 directional antenna has been developed for installation around a triangular tower section.

An Audio Console Designed for the Future—A. C. Angus (p. 11)

Circuit Theory

Vol. CT-5, No. 3, September, 1958

Abstracts (p. 154)

Network Realization of Optimum Amplifier Noise Performance—R. B. Adler and H. A. Haus (p. 156)

Network realizations of the optimum noise performance (lowest noise figure at high gain) of a two-terminal-pair amplifier are presented. Two amplifier classes are distinguished: 1) networks that can both generate and absorb power and 2) networks that only generate power, or negative resistance networks. Amplifiers of class 1) can be optimized by first making them unilateral, subsequently employing input mismatch. Negative resistance amplifiers can be first brought into "canonic" form. Subsequent imbedding of part of the canonic network in an ideal circulator optimizes the noise performance. Both optimizations result in source impedances having a positive real part. High gain is achieved by subsequent cascading. The optimization using the ideal circulator yields maser noise performance optimization.

Canonical Form of Linear Noisy Networks—H. A. Haus and R. B. Adler (p. 161)

At any single frequency, every n-terminal-pair noisy linear network has at most n real parameters that are invariant with respect to all lossless "imbeddings" of that network. Such an "imbedding" is defined by constructing an arbitrary lossless $2n$-terminal-pair network, n of whose terminal pairs are connected to those of the original network, and the remaining n of which form a new set of n terminal pairs. Moreover, by a suitable choice of this imbedding structure, the original network can always be reduced to a canonical form which places clearly in evidence its n invariants. The canonical form consists of n *isolated* one-terminal-pair networks each of which comprises a (negative or positive) resistance in series with a noise voltage generator, and these various noise generators are mutually *uncorrelated*. The n exchangeable powers from the n isolated terminal pairs are the n invariants of the original network.

The invariants have other physical meanings. Each meaning is best brought out by a corresponding particular matrix description of the network. Transformations between matrix descriptions are studied and applied to show that the invariants are interpretable as the n stationary values of the exchangeable power obtainable from any *one* of the new terminal pairs created by a lossless imbedding, as the imbedding network is varied through all lossless forms.

Finally, the two invariants of a two-terminal-pair network are shown to fix the extrema of its noise measure, one of which is known to represent, for an amplifier, the minimum excess noise figure achievable at high gain.

Synthesis of Lossless Networks for Prescribed Transfer Impedances Between Several Current Sources and a Single Resistive Load—A. B. Macnee (p. 168)

A technique is presented for the synthesis of lossless networks open-circuited at one end and paralleled across a single resistance at the other end. The synthesis is for prescribed transfer impedances between the open-circuited terminals and the resistive termination. Such networks can be applied to a variety of frequency multiplexing problems, including the design of multichannel amplifiers. Examples are included, and some practical limitations of such networks are considered.

A Synthesis Procedure for Transmission Line Networks—Alfred I. Grayzel (p. 172)

Richards has shown that by a suitable frequency transformation, networks composed of transmission lines all of a fixed length and resistors behave over a range of frequencies zero to f_0 as lumped constant networks behave over the frequency range zero to infinity.

In the paper the synthesis procedure of a general class of lossless filters using transmission line components is considered. This is the class of filters having all of its transmission zeros at zero frequency and at infinite frequency in the transformed frequency plane, which corresponds to transmission zeros at zero frequency and frequency f_0 along the real frequency axis. This class includes the high-pass and low-pass configuration as special cases. It is proven that if a transmission characteristic is realizable using lumped constant elements, it can be realized in the transformed frequency plane using transmission line components. The transmission line components used are series or shunt shorted and open stubs and series lines. The series stubs are discussed and their feasibility demonstrated. It is shown that series transmission lines can be placed between elements whenever necessary, so that it is physically possible to build these networks.

Matrix Analysis of Oscillators and Transistor Applications—A. J. Cote, Jr. (p. 181)

The use of matrix techniques leads to the classification of feedback harmonic oscillators into four basic types. The oscillator is considered to be made up of two two-port networks: one contains the active element; the other the feedback network. The equations for oscillation are expressed in terms of the two-port parameters.

The method is applied specifically to the Hartley and Colpitts oscillators and their duals. The use of matrices in the analysis brings out the similarities between the oscillators. The Colpitts and Hartley circuits are of one class and require a small L/C ratio to reduce the effect of the active element upon frequencies, whereas their duals require a small C/L ratio.

While the equations are derived for the low frequency case, two methods of high-frequency analysis are presented.

The application of the equations to transistors is considered and several practical circuits for the dual oscillators are given. A short discussion of the bias elements and their effect on frequency and starting conditions is also included.

Axioms on Transactors—Gerald E. Sharpe (p. 189)

The introduction of semiconductor elements has greatly stimulated interest in active, lumped, nonbilateral network theory.

This paper sets out to answer the following fundamental question: Are there, by analogy to the three ideal passive elements, R, L and C, a group or set of ideal active elements, and if so, what are their properties?

The search for an answer leads to the postulate of an hypothesis on electromagnetism which states: Every electromagnetic action is of a causal and irreversible physical nature.

On this hypothesis is based a dual pair of *ideal active* elements also called the *transactor* elements. Their properties are discussed at length and a symbolism is introduced which extends and modifies network topology.

The study of the resistive feedback connection of these elements leads to the conclusion that Ohm's law in its present form is incompatible with a consistent, harmonious theory of networks. After lengthy discussion, Ohm's law is modified and an hypothesis on dissipation is stated.

Finally it is shown that only transactor elements having real transmittance need be considered fundamental and this is summarized by an hypothesis on activity.

On the Transient Responses of Ladder Networks—A. H. Zemanian and P. E. Fleischer (p. 197)

This paper considers bounds that may be obtained on the transient response of ladder networks. These results are developed by means of the superposition integral from the known bounds on the responses of the series and shunt elements of the ladder. Bounds on the response of a fairly general class of one-port networks are also given. Finally, several examples of the method are presented.

Theory of Low-Distortion Reproduction of FM Signals in Linear Systems—Elie J. Baghdady (p. 202)

Certain fundamental aspects of linear-system response to variable-frequency excitations are discussed. A unified argument is presented to simplify the derivation and define the convergence properties of the Carson and Fry and van der Pol-Stumpers expansions. Upper bounds on errors incurred in restricting each expansion to a finite number of terms are derived. This analysis leads to a more complete, more general statement of the conditions for low-distortion transmission and FM-to-AM conversion of FM signals than has heretofore been published. This statement shows that the most significant property of a frequency modulation is its maximum slope, and that the sluggishness properties of a linear system are completely specified by its "sluggishness ratio," $|Z''(j\omega)/Z(j\omega)|$, where $Z(j\omega)$ is the system function. Plots of this ratio for various important filters are presented. The newly derived condition for quasi-stationary response is proposed as a more complete criterion for specifying FM system bandwidths, and an analysis of the distortion in the quasi-stationary response is presented.

Minimum-Loss Two-Conductor Transmission Lines—Gordon Raisbeck (p. 214)

Of all two-conductor transmission lines in which the harmonic mean of the perimeters of the two conductors is fixed, the one having the lowest loss is a conventional round coaxial line. It is conjectured that the same is true of the class having fixed cross section area.

Realizability Conditions on n-Port Networks—Louis Weinberg and Paul Slepian (p. 217)

It is well known that the positive real (pr) concept is one of the most important in network theory. Its importance derives from the following two facts:

1) A necessary and sufficient condition for a real rational function to be realizable as the driving-point impedance of a one-port network is that it be a pr function.
2) A necessary and sufficient condition for a symmetric nth-order matrix of real rational functions to be realizable as the open-circuit impedance matrix of an n-port network is that it be a pr matrix.

Sets of necessary and sufficient conditions equivalent to the definition of a pr function and a pr matrix have been presented in the literature. In this paper new sets of necessary and sufficient conditions are formulated for a rational function and a matrix of rational functions to be pr. These conditions give insights that may be useful in research on unsolved synthesis problems; some of these problems are now being studied by the authors. When used for testing purposes none of the new conditions requires root solving, and thus in many cases much of the tedium of previous tests is eliminated.

Reviews of Current Literature (p. 222)

Correspondence (p. 224)

Electronic Computers

Vol. EC-7, No. 3, September, 1958

The Chairman's Column—Willis H. Ware (p. 189)

Frontispiece—Willis H. Ware (p. 190)

Design of AC Computing Amplifiers Using Transistors—C. A. Krause and R. R. Lowe (p. 191)

A design philosophy for transistorized analog computing amplifiers is presented. A design procedure for a summing amplifier to drive a specific resolver in a 400-cps system is described, and the performance of the resulting circuit is evaluated. Whereas experience with vacuum tube amplifiers in similar applications has led to the conclusion that the amplifier input impedance should be as large as possible, the inverse is true in the transistor amplifier.

A Note on Contact Networks for Switching Functions of Four Variables—Roderick Gould (p. 196)

Several corrections are given to a recent tabulation of two-terminal contact networks realizing the switching functions of four variables. Nineteen new networks which are more economical in contacts than those previously tabulated are also presented and certain four-variable functions possessing a useful complementary relationship are listed. In conclusion this paper indicates an area where further work on four-variable contact network synthesis is needed.

On the Loop- and Node-Analysis Approaches to the Simulation of Electrical Networks—Joseph Otterman (p. 199)

The number of integrators in an analog-computer setup should be equal to the order of the differential equation describing the system. This paper presents a new procedure for tracing the loop currents which results in one-to-one correspondence between the number of integrators in the simulation setup and the count of independent energy-storing elements in the network, *i.e.*, the degree of the system's characteristic equation. The generality of the procedure proves that it is always possible to trace the loop currents in such a way that excess integrators are avoided. The loop-analysis and the branch-variables-analysis approaches are discussed and examples given.

Generalized Parity Checking—Harvey L. Garner (p. 207)

The usual definition given for the parity check is unwieldy and not particularly suited for the analysis or the study of the arithmetic properties of parity checking. The definition of parity by means of congruences provides a convenient mathematical basis for the concepts of the parity check. In this paper congruence notation is used to generalize the concepts of parity to include nonbase two number systems. Consideration is given to the cases where the check base is equal to the number base, and where it is not equal to the number base. The arithmetic properties of each case are considered by means of congruences.

Investigations of Magnetic Amplifiers with Feedback—Harry J. Gray, Jr. (p. 213)

Sine wave carrier excited magnetic amplifiers have been investigated to determine if the figure of merit can be improved through the use of feedback techniques. It is shown that the power gain can be made unlimited but that a finite rise time is preserved. Hence the figure of merit as ordinarily defined becomes meaningless. It is shown, however, that voltage gain divided by rise time remains nearly constant under feedback and is a more suitably defined figure of merit.

A New Class of Digital Division Methods—James E. Robertson (p. 218)

This paper describes a class of division methods best suited for use in digital computers with facilities for floating point arithmetic. The division methods may be contrasted with conventional division procedures by considering the nature of each quotient digit as generated during the division process. In restoring division, each quotient digit has one of the values $0, 1, \cdots, r-1$, for an arbitrary integer radix r. In nonrestoring division, each quotient digit has one of the values $-(r-1), \cdots, -1, +1, \cdots, +(r-1)$. For the division methods described here, each quotient digit has one of the values $-n, -(n-1), \cdots, -1, 0, 1, \cdots, n-1, n$, where n is an integer such that $\frac{1}{2}(r-1) \leq n \leq r-1$. A method for serial conversion of the quotient digits to conventional (restoring) form is given. Examples of new division procedures for radix 4 and radix 10 are given.

Magnetic Core Pulse-Switching Circuits for Standard Packages—Jack L. Rosenfeld (p. 223)

A new method for the logical design of magnetic core pulse-switching circuits is presented. This method has features which make it excellent for use in standard packages. These features are the absence of spurious noise signals at the output; the fact that outputs are independent of the order of arrival of input pulses; the fact that interchanging components does not affect circuit behavior; and the fact that moderate changes in clock pulse amplitude and duration do not cause false operation. Furthermore, the number of components required by this system compares favorably with the numbers required by other systems. A computing system can be built by properly interconnecting a few different types of such packages.

The new system uses advance current drive but performs the logical operations with both forward and backward windings in an output network. The use of both types of windings permits a reduction in the total number of cores required.

Tests performed on actual circuits yielded very encouraging results. The circuits operated as predicted, and the performance was most satisfactory.

The Switching Characteristics of 4-79 Permalloy Cores with Different Anneals—T. D. Rossing, W. M. Overn, and V. J. Korkowski (p. 228)

The magnetic properties of 4-79 Permalloy cores, which have been annealed at different temperatures, are discussed. Cores annealed at relatively low temperatures are characterized by high coercivity, slower switching, insensitivity to strain, magnetization difficult to rotate, and insensitivity to an applied transverse field. Some cores exhibit a preference to one remanent state over the opposite state.

Formal Analysis and Synthesis of Bilateral Switching Networks—Raymond E. Miller (p. 231)

Formal procedures for the analysis and synthesis of two-terminal combinational bilateral switching networks are presented. A bilateral switching network is one which contains only elements having the same switching transmission characteristic in both directions.

Following the definitions for the terminology and notation, where some new terms are introduced, the definitions for a series-parallel network, a bridge element, and a bridge network are given. A condition, called the bridge condition, to test a given transmission function for possible bridge network realizations is presented.

A stepwise decomposition procedure is developed which may be used for the analysis and synthesis of the series and parallel parts of the network. The steps are described both with linear graphs and connection matrices. The bridge condition partially formalizes bridge network synthesis. Redundant variables also are considered as an aid to network synthesis. Under certain conditions, the synthesis yields network realizations with the fewest possible number of elements.

A Transistor Pulse Generator for Digital Systems—Douglas J. Hamilton (p. 244)

A design procedure is developed for a new transistor pulse generator circuit suitable for use as a building block in a digital system. The circuit produces a pulse whose shape is relatively independent of variations in transistor parameters and load current. Pulse durations in the range 0.5 microsecond to 20 microseconds and load currents of several hundred milliamperes may be obtained.

Correction to "Logical Machine Design: A Selected Bibliography"—Douglas B. Netherwood (p. 250)

Correction to "Switching Functions of Three Variables"—D. W. Davies (p. 250)

Correspondence (p. 251)

Contributors (p. 252)

SENEWS, Science Education Subcommittee Newsletter (p. 254)

PGEC News (p. 259)

Industrial Electronics

PGIE-7, August, 1958

Automation in Highway Design—J. M. Cahn (p. 1)

The Semiautomatic Circuit Component Tester—F. C. Brammer (p. 4)

Process Instrumentation for the Measurement and Control of Level—G. Revesz (p. 11)

The use of capacitance-type measuring methods is described for indicating and controlling the level of liquid, granular or powdery materials. The purpose of this paper is twofold. First, it summarizes commercially available devices for various requirements (on-off control, proportional indication, proportional control, or combinations of these). Second, it formulates a method of analysis enabling users to choose suitable probe designs for specific applications.

Automatic Job Control Data System—C. Pilnick (p. 17)

In most industrial plants today, the system generally in use for acquiring and recording sufficient job data for accounting and planning purposes includes the following procedures:

1) Introduction of worker "time in, time out" and identification data onto a time card by means of a time clock.
2) Introduction of such variable data as job number, time spent on each job per day, craft code, etc., onto time sheets or records, usually performed manually.
3) Gathering of all such job data from various source records, again performed manually.
4) Transcribing the data into a format convenient for analysis and computation, either a manual or semiautomatic process.
5) Performing the desired computation or evaluation of the data for such end-item functions as payroll preparation, cost accounting, project analysis or compilation of statistics for job planning.

The complete job control data acquisition and recording process involves laborious manual transcription with the possibility of human error at many stages. This field therefore represents an exceptionally fruitful one for the application of automatic techniques, if the cost of an automatic system is low enough to pay for itself in a reasonable period of time.

A basic automatic system is described below. The system is designed for maximum cost, but is sufficiently flexible so that modifications custom-tailored to almost any requirements may be incorporated.

Application of Automatic Techniques in the Handling of Physical Data for a Modern Refinery—W. G. Deutsch (p. 23)

The modern refinery is perhaps the test example of continuous flow processing in American industry. This paper shows how the concept of automatic data handling was applied in the design, construction, and instrumentation of one of the world's most modern refineries. Benefits made available through the integration of a modern automatic data handling system accrue not only from manpower savings, but from many other sources such as reduction in other instrument requirements, timeliness of information, etc.

The primary concern of this paper is to show how the automatic data handling system is incorporated in the conceptual design of the plant, and how once installed, it is commissioned, and its data correlated with that of other information sources in such a plant. As a further point of interest, other potential applications for automatic physical data handling systems are suggested by the author.

Automatic Techniques, Large Computers, and Engineering Calculations—V. Paschkis (p. 27)

This three-part paper first discusses (*a*) large-scale computers preparing automation; (*b*) computing devices in the automatized plant; (*c*) computing devices and engineering calculations. Next the author discusses the organization of a computing laboratory for engineering calculations. In the final part some implications of automation and large computing devices are considered.

Applying the Electro-Hydraulic Servo Valve to Industry—R. Spencer (p. 33)

The industrial control field is constantly adapting new techniques and procedures. These changes are motivated by industry's need to turn out their products faster and with greater precision. To make these improvements possible the manufacturers of mechanical, electrical, pneumatic, and hydraulic equipment are constantly developing new components and systems. Some components are developed on the basis of a general industry need and others for specific applications. The latter group of components, though designed for specific applications, become standard components as control-system designers begin to visualize how they may be applied to other control problems.

The electro-hydraulic servo valve is in its transition period. The success achieved in military and machine-tool applications indicates that its potential for industrial control problems is very high. To apply the servo valve, the industrial control-system designer must become familiar with its functions, capabilities, reliability, economics, and some special considerations. These factors are quite interrelated and it is the over-all evaluation of these factors which determines its suitability. This paper hopes to assist the industrial-control field toward a better understanding of the servo valve.

Basic Gages and Gaging Considerations for Automatic Machine Control—J. W. Hopper (p. 40)

In considering automatic techniques, many and varied definitions of greatly overused and misused words are applied. Certainly "automatic," "machine," and "control" are out in front in so far as repetition is concerned. In order to chart a course through the material to be presented in this paper, I will arbitrarily consider that automatic machine control is a condition whereby material is manufactured by a piece of machinery, with suitable equipment to measure the product while it is being manufactured and provide corrections to the machine itself to produce material within desired limits. The gages in this configuration of measuring equipment will be dimensional measuring devices indicating diameter, length, thickness, and so on.

Logical Development of the Design for Sequential Control of Chemical Batch Processes—J. P. Laird (p. 44)

Chemical manufacturing processes frequently require safety interlock circuits which warn operating personnel of undesirable conditions or automatically act to avoid an accident. Batch-type manufacturing operations require that a succession of steps be carried out one after another, and successful operation depends on taking the proper action at the proper moment in a reproducible manner.

In the past there have been serious difficulties in communication among technical personnel who are concerned with these problems. Written descriptions are frequently either vague or confusing. What is needed are techniques which will aid in reading and writing of thought and reason. This paper attempts to aid in the solution of the problem.

A Survey of the Application of Automatic Devices for Electric Power Generation—A. C. Hartranft and F. H. Light (p. 55)

Twenty-five years ago power plant control and load dispatching were principally manual operations. Today, automatic devices are widely used and, in many cases, essential to safe and reliable operation. Much progress has been made in automation of power generation and distribution equipment. It is continuing. New developments include automatic data logging, automatic load control, network analysis by computers, and improved control systems.

It is the purpose of this survey to describe progress made in past years and briefly discuss new developments which are indicative of future trends. With this background, we are better able to judge the merits of automation and its potential advantages. These benefits are reduced operating costs, manpower savings, improved reliability, and more efficient use of manpower that has been relieved from routine duties.

The potential advantages of automation increase as electric systems grow in size and complexity. Large turbine-generating units require automatic controls and protective devices for reliable operation. Interconnection of systems makes automatic control necessary for regulation of interchange power flow.

An accurate evaluation of automatic control is difficult and requires careful study and judgment. Many of the advantages gained are intangible. Studies made by others provide valuable background information. This survey includes a bibliography of papers on automation in the electric power industry for the years 1950 to date.

The Application of the Punch Card to Automatic Weighing of Bulk Materials—W. M. Young (p. 63)

The automatic control of a dynamic batch-weighing system integrates many functions, more commonly associated with automation in the machine-tool industry. They are:

1) Power converting
2) Power actuating
3) Sensing
4) Regulating
5) Communicating
6) Programming
7) Computing
8) Data converting
9) Data storing
10) Data presenting.

Data storing and data presenting are the functions that directly involve the use of a punch card and similar information-storage media, and will be developed in detail.

Reliability and Quality Control

PGRQC-14, September, 1958

The papers in this issue were presented at the Fourth National Symposium on Reliability and Quality Control, Washington, D. C., January 6 to 8, 1958. They were not available in time for printing in the *Proceedings* of that meeting.

The Impact of Reliability Requirements on Organization in the Manufacture of Airborne Electronic Equipment—J. J. Crowley (p. 1)

Current Military Reliability Specifications—E. F. Dertinger and D. W. Pertschuk (p. 6)

Reliability Techniques for Electronic Circuit Design—L. Hellerman and M. P. Racite (p. 9)

Air Force Electronic Reliability Program—J. S. Lambert (p. 17)

Reliable Design and Development Techniques—J. E. McGregor (p. 22)

Mechanical concepts must be applied to modify electronic circuit design in order that large scale computer equipment can attain practical levels of reliability. This paper cites some specific mechanical design problems with regard to the reliability of a particular computer system, the AN/FSQ-7.

The Navy Specification Program for Reliability—E. J. Nucci (p. 27)

The objective of this paper is to simply relate the role of the specification in the Navy's Electronics Reliability Program over the past years and to outline what appears to be the specification aspect of reliability for the future. In my discussion I will deal for the most part with full equipments and systems reliability and specifications.

Accelerated Life Test in Airframe Manufacture—N. H. Simpson (p. 33)

System Aspects—M. M. Tall (p. 50)

Reliable System Design by Part Engineering—C. G. Walance (p. 55)

This paper will concern itself with the organization and activity of a component application engineering organization and the part it plays in the development of electronic systems with particular emphasis on those aspects which influence the reliability of the system.

The Challenge of Reliability to Management—W. W. Wooldridge (p. 57)

Utilization of Component Part Reliability Information in Circuit Design—M. A. Xavier, L. L. Schneider, and P. Gottfried (p. 60)

Component part reliability testing programs of varying scope are in progress in many areas of the electronics industry today. These programs differ in magnitude, levels of environmental and electrical stress, and types of component parts tested, but properly designed programs have one aspect in common: They can result not only in reliability evaluation, but also in reliability improvement. This paper will discuss techniques for optimizing circuit reliability by application of component characteristic data obtained from reliability testing.

An Application of the Box Technique to the Evaluation of Electrical Components (Addendum)—R. Glaser (p. 69)

Presented here are examples of the statistical analysis of the responses for two of the variables, Pulse Response Factor, and Rcs referred to in the titled paper. It is intended to show a step-by-step procedure in analyzing the results with particular emphasis placed on the details in preparing the Analysis of Variance Table.

Abstracts and References

Compiled by the Radio Research Organization of the Department of Scientific and Industrial Research, London, England, and Published by Arrangement with that Department and the *Electronic and Radio Engineer*, incorporating *Wireless Engineer*, London, England

NOTE: The Institute of Radio Engineers does not have available copies of the publications mentioned in these pages, nor does it have reprints of the articles abstracted. Correspondence regarding these articles and requests for their procurement should be addressed to the individual publications, not to the IRE.

The Index to the Abstracts and References published in the PROC. IRE from February, 1957 through January, 1958 is published by the PROC. IRE, May, 1958, Part II. It is also published by *Electronic and Radio Engineer*, incorporating *Wireless Engineer*, and included in the March, 1958 issue of that journal. Included with the Index is a selected list of journals scanned for abstracting with publishers' addresses.

The number in heavy type at the upper left of each Abstract is its Universal Decimal Classification number. The number in heavy type at the top right is the serial number of the Abstract. DC numbers marked with a dagger (†) must be regarded as provisional.

ACOUSTICS AND AUDIO FREQUENCIES

534:061.3 **3308**
Symposium on Unsolved Problems in Acoustics—(*J. Acoust. Soc. Amer.*, vol. 30, pp. 375–398; May, 1958.) The text is given of papers read at the 54th meeting of the Acoustical Society of America held at Michigan, October, 24–26, 1957, including the following:
1) **Electroacoustics and Transducers**—F. V. Hunt. (pp. 375–377.)
2) **Speech and Communication**—G. A. Miller. (pp. 397–398.)

534.1–8:538.222 **3309**
Paramagnetic Centres as Detectors of Ultrasonic Radiation at Microwave Frequencies—Kittel. (See 3416 below.)

534.13–8–16:538.69 **3310**
A Proposal for Determining the Fermi Surface by Magneto-acoustic Resonance—A. B. Pippard. (*Phil. Mag.*, vol. 2, pp. 1147–1148; September, 1957.)

534.22.08–16 **3311**
The Velocity of Sound in Metals at High Temperatures—J. F. W. Bell. (*Phil. Mag.*, vol. 2, pp. 1113–1120; September, 1957.) A pulse method of measuring the sound velocity in thin rods over a wide temperature range is described.

534.75 **3312**
Effect of the Transmission Characteristic of the Ear on the Threshold of Audibility—J. Zwislocki. (*J. Acoust. Soc. Amer.*, vol. 30, pp. 430–432; May, 1958.) Sensitivity/frequency curves are given based on Békésy's results (*e.g.*, 2121 of 1949).

534.75 **3313**
Creation of Pitch through Binaural Interaction—E. M. Cramer and W. H. Huggins. (*J. Acoust. Soc. Amer.*, vol. 30, pp. 413–417; May, 1958.) A faint pitch quality is detected when white noise presented at one ear is shifted in phase and presented to the other ear. An investigation of this phenomenon shows that phase information is of importance in pitch perception at frequencies up to 1.6 kc.

534.75:621.391 **3314**
Information Transmission with Elementary Auditory Displays—W. H. Sumby, D. Chambliss, and I. Pollack. (*J. Acoust. Soc. Amer.*, vol. 30, pp. 425–429; May, 1958.) The transmission of the letters of the alphabet by tone-coded signals is investigated using codes with two, three or five alternatives per letter and varying each of the four tonal variables. The highest reception rate was obtained with a three-alternative, frequency-coded display.

534.75:621.391 **3315**
Confidence Ratings and Message Reception for Filtered Speech—L. Decker and I. Pollack. (*J. Acoust. Soc. Amer.*, vol. 30, pp. 432–434; May, 1958.)

534.771:534.78 **3316**
Fundamentals of Testing the Hearing of Speech—F. J. Meister. (*Arch. Tech. Messen*, no. 264, pp. 7–8; January, 1958.) The problems are outlined of selecting suitable speech material and of evaluating test results in physiological measurements of hearing ability. For details of normal measurement technique see *ibid.*, no. 265, pp. 21–24; February, 1958.

534.79 **3317**
Proposal for an Explanation of Limens of Loudness—J. R. Pierce. (*J. Acoust. Soc. Amer.*, vol. 30, pp. 418–420; May, 1958.) The root-mean-square deviation in the number of pulses produced in a given time is suggested as a measure of the limen of loudness.

ANTENNAS AND TRANSMISSION LINES

621.315.212.3 **3318**
Transmission Characteristics of a Three-Conductor Coaxial Transmission Line with Transpositions—G. Raisbeck and J. M. Manley. (*Bell Sys. Tech. J.*, vol. 37, pp. 835–876; July, 1958.) The design, manufacture and some experimental results are described. The effective cross-section of the center conductor is increased by using a solid central member and a thin concentric shell. The reduction of skin-effect losses, compared with a two conductor cable of the same diameter, gives lower attenuation from 1 to 10 mc with a reduction of 17 per cent at 4 mc.

621.315.616 **3319**
Plastics in Cables—E. E. L. Winterborn. (*P.O. Elec. Eng. J.*, vol. 51, pp. 33–39; April, 1958.) The application to telephone exchanges, underground and antenna telephone cables, and to the protection of cables from corrosion, is discussed.

621.372 **3320**
Group and Phase Velocity—(*Wireless World*, vol. 64, pp. 445–449; September, 1958.) A simplified explanation of the terms is given and is applied to line and waveguide transmission.

621.372.2 **3321**
Calculation of Transmission Line Equations with New System Parameters—W. Doebke. (*Arch. elekt. Übertragung*, vol. 11, pp. 495–503; December, 1957.) Mathematical difficulties in the solution of line equations can be reduced by adopting the parameters on which the scattering-matrix concept is based. See *e.g.*, 1660 of 1958 (Carlin).

621.372.2.029.6:621.317.74 **3322**
High-Frequency Measuring Lines— Moerder. (See 3577.)

621.372.22 **3323**
The Nonuniform Transmission Line as a Broadband Termination—I. Jacobs. (*Bell Sys. Tech. J.*, vol. 37, pp. 913–924; July, 1958.) The transmission-line equations are solved for a line in which the fractional change in shunt admittance/wavelength is constant. It is shown that a fixed length of line can be made to have as large an effective length as desired, and complete absorption of all energy will occur if the line has a small loss term.

621.372.8+621.396.677.7 **3324**
Some Aspects of Waveguide Technique—J. C. Parr. (*J. Telev. Soc.*, vol. 8, pp. 413–422; April/June, 1958.) Fundamental properties of electromagnetic waves and the generation of various modes of propagation inside a waveguide are discussed. Modes in resonant cavities are also considered, and three devices—the cavity wavemeter, the hybrid T junction and the slotted-waveguide array—are described.

621.372.8 **3325**
Determination of Higher-Order Propagating Modes in Waveguide Systems—M. P. Forrer and K. Tomiyasu. (*J. Appl. Phys.*, vol. 29, pp. 1040–1045; July, 1958.) A theoretical analysis and an experimental method are given

for determining the power level and relative phase of all propagating modes in a rectangular waveguide. Practical details are quoted for a 5 mw, S-band magnetron.

621.372.8 3326
Local Reflections in Waveguides of Variable Cross-Section—V. Pokrosvkii, F. Uiinich, and S. Savvinykh. (*Dokl. Akad. Nauk S.S.S.R.*, vol. 120, pp. 504–506; May 21, 1958.) Mathematical analysis of the reflection and scattering produced by discontinuities.

621.372.823:621.317.7:538.566 3327
Double-Probe Polarimetric Analyser for the 1000-Mc/s Band—Picherit. (See 3574.)

621.372.823:621.372.83 3328
Circular-Waveguide Taper of Improved Design—H. G. Unger. (*Bell Sys. Tech. J.*, vol. 37, pp. 899–912; July, 1958.) Conical tapers with gradual change of cone angle transform cylindrical waves into spherical waves in the transition region. Optimal and almost optimal tapers are found for which the power conversion from TE_{01} transmission to spurious modes is small for frequencies up to 75 kmc.

621.372.826:537.226 3329
Surface Waveguide—S. K. Chatterjee and R. Chatterjee. (*J. Inst. Telecommun. Eng., India*, vol. 4, pp. 90–95; March, 1958.) Characteristic equations are given for surface-wave propagation along a solid conductor embedded in three coaxial dielectrics. See also 1017 of 1958.

621.372.85:621.318.134 3330
Use of Microwave Ferrite Toroids to Eliminate External Magnets and Reduce Switching Power—M. A. Treuhaft and L. M. Silber. (Proc. IRE., vol. 46, p. 1538; August, 1958.) Experiments show that toroids may replace slabs in some microwave devices, eliminating the need for external magnetizing currents and permitting higher switching rates.

621.372.852.22 3331
X-Band Phase Shifter without Moving Parts—W. H. Hewitt, Jr., and W. H. von Aulock. (*Electronics*, vol. 31, pp. 56–58; July 4, 1958.) The unit comprises two transversely magnetized ferrite slabs in the narrow walls of a rectangular waveguide. Continuous phase variation from 0 to 360 degrees is obtainable for up to 15 kw peak power. Maximum insertion loss is 0.75 db, and voltage SWR 1.08.

621.372.852.3:621.372.823 3332
The Frequency Response of Waveguide Potential Dividers with Coaxial Launching and Pick-Up—A. Sander. (*Nachrichtentech. Z.*, vol. 11, pp. 1–5; January, 1958.) The types of piston attenuator are discussed, with reference to theory presented earlier (2292 of 1956). Forty references.

621.372.852.323:621.318.134:621.317.74 3333
High-Power Testing of Ferrite Isolators—Wantuch. (See 3578.)

621.396.67:517.512.2(083.5) 3334
A New Table of the Amplitude Functions of the Iterated Sine and Cosine Integrals and Some Comments on the Aperiodic Functions in Hallén's Antenna Theory—P. O. Brundell. (*Acta polyt., Stockholm*, no. 217, 14 pp; 1957. *Kungl. tek. Högsk. Handl., Stockholm*, no. 108; 1957.) See also 1873 of 1955 (Hallén).

621.396.673.029.4 3335
A Study of Earth Currents near a VLF Monopole Antenna with a Radial Wire Ground System—J. R. Wait. (Proc. IRE, vol. 46, pp. 1539–1541; August, 1958.) The results of experimental studies are briefly reported and confirm the author's earlier theoretical work. See also 334 of 1955 (Wait and Pope).

621.396.677 3336
Suppression of Undesired Radiation of Directional HF Antennas and Associated Feed Lines—H. Brueckmann. (Proc. IRE, vol. 46, pp. 1510–1516; August, 1958.) Practical measurements of rhombic antennas show large sidelobes which may contribute to interference in the HF band. Antenna arrays using nonuniform amplitude distributions and a tapered-aperture horn are briefly described, in which the sidelobes are substantially reduced. Coaxial feeders coupled to wide-band transformers are suggested in place of open-wire lines which are difficult to balance accurately.

621.396.677.001.57 3337
Use of Scale Model Techniques in the Design of V.H.F. and U.H.F. Antennas—F. J. H. Charman, J. Thraves and E. F. Walker. (*Electronic Eng.*, vol. 30, pp. 498–501; August, 1958.)

621.396.677.3:523.164 3338
Optimum Arrays for Direction Finding—N. F. Barber. (*N.Z. J. Sci.*, vol. 1, pp. 35–51; March, 1958.) The design of an array of receivers suitable for exploring the distribution of wave power with wave direction is discussed. Examples of practical arrays, including the Mills Cross, for the determination of power distribution with the minimum mean square error are examined.

621.396.677.3:523.164 3339
Gain Measurements of Large Antennas used in Interferometer and Cross-Type Radio Telescopes—A. G. Little. (*Aust. J. Phys.*, vol. 2, pp. 70–78; March, 1958.) A method is described using strong, discrete radio sources whose intensity need not be known. The method is applied to the 3.5-m Mills Cross radio telescope at Sydney [1126g of 1958 (Mills, *et al.*)].

621.396.677.73 3340
A New Ultra-Wide-Band Microwave Antenna—T. Sakurai. (*Rep. Elec. Commun. Lab., Japan*, vol. 6, pp. 40–45; February, 1958.) The antenna described is matched over the frequency band 4000–9400 mc with a voltage SWR better than 1.12. The gains are 32 and 40 db at the ends of the band.

621.396.677.8.029.6 3341
Polarization-Transforming Plane Reflector for Microwaves—J. Aagesen. (*Acta polyt., Stockholm*, no. 239, 27 pp.; 1957.) The infinite reflector investigated consists of a perfectly conducting surface in front of which is a parallel, anisotropically conducting surface. The intervening space is filled with a perfect dielectric. By a suitable choice of the thickness of the dielectric and the plane of polarization of the incident wave it is always possible to obtain a circularly polarized reflected wave.

621.396.677.833 3342
A 360° Scanning Microwave Reflection—J. A. C. Jackson and E. G. A. Goodall. (*Marconi Rev.*, vol. 21, no. 128, pp. 30–38; 1958.) The design and construction are described for a parabolic-torus reflector in the form of a radome with a wire grating inserted in its surface. A beam width of 3.5 degrees for −6 db with sidelobes at −25 db is possible for *X*-band frequencies using a 6-foot diameter reflector.

AUTOMATIC COMPUTERS

681.142 3343
Electronic Computer Research—(*Tech. News Bull., Natl. Bur. Stand.*, vol. 42, pp. 57–79; April, 1958.) A note on the research program of the National Bureau of Standards followed by ten short papers with titles as under.

a) **A High-Speed Multiplier for Electronic Digital Computers**—(pp. 58–59).

b) **Processing Pictorial Information on Digital Computers**—(pp. 60–63).

c) **Low-Power Plug-In Packages for Electronic Computer Circuitry**—(pp. 63–65).

d) **SEAC Converted to Applications Research Facility**—(pp. 65–66).

e) **A Function Generator for Two Independent Variables**—(p. 67).

f) **Man-Machine Simulation System**—(pp. 68–70).

g) **Problem Solving on the High-Speed Computer**—(pp. 71–75).

h) **Chemical Structure Searching with Automatic Computers**—(pp. 75–76).

i) **Magnetic Amplifiers for Digital Computers**—(pp. 77–78).

j) **Diode Amplifier Shift Register**—(pp. 78–79).

681.142 3344
Electronic Computers 1957—K. Prause. (*VDI Z.*, vol. 100, pp. 701–708; June 1, 1958.) A survey with tabulated data on German equipment. Ninety-four references.

681.142 3345
Accuracy Control in Electronic Business Data Processing Systems—J. C. Hammerton. (*Electronic Eng.*, vol. 30, pp. 483–486; August, 1958.)

681.142 3346
Digital Codes in Data-Processing Systems—M. P. Atkinson. (*Trans. Soc. Instr. Tech.*, vol. 10, pp. 87–90; June, 1958.) Discussion on 1981 of 1958.

681.142 3347
Simple Digital Correlator—C. Collins. (*Rev. Sci. Instr.*, vol. 29, pp. 487–490; June, 1958.) "A description is given of a simple electronic correlator which employs punched-tape input and visual digital readout. Cold-cathode counting tubes are used in the arithmetic unit. Several basic design considerations are briefly discussed, and an outline is given of the recent application of the correlator to a problem in meteor physics."

681.142 3348
An Improved Technique for Fast Multiplication on Serial Digital Computers—M. Shimshoni. (*Electronic Eng.*, vol. 30, pp. 504–505; August, 1958.)

681.142 3349
Half-Adders Drives Simultaneous Computer—F. B. Maynard. (*Electronics*, vol. 31, pp. 80–82; July 18, 1958.) A combination of transistorized half and full adders, emitter followers, output amplifiers and multiplier gates provides simultaneous binary addition of digital inputs.

681.142 3350
Relay-Scanning-Design Technique Generates High Accuracy and Speed in Analogue-to-Digital Transducer Measurements—A. F. Kay. (*Commun. and Electronics*, no. 36, pp. 248–250; May, 1958.) The converter is designed to handle three decades of binary decimal pulses; each decimal unit is equivalent to 20 μv input. The converter scans an internal voltage until it becomes equal to the unamplified input voltage and supplies a serial pulse output.

681.142 3351
The Design of Function Generators using Short-Time Memory Devices and Nonlinear Elements—A. W. Revay and D. J. Ford. (*Commun. and Electronics*, no. 36, pp. 143–152; May, 1958.) The various types of function

generator discussed have easily controllable output waveforms which can be made to approximate to any desired shape with a high degree of accuracy.

681.142 3352
An Electronic Differential Analyser—A. K. Choudhury and B. R. Nag. (*Indian J. Phys.*, vol. 32, pp. 91–108; February, 1958.) Equations are derived to show the effect of errors due to circuit elements, and some experimentally obtained solutions are compared with calculated values.

681.142:512.3 3353
On the Application of an Electronic Differential Analyser for Finding the Roots of a Polynomial—B. R. Nag. (*Indian J. Phys.*, vol. 32, pp. 212–217; May, 1958.) A transfer function is used with the polynomial as numerator and another suitable function as denominator. The roots are given by the zeros of the output of the system.

681.142:517.9 3354
Digital Field Computers—B. Meltzer and I. F. Brown. (*Nature, London*, vol. 181, pp. 1384–1385; May 17, 1958.) To eliminate the speed limitation of conventional digital techniques for field computations, a nonuniversal unitary system is proposed, based on the analogy between electron flow through a resistance network and the flow of pulses through a network of computer units. An integral number N is represented by N pulses, and a basic unit generates a train of $\frac{1}{2}(N_1+N_2)$ synchronized pulses from two input pulse trains of N_1 and N_2 pulses. The interconnection of a lattice of basic units gives a finite-difference representation of the general field equation.

681.142:518.4 3355
An Automatic Graph Plotter—J. J. Morrison. (*Trans. Soc. Instr. Tech.*, vol. 10, pp. 55–66; June, 1958.) The adaptation of an analog plotting table for accepting input data in digital form is described.

681.142:621.039 3356
The Application of Digital Computers to Nuclear-Reactor Design—J. Howlett. (*Proc. IEE*, vol. 105, pp. 331–336; July, 1958. Discussion, pp. 365–369.) The main computational problems are reviewed, together with examples of the treatment of neutron transport problems. An assessment is made of the performance requirements of future computers.

681.142:621.372.5 3357
Use of Laguerre Filters for Realisation of Time Functions and Delay—A. K. Choudhury and N. B. Chakrabarti. (*Indian J. Phys.*, vol. 32, pp. 205–211; May, 1958.)

681.142:621.385.832 3358
Analogue Multiplier and Function Generator with Cathode-Ray Tube—A. K. Choudhury and B. R. Nag. (*Indian J. Phys.*, vol. 32, pp. 141–148; March, 1958.) A capacitive pick-up device is mounted outside the CR tube in front of the screen; it is easily replaced so that the same tube can be used as multiplier or for generating different types of functions.

681.142:621.396.11 3359
An Electronic Computer for Statistical Analysis of Radio Propagation Data—M. Grønlund and C. O. Lund. (*Acta polyt., Stockholm*, no. 222, 26 pp., 18 plates; 1957.)

CIRCUITS AND CIRCUIT ELEMENTS

621.3.049.75 3360
Printed Circuits—A. Roos. (*Metal Ind., Lond.*, vol. 92, pp. 467–470; June 6, 1958.) Review of materials and manufacturing processes.

621.318.4.045 3361
Coils for Magnetic Fields—G. M. Clarke. (*Electronic Radio Eng.*, vol. 35, pp. 298–306; August, 1958 and pp. 340–344; September, 1958.) A comparison between wire-wound, foil-wound and coaxial-cable-wound solenoids, considering the limitations of temperature-rise and weight. Equations relating field, power and internal temperature difference are obtained from which the performance of any coil can be calculated. The relative advantages of Al or Cu windings are considered.

621.319.4 3362
A Note on the Self-Resonance of Ceramic Capacitors—J. Bork. (*Proc. IRE, Aust.*, vol. 18, pp. 159–162; May, 1957.) Details of changes in self-resonant frequency with a capacitor type, length of connecting leads and method of mounting are given. Practical applications of the self-resonance of these components in VHF circuits are suggested.

621.372:512.831 3363
Certain Applications of Matrices to Circuit Theory—L. A. Pipes. (*Commun. and Electronics*, no. 36, pp. 251–256; May, 1958.) Matrices can be constructed for circuits so that their eigenvalues and vectors relate to the circuit parameters. Propagation constants, characteristic impedances and symmetrical components in polyphase systems are considered from this point of view.

621.372.2:621.318.5 3364
Synthesis of Series-Parallel Network Switching Functions—W. Semon. (*Bell Sys. Tech. J.*, vol. 37, pp. 877–898; July, 1958.) "From the switching functions of n variables, those which correspond to networks are abstracted and called network functions. Properties of those network functions corresponding to series-parallel networks are studied and a method for synthesis is developed."

621.372.414 3365
High-Power Radio-Frequency Broad-Band Transformers—E. R. Broad (*P.O. Elec. Eng. J.*, vol. 51, pp. 8–13; April, 1958.) "The design of wide-band transformers composed of simple transmission line elements and capable of handling radio-frequency power of the order of 20 kw is discussed. Examples are given of devices matching 75-ohm coaxial cable to balanced-pair transmission lines with a standing-wave ratio of less than 1.3 over the band 4–28 mc."

621.372.51 3366
Complex Matching—D. Steffen. (*Elektronische Rundschau*, vol. 12, pp. 3–9; January, 1958.) The conditions are investigated for obtaining maximum real power at the input of a complex load matched to a generator with complex internal impedance.

621.372.54:621.396.96 3367
Analysis and Synthesis of Delay-Line Periodic Filters—H. Urkowitz. (IRE Trans. on Circuit Theory, vol. CT-4, pp. 41–53; June, 1957. Abstract, Proc. IRE, vol. 45, p. 1432; October, 1957.)

621.372.543.2 3368
Pulse Distortion by Band Filters—K. Emden. (*Arch. elekt. Übertragung*, vol. 11, pp. 509–512; December, 1957.) The roots of the homogeneous differential equations for image-parameter (Zobel) band-pass filters with one to four stages are tabulated. The integration constants are determined for the case of a square-wave-modulated carrier equal to the mid-band frequency of the filter.

621.372.543.2 3369
Design of Unsymmetrical Band-Pass Filters—R. F. Baum. (IRE Trans. on Circuit Theory, vol. CT-4, pp. 33–40; June, 1957. Abstract, Proc. IRE, vol. 45, pp. 1431–1432; October, 1957.)

621.372.553 3370
Simplifying Phase Equalizer Design—W. J. Judge. (*Electronic Ind.*, vol. 17, pp. 76–77; April, 1958.) A graphical method using bridged-T and all-pass lattice networks.

621.372.57:621.314.7 3371
Power Amplification × Bandwidth Figure of Merit for Transducers including Transistors—L. J. Giacoletto. (*J. Electronics Control*, vol. 4, pp. 515–522; June, 1958.) A figure of merit based on spot-frequency maximum power amplification×bandwidth is derived for a transducer which is unilateralized and conjugately matched, the result being simplified by assuming a bell-shaped frequency response. Specfic formulas are given for tube and transistor circuits. See *e.g.*, 2238 of 1953.

621.372.6 3372
On the Synthesis of Three-Terminal Networks Composed of Two Kinds of Elements—K. M. Adams. (*Philips Res. Rep.*, vol. 13, pp. 201–264; June, 1958.) "A set of necessary and sufficient conditions and a method of realization of all sets of series-parallel *LC* three-terminal network functions from the zeroth to the sixth degree are given."

621.372.632:621.396.621 3373
A Low-Noise Crystal-Controlled Converter for 144 Mc/s—G. R. Jessop. (*R.S.G.B. Bull.*, vol. 33, pp. 510–512; May, 1958.) Construction details of a converter providing satisfactory reception of signals of about 3 db above noise level.

621.373.1.018.756 3374
Millimicrosecond Pulse Generator—O. H. Davie. (*Electronic Radio Eng.*, vol. 35, pp. 332–335; September, 1958.) The generator uses a length of high-frequency cable which is charged from a known dc potential. The cable is then discharged into the load by a magnetically operated mercury switch at pulse repetition frequencies up to 120 cps for pulses of 1-mμsec rise time.

621.373.1.029.4 3375
Calculations for a Capacitor with Rotating Armatures Piloting a Very-Low-Frequency Generator—P. Dupin, R. Lacoste, and H. Martinot. (*Compt. Rend. Acad. Sci., Paris*, vol. 246, pp. 1172–1175; February 24, 1958.) See 1699 of 1957 (Dupin).

621.373.421.13 3376
Fluctuations in Quartz Crystal Oscillators—M. E. Zhabotinskiĭ and P. E. Zil'berman. (*Dokl. Akad. Nauk S.S.S.R.*, vol. 119, pp. 918–921; April 11, 1958.) Results of an analysis using symbolic differential equations show that the noise and thermal fluctuations are not determining factors for stability. See also 1996 of 1956 (Rytov).

621.373.421.13 3377
Thermally Compensated Crystal Oscillator—(*Wireless World*, vol. 64, p. 441; September, 1958.) Frequency stabilization without the use of a temperature-controlled oven is obtained by varying the effective shunt load of the crystal, a thermistor head being the temperature-sensitive element.

621.373.52.072.6 3378
Transistor Circuit Varies Reactance—F. F. Radcliffe. (*Electronics*, vol. 31, pp. 76–80; July 4, 1958.) Frequency control of a 2.5-kc oscillator to within 0.1 cps is achieved by means of a variable-reactance circuit which produces an effective capacitance change of up to 3500 pf for a change in emitter current from zero to 700 μa.

621.374.3:681.142 3379
A Neon Pulser for the Computer Laboratory—R. L. Ives. (*Electronic Ind.*, vol. 17, pp. 98–100; April, 1958.) An output of 70 volt peak, positive or negative, at pulse repetition frequencies from less than 1 cps to 2.5 kc is obtained.

621.374.32 3380
High-Speed Pulse Amplitude Discriminator—F. J. M. Farley. (*Rev. Sci. Instr.*, vol. 29, pp. 595–596; July, 1958.) A circuit is described for use in fast counting systems. It handles pulses of amplitude 1–21 volts generating a positive output pulse of constant amplitude whose length is determined by the length of the input pulse. Dead time is about 20 mμsec and peaks 40 mμsec apart are separated.

621.375.012:621.396.822 3381
Optimum Noise Performance of Linear Amplifiers—H. A. Haus and R. B. Adler. (PROC. IRE, vol. 46, pp. 1517–1533; August, 1958.) A single quantitative measure of amplifier "spot noise" performance $(M_e)_{opt}$ is established which removes difficulties associated with the effect of feedback on the noise figure as it is a function only of the amplifier noise and circuit parameters. It determines the lowest noise figure obtainable at high gain with a given amplifier used alone, or passively connected to other amplifiers of the same $(M_e)_{opt}$, and it provides an index of the absolute quality of noise performance.

621.375.024 3382
Performance Calculations for DC Chopper Amplifiers—I. C. Hutcheon. (*Electronic Eng.*, vol. 30, pp. 476–480; August, 1958.) Switched chopping and demodulating circuits are analyzed, and methods of calculating the essential parameters are described.

621.375.024:[621.317.725:621.385 3383
D.C. Amplifier Expands Input Voltage Range—V. D. Schurr. (*Electronics*, vol. 31, pp. 87–89; June 6, 1958.) A direct-coupled dc amplifier with infinite input-voltage range and infinite input impedance is described, and details are given of its application in a differential tube-voltmeter without input voltage dividers for measurements at mean levels between −150 and +300 volts.

621.375+621.385].029.65 3384
The Generation and Amplification of Millimetre Waves—W. Kleen and K. Pöschl. (*Nachrtech. Z.*, vol. 11, pp. 8–19; January, 1958 and pp. 77–84; February, 1958.) A detailed survey of techniques and devices including the maser and the harmodotron. Eighty-eight references.

621.375.126:621.396.96 3385
The Design of Primary and Secondary Radar I.F. Amplifiers—N. N. Patla. (*J. Inst. Telecommun. Eng., India*, vol. 4, pp. 102–111; March, 1958.) The features of synchronous and stagger-tuned circuit arrangements are discussed and design procedures outlined. Practical considerations such as feedback coil design and heat dissipation, and the design of amplifiers having logarithmic characteristics are also covered.

621.375.2:621.317.755 3386
Direct or A.C. Coupling for Deflexion Amplifiers—H. L. Mansford. (*Electronic Eng.*, vol. 30, pp. 473–475; August, 1958.) A quasi-dc coupling system using a vertical-deflection amplifier input switch providing dc reference pulses for level clamping is described. It is suitable for the range dc–100 mc, and the range of dc shift can be extended indefinitely as far as insulation permits.

621.375.2.132.3 3387
A Direct-Coupled Phase-Splitter—C. Billington. (*Electronic Eng.*, vol. 30, pp. 480–482; August, 1958.) A precision cathode-follower and inverter are described having an output resistance of about 3Ω and a frequency response from dc to beyond 100 kc.

621.375.226:621.396.96 3388
Ringing Amplifier—S. Rozenstein and E. Gross. (*Electronic Radio Eng.*, vol. 35, pp. 327–332; September, 1958.) A circuit for amplifying 0.2 μsec pulses by 110 db in a radar transponder is described. Damped oscillations, produced by the transient response of a tuned circuit, are amplified, and the second half-cycle selected to trigger the transponder. The unit is of small size and has a low power consumption and a fixed internal delay of 0.4 μsec.

621.375.23 3389
Bootstrap Circuit Technique—A. W. Keen. (*Electronic Radio Eng.*, vol. 35, pp. 345–354; September, 1958.) "The normal amplifier, the bootstrapped amplifier, the cathode-follower and the anode-follower are shown to comprise a set of four circuits related to one another by simple circuit transformations. Three methods of excitation are distinguished. Each circuit may be put into feedback form, and the four basic feedback configurations applicable to bootstrap amplifiers are given. A number of practical examples are described."

621.375.3 3390
Magnetic Amplifiers—D. Katz. (*Bell Lab. Rec.*, vol. 36, pp. 294–297; August, 1958.) The use of magnetic amplifiers as static switching devices is discussed. Switching action is obtained by biasing to saturated or unsaturated states. A binary to quaternary decoder using this principle is described.

621.375.3 3391
Magnetic-Amplifier Design—R. E. Anderson. (*Commun. and Electronics*, no. 36, pp. 160–175; May, 1958.) Commencing with the basic information of power supply frequency, desired gain and time constant, charts are developed to determine the core design, with reference to load voltage and current. With a specified core, additional charts are presented to determine the design of the winding layout.

621.375.3:537.312.62 3392
Superconducting Rectifier and Amplifier—J. L. Olsen. (*Rev. Sci. Instr.*, vol. 29, pp. 537–538; June, 1958.) To avoid heat losses due to heavy-current leads in apparatus at liquid-helium temperatures, a high-voltage ac supply is applied to a transformer which is coupled to the load through a coil of superconducting material. By applying a magnetic field parallel to the axis of the coil a dc component is produced in the load. A current amplification factor of 10 is obtained at 4.2°K using coils of 0.6-mm wire drawn from lead-tin solder. See also 2675 of 1958 (De Vroomen and Van Baarle).

621.375.4 3393
Collector Bias, the Transistor Equivalent of Cathode Bias, and some Applications—R. F. Treharne. (*Proc. IRE, Aust.*, vol. 18, pp. 149–159; May, 1957.) " A self-bias circuit for stabilizing the operating point of a transistor amplifier without unduly decreasing the gain at very low frequencies is discussed. Expressions for the frequency response, stability and input impedance are derived and the application of the circuit to amplifiers, oscillators and active filters is considered."

621.375.4 3394
Diode cuts Transistor Cut-off-Current Drift—H. H. Hoge. (*Electronics*, vol. 31, p. 83; July 18, 1958.) Amplified thermal variations of cut-off current in grounded-emitter amplifiers can be compensated by connecting a diode, experiencing the same thermal changes and having similar collector/base junction saturation current characteristics, across the transistor base/emitter junction.

621.375.4.024 3395
A Stabilized D.C. Differential Transistor Amplifier—L. Depian and R. E. Smith. (*Commun. and Electronics*, no. 36, pp. 157–159; May, 1958.) Design details and performance characteristics of a circuit which is insensitive to temperature changes. The method employed eliminates feedback and compensating circuits with their attendant complications and disadvantages.

621.375.43 3396
Designing Multiple Feedback Loops—F. H. Blecher. (*Electronic Ind.*, vol. 17, pp. 78–82; April, 1958 and pp. 64–68; May, 1958.) Design considerations applicable to transistors in the common-cathode, common-base or common-emitter connections are discussed. Theorems for determining the gain of any multiple-loop circuit and a stability criterion are given

621.375.9:538.569.4.029.6 3397
The Saturation Effect in a System with Three Energy Levels—Fain. (See 3420.)

621.375.9:538.569.4.029.64 3398
A Three-Level Solid-State Maser—H. E. D. Scovil. (*Bell Lab. Rec.*, vol. 36, pp. 243–246; July, 1958.) Nonmathematical description of three-level maser operation, including a mechanical analogy. Some constructional details and operating characteristics of a particular model amplifying at 6 kmc are given.

621.375.9.029.64:621.3.011.23:621.314.63 3399
Low-Noise Amplifier—(*Bell Lab. Rec.*, vol. 36, pp. 250–251; July, 1958.) Description of a 6-kmc parametric amplifier using a variable capacitance in the form of a diffused-base Si diode with an active area 0.002 inch in diameter. Advantages and applications of such amplifiers are discussed.

621.376.22:621.314.63 3400
Ring Modulator Reads Low-Level D.C.—E. J. Keonjian and J. D. Schmidt. (*Electronic Ind.*, vol. 17, pp. 86–89; April, 1958.) DC signals in the range $10^{-10}-10^{-3}$A are fed via a logarithmic Si-diode attenuator to a ring modulator and converted to ac, which is amplified and serves as a measure of the dc input. See also 1663 of 1956 (Moody).

GENERAL PHYSICS

535.33-1 3401
The Forty-Eighth Kelvin Lecture: "Infrared Radiation"—G. B. B. M. Sutherland. (*Proc. IEE*, vol. 105, pp. 306–316; July, 1958.) Historical survey with details of applications in the field of infrared spectroscopy. Thirty-three references.

537.122:53.08 3402
Importance of the Faraday to Elemental Constants and Electricity Standards—A. G. McNish and R. D. Huntoon. (*Nature, London*, vol. 181, p. 1194; April 26, 1958.) The ratio e/m can be determined with high accuracy and without uncertainties due to electrical standards and the acceleration of gravity, using the value of the gyromagnetic ratio of the proton determined from precision measurements (see *Nuovo Cim.*, vol. 6, pp. 146–184; 1957) the cyclotron frequency of the proton, and the faraday determined electrochemically.

537.226:621.396.677.8 3403
Anisotropic Effects in Geometrically Isotropic Lattices—Z. A. Kaprielian. (*J. Appl.*

Phys., vol. 29, pp. 1052–1063; July, 1958.) An analysis of the anisotropy produced by an arbitrary ratio of element spacing to wavelength in an artificial lattice dielectric. The "granularity" which is important at high frequencies is considered in detail. See also 1671 of 1956.

537.226.31 3404

The Electric Properties of a Dielectric with a Variable Number of Relaxation Centres—N. P. Bogoroditskiĭ, Yu. M. Volokobinskiĭ, and I. D. Fridberg. (*Dokl. Akad. Nauk S.S.S.R.*, vol. 120, pp. 487–490; May 21, 1958.) Expressions are derived for permittivity and of dielectric loss tangent. It is shown that the number of ions and dipoles which give rise to relaxation polarization increases with temperature, leading to an increase of permittivity.

537.311.31 3405

Plasma Approach to Metallic Conduction—L. Gold. (*Nature, London*, vol. 181, pp. 1316–1317; May 10, 1958.) Normal and superconductive response in metals may be construed as limiting modes of metallic conduction using a theory of plasma interaction.

537.311.33:539.2:061.3 3406

Report on the 5th Course of the International School of Physics of the Italian Physical Society, Varenna, 14th July–3rd August 1957—(*Nuovo Cim.*, vol. 7, pp. 165–736; 1958.) Report of the proceedings of the course on solid-state physics held at the Villa Monastero, Varenna. The text is given of lectures and discussions, including the following:

a) **Optical Properties of Solids**—D. L. Dexter. (pp. 245–286. In English.) Fifty-three references.

b) **The Transition from the Metallic to the Nonmetallic State**—N. F. Mott. (pp. 312–328. In English.)

c) **Electrons and Plasmons**—D. Pines. (pp. 329–352. In English.)

d) **Transport Properties of Solids**—J. M. Ziman. (pp. 353–376. In English.)

e) **Point Imperfections in Solids**—F. Seitz. (pp. 414–443. In English.)

f) **Dislocations in Germanium and Silicon**—H. G. van Bueren, J. Hornstra, and P. Penning. (pp. 646–660. In English.)

g) **Properties of Semiconductors**—H. Y. Fan. (pp. 661–695. In English.)

h) **Semiconducting Compounds**—G. A. Busch. (pp. 696–712. In English.)

i) **Shallow Impurity States in Semiconductors**—W. Kohn. (pp. 713–723. In English.)

j) **Recombination Processes in Semiconductors**—P. Aigrain. (pp. 724–729. In English.)

k) **Semiconductors with Charge Carriers of Low Apparent Mass**—O. Madelung. (pp. 730–736. In German.)

537.311.62 3407

The Theory of the Anomalous Skin Effect in Metals—V. P. Silin. (*Zh. eksp. teor. Fiz.*, vol. 33, pp. 1282–1286; November, 1957.) Information concerning the Fermi surface obtained from measurements of surface impedance in the region of the anomalous skin effect does not depend on whether the conduction electrons are considered as a gas or as a degenerate fluid.

537.311.62 3408

Skin Effect with Shock Waves—L. Castagnetto. (*Compt. Rend. Acad. Sci., Paris*, vol. 246, pp. 916–918; February 10, 1958.) Approximate formulas are given for the skin effect in a cylindrical conductor traversed by a shock wave.

537.523 3409

The Impulse Breakdown Characteristic of a Point/Plane Gap in Air—J. J. Kritzinger and G. R. Bozzoli. (*Nature, London*, vol. 181, p. 1259; May 3, 1958.) The influence of the duration of the impulse wave on the breakdown characteristics for both polarities was investigated for air at a pressure of 62.5 cm Hg and temperature 25°C.

537.533:621.385.029.6 3410

The Complex Formulation of the Equations for Two-Dimensional Space-Charge Flow—P. T. Kirstein. (*J. Electronics Control*, vol. 4, pp. 425–433; May, 1958.) The equations satisfied by an electron for congruent space-charge flow are solved using a complex-variable formulation, for a constant magnetic field normal to the flow. Solutions are also obtained in the presence of space charge but with absence of magnetic fields, and for flow along the level lines of a harmonic function.

537.56:538.56 3411

Containment of a Fully Ionized Plasma by Radio-Frequency Fields—H. A. H. Boot, S. A. Self, and R. B. R. Shersby-Harvie. (*J. Electronics Control*, vol. 4, pp. 434–453; May, 1958.) A fully ionized plasma is treated as a compressible loss-free dielectric in a RF field. It is shown that there are steady forces which may be used to confine a body of dense plasma in a conducting cavity resonant in a suitable mode. A particular solution, the E_0 cutoff mode, for which extensive numerical calculations have been made is discussed in some detail and interpreted in terms of possible physical experiments.

537.56:538.6:538.56.029.53 3412

Investigations on the Occurrence of High-Frequency Oscillations in an Ion Source with Magnetic Guiding Field—H. Kühn. (*Z. Phys.*, vol. 149, pp. 267–275; October 19, 1957.) Oscillations at about 1 mc were observed in H_2 and A, and their amplitude and frequency was measured under various conditions. The effect is interpreted as an acoustic type of plasma oscillation.

537.56:538.63 3413

Oscillations in a Plasma with Oriented (D.C.) Magnetic Field—L. Gold. (*J. Electronics Control*, vol. 4, pp. 409–416; May, 1958.) The angular dependence of the double resonances representing coupling of a low-energy plasma and cyclotron oscillations is studied for all orientations of the dc electric and magnetic fields, using a nonlinear phenomenological approach. Conditions favorable for manifestation of these modes are indicated.

538.221 3414

Statistics of the Ising Ferromagnet—A. Levitas and M. Lax. (*Phys. Rev.*, vol. 110, pp. 1016–1027; June 1, 1958.) The Ising model is treated by synthesizing a cluster treatment with the spherical model which is used to determine approximately the molecular field acting on the cluster, and the effective interactions between dipoles of the cluster. The method is applied to the square net and to the cubic lattice and the critical temperatures are obtained.

538.221:537.228.4 3415

The Use of the Kerr Effect for Studying the Magnetization of a Reflecting Surface—E. W. Lee, D. R. Callaby, and A. C. Lynch. (*Proc. Phys. Soc.*, vol. 72, pp. 233–243; August 1, 1958.) If a domain wall moving in an alternating field crosses a small area illuminated with plane-polarized light, the change in intensity of the reflected light passing through a nearly crossed analyzer can be detected by use of a photomultiplier cell and by amplification of the alternating component of its output signal. Experimental results agree well with theoretical predictions. See also 2441 of 1954 (Fowler and Fryer).

538.222:534.1–8 3416

Paramagnetic Centres as Detectors of Ultrasonic Radiation at Microwave Frequencies—C. Kittel. (*Phys. Rev. Lett.*, vol. 1, pp. 5–6; July 1, 1958.) It may be possible to detect microwave phonons generated by an electromechanical or magnetomechanical transducer by observing their effect on the saturation of an electron-spin resonance line. The quantitative aspects of this are estimated.

538.3:535.13 3417

The Equations of Electromagnetic Induction—Pham Mau Quan. (*Compt. Rend. Acad. Sci., Paris*, vol. 246, pp. 707–710; February 3, 1958.) The association of Maxwell's electromagnetic equations with Einstein's space-time equations is considered.

538.569.4:535.34:621.372.413 3418

Stark-Effect, Resonant-Cavity Microwave Spectrograph—P. H. Verdier. (*Rev. Sci. Instr.*, vol. 29, pp. 646–647; July, 1958.) The construction and use of a cavity for a *K*-band Stark modulated spectrograph are described. The cavity is a circular cylinder of variable length operating in the TE_{01p} modes. See also 1632 of 1955 (Collier).

538.569.4.029.6:535.33 3419

Improvement in Millimetre-Wave Detection—W. E. Tolberg, W. D. Henderson, and A. W. Jache. (*Rev. Sci. Instr.*, vol. 29, pp. 660–661; July, 1958.) A modification of the detector used in mm-λ spectroscopy [2079 of 1954 (King and Gordy)] is described which facilitates the adjustment of the cat's whisker.

538.569.4.029.6:621.375.9 3420

The Saturation Effect in a System with Three Energy Levels—V. M. Fain. (*Zh. eksp. teor. Fiz.*, vol. 33, pp. 1290–1294; November, 1957.) Mathematical analysis of the effect of a high-frequency alternating field with given harmonics on a system with three energy levels. Expressions are derived for dielectric constant or permeability applicable to maser operation.

539.2:538.56 3421

Spin-Lattice Relaxation Resonances in Solids—H. S. Gutowsky and D. E. Woessner (*Phys. Rev. Lett.*, vol. 1, pp. 6–8; July 1, 1958.) Preliminary experiments suggest the importance of a spin-lattice relaxation mechanism in certain cases. Possible applications to spin-echo storage devices and to masers are outlined.

539.2:548.0 3422

Some Features of the Motion of Rapid Current Carriers in Polar Crystals—Yu. I. Gorkun and K. B. Tolpygo. (*Dokl. Akad. Nauk S.S.S.R.*, vol. 120, pp. 491–495; May 21, 1958.) Investigation of the behavior of polarons (majority current carriers in ionic crystals) with increase of energy.

GEOPHYSICAL AND EXTRATERRESTRIAL PHENOMENA

523.164:621.396.677.3 3423

Gain Measurements of Large Antennas used in Interferometer and Cross-Type Radio Telescopes—Little. (See 3339.)

523.164:621.396.677.833 3424

Radio Telescope Sees 2 Billion Light Years—C. N. Kington. (*Electronics*, vol. 31, pp. 70–75; June 6, 1958.) Details are given of the drive control system associated with the Jodrell Bank radio telescope. See also 108 of 1958.

523.164:621.396.677.833 3425

The Computer and Control for the Telescope at Jodrell Bank. (*Electronic Eng.*, vol. 30, pp. 466–472; August, 1958.) The analog computer and the drive and correction systems which it controls are described.

523.164.3:523.4 3426
Further Observations of Radio Emission from the Planet Jupiter—F. F. Gardner and C. A. Shain. (*Aust. J. Phys.*, vol. 2, pp. 55–69; March, 1958.) Characteristics of radiation at 19.6 mc are described in detail. The radiation appears to be random noise varying rapidly in intensity and its short-term characteristics can be affected markedly by the terrestrial ionosphere. Three main sources of noise are apparent but none can be identified with visual features. The great variability and spectral concentration of the radiation suggests an origin in some form of plasma oscillation in an ionized region having a critical frequency of about 20 mc. See also 406 of 1956 (Shain).

523.164.32:523.74 3427
The Variation of Decimetre-Wave Radiation with Solar Activity—C. W. Allen. (*Mon. Not. R. Astr. Soc.*, vol. 117, pp. 174–188; July, 1957.) "A statistical method is used to segregate the quiet component from the slowly varying component of solar decimetre-wave radiation in the period 1947–54. For this purpose the radiations at frequencies 2800, 1200, and 600 mc have been correlated with sunspot numbers, sunspot areas, and faculae. The mean lives of the various radiations and activities have been estimated and compared. There is an increase of life with decreasing radio frequency. The life of 2800 mc radiation is about the same as sunspots but measurements of the latter show some anomalies. The slowly varying radiation flux is proportional to frequency in the range studied. The quiet sun flux has a small but significant variation with solar activity, the relative change being greater for smaller frequencies. The possibility that this variation may be associated with uncorrelated local sources, such as prominences, is not entirely excluded."

523.165:523.745 3428
Changes in Amplitude of the 27-Day Variation in Cosmic Ray Intensity during the Solar Cycle of Activity—D. Venkatesan. (*Tellus*, vol. 10, pp. 117–125; February, 1958.) The amplitude variation is in general agreement with the changes in solar activity, assessed by the sunspot number, only for the years 1937–1946 and 1952–1955. The poor correlation for the years 1946–1952 may be explained by the changes in the electromagnetic conditions in interplanetary space during the solar cycle.

523.165:523.75 3429
On the Increase in Cosmic Ray Intensity and the Electromagnetic State in Interplanetary Space during the Solar Flare of Feb. 23, 1956—D. Eckhartt. (*Tellus*, vol. 10, pp. 126–136; February, 1958.) A detailed analysis of the onset times of the increase in intensity is used in the study of the electromagnetic state. The existence of deflecting magnetic fields between the sun and the earth is demonstrated. A probable mechanism is discussed whereby flare low-energy cosmic-ray particles could be trapped and guided by a solar beam, which could also have caused the large magnetic storm observed two days after the flare.

523.165:550.385 3430
Geomagnetic Latitude Effect of the Cosmic-Ray Nucleon and Meson Components at Sea Level from Japan to the Antarctic—M. Kodama and Y. Miyazaki. (*Rep. Ionosphere Res. Japan*, vol. 11, pp. 99–115; September, 1957.) Preliminary report on results of measurements made on board the ice-breaker "Sōya" from November, 1956 to April, 1957. The effects of a cosmic-ray storm in the Antarctic are described.

523.5:621.396.11.029.62 3431
A Theoretical Rate-Amplitude Relation in Meteoric Forward Scattering—Hines. (See 3608.)

523.5:621.396.11.029.62 3432
Observations of Angle of Arrival of Meteor Echoes in V.H.F. Forward Scatter Propagations—Endresen, Hagfors, Landmark, and Rödsrud. (See 3609.)

523.5:621.396.11.029.62 3433
The Fading of Long-Duration Meteor Bursts in Forward Scatter Propagation—Landmark. (See 3610.)

523.53 3434
The 1956 Phoenicid Meteor Shower—A. A. Weiss. (*Aust. J. Phys.*, vol. 2, pp. 113–117; March, 1958.) From radio observations at Adelaide six hours before peak activity, the radiant coordinates are estimated to be 15 ± 2, -55 ± 3. The radio rate of 30/hour measured on high-sensitivity equipment is much lower than that expected from visual rates of 20 to 100/hour reported 1 to 9 hours later. See also 771 of 1958.

523.75:550.386:621.396.11 3435
Sunspot and Magnetic Activity—A. M. Humby. (*Wireless World*, vol. 64, pp. 435–438; September, 1958.) Unusual features of sunspot and magnetic activity in the years 1950–1957 and their effects on the performance and frequency usage of some HF radio-teletype circuits are examined.

523.78 3436
The Swedish Radio-Scientific Solar Eclipse Expedition to Italy, 1952—S. I. Svensson, G. Hellgren, and O. Perers. (*Acta polyt., Stockholm*, no. 212, 30 pp.; 1957. *Chalmers tek., Högsk. Handl.*, no. 181, 1956.) Preliminary report on observations of the solar eclipse of February 25, 1952. See, *e.g.*, 3378 of 1956 (Minnis).

523.78:551.510.535 3437
Nonuniformity in the Brightness of the Sun's Disk during the Eclipse of 30 June 1954—C. M. Minnis. (*J. Atmos. Terr. Phys.*, vol. 12, pp. 266–271; July, 1958.) The brightness distributions derived from British and Norwegian ionospheric measurements are presented so as to show their underlying similarity. Quantitative data for the most probable distribution are given and a comparison is made with radio noise measurements at 10.7 cm γ during the eclipse. See also 442 of 1957.

550.372(481) 3438
A Survey of Ground Conductivity and Dielectric Constant in Norway within the Frequency Range 0.2–10 Mc/s—K. E. Eliassen. (*Geofys. Publ.*, vol. 19, no. 11, pp. 1–30; 1957.) Measurements were made using the wave tilt method, and a ground conductivity map of Southern Norway has been prepared.

550.385+551.594.5 3439
On the Theory of Magnetic Storms and Aurorae—H. Alfvén. (*Tellus.*, vol. 10, pp. 104–116; February, 1958.) It is shown that the nonmagnetic beam of ionized gas assumed in the Chapman-Ferraro theory is inconsistent with cosmic-ray observations, and that the main phase of the storm cannot be explained in terms of a nonmagnetic beam. The arguments of Chapman (1356 of 1953) and Cowling (13 of 1943) against the electric field theory are discussed and shown to be invalid.

550.385 3440
Statistical Investigation of Magnetic Crochets at Tamanrasset—F. Duclaux and B. Leprêtre. (*Compt. Rend. Acad. Sci., Paris*, vol. 246, pp. 1243–1245; February 24, 1958.)

550.385 3441
Sub-audible Geomagnetic Fluctuations—H. J. Duffus, P. W. Nasmyth, J. A. Shand, and C. Wright. (*Nature, London*, vol. 181, pp. 1258–1259; May 3, 1958.) The observations of Duffus and Shand (3076 of 1958) have been extended to cover the frequency range 0.1–30 cps. Records obtained at a portable subsidiary station about 200 miles from the main station near Victoria, B.C., in the same magnetic latitude, showed no phase shift of the normal day-time oscillations.

550.385 3442
Large-Amplitude Hydromagnetic Waves above the Ionosphere—A. J. Dessler. (*Phys. Rev. Lett.*, vol. 1, pp. 68–69; July 15, 1958.) The hydromagnetic-wave velocity is calculated as a function of altitude. There are two regions where the wave velocity changes very rapidly with altitude and it is concluded that hydromagnetic waves above the ionosphere have an amplitude greater than the geomagnetic fluctuations they produce at the surface of the earth. See also 3077 of 1958.

550.385.1:523.75 3443
Method of Magnetic-Storm Forecasting from the Activities of Flares accompanied by Solar Radio Noise Outbursts—K. Sinno. (*Rep. Ionosphere Res. Japan*, vol. 11, pp. 195–204; December, 1957.) A statistical study indicates that solar flares accompanied by 200-mc radio noise bursts have a close correlation with terrestrial magnetic storms. See also 446 of 1958.

550.385.4:523.165 3444
On the Magnetic Clouds responsible for Variations of Cosmic-Ray and Geomagnetic Field—M. Hirono. (*Rep. Ionosphere Res. Japan*, vol. 11, pp. 205–228; December, 1957.) Discussion of the mechanism suggested by Morrison (*Phys. Rev.*, vol. 101, pp. 1397–1404; February 15, 1956) by which large ionized gas clouds carrying tangled magnetic fields are emitted from the sun and modulate the galactic cosmic rays reaching the earth. It is shown to be more probable that smaller magnetic clouds are intermittently ejected from the sun and slowed down by the interplanetary gas. The velocity of accompanying unmagnetized streams is unaffected, and the different velocities account for the observed initial and main phases of terrestrial magnetic storms; the model also explains some solar cosmic ray phenomena. Thirty-nine references.

550.389.2:621.396.11 3445
Radio Studies during the International Geophysical Year 1957–8—W. J. G. Beynon. (*J. Brit. IRE*, vol. 18, pp. 401–412; July, 1958. Discussion, pp. 412–416.) Studies are discussed under five headings: a) vertical soundings, b) ionospheric drift measurements, c) backscatter, d) radio noise and atmospheric studies, and e) rockets and satellites. The history, program and organization of the I.G.Y. are briefly outlined.

550.389.2:629.19 3446
Theoretical Analysis of Doppler Radio Signals from Earth Satellites—W. H. Guier and G. C. Weiffenbach. (*Nature, London*, vol. 181, pp. 1525–1526; May 31, 1958.) The analysis is briefly described and its application to the calculation of the orbits of two satellites (Sputnik I and Explorer I) from isolated observations made at one station is given.

550.389.2:629.19 3447
Observations of the U.S. Satellites Explorers I and III by C.W. Reflection—J. D. Kraus, R. C. Higgy and J. S. Albus. (PROC. IRE, vol. 46, p. 1534; August, 1958.) The passage of satellites Explorer I and III may be detected by the increased signal strength of WWV as a result of ionization from the satellite paths. See also 1724 of 1958 (Kraus).

550.389.2:629.19 3448
Continuous Phase-Difference Measurements of Earth Satellites—J. W. Herbstreit

and M. C. Thompson, Jr. (Proc. IRE, vol. 46, p. 1535; August, 1958.) Two similar receivers are used, operated from a common local oscillator. The phase-meter compares the AF tones from the two receivers. See also 234 of 1956.

550.389.2:629.19 3449

On the Interpretation of the Doppler Effect from Senders in an Artificial Satellite—K. Weekes. (*J. Atmos. Terr. Phys.*, vol. 12, pp. 335–338; July, 1958.) The Doppler effect is simply related to the angle of incidence of the transmitted signal if the geomagnetic field is ignored, otherwise the relationship is complex, and an investigation of the actual ray-paths is necessary even for the deduction of approximate numerical values.

550.389.2:629.19:551.510.535 3450

The Effect of the Ionosphere on the Doppler Shift of Radio Signals from an Artificial Satellite—F. H. Hibberd. (*J. Atmos. Terr. Phys.*, vol. 12, pp. 338–340; July, 1958.) Application of Snell's law to a ray passing through a spherically stratified ionosphere to a receiver on the ground leads to a relation between Doppler shift and angle of incidence at the ground.

551.510.3 3451

High-Atmosphere Densities—M. Nicolet. (*Science*, vol. 127, pp. 1317–1320; June 6, 1958.) Models of the upper atmosphere are modified to allow for diffusion and other factors in order to conform to the results obtained from satellite observations.

551.510.53:550.38:523.165 3452

Distortion of the Magnetic Field in the Outer Atmosphere due to the Rotation of the Earth—K. Maeda. (*Rep. Ionosphere Res. Japan*, vol. 11, pp. 116–129; September, 1957.) Assuming a cavity surrounding the earth, caused by the earth's revolution, the equations of the fields inside and outside this cavity imply a westward shift of the dip equator in the outer atmosphere, in agreement with cosmic-ray evidence. See *e.g.*, 3721 of 1956 (Simpson, *et al.*).

551.510.535 3453

Anomalies in Ionosonde Records due to Travelling Ionospheric Disturbances—L. H. Heisler. (*Aust. J. Phys.*, vol. 2, pp. 79–90; March, 1958.) Anomalies in ionosonde records of the *F* region during the passage of traveling disturbances are classified into four main types. The diurnal and seasonal variation of their occurrence is discussed and it is suggested that the ion distribution at a height of 200 km governs the type of anomaly observed. See also 1434 of 1957 (Munro and Heisler).

551.510.535 3454

Travelling Ionospheric Disturbances in the *F* Region—G. H. Munro. (*Aust. J. Phys.* vol. 2, pp. 91–112; March, 1958.) Data obtained from April, 1948, to March, 1957, on the horizontal movements of the disturbances are analyzed for a single radio frequency. The monthly means of direction show a seasonal change from 30° in winter to 120° in summer with a small change in mean speed from 8 km/min to 7 km/min respectively.

551.510.535:523.3 3455

Measurement of the Ionospheric Faraday Effect by Radio Waves Reflected from the Moon—F. B. Daniels and S. J. Bauer. (*Nature, London*, vol. 181, pp. 1392–1393; May 17, 1958.) Continuous waves at 151.11 mc were transmitted from Belmar, N. J., and received at Urbana, Ill., after reflection from the moon. From 2333–0600 CST the change in total electron content deduced from measurements made during the night of January 8–9, 1958, was about 2.2 times the change computed for a parabolic layer from vertical-incidence recordings at the transmitter site.

551.510.535:523.72 3456

The Effect of Certain Solar Radiations on the Lower Ionosphere—R. E. Houston, Jr. (*J. Atmos. Terr. Phys.*, vol. 12, pp. 225–235; July, 1958.) "An electron density distribution in the *D* and *E* regions of the ionosphere is computed. Lyman alpha, Lyman beta, the Lyman continuum and X-radiations are considered. The resulting electron distribution is used to compute parameters which may then be compared with data from rocket and long wave radio experiments. In general, there is good agreement between experimental results and the values predicted by the model."

551.510.535:523.75 3457

On the Ionospheric Current System of the Geomagnetic Solar Flare Effect (S.F.E.)—H. Volland and J. Taubenheim. (*J. Atmos. Terr. Phys.*, vol. 12, pp. 258–265; July, 1958.) The analysis of 16 magnetograms obtained at Niemegk (near Berlin) between 1951 and 1957 shows that the s.f.e. current system is independent of the S_q system and situated at a lower level. Contributions to the geomagnetic s.f.e. apparently come from both the *D* and *E* regions. See also 3866 of 1957 (Taubenheim).

551.510.535:523.78 3458

The Interpretation of Changes in the *E* and *F*-Layers during Solar Eclipses—C. M. Minnis. (*J. Atmos. Terr. Phys.*, vol. 12, pp. 272–282; July, 1958.) Results obtained during a series of eclipses support an interpretation of ionospheric changes in terms of the response of a Chapman layer to the obscuration of a solar disk where localized sources of ionizing radiation are superposed on a uniformly bright background. An alternative hypothesis of a uniform disk and a complex layer with two different species of ion does not adequately explain observed characteristics. Experimental results indicate that errors due to layer tilts are probably not important. See also 3437 above.

551.510.535:551.557 3459

Method of Measuring Ionospheric Winds by Fading at Spaced Receivers—R. B. Banerji. (*J. Atmos. Terr. Phys.*, vol. 12, pp. 248–257; July, 1958.) Current statistical methods of measurement are critically reviewed and compared. As a result a method is suggested that may be less laborious than the autocorrelation methods but of comparable accuracy. See, *e.g.*, 3216 of 1954 (Ratcliffe).

551.510.535:621.396.11 3460

On the Bearing of Ionospheric Radio Waves—K. Miya, M. Ishikawa, and S. Kanaya. (*Rep. Ionosphere Res. Japan*, vol. 11, pp. 130–144; September, 1957.) Systematic measurements of bearings obtained by means of special DF equipment [465 of 1958 (Miya, *et al.*) are analyzed, and fluctuations are interpreted with regard to propagation modes and distance. When the great-circle m.u.f. exceeds the signal frequency the mean bearing coincides with the direction of the main beam of the transmitter aerial, but deviates considerably when the great-circle MUF falls below the signal frequency. The changes are attributed to a major deviation from the great-circle path combined with a final scatter hop from continental land masses. Deviation of antipodal signal bearings are explained assuming that the signals follow paths of low absorption ("night zones").

551.510.535:621.396.11:621.317.799 3461

An Automatic Recorder For Measuring Ionospheric Absorption—S. C. Mazumdar. (*J. Inst. Telecommun. Eng., India*, vol. 4, pp. 81–86; March, 1958.) Ionospheric absorption is deduced from the ratio of the amplitudes of singly and doubly reflected vertical incidence pulses. The two pulses are separated by adjustable gates and applied to two logarithmic amplifiers followed by a difference circuit operating a chart recorder. In the absence of a second reflection a local reference pulse can be used, the system being calibrated subsequently. See 1444 of 1957 (Mitra and Mazumdar).

551.510.535:621.396.11.029.45/.5 3462

Low-Frequency Reflection in the Ionosphere—Poeverlein. (See 3604.)

551.510.536 3463

The Transition from the Ionosphere to Interplanetary Space—D. E. Blackwell. (*Nature, London*, vol. 181, pp. 1237–1238; May 3, 1958.) Report of a discussion held by the Royal Astronomical Society in London, February 21, 1958, including five short talks concerning the solar corona, zodiacal light, radio echoes from the moon, earth-satellite observations, and AF atmospherics.

551.551:551.508.822 3464

Free-Air Turbulence—A. D. Anderson. (*J. Met.*, vol. 14, pp. 477–494; December, 1957.) Measurements of the altitude distribution between 3000 and 18,300 m of layers of turbulence made by means of a "gustsonde" incorporating a VHF transmitter are analyzed.

551.594.21 3465

Thunderstorm Charge Separation—S. E. Reynolds, M. Brook and M. F. Gourley. (*J. Met.*, vol. 14, pp. 426–436; October, 1957.) Laboratory experiments show that charge separation may arise from the collison between graupel pellets and ice crystals, from friction between ice formations at different temperatures or with different amounts of contamination, and from the resolidification of a liquid layer in contact with ice.

551.594.5:621.396.11.029.6 3466

Low-Latitude Reflection from the Aurora Australis—T. J. Seed and C. D. Ellyett. (*Aust. J. Phys.*, vol. 2, pp. 126–129; March, 1958.) Observations of radar reflections for the period March–June, 1957, are reported. Records of radar, visual and geomagnetic observations for one day are compared.

551.594.6:621.396.11.029.45 3467

Velocity of Propagation of Electromagnetic Waves at Audio Frequencies—Al'pert and Borodina. (See 3605.)

LOCATION AND AIDS TO NAVIGATION

621.396.93 3468

Methods and Installations for Long-Distance Radio Navigation—W. Stanner. (*Elektrotech. Z., Ed. A.*, vol. 79, pp. 322–329; May 1, 1958.) A review of the principal present-day systems including Loran, Consol and Decrra.

621.396.93 3469

Improvements in H.F. Direction Finding by Automatic Time Averaging—J. F. Hatch and D. W. G. Byatt. (*Marconi Rev.*, vol. 21, pp. 16–29; 1958.) Equipment is described for use with CW or ICW signals which gives automatically the mean bearing averaged over a range of time intervals. The improvement is assessed by comparison with simultaneous bearings observed on twin-channel CRDF equipment.

621.396.93(94) 3470

The Australian D.M.E. System—E. Stern. (*Proc IRE, Aust.*, vol. 18, pp. 318–327; September, 1957.) Description of the development and operation of the system. See 3471 below.

621.396.93.029.62 3471

Echo Interference in a 200-Mc/s Double-Pulse D.M.E. System—B. R. Johnson. (*Proc. IRE, Aust.*, vol. 18, pp. 309–317; September, 1957.) In DME systems such as the Australian system using double-pulse interrogation coding as a means of channel selection, echo interference may cause a) interrogation of off-channel beacons, b) incorrect range indication, or c) masking of beacon identification code. Theoretical analysis and experimental work indicate what type of reflectors may be troublesome, and how echo interference can be minimized.

621.396.933 3472
Factors in the Design of Airborne Doppler Navigation Equipment—E. G. Walker. (*J. Brit. IRE*, vol. 18, pp. 425–442; July, 1958. Discussion, pp. 442–444.) "The paper describes the use of a Doppler-sensor of aircraft component-velocities as an input for self-contained dead-reckoning navigation. Choice of radio frequencies, beam configuration, radiated power and other system parameters is discussed and some basic quantitative expressions derived. Design features of the individual units of the sensor are given and requirements of computer and heading-reference outlined. System accuracy is discussed and the heading information is shown to be the factor presently limiting system performance."

621.396.933.1:621.396.824 3473
Sudden Changes in Bearing Indication on Medium-Wave Four-Course Radio Ranges using Cathode-Ray Direction-Finders—A. R. Wendlinger. (*Elektronische Rundschau.*, vol. 12, pp. 10–12; January, 1958.) Experimental investigations of the Stavanger effect show that it is due to interference at the receiver between signals emitted by two different radio beacons operating at almost identical frequencies.

621.396.96 3474
The Influence of Atmospheric Conditions on Radar Performance—J. A. Saxton. (*J. Inst. Nav.*, vol. 11, pp. 290–303; July, 1958.) The effects of gaseous absorption and of various forms of precipitation upon the performance of radars at 3 cm λ are reviewed. Heavy widespread rain can cause serious reduction in range. The effects of superrefraction are discussed, and it is shown how skip effects can occur.

621.396.96 3475
A 3-cm Airport Control Radar System—F. W. Garrett. (*Marconi Rev.*, vol. 21, no. 128, pp. 3–15; 1958.)

621.396.96 3476
Four Ways to Simulate Radar Targets—J. I. Leskinen. (*Electronics*, vol. 31, pp. 82–86; June 6, 1958.) Pulses are generated to simulate azimuth, elevation and range of targets moving at speeds up to 2400 knots. Land and sea clutter effects are also produced.

621.396.96:621.375.226 3477
Ringing Amplifier—Rozenstein and Gross. (See 3388.)

621.396.969.33 3478
The Planning of Shore-Based Radar Installations for Marine Navigation—H. Bürkle. (*Telefunken Ztg.*, vol. 30, pp. 236–245; December, 1957. English summary, p. 287.) Factors governing the choice of site and coverage and transmitter and antenna characteristics are examined. Avoidance of interference from neighboring stations, and systems of transmitter control are also considered.

MATERIALS AND SUBSIDIARY TECHNIQUES

535.215 3479
Photoconductivity of Zinc Selenide Crystals and a Correlation of Donor and Acceptor Levels in II-VI Photoconductors—R. H. Bube and E. L. Lind. (*Phys. Rev.*, vol. 110, pp. 1040–1049; June 1, 1958.) Photosensitive crystals of ZnSe were prepared by incorporating suitable proportions of group-VII donors and either group-I or group-V acceptors in crystals prepared from the vapor phase. Photoconductivity phenomena characteristic of other group II–VI photoconductors were also found for ZnSe.

535.215 3480
Photo-effects with Anodic Oxide Layers on Tantalum and Aluminium—W. C. van Geel, C. A. Pistorius, and P. Winkel. (*Philips Res. Rep.*, vol. 13, pp. 265–276; June, 1958.) The photoelectric properties of the system Ta/Ta_2O_5/electrolyte during irradiation with ultraviolet light are investigated, and an attempt is made to explain the observed phenomena by assuming that the work function for Ta/Ta_2O_5 is smaller than that for electrolyte/Ta_2O_5.

535.37 3481
Phosphorescence and Fluorescence Quantum Yield Ratios as related to the Position of the Fluorescence Spectrum—V. V. Zelinskiĭ and V. P. Kolobkov. (*Dokl. Akad. Nauk S.S.S.R.*, vol. 119, pp. 922–925; April 11, 1958.)

535.37 3482
Investigations in the $CuGaS_2$-ZnS and $AgGaS_2$-ZnS Systems—E. F. Apple. (*J. Electrochem. Soc.*, vol. 105, pp. 251–255; May, 1958.)

535.37:546.472.21 3483
Some Remarks on the "Self-Activation" of ZnS—E. A. Schwager and A. Fischer. (*Z. Phys.*, vol. 149, pp. 345–346; October 19, 1957.) The effect is interpreted as a shift of Schottky-type defect equilibrium according to the conditions of phosphor preparation.

535.37:546.472.21 3484
A Sensitive Method of Detecting Lead, and the Inclusion of Lead in Zinc Sulphide—E. A. Schwager and A. Fischer. (*Z. Phys.*, vol. 149, pp. 347–352; October 19, 1957.) Activation of ZnS by Pb is discussed.

535.376 3485
The Effect of Electric Fields on Scintillations in Crystalline Zinc Sulphide—G. F. Alfrey and K. N. R. Taylor. (*J. Electronics Control*, vol. 4, pp. 417–424; May, 1958.) In electroluminescent crystals brightness is reduced when α particles are incident on the negative electrode. Observations have been interpreted in terms of a cathode barrier in ynS which changes in thickness with frequency, the variation being considered to be a change in dielectric constant. Results agree with earlier work [782 of 1956 (Ince and Oatley)] and are supported by observations of the electroluminescence threshold voltage.

535.376:621.385.832 3486
Electron Excitation of Bilayer Screens—L. R. Koller and H. D. Coghill. (*J. Appl. Phys.*, vol. 29, pp. 1064–1066; July, 1958.) "The control of the color of the luminescence of thin transparent superimposed phosphor films when excited by electron beams of varying voltage is discussed. The quantitative relations are found to be in agreement with a theory based on the laws of electron penetration and scattering."

537.226/.228.1:546.431.824–31 3487
Some Studies on the Ternary System (Ba-Pb-Ca)TiO_3—T. Ikeda. (*J. Phys. Soc. Japan*, vol. 13, pp. 335–340; April, 1958.) The phase diagram for the system is investigated while the Ca concentration is increased, and it is shown that the ferroelectric and tetragonal phase changes to the orthorhombic structure of $CaTiO_3$, passing through cubic and pseudocubic phases. The dielectric, piezoelectric and mechanical properties of the system are also examined.

537.226/.227:546.431.824–31 3488
Barkhausen Pulses in Barium Titanate—A. G. Chynoweth. (*Phys. Rev.*, vol. 110, pp. 1316–1332; June 15, 1958.) An investigation of the Barkhausen pulses that occur during polarization reversal. The pulse shapes and in particular their heights and rise times have been studied as a function of the crystal thickness and the applied field strength. The observations are not consistent with the usual jerky domain-wall motion models for the generation of Berkhausen pulses. It is suggested that the pulses could represent the nucleation and initial stages of growth of new spike-shaped domains extending along the *c* axis, and that the fixed numbers of pulses given by a crystal would then indicate a definite number of nucleating sites on the crystal surfaces.

537.226/.227:546.431.824–31 3489
Decay Effects in Barium Titanate Ceramics—H. L. Allsopp. (*Phil. Mag.*, vol. 2, pp. 1100–1102; September, 1957.) Variations of dielectric and electromechanical properties following the application and removal of a strong alternating field are described.

537.226/.227:546.431.824–31 3490
Electron Spin Resonance in Single Crystals of $BaTiO_3$—W. Low and D. Shaltiel. (*Phys. Rev. Lett.*, vol. 1, pp. 51–52; July 15, 1958.) The very intense spectrum observed at 3 cm λ is attributed to the ferroelectric state of $BaTiO_3$ and not to any paramagnetic impurity.

537.226:546.824–31 3491
Dielectric Losses in TiO_2 Single Crystals—J. Van Keymeulen. (*Naturwissenschaften*, vol. 45, p. 56; February, 1958. In English.)

537.227 3492
The Polarization Reversal Process in Ferroelectric Single Crystals—M. Prutton. (*Proc. Phys. Soc.*, vol. 72, pp. 307–308; August 1, 1958.)

537.227 3493
New Room-Temperature Ferroelectric—R. Pepinsky, K. Vedam, and Y. Okaya. (*Phys. Rev.*, vol. 110, pp. 1309–1311; June 15, 1958.) The neutral-salt complex with glycine $(NH_2CH_2COOH)\cdot MnCl_2\cdot 2H_2O$ is found to be ferroelectric from low temperatures to +55°C. Details of measurements on this salt are given.

537.227 3494
Ferroelectric and Optical Properties of Na(K-NH_4)-Tartrate Mixed Crystals—Y. Makita and Y. Takagi. (*J. Phys. Soc. Japan*, vol. 13, pp. 367–377; April, 1958.) In 90.5 per cent $NaNH_4$ tartrate crystals three kinds of polymorphic modification have been found: a) a ferroelectric phase with spontaneous polarization along the *a* axis; b) a ferroelectric phase with polarization along the *b* axis; c) a paraelectric phase. The complete phase diagram of the system is examined.

537.311.3:539.23 3495
Remarks on some Electrical Properties of Very Thin Films of Silver—C. Uny and N. Nifontoff. (*Compt. Rend. Aacd. Sci., Paris*, vol. 246, pp. 906–909; February 10, 1958.) Techniques used in the preparation of regular and stable thin films are noted, and measurements of resistance variation with time and with current are reported. See also 2167 of 1957.

537.311.33 3496
Statistics of Compensated Divalent Impurities in Semiconductors—W. Mercouroff. (*Compt. Rend. Acad. Sci., Paris*, vol. 246, pp. 1175–1177; February 24, 1958.) The introduction of compensating monovalent impurity centers considerably modifies the variation in the number of free carriers as a function of temperature. Analytical results have been confirmed by experiments on Zn-doped Ge compensated by Sb.

537.311.33 3497

Theory of an Experiment for Measuring the Mobility and Density of Carriers in the Space-Charge Region of a Semiconductor Surface—R. L. Petritz. (*Phys. Rev.*, vol. 110, pp. 1254–1262; June 15, 1958.) Two models are considered: a) a single crystal composed of two regions, a surface region of thickness of the order of a Debye length and a bulk region, and b) a single crystal with continuous variation of the potential in the direction perpendicular to the surface. Rigorous expressions are derived for the Hall coefficient and magnetoresistance.

537.311.33 3498

Oxides of the 3d Transition Metals—F. J. Morin. (*Bell Sys. Tech. J.*, vol. 37, pp. 1047–1084; July, 1958.) An examination of the magnetic, electrical and optical properties leads to a tentative energy-band scheme for the oxides of scandium, titanium and vanadium. The remaining *3d* metal oxides do not have a conduction band, and an energy level scheme for these is calculated from electrostatics. Forty-seven references.

537.311.33 3499

Compound Semiconductors—H. P. R. Frederikse. (*J. Metals, New York*, vol. 10, pp. 346–350; May, 1958.) "A survey of the characteristics of compound semiconductors as deduced from measurements of their mechanical, optical, electrical, magnetic, and thermal properties."

537.311.33 3500

Solid Solution in $A^{III}B^{V}$ Compounds—J. C. Wooley and B. A. Smith. (*Proc. Phys. Soc.*, vol. 72, pp. 214–223; August 1, 1958.) Investigations show that in most of the compounds considered, complete solid solution can be obtained throughout the whole range of composition under special conditions of temperature and annealing time.

537.311.33 3501

Adsorption and Charge Transfer on Semiconductor Surfaces—H. J. Krusemeyer and D. G. Thomas. (*Phys. Chem. Solids*, vol. 4, nos. 1/2, pp. 78–90; 1958.) A theoretical evaluation of the concentration of ions and neutral atoms adsorbed on a semiconductor surface, from a mixture of two gases, one giving positive, the other negative, adions. Numerical results are calculated for semiconductors such as ZnO with a large forbidden gap at temperatures below the intrinsic range.

537.311.33 3502

Space-Charge Calculations for Semiconductors—R. Seiwatz and M. Green. (*J. Appl. Phys.*, vol. 29, pp. 1034–1040; July, 1958.) A derivation of the general equation relating the electric field at the semiconductor surface to the electrostatic potential difference across the space charge region. The treatment considers degenerate free carrier distributions and partial ionization of impurities.

537.311.33 3503

Sweep-Out Effects in the Phase-Shift Method of Carrier-Lifetime Measurements—N. B. Grover and E. Harnick. (*Proc. Phys. Soc.*, vol. 72, pp. 267–269; August 1, 1958.) The particular case of thin rectangular filaments with ohmic contacts and low-level sinusoidally modulated illumination is considered with a view to determining an upper limit for the value of the applied field consistent with negligible sweep-out effects.

537.311.33 3504

Infrared and Microwave Modulation using Free Carriers in Semiconductors—A. F. Gibson. (*J. Sci. Instrum.*, vol. 35, pp. 273–278; August, 1958.) The failures and successes of the classical Drude-Zener theory in relation to experimental results are discussed. Methods are described for modulating the conductivity of a semiconductor and for applying these techniques to the study of its optical and microwave properties.

537.311.33:061.3 3505

Report on the Second Symposium on the Physics of Semiconductors—F. Herman. (*Phys. Chem. Solids*, vol. 2, pp. 72–82; March, 1957.) Summary of papers presented at a symposium in Washington, D. C., October 24–26, 1956, covering work on conduction mechanisms, the effect of magnetic fields, and investigations of paramagnetic resonance.

537.311.33:538.569.4 3506

Observation of Microwave Cyclotron Resonance by Cross Modulation—H. J. Zeiger, C. J. Rauch, and M. E. Behrndt. (*Phys. Rev. Lett.*, vol. 1, pp. 59–60; July 15, 1958.) The sample was placed in the high *E*-field region of a microwave cavity, the resonance peaks being observed by detecting changes in dc resistance of the sample. The microwave power applied was amplitude-modulated at 260 cps and cross-modulation was observed on samples of pure Ge and *p*-type InSb.

537.311.33:538.63 3507

Variation of Hall Mobility of Carriers in Nondegenerate Semiconductors with Electric Field—M. S. Sodha and P. C. Eastman. (*Phys. Rev.*, vol. 110, pp. 1314–1316; June 15, 1958.) An expression is obtained for the Hall mobility applicable in a large range of fields and non-Maxwellian distribution of velocities of carriers.

537.311.33:538.63 3508

Hall and Transverse Magnetoresistance Effects for Warped Bands and Mixed Scattering—A. C. Beer and R. K. Willardson. (*Phys. Rev.*, vol. 110, pp. 1286–1294; June 15, 1958.) The transport integrals for warped bands were evaluated for relaxation times determined by mixed scattering from acoustic phonons and ionized impurities. Hall and transverse magnetoresistance coefficients were calculated for parameters characteristic of the degenerate valence bands in Ge and Si, the results being consistent with experimental observations.

537.311.33:538.63 3509

The Change of Carrier Concentration in the Simple Semiconductors with Static Magnetic Field—Y. Uemura and M. Inoue. (*J. Phys. Soc. Japan*, vol. 13, pp. 377–381; April, 1958.) Three solutions are considered depending on the trapping-center concentration: a) with distinct trapping levels the carrier concentration n decreases with the magnetic field H; b) with sufficient levels to form an impurity band whose width is less than kT, n increases or decreases depending on the effective carrier mass; c) n increases with H for large effective carrier mass when the width of the impurity band is greater than kT.

537.311.33:[546.28+546.289 3510

The Magnetic Susceptibility and Effective Mass of Charge Carriers in Silicon and Germanium—D. Geist. (*Naturwissenschaften*, vol. 45, pp. 33–34; January, 1958.) Preliminary report on measurements of susceptibility at constant temperatures, from which any temperature dependence of the effective mass can be determined.

537.311.33:546.28 3511

Ion Pairing in Silicon—J. P. Maita. (*Phys. Chem. Solids*, vol. 4, nos. 1/2, pp. 68–70; 1958.) "The occurrence of ion pairing in Si is demonstrated. The pairing process is used to determine the diffusivity of Li in Si at low temperatures and the distance of closest approach between the ions forming the pair."

537.311.33:546.28 3512

Lifetime in *p*-Type Silicon—J. S. Blakemore. (*Phys. Rev.*, vol. 110, pp. 1301–1308; June 15, 1958.) Lifetime is measured as a function of excess electron density in the temperature range 200–400°K. A stronger dependence is found at electron densities $<10^{12}cm^{-3}$ than at larger densities. The data are discussed in terms of two separate recombinative levels.

537.311.33:546.28 3513

Magnetic Properties of *N*-Type Silicon—E. Sonder and D. K. Stevens. (*Phys. Rev.*, vol. 110, pp. 1027–1034; June 1, 1958.) The magnetic susceptibility of *n*-type Si samples with a wide range of donor concentrations has been measured as a function of temperature from 3°K to 300°K. By utilizing conduction-electron concentrations obtained from Hall coefficient measurements on comparison specimens over the range 50°K–400°K, the contributions to the susceptibility arising from the conduction electrons and electrons trapped on donor atoms have been analyzed. In the upper range of temperature the diamagnetic contribution of conduction electrons is dominant and is consistent with the model of six energy minima in the conduction band. However, comparison of the squared reciprocal mass ratio with that obtained from cyclotron-resonance experiments reveals that the former is appreciably smaller than the latter.

537.311.33:546.28 3514

Effect of Dislocations on Breakdown in Silicon *p-n* Junctions—A. G. Chynoweth and G. L. Pearson. (*J. Appl. Phys.*, vol. 29, pp. 1103–1110; July, 1958.) A description of experiments providing definite correlations between the light-emission patterns at breakdown and dislocations, the latter being revealed by etching. The possible explanations of this effect are discussed. See *e.g.*, 3527 of 1957 (Chynoweth and Pearson).

537.311.33:546.28 3515

Electron-Bombardment Damage in Silicon—G. K. Wertheim. (*Phys. Rev.*, vol. 110, pp. 1272–1279; June 15, 1958.) It is shown that the bombardment imperfections consist of sites containing at least two electrically active point defects. The relation between these sites and the energy levels in the forbidden gap found in an earlier investigation is established. See also 2807 of 1957.

537.311.33:546.28 3516

Method for the Detection of Dislocations in Silicon by X-Ray Extinction Contrast—J. B. Newkirk. (*Phys. Rev.*, vol. 110, pp. 1465–1466; June 15, 1958.)

537.311.33:546.28 3517

Sintering Method for Semiconductor Material—G. K. Gaulé, J. T. Breslin, and J. R. Pastore. (*Rev. Sci. Instr.*, vol. 29, pp. 565–567; July, 1958.) A sintering process is described for forming small grains of pure Si into rods suitable for feeding a crystal-growing apparatus [see *e.g.*, 3255 of 1954 (Keck, *et al.*)]. The rods are sintered by application of pressure, alternating current and a RF field without using a binder.

537.311.33:546.28 3518

Control of Surface Concentration in the Diffusion of Phosphorus in Silicon—M. J. Coupland (*Nature, London*, vol. 181, pp. 1331–1332; May 10, 1958.) Desired values of surface concentration over the range 5×10^{16}–5×10^{-18} atoms/cm³ are obtained by controlling the phosphorus vapor pressure in closed a evacuated tube, one end of which, containing Si slices, is held in a diffusion furnace, while the other, containing yellow phosphorus, is maintained at temperatures in the range −30°C to +35°C.

537.311.33:546.28 3519

The Interaction of Oxygen with Clean Silicon Surfaces—J. T. Law. (*Phys. Chem. Solids*, vol. 4, nos. 1/2, pp. 91–100; 1958.)

537.311.33:546.28:538.632 3520

The Electrical Conductivity and Hall Effect of Silicon—E. H. Putley and W. H. Mitchell. (*Proc. Phys. Soc.*, vol. 72, pp. 193–200; August 1, 1958.) Measurements have been made in the temperature range 20°–500°K on single crystals of Si with extrinsic carrier concentrations between 2 and 5×10^{12} cm^{-3} to estimate the purity of the material and to study the Hall mobility. Mobilities of electrons and holes are greater than previously observed [*e.g.*, 2184 of 1957 (Cronemeyer)].

537.311.33:546.289 3521

Predicted Intervalley Scattering Effects in Germanium—W. Shockley. (*Phys. Rev.*, vol. 110, pp. 1207–1208; June 1, 1958.) Two methods for studying intervalley scattering effects are described. One is the study of the admittance of an *n-p* junction at high frequencies; the other method uses an *n-p-n* transistor with suitable properties.

537.311.33:546.289 3522

Impact Ionization of Impurities in Germanium—N. Sclar and E. Burstein. (*Phys. Chem. Solids*, vol. 2, pp. 1–23; March, 1957.) The low-temperature electrical breakdown effect is investigated experimentally as a function of temperature, magnetic field, background radiation, type and concentration of impurities, geometry, surface effects, orientation of the specimens and time dependence. The effect is attributed to the impact ionization of impurities by free charge carriers, and a mean-value theory is developed for the critical breakdown field. See also 1796 of 1957 (Schlar).

537.311.33:546.289 3523

Effect of the Impurity Band in Germanium Doped with Zinc, at Very Low Temperatures—W. Mercouroff. (*Compt. Rend. Acad. Sci., Paris*, vol. 246, pp. 1013–1015; February 17, 1958.) At low temperatures, Hall effect and conductivity in samples of Ge, heavily doped with Zn and compensated with Sb, were found to vary with the applied electric field.

537.311.33:546.289 3524

The Effect of Ion Pair and Ion Triplet Formation on the Solubility of Lithium in Germanium—Effect of Gallium and Zinc—H. Reiss and C. S. Fuller. (*Phys. Chem. Solids*, vol. 4, pp. 58–67; 1958.) Theoretical predictions of the effect of ion pairing or association on solubility are confirmed. By taking account of ion association effects a more accurate curve for the solubility of Li in undoped Ge is obtained.

537.311.33:546.289 3525

Preparation and Regeneration of Clean Germanium Surfaces—S. P. Wolsky. (*J. Appl. Phys.*, vol. 29, pp. 1132–1133; July, 1958.) A summary of a) a modified method designed to improve the cleaning efficiency of the ion bombardment process, and b) thermal restoration effects in Ge surfaces exposed to oxygen.

537.311.33:546.289 3526

Temperature Dependence of Point-Contact Injection Ratio in Germanium—D. Gerlich. (*Proc. Phys. Soc.*, vol. 72, pp. 264–267; August 1, 1958.) A method is described for the measurement of point-contact injection ratio by direct compensation. Results are given for *n* and *p*-type material for the temperature range 150–350°K. See also 1821 of 1957.

537.311.33:546.289:538.63 3527

Magneto-surface Experiments on Germanium—J. N. Zemel and R. L. Petritz. (*Phys. Rev.*, vol. 110, pp. 1263–1271; June 15, 1958.) Ambient-induced changes in the conductivity, Hall coefficient, and magnetoresistance of thin samples of intrinsic Ge have been studied. The data are analyzed using the theory of Petritz (3497 above). The results indicate that light holes play an important role in the transport process in the surface. There is a reduction of the mobility of surface electrons in qualitative agreement with the predictions of Schrieffer (2322 of 1955).

537.311.33:546.289:538.63 3528

Magnetoresistance Symmetry Relation in *n*-Germanium—C. Goldberg and W. E. Howard. (*Phys. Rev.*, vol. 110, pp. 1035–1039; June 1, 1958.) Careful measurement of the weak-field magnetoresistance coefficients of *n*-type Ge indicates that the magnetoresistance symmetry relation is obeyed for samples with carrier concentrations as high as 6×10^{15} cm^{-3}. For a 3×10^{16} sample, the deviation, if any, is still quite small. For samples with larger concentrations there is definite evidence of some deviation.

537.311.33:546.289:538.63:535.376 3529

The Electromagnetoluminescence Effect in Germanium—M. Bernard and J. Loudette. (*Compt. Rend. Acad. Sci., Paris*, vol. 246, pp. 1177–1180; February 24, 1958.) The emission of infrared radiation by a sample of Ge placed in an electric field at right angles to a magnetic field is due to the recombination of electrons and holes. This has been studied experimentally.

537.311.33:546.289:541.135 3530

The Rectifying Effect of Germanium/Electrolyte Contacts—G. Déjardin, G. Mesnard and A. Dolce. (*Compt. Rend. Acad. Sci., Paris*, vol. 246, pp. 1016–1018; February 17, 1958.) Measurements have been made of the *I/V* characteristics of single-crystal *n*-type Ge in contact with a 0.1 N solution of HCl, using 12-volt pulses of duration several microseconds, with and without a superimposed polarizing voltage of about 1 volt.

537.311.33:546.289:621.314.63 3531

On the Backward Leakage Current in the Alloyed Germanium *p-n* Junction—M. Kikuchi. (*J. Phys. Soc. Japan*, vol. 13, pp. 350–362; April, 1958.) Experimental procedure and results are described for the observation of "creep" phenomena (*i.e.*, variation of current with a fixed applied voltage). Creep is observed in the leakage current component and it is also found that, in some alloy-junction transistors, the creep in the emitter junction influences the characteristics of the collector junction. Some theoretical considerations are suggested which partially explain the experimental results.

537.311.33:546.57.24 3532

Electrical Properties of Ag_2Te—S. Miyatani. (*J. Phys. Soc. Japan*, vol. 13, pp. 341–350; April, 1958.) Measurements of electronic conductivity, Hall constant and thermoelectric power have been made, for varying ratios of Ag/Te, using a galvanic cell Ag/AgI/Ag_2Te/Pt. The EMF of the cell represents the position of the Fermi level relative to Ag-saturated Ag/Te.

537.311.33:546.682.86 3533

High-Electric-Field Effects in *n*-Indium Antimonide—M. Glicksman and M. C. Steele. (*Phys. Rev.*, vol. 110, pp. 1204–1205; June 1, 1958.) Pulsed current/voltage measurements have been made at 77°K on a single crystal of *n*-type InSb up to a current density of 10^4 a/cm^2. Beyond about 2×10^3 a/cm^2 the current increased rapidly for small further increases in voltage. The mechanism of electron-hole pair creation is used to explain the results. See also 2148 of 1958 (Prior).

537.311.33:546.682.86 3534

Theory of Cyclotron Resonance Absorption by Conduction Electrons in Indium Antimonide—R. F. Wallis. (*Phys. Chem. Solids*, vol. 4, nos. 1/2, pp. 101–110; 1958.) A semiclassical treatment, assuming a simple conduction band with a minimum at $k=0$, and neglecting spin interactions.

537.311.33:546.682.86 3535

Influence of Crystal Orientation on the Surface Behaviour of InSb—M. C. Lanine, A. J. Rosnberg and H. C. Gatos. (*J. Appl. Phys.*, vol. 29, pp. 1131–1132; July, 1958.)

537.311.33:[546.682.86+546.289]:535.33–1 3536

The Infrared Emissivities of Indium Antimonide and Germanium—T. S. Moss and T. D. H. Hawkins. (*Proc. Phys. Soc.*, vol.72, pp. 270–273; August 1, 1958.)

537.311.33:546.682.86:538.63 3537

Magnetoresistance and Field Dependence of the Hall Effect in Indium Antimonide—G. Fischer and D. K. C. MacDonald. (*Canad. J. Phys.*, vol. 36, pp. 527–538; May, 1958.) Measurements of resistance and Hall effect show both to be highly dependent on magnetic field. The classical two-band model, often proposed to account for the behavior of metals, is found to account quite well for the observed results up to the highest fields used. The underlying assumptions of this theory are reviewed and simple formulas are derived, allowing the concentration and mobilities of both types of carrier to be calculated from the magnetic-field dependence of the resistivity and Hall effect.

537.311.33:621.314.63:537.52 3538

The Avalanche Breakdown Voltage of Narrow $p^+\nu n^+$ Diodes—J. Shields. (*J. Electronics Control*, vol. 4, pp. 544–548; June, 1958.) Considerable reduction in breakdown voltage can occur when the width of the junction is reduced below a limiting value, the effect becoming more pronounced as the net impurity concentration in the ν region is decreased. The breakdown voltage is much higher than the voltage at which penetration of the space-charge region occurs. See also 2152 of 1958.

537.311.33:621.315.61 3539

Simplified Theory of One-Carrier Currents with Field-Dependent Mobilities—M. A. Lampert. (*J. Appl. Phys.*, vol. 29, pp. 1082–1090; July, 1958.) A general method is presented for the calculation of steady-state, one-carrier currents in nonmetallic solids where the mobility is field-dependent. See also 832 of 1957.

537.312.62:534.23–8 3540

Ultrasonic Attenuation in Superconductors—H. E. Bömmel and W. P. Mason. (*Bell Lab. Rec.*, vol. 36, pp. 253–256; July, 1958.) Metals in the normal resistivity state give large attenuation for ultrasonic waves of sufficiently high frequency, but in the superconducting state the attenuation drops to zero as the temperature approaches 0°K. Results for lead and for very pure tin are given and the effect of an applied magnetic field is discussed.

538.22 3541

Magnetic Structures of MnO, FeO, CoO, and NiO—W. L. Roth. (*Phys. Rev.*, vol. 110, pp. 1333–1341; June 15, 1958.)

538.22:538.569.4 3542

Quantitative Theory of Faraday Rotation at Centimetre Wavelengths in Chrome Alum, and its Experimental Verification—B. C. Unal, A. Chevalier, and T. Kahan. (*Compt. Rend. Acad. Sci., Paris*, vol. 246, pp. 901–903; February 10, 1958.) The theory is valid for the region of parametric transparency where the spin-spin interaction does not occur.

538.22:546.65/.66 3543
Magnetic Properties of the Gd-La and Gd-Y Alloys—W. C. Thoburn, S. Legvold, and F. H. Spedding. (*Phys. Rev.*, vol. 110, pp. 1298–1301; June 15, 1958.)

538.221 3544
Excitation of Spin Waves in a Ferromagnet by a Uniform R.F. Field—C. Kittel. (*Phys. Rev.*, vol. 110, pp. 1295–1297; June 15, 1958.) It is possible to excite exchange and magnetostatic spin waves in a ferromagnet by a uniform RF field provided that spins on the surface of the specimen experience anistropy interactions different from those acting on spins in the interior.

538.221 3545
Theory of the Curvature of Bloch Walls under the Influence of Stray Fields—H. D. Dietze. (*Z. Phys.*, vol. 149, pp. 276–298; October 19, 1957.) The influence of stray fields on the initial permeability is investigated with reference to Kersten's theory (see *e.g.*, 1825 of 1957).

538.221 3546
Experimental Investigation of the Kinetics of Magnetic Moments in Iron above the Curie Point—M. Ericson and B. Jacrot. (*Compt. Rend. Acad. Sci., Paris*, vol. 246, pp. 1018–1020; February 17, 1958.)

538.221:538.652 3547
Magnetostriction Curves of Polycrystalline Ferromagnetics—E. W. Lee. (*Proc. Phys. Soc.*, vol. 72, pp. 249–258; August 1, 1958.)

538.221:539.23 3548
Thin Ferromagnetic Layers. Electrical Properties of Thin Films of Nickel—G. Goureaux and A. Colombani. (*Compt. Rend. Acad. Sci., Paris*, vol. 246, pp. 741–744; February 3, 1958.)

538.221:621.318.122 3549
Hysteresis Loops associated with a Simple Domain Structure—A. Hart. (*Proc. Phys. Soc.*, vol. 72, pp. 244–248; August 1, 1958.)

538.221:621.318.124 3550
Origin of Magnetic Anisotropy in Cobalt-Substituted Magnetite—J. C. Slonczewski. (*Phys. Rev.*, vol. 110, pp. 1341–1348; June 15, 1958.)

538.221:621.318.12.029.65 3551
Magnetic Materials for Use at High Microwave Frequencies (50–90 kmc/s)—F. K. du Pré, D. J. De Bitetto, and F. G. Brockman. (*J. Appl. Phys.*, vol. 29, pp. 1127–1128; July, 1958.) Experimental results show that the no-field resonance line in oriented ferroxdure ($BaO \cdot 6Fe_2O_3$) can be placed at any frequency in the 50–90-km range by partial substitution of Fe_2O_3 by Al_2O_3. Similar effects occur in $SrO \cdot 6Fe_2O_3$. See also Guillaud and Villers (3451 of 1956).

538.221:621.318.134 3552
Switching in Rectangular-Loop Ferrites containing Air Gaps—U. F. Gianola. (*J. Appl. Phys.*, vol. 29, pp. 1122–1124; July, 1958.) Switching waveforms produced by ferrite magnetic cores with or without air gaps are given and discussed with reference to predicted characteristics.

538.221:621.318.134 3553
Magnetization Processes in a Polycrystalline Manganese Zinc Ferrite—L. F. Bates, H. Clow, D. J. Craik, and P. M. Griffiths. (*Proc. Phys. Soc.*, vol. 72, pp. 224–232; August 1, 1958.) A description is given of Bitter-figure, magnetothermal and Barkhausen-effect studies which indicate that the processes of magnetization are entirely rotational.

538.221:621.318.134:538.569.4 3554
Ferromagnetic Resonance Line Width in Yttrium Iron Garnet Single Crystals—R. C. LeCraw, E. G. Spencer, and C. S. Porter. (*Phys. Rev.*, vol. 110, pp. 1311–1313; June 15, 1958.) Waveguide cavity perturbation techniques are used with samples of diameter 0.013–0.020 inch. An extremely narrow line width of 520 milli-oersteds (the full width) is observed at 9300 mc along the hard axis [100]. The approximate invariance of the line width with frequency is compared with theoretical predictions. See also 21569 of 1958.

538.221:621.318.134:621.372.8 3555
Investigation of the Dependence of Certain Properties of Ferrites on Temperature in the Centimetre-Wave Range—V. A. Kuseleva and E. I. Kondorskii. (*Dokl. Akad. Nauk S.S.S.R.*, vol. 119, pp. 926–928; April 11, 1958.) Experiments carried out on samples of $Ni_{0.7}+Mg_{0.3}Fe_2O_4$ in circular and rectangular waveguides showed that with rise of temperature resonance occurs at reduced field strength. This seems to be related to the variation of the field anisotropy. The rotation of the plane of polarization due to a magnetic field for different temperatures, and the temperature dependence of the resonance field are shown. Ellipticity and attenuation ratios for temperatures between −196 and +220°C and different magnetic field strengths are tabulated.

549.514.51:537.228.1 3556
Elastic and Piezoelectric Constants of Alpha-Quartz—R. Bechmann. (*Phys. Rev.*, vol. 110, pp. 1060–1061; June 1, 1958.) Results obtained by the resonance method (2116 of 1958) are tabulated.

621.315.612:537.311.3 3557
The Effect of Temperature and Thickness on the Electrical Resistivity of Ceramic Coatings—W. H. Fischer. (*J. Electrochem. Soc.*, vol. 105, pp. 201–203; April, 1958.)

MATHEMATICS

517.566:621.396.822 3558
The Axis-Crossing Intervals of Random Functions—J. A. McFadden. (IRE TRANS. ON INFORMATION THEORY, vol. IT-2, pp. 146–150; December, 1956. Abstract, PROC. IRE, vol. 45, p. 575; April, 1957.)

517.9:512.831 3559
Differential Equations, Difference Equations and Matrix Theory—P. D. Lax. (*Commun. Pure Appl. Math.*, vol. 11, pp. 175–194; May, 1958.) For comments by H. F. Weinberger see *ibid.*, pp. 195–196.

517.9:534.1 3560
On the Periodic Solutions of the Forced Oscillator Equation—R. M. Rosenberg. (*Quart. Appl. Math.*, vol. 15, pp. 341–354; January, 1958.)

519.2:621.391 3561
Some General Aspects of the Sampling Theorem—D. L. Jagerman and L. J. Fogel. (IRE TRANS. ON INFORMATION THEORY, vol. IT-2, pp. 139–146; December, 1956. Abstract, PROC. IRE, vol. 45, p. 575; April, 1957.

MEASUREMENTS AND TEST GEAR

529.78:621.374 3562
The Accurate Measurement of a Time Interval—A. E. Cawkell and H. Ristlaid. (*Electronic Eng.*, vol. 30, pp. 502–503; August, 1958.) A method is described for measuring the time interval between trigger pulse and output pulse in a delay unit. Measurements accurate to within ±0.02 per cent can be made of a time interval in the ms range.

529.786:621.317.7.087.6 3563
A System for the Electrical Recording of Time Intervals—G. Becker. (*Elektrotech. Z., Ed. A*, vol. 79, pp. 358–361; May 11, 1958.) Equipment is described for the continuous comparison of the frequencies of two quartz clocks. A mechanism similar to a synchronous stopwatch, and a magnetic counting system are used to derive a recorder voltage proportional to the time interval being measured.

53.087.64 3564
Automatic Calibrator for Chart Recorders—J. L. Durand. (*Rev. Sci. Instr.*, vol. 29, pp. 534–535; June, 1958.) A circuit is outlined which produces calibration pips on a magnetic-resonance spectrometer chart.

621.3.018.41(083.74):621.396.712 3565
WWV Standard-Frequency Transmissions—W. D. George. (PROC. IRE, vol. 46, pp. 1534–1535; August, 1958.) A note on the accuracy of WWV and WWVH transmissions during May, 1958.

621.3.082+621.3.078 3566
How Transducers Measure and Control—R. K. Jurgen. (*Electronics*, vol. 31, pp. 59–70; July 4, 1958.) A general survey of the transducer field, together with applications.

621.317.332.6.029.6. 3567
Measurement of Low Reflection Coefficients at High Frequencies in Terms of Magnitude and Phase—A. Linnebach. (*Arch. Elekt. Übertragung*, vol. 11, pp. 471–477; December, 1957.) The conventional reflectometer method is extended to cover the measurement of phase angle by the insertion of a quadripole with variable stub lines.

621.317.35:621.396.84 3568
Errors of Selectivity Measurement—W. Rotkiewicz. (*Nachrtech. Z.*, vol. 8, pp. 22–24; January, 1958.) The causes of errors and their elimination in receiver selectivity measurements are discussed.

621.317.411.029.6:538.221 3569
Measurement of Permeability at V.H.F. using Transmission-Line Technique—J. C. Anderson. (*J. Brit. IRE*, vol. 18, pp. 417–424; July, 1958.) Accurate measurements may be made without the aid of calibrated instruments or standing-wave detectors. These measurements are sufficiently precise to show detailed structure in the permeability/frequency curves. Results are given for strips of permalloy B and C, mumetal, and for pure nickel wire.

621.317.42:621.375.13 3570
The Control of Flux Waveforms in Iron Testing by the Application of Feedback Amplifier Techniques—J. McFarlane and M. J. Harris. (*Proc. IEE*, vol. 105, pp. 395–402; Discussion, pp. 402–405; August, 1958.)

621.317.42:621.383 3571
The Construction of a Photoelectric Electronic Fluxmeter—M. Sauzade. (*Compt. Rend. Acad. Sci., Paris*, vol. 246, pp. 727–730; February 3, 1958.) Description of the design of an integrating system comprising a galvanometer, photocell and amplifier, with capacitive feedback, of the type described by Edgar [see 2163 of 1956 (Kapitsa)]. See also 435 of 1949 (Dicke).

621.317.44 3572
A Ferrometer for the Determination of the A.C. Magnetization Curve and the Iron Losses of Small Ferromagnetic Sheet Samples—H. Blomberg and P. J. Karttunen. (*Proc. IEE*, vol. 105, pp. 375–384; August, 1958. Discussion, pp. 402–405.)

621.317.44 3573
Direct-Reading Iron-Loss Testing Equip-

ment for Single Sheets, Single Strips and Test Squares—J. McFarlane, P. Milne, and J. K. Darby. (*Proc. IEE*, vol. 105, pp. 385–394; August, 1958. Discussion, pp. 402–405.)

621.317.7:538.566:621.372.823 3574

Double-Probe Polarimetric Analyser for the 1000-mc/s Band—F. Picherit. (*Compt. Rend. Acad. Sci., Paris*, vol. 246, pp. 911–913; February 10, 1958.) Description of apparatus for accurate measurement of wave rotation in a circular waveguide, using a graduated rotatable section provided with two probes with a fixed angular separation of 90 degrees.

621.317.73:537.312.9.082.73 3575

Apparatus for Piezoresistance Measurement—M. Pollack. (*Rev. Sci. Instr.*, vol. 29, pp. 639–641; July, 1958.) The piezoresistance effect in semiconductors is measured using a 29-cps alternating stress. The method is sensitive and suitable for low-resistivity materials; the measurements are adiabatic. See also 1192 of 1958 (Potter).

621.317.733:621.317.4:538.221 3576

Improved Bridge Method for the Measurement of Core Losses in Ferromagnetic Materials at High Flux Densities—W. P. Harris and I. L. Cooter. (*J. Res. Natl. Bur. Stand.*, vol. 60, Rep. 2865, pp. 509–516; May, 1958.) An amplifier having negative output resistance was devised and is used in a manner that automatically allows accurate compensation for the harmonic components of the excitation current. See also 530 of 1957 (Cooter and Harris).

621.317.74:621.372.2.029.6 3577

High-Frequency Measuring Lines—C. Moerder. (*Arch. Tech. Messen.*, no. 265, pp. 37–40; February, 1958.) The use of calibrated transmission lines for the measurement of circuit and line characteristics is described. Particular reference is made to the Smith chart and to commercial test equipment incorporating an artificial line with a CRO display of the measured parameters on a Smith-chart graticule.

621.317.74:621.372.852.323:621.318.134 3578

High-Power Testing of Ferrite Isolators—E. Wantuch. (*Electronic Ind.*, vol. 17, pp. 83–85; April, 1958.) Description of methods for determining insertion loss, input SWR under matched-load, and isolation under mismatched-load conditions.

621.317.74:621.374 3579

An Electronic Pulse-Duration Analyser—E. Newell and A. A. Makemson. (*P.O. Elec. Eng. J.*, vol. 51, pp. 64–69; April, 1958.) Description of apparatus for determining the duration and frequency of occurrence of transient irregularities on HF trunk telephone routes. Irregularities longer than 2 ms are recorded on cold-cathode counters, simultaneous recordings being made of durations exceeding four predetermined values in the range 2–50 ms.

621.317.75:621.376.3 3580

Testing the Linearity of Modulators and Demodulators in Multichannel F.M. Transmitters and Receivers—G. C. Davey. (*Electronic Eng.*, vol. 30, pp. 487–489; August, 1958.) Design principles are described of equipment which displays the slope of a demodulator characteristic and discriminates changes in slope of 1 per cent. Modulators can be tested indirectly and the equipment may be used for conventional sweep tests in aligning IF amplifiers.

621.317.755 3581

A New Eight-Channel Oscillograph—H. H. Feldmann. (*Elektrotech. Z., Ed. B*, vol. 10, pp. 206–209; May 21, 1958.) A single-tube CRO is described which provides facilities for the simultaneous display of four functions. The 2×4 variables are applied to the vertical and horizontal amplifiers, via an electronic switching circuit.

621.317.755:621.385.029.6 3582

Fractional-Millimicrosecond Oscilloscope System Utilizing Commercially Available Components—C. N. Winningstad. (*Rev. Sci. Instr.*, vol. 29, pp. 578–584; July, 1958.) The oscilloscope described uses a traveling-wave CR tube with a synchronizing system which does not appreciably distort the applied pulse.

621.317.755.087.6 3583

Electronic Tracing of Oscilloscope Displays—C. H. Hertz and E. Möller. (*Rev. Sci. Instr.*, vol. 29, pp. 611–613; July, 1958.) A gated charging circuit is described for sampling the waveform applied to a CRO and driving a pen recorder. Frequencies up to 10 kc can be recorded.

621.317.789 3584

Ergmeter measures Bursts of Energy—L. A. Rosenthal. (*Electronics*, vol. 31, pp. 79–81; June 6, 1958.) Energy surges unbalance a bolometer bridge whose output is amplified and applied to a peak-holding voltmeter; the instrument is calibrated by using an internally generated pulse of known energy content.

621.317.799:551.510.535:621.396.11 3585

An Automatic Recorder for Measuring Ionospheric Absorption—Mazumdar. (See 3461.)

621.317.799:621.316.82 3586

Potentiometer Tester—S. Morleigh. (*Wireless World*, vol. 64, pp. 450–452; September, 1958.) Description of circuits for locating bad contacts and for measuring contact resistance in precision variable resistors and inductive potentiometers.

621.317.799:621.396.61/.62 3587

Recent Developments in Communications Measuring Instruments—E. Garthwaite and A. G. Wray. (*J. Brit. IRE*, vol. 18, pp. 387–397; July, 1958.) Improvements in design and advances in measuring techniques are illustrated by reference to specific instruments. Future trends are briefly discussed.

621.317.799:621.396.933.029.6 3588

A Standing-Wave-Ratio Measuring Instrument for Use in the Maintenance of Aircraft Installations—A. G. Hancock and T. S. Kepner. (*A.W.A. Tech. Rev.*, vol. 10, pp. 90–99; October, 1957.) A portable instrument for measuring SWR on transmission lines in VHF aircraft installations is described. The battery operated equipment includes bridges for 50-Ω and 70-Ω installations, and fixed and variable oscillators.

OTHER APPLICATIONS OF RADIO AND ELECTRONICS

53.087.5 3589

Digital and Pictorial Photographic Electronic Recorder—R. G. McPherson and I. A. Sonderby. (*Commun. and Electronics*, no. 36, pp. 194–196; May, 1958.) Digital recording is achieved by photographing square spots or bits in rows on the film. With a bit size of 10 mils and 40 bits/row, 4000 bits/inch may be stored on 16-mm film. Playback is effected by mechanical or electrical scanning.

53.087.9:621.395.625.3 3590

Magnetic Tape for Data Recording—C. D. Mee. (*Proc. IEE*, vol. 105, pp. 373–380; July, 1958. Discussion, pp. 380–382.) The occurrence of "drop-outs" in both the recording and reproduction of pulse signals is investigated and applied to "return to zero" and "non return to zero" recording. Methods are considered which would improve reliability. Equipment is described for testing tape under widely varying recording conditions. Commercial tapes are assessed and an economical performance specification is suggested.

551.508.822 3591

Comparison of Aerological Soundings made Simultaneously by Radiosonde and Aircraft—F. H. Ludlam and P. M. Saunders. (*Tellus*, vol. 10, pp. 83–87; February, 1958.) The results of five soundings by Väisälä radiosonde and by aircraft fitted with electrical resistance thermometers show that the temperatures given by the radiosonde were usually 1–1½°C, but occasionally 2½–3½°C, too great. Shallow layers of very dry air were often not revealed by the radiosonde due to the large time lag of the hygrometer unit.

621.362:536.8 3592

Measured Thermal Efficiencies of a Diode Configuration of a Thermo-electron Engine—G. N. Hatsopoulos and J. Kaye. (*J. Appl. Phys.*, vol. 29, pp. 1124–1125; July, 1958.) Note on a practical engineering method of converting heat directly into electricity.

621.384.612 3593

Electron Losses due to Phase Oscillations Induced by Radiation Fluctuations in Synchrotrons—A. N. Matveev. (*Zh. Eksp. Teor. Fiz.*, vol. 33, pp. 1254–1260; November, 1957.) An approximate method of calculation is described taking account of nonlinear effects by considering appropriate boundary conditions in linear theory.

621.384.7:537.533.8 3594

Source of Ions due to Electron Bombardment—D. Blanc and A. Degeilh. (*Compt. Rend. Acad. Sci., Paris*, vol. 246, pp. 936–939; February 10, 1958.) The characteristics of an ion source of Nier type (see *Rev. Sci. Instr.*, vol. 18, pp. 398–411; June, 1957) without an auxiliary magnetic field are described.

621.385.833:061.3 3595

Summarized Proceedings of a Conference on Electron Microscopy—Bangor, September 1957—H. W. Emerton. (*Brit. J. Appl. Phys.*, vol. 9, pp. 306–312, 322; August, 1958.)

621.385.833:537.533.72 3596

Magnetic Deflexion of Electron Beams without Astigmatism—G. D. Archard and T. Mulvey. (*J. Sci. Instr.*, vol. 35, pp. 279–283; August, 1958.) The system described uses circular pole pieces from which semicircular portions have been removed. An application to reflection-type electron microscopes is described.

621.385.833:621.373.44 3597

Construction of a 100-kV Pulse Generator—J. Gardez. (*Compt. Rend. Acad. Sci., Paris*, vol. 246, pp. 1023–1025; February 17, 1958.) A pulse generator for an electron microscope is described, with pulse length 2 μsec, and repetition frequency 200/sec.

621.387.4 3598

The Design, Performance and Use of Fission Counters—W. Abson, P. G. Salmon, and S. Pyrah. (*Proc. IEE*, vol. 105, pp. 349–356; July, 1958. Discussion, pp. 365–369.) General design criteria applicable to the measurement of fission cross sections, the analysis of neutron spectra and the relative measurement of neutron flux are discussed.

621.387.424 3599

Firing Characteristics of Halogen-Quenched Geiger-Müller Counters—S. P. Puri and P. S. Gill. (*Proc. Natl. Inst. Sci. India*, vol. 24, pp. 66–77; January 26, 1958.)

621.387.426.2 3600
Boron Trifluoride Proportional Counters—W. Abson, P. G. Salmon, and S. Pyrah. (*Proc. IEE*, vol. 105, pp. 357–365; July, 1958. Discussion, pp. 365–369.) Operating characteristics and the effect of circuit parameters on output pulse amplitude are discussed.

621.398:623.454.91–519 3601
Telemeter Transmitter for Vanguard Rocket—N. Raskhodoff. (*Electronics*, vol. 31, pp. 46–47; July 4, 1958.) Details of engine performance are relayed using a PWM/FM system.

PROPAGATION OF WAVES

621.396.11:551.510.535 3602
Electromagnetic Propagation in an almost Homogeneous Medium—V. W. Bolie. (*Aust. J. Phys.*, vol. 2, pp. 118–125; March, 1958.) An equation is derived for calculating the scattering energy resulting from a single Gaussian perturbation in refractive index. A turbulent ionosphere may be considered as being composed of such perturbations.

621.396.11:551.510.535 3603
Single-Hop Propagation of Radio Waves to a Distance of 5300 km—F. Kift. (*Nature, London*, vol. 181, pp. 1459–1460; May 24, 1958.) Path lengths and angles of elevation of rays arriving at Slough from Ottawa have been calculated from the Appleton and Beynon equations for propagation via a parabolic F_2 layer, and show good agreement with experimental results of Warren and Hagg (2202 of 1958).

621.396.11.029.45/.5:551.510.535 3604
Low-Frequency Reflection in the Ionosphere—H. Poeverlein. (*J. Atmos. Terr. Phys.*, vol. 12, nos. 3/4, pp. 126–139; 1958 and no. 4, pp. 236–247; 1958. Correction, *ibid.*, p. 352.) Theoretical investigation of ionospheric reflection in the frequency range 1–100 kc approximately. The ionospheric layer is considered as a thin conductive sheet or as consisting of many thin sublayers. Some typical cases are discussed with reference to observational results.

621.396.11.029.45:551.594.6 3605
Velocity of Propagation of Electromagnetic Waves at Audio Frequencies—Y. L. Al'pert and S. V. Borodina. (*Zh. Eksp. Teor. Fiz.*, vol. 33, pp. 1305–1307; November, 1957.) Note of an investigation covering the frequency range 1–30 kc based on waveform analysis of thunderstorm discharges at distances of 800–3100 km. Experimental and theoretical values deviate significantly below 3 kc, at which frequencies the model of the ionosphere used in the calculations may be inappropriate. See also 920 of 1957.

621.396.11.029.53:551.510.535 3606
Investigation of Magneto-ionic Fading in Oblique-Incidence Medium-Wave Transmissions—M. S. Rao and B. R. Rao. (*J. Atmos. Terr. Phys.*, vol. 12, pp. 293–305; July, 1958.) "Periodic fading of magneto-ionic origin observed in oblique-incidence medium-wave records is interpreted theoretically by calculating the phase paths by a graphical integration method assuming Chapman and parabolic ion distribution. Analytical expressions have also been derived for phase paths of both magneto-ionic components by an approximate method involving the use of an empirical formula for *q-x* curves. The theoretical values of fading periods compared very well with the experimental data, the agreement being particularly good for the case of Chapman distribution."

621.396.11.029.6:551.510.5 3607
Atmospheric Effects on V.H.F. and U.H.F. Propagation—G. H. Millman. (Proc. IRE, vol. 46, pp. 1492–1501; August, 1958.) Tropospheric refractive-index profiles and ionospheric electron-density models representative of average conditions are presented, and mathematical relations are derived for calculating refraction effects, time delays, Doppler errors, polarization changes, and attenuation experienced by radio waves traversing the entire atmosphere.

621.396.11.029.62:523.5 3608
A Theoretical Rate Amplitude Relation in Meteoric Forward Scattering—C. O. Hines. (*Canad. J. Phys.*, vol. 36, pp. 539–554; May, 1958.) The theory of forward scattering of radio waves by ionized meteor trails is applied to the development of a relation which expresses the expected occurrence rate of scattered signals exceeding a given amplitude level as a function of that level. Comparison with provisional observational data shows good agreement qualitatively and quantitatively. Closest agreement is obtained only with an appropriate choice of two scaling factors which provide a convenient condensed version of the observations for further interpretation.

621.396.11.029.62:523.5 3609
Observations of Angle of Arrival of Meteor Echoes in V.H.F. Forward-Scatter Propagation—K. Endresen, T. Hagfors, B. Landmark and J. Rodsrud. (*J. Atmos. Terr. Phys.*, vol. 12, pp. 329–334; July, 1958.) Observations were made in November and December, 1957 near Tronsö, using a frequency of 46.8 mc. Histograms show the properties of background meteor reflections as well as of shower reflections as a function of azimuth. Diurnal variations agree well with present theories.

621.396.11.029.62:523.5 3610
The Fading of Long-Duration Meteor Bursts in Forward-Scatter Propagation—B. Landmark. (*J. Atmos. Terr. Phys.*, vol. 12, pp. 341–342; July, 1958.) Application of the theory presented by L. A. Manning at the 12th General Assembly of URSI, 1957, Boulder, Colo., allows the seasonal variations of wind sheer in the lower E layer to be studied.

621.396.11.029.62:551.510.535 3611
Preliminary Results of Studies of the Angular Distribution of a V.H.F. Ionospheric Forward-Scatter Signal—T. Hagfors. (*J. Atmos. Terr. Phys.*, vol. 12, pp. 340–341, plate; July, 1958.) The angular spectrum is determined by correlation over the wavefront. Results obtained at 46.8 mc over a 1150-km N-S path indicate that the Rayleigh-type background is not due to the overlapping of many small meteoric echoes.

621.396.11.029.62:621.397.81 3612
Phase-Coherent Back-Scatter of Radio Waves at the Surface of the Sea—E. Sofaer. (Proc. IRE, vol. 105, pp. 383–394; July, 1958.) An investigation into interference with reception of the B.B.C. Devon television transmitter in coastal regions near Plymouth. Rhythmic variations in amplitude due to beating between direct and back-scattered signals occur when sea waves within the irradiated area are correctly spaced and suitably oriented with respect to frequency and geometry of the transmitter /receiver circuit. The effect is studied theoretically and correlated with meteorological data.

621.396.11.029.64 3613
Multipath Propagation of Microwaves—T. Omori and R. Sato. (*Rep. Elec. Commun. Lab., Japan.* vol. 6, pp. 1–11; January, 1958.) Results are given for five different paths at frequencies near 4 kmc; frequency-sweep and pulse techniques were both used to measure the delayed signals. The mean value of the instantaneous distortion in the worst 1-hour period was shown to be negligibly small.

RECEPTION

621.376.2 3614
The Demodulation of Linearly Distorted A.M. Spectra—H. Schneider and G. Petrich. (*Nachrtech. Z.*, vol. 8, pp. 17–21; January, 1958.) Continuation of 2893 of 1957 dealing with s.s.b. and common-frequency reception and the distortion effects of overmodulation.

621.376.23:621.396.822 3615
The Rectification of Non-Gaussian Noise—J. A. Mullen and D. Middleton. (*Quart. Appl. Math.*, vol. 15, pp. 395–419; January, 1958.) A noise model in which the noise events occur with a Poisson distribution in time is analyzed. Atmospherics and some types of radar clutter may approximate to this model. The influence of linear and quadratic detectors on the noise is studied, and account is taken of narrow-band filters preceding the detector.

621.376.23:621.396.822 3616
Effects of Signal Fluctuation on the Detection of Pulse Signals in Noise—M. Schwartz. (IRE Trans. on Information Theory, vol. IT-2, pp. 66–71; June, 1956. Abstract, Proc. IRE, vol. 44, p. 1642; November, 1956.)

621.396.822:621.376.23 3617
Rectification of Two Signals in Random Noise—L. L. Campbell. (IRE Trans. on Information Theory, vol. IT-2, pp. 119–124; December, 1956. Abstract, Proc. IRE, vol. 45, p. 575; April, 1957.)

621.376.23:621.396.822 3618
Optimum Detection of Random Signals in Noise, with Applications to Scatter-Multipath Communication: Part I—R. Price. (IRE Trans. on Information Theory, vol. IT-2, pp. 125–135; December, 1956. Correction, *ibid.*, vol. IT-3, p. 256; December, 1957. Abstract, Proc. IRE, vol. 45, p. 575; April, 1957.)

621.376.23:621.396.822 3619
A Coincidence Procedure for Signal Detection—M. Schwartz. (IRE Trans. on Information Theory, vol. IT-2, pp. 135–139; December, 1956. Abstract, Proc. IRE, vol. 45, p. 575; April, 1957.)

621.376.332:621.3.018.78 3620
Amplitude Modulation Suppression in F.M. Systems—C. L. Ruthroff. (*Bell Sys. Tech. J.*, vol. 37, pp. 1023–1046; July, 1958.) Limiter circuits are analyzed in terms of low-index modulation theory. The analysis of a diode limiter shows that perfect AM suppression is possible with only small loss to the FM signal. Experimental verification is given.

621.396.62:621.396.662 3621
A Novel Sideband Selector System—E. P. Alvernaz. (*QST*, vol. 42, pp. 18–20; May, 1958.) Two mixers and a common VFO are used in a selector system by means of which an incoming signal, or any part of it, can be placed in or out of the pass band of a fixed-frequency band-pass filter without changing the receiver tuning.

621.396.662 3622
Some Aspects of Permeability Tuning—W. D. Meewezen. (*Proc. IRE, Aust.*, vol. 18, pp. 263–275; August, 1957.) Capacitance and permeability-tuned circuits are compared, and the construction and applications of permeability tuners are described.

621.396.8:519.2 3623
Cumulative Frequency Curves of Eccentric Rayleigh Distribution and their Application to Propagation Measurements—H. Zuhrt. (*Arch. elekt. Übertragung*, vol. 11, pp. 478–484; December, 1957.) Equations and curves of eccentric Rayleigh distribution are given which are

applicable to received voltage waveforms considered as a number of statistically fluctuating interference waves superimposed on the signal waveform. Probability distribution curves based on propagation measurements at 2.5, 4.15 and 15 kmc are compared with the theoretical curves; agreement is closed except for short-term probabilities.

621.396.82 3624
Radio Interference: Part 3—Suppression—R. A. Dilworth. (*P.O. Elec. Eng. J.*, vol. 51, pp. 40–45; April, 1958.) Interference produced by sparking from electrical appliances is discussed. Reduction of interference by measures taken at the receiving installation, and by suppression at source are considered. Practical suppression arrangements are described and illustrated for various kinds of appliance. Part 2: 2213 of 1958 (Britton).

621.396.821 3625
Atmospheric Noise Interference to Medium-Wave Broadcasting—S. V. C. Aiya. (PROC. IRE, vol. 46, pp. 1502–1509; August, 1958.) The electrical discharges associated with a tropical thundercloud are described. It is suggested that discharge mechanisms within the cloud contribute noise only on frequencies above 2.5 mc. The power radiated by a flash in the medium-wave band is deduced by assuming that the energy is produced by the first stepped leader propagated as an air or ground discharge. See also 1866 of 1958.

STATIONS AND COMMUNICATION SYSTEMS

621.391 3626
Bits of Information—A. S. Zamanakos. (*Commun. and Electronics*, no. 36, pp. 197–201; May, 1958.) Concepts of information, channel capacity and equivocation are reviewed. The probability of an error is used to calculate the equivocation. The method of coding a message to incorporate error detecting and correcting information is explained, and examples are given of a parity checking procedure.

621.391 3627
On the Shannon Theory of Information Transmission in the Case of Continuous Signals—A. N. Kolmogorov. (IRE TRANS. ON INFORMATION THEORY, vol. IT-2, pp. 102–108; December, 1956.)

621.391 3628
On Noise Stability of a System with Error-Correcting Codes—V. I. Siforov. (IRE TRANS. ON INFORMATION THEORY, vol. IT-2, pp. 109–115; December, 1956. Abstract, PROC. IRE, vol. 45, p. 575; April, 1957.)

621.391 3629
Optimum, Linear, Discrete Filtering of Signals containing a Nonrandom Component—K. R. Johnson. (IRE TRANS. ON INFORMATION THEORY, vol. IT-2, pp. 49–55; June, 1956. Abstract, PROC. IRE, vol. 44, p. 1642; November, 1956.)

621.391:519.272 3630
Correlation Electronics—F. H. Lange. (*Nachrtech. Z.*, vol. 8, pp. 3–11; January, 1958.) The principles and purpose of correlation analysis are outlined with examples of applications in communications and electroacoustics.

621.391:519.272 3631
Simple Methods of Correlation Measurements—R. Fey. (*Nachtech. Z.*, vol. 8, pp. 12–16; January, 1958.) The analytical bases of four methods of determining autocorrelation functions are discussed, with an outline of appropriate measurement techniques.

621.391:534.75 3632
Information Transmission with Elementary Auditory Displays—Sumby, Chambliss, and Pollack. (See 3314.)

621.391:534.75 3633
Confidence Ratings and Message Reception for Filtered Speech—Decker and Pollack. (See 3315.)

621.391:621.396.822 3634
Probability Densities of the Smoothed "Random Telegraph Signal"—W. M. Wonham and A. T. Fuller. (*J. Electronics Control*, vol. 4, pp. 567–576; June, 1958.) The probability distribution of the output from a simple *RC* smoothing network is found when the input is a sequence of random square waves generated by a Poisson process. Results suggest a convenient experimental method for generating LF noise with Gaussian, rectangular, parabolic or elliptical probability density functions.

621.391:621.396.822 3635
Nonstationary Velocity Estimation—T. M. Burford. (*Bell Sys. Tech. J.*, vol. 37, pp. 1009–1021; July, 1958.) A nonstationary noise is approximated by the product of a stationary noise and a deterministic function of time. From observations of the sum of such a nonstationary noise and a linear signal, an estimate of the rate of change of the signal is obtained.

621.396.4:551.510.52 3636
White Alice—a New Radio Voice for Alaskan Outposts—W. H. Tidd. (*Bell Lab. Rec.*, vol. 36, pp. 278–283; August, 1958.) A tropospheric-scatter system is described for multichannel telephone and telegraph communication between points 100–200 miles apart. 10-kw transmitters and 60-foot parabolic antennas are used at frequencies in the 750–950 mc band.

621.396.41 3637
Compressed Time boosts Single-Sideband Capacity—M. I. Jacob and J. Mattern. (*Electronics*, vol. 31, pp. 52–55; July 4, 1958.) Description of a time-sharing multiplex system which needs only one RF channel, with a single transmitter and receiver at each station. Received information is stored, and then expended and read-out between transmissions.

621.396.41:621.396.65 3638
The Simultaneous Transmission of Television and Telephone Multiplex over a Single Microwave Channel on the Trans-Canada TD-2 System—H. E. Curtis, V. C. P. Strahlendorf, and A. J. Wade. (*Commun. and Electronics*, no. 36, pp. 185–190; May, 1958.) Transmission considerations, terminal circuits and tests are discussed for a system simultaneously transmitting a television signal and a maximum of 180 telephone channels.

621.396.61/.62:535–14 3639
500-Million-Mc/s Transceiver—H. Pallatz. (*Radio-Electronics*, vol. 28, pp. 93–94; October, 1957.) Simple voice-communication equipment using a caesium-vapour lamp as transmitter is described.

621.396.932 3640
The Development of Radio Services for Coastal Traffic, Inland Waterways and Harbours—J. Mohrmann. (*Telefunken Ztg.*, vol. 30, pp. 225–232; December, 1957. English summary, p. 286.) The development of R/T services for ship-to-shore communication in Germany is outlined and details of some modern installations, including VHF services, are given.

SUBSIDIARY APPARATUS

621.316.5.004.6 3641
Physical Processes in Contact Erosion—L. H. Germer. (*J. Appl. Phys.*, vol. 29, pp. 1067–1082; July, 1958.) A general survey of erosion effects for relatively low voltages and currents.

621.316.721/.722:621.314.7 3642
Transistor Voltage and Current Stabilizers—E. Cassignol and G. Giralt. (*Compt. Rend. Acad. Sci., Paris*, vol. 246, pp. 1020–1023; February 17, 1958.) Details are given of a current generator and a voltage generator using transistors and a Zener diode. Coupled together, the circuits provide a stabilized current supply of up to 300 ma.

621.316.93:621.314.63 3643
Electrical Protection for Transistorized Equipment—J. W. Phelps. (*Bell Lab. Rec.*, vol. 36, pp. 247–249; July, 1958.) Semiconductor diodes are used to limit excessive voltages accidentally placed on telephone circuits.

621.353/.355 3644
New Batteries for the Space Age—D. Linden and A. F. Daniel. (*Electronics*, vol. 31, pp. 59–65; July 18. 1958.) A survey of short-life electrochemical batteries, developed for extreme reliability at high discharge rates under stringent operating conditions. The main characteristics of recent types are given in tabulated form.

TELEVISION AND PHOTOTELEGRAPHY

621.397.5 3645
567 Lines—P. T. Weston. (*Wireless World*, vol. 64, pp. 442–443; September, 1958.) An alternative to the British 405-line television system is suggested in which a greater number of lines is achieved with a minimum of equipment changes.

621.397.5:535.623 3646
A Method for Controlling the Gray-Scale Equivalent of Colours used in Live and Filmed Television Scenic and Graphic Art—W. J. Wagner. (*J. Soc. Mot. Pict. Telev. Eng.*, vol. 67, pp. 369–373; June, 1958. Discussion.) Greys are graded in a scale of 20 steps from white to black, and the equivalence of colors presented on a monochromatic screen is based on this scale.

621.397.6.029.63 3647
A UHF Television Link for Outside Broadcasts—K. C. Quinton. (*B.B.C. Eng. Div. Monographs*, no. 19, pp. 1–20; June, 1958.) The merits of FM and AM systems are considered, and preliminary comparison tests over a short link with a mobile transmitter at 190 and 511 mc indicated FM to be preferable. A mobile transmitter delivering 17 watts at about 630 mc with 6-mc deviation to either a Yagi or corner-reflector antenna is described. Receiver IF is either 30 or 60 ms, with a noise factor of 14 db. Multipath distortion is still troublesome over such links, and possible means of reducing it are suggested.

621.397.611 3648
Improved Television Standards Converter—T. Worswick. (*Wireless World*, vol. 64, pp. 443–444; September, 1958.) For the B.B.C. Eurovision converter system an improvement of 10 db in signal/noise ratio has been achieved by using a 4½-inch image orthicon tube Type P812 in place of a 3-inch Type P807.

621.397.611:535.623 3649
A Flying-Spot Film Scanner for Colour Television—H. E. Holman, G. C. Newton, and S. F. Quinn. (*Proc. IEE*, vol. 105, pp. 317–328; July, 1958. Discussion pp. 329–330.) Film moving with uniform velocity is scanned by a series of displaced rasters in such a sequence that the system is applicable to 50 or 60-cps conditions. Three photomultipliers provide color analysis of the image, element by element, and directly

produce a video-frequency signal. A particular equipment is described.

621.397.611.2 3650
A French Portable TV Camera—J. Polonsky. (*J. Telev. Soc.*, vol. 8, pp. 423–431; April/June, 1958.) Technical requirements and design considerations are described for the Type-CP103 equipment weighing about 29 pounds and based on a vidicon camera tube. Transistors are used in the power supply circuits and synchronizing generator.

621.397.62 3651
Ultrasonic Tones Select TV Channels—N. Frihart and J. Krakora. (*Electronics*, vol. 31, pp. 68–69; June 6, 1958.) Television receiver tuning and power supply are remotely controlled by means of an ultrasonic magnetostriction transducer with transistor oscillator transmitting via an air path to a microphone in the receiver. See also 3669 of 1957 (Adler, *et al.*).

TRANSMISSION

621.376.222 3652
Some Aspects of High-Level Modulation—A. H. Koster. (*R.S.G.B. Bull.*, vol. 33, pp. 552–556; June, 1958.) The effects of speech compression on the output of a typical transmitter, together with circuits for reducing the resulting distortion, are described.

621.396.61:621.396.967 3653
The Frequency Stability of Self-Excited Transmitters Connected to a Load with Variable Phase—H. Schwindling. (*Telefunken Ztg.*, vol. 30, pp. 246–250; December, 1957. English summary, pp. 287–288.) The Rieke-diagram method is used to investigate the "long-line" effect with reference to rotating radar antennas.

TUBES AND THERMIONICS

621.314.63+621.314.7 3654
Crystal Valves—T. R. Scott. (*J. Telev. Soc.*, vol. 8, pp. 401–412; April/June, 1958.) The development of the crystal tube is reviewed with particular reference to economic aspects. The likely future relation between the economics of crystal and thermionic tubes is discussed and the role of the former in various fields of electronic application is examined. The difficulties and advantages of the manufacture and use of crystal tubes is also discussed.

621.314.63:621.372.652 3655
Shot Noise in *p-n*-Junction Frequency Converters—A. Uhlir, Jr. (*Bell Sys. Tech. J.*, vol. 37, pp. 951–988; July, 1958.) General equations for the noise figure of a *p-n*-junction diode with arbitrary minority-carrier storage are derived, and it is shown that a junction with purely capacitive nonlinear admittance, in theory, permits noiseless amplification. Nonlinear-resistance diodes can give low-noise frequency conversion with pulsed local-oscillator current, but cannot amplify. See also 3897 of 1956.

621.314.63:621.372.632 3656
Gain and Noise Figure of a Variable-Capacitance Up-Converter—D. Leenov. (*Bell Sys. Tech. J.*, vol. 37, pp. 989–1008; July, 1958.) The upper-sideband frequency conversion performance of a *p-n*-junction nonlinear-capacitance diode is analyzed. The maximum available gain and the noise figure are derived for the equivalent circuit consisting of a time-varying capacitance and constant series resistance. Over-all noise figures are given for three types of receiver with diode preamplifiers.

621.314.7 3657
The Tecnetron—Competitor to the Transistor?—E. Aisberg. (*Radio-Electronics*, vol. 29, pp. 60–61; May, 1958.) Description of a semiconductor device invented by S. Teszner (see *e.g.*, 3599 of 1954). It consists of a small rod of *n*-type Ge 0.5 mm in diameter with a central portion reduced to 30μ and surrounded by a cylinder of indium. Transconductance increases with frequency and in experiments a gain of 16 db was obtained at 200 mc. See also *Toute la Radio*, vol. 25, pp. 47–48; February, 1958, and *Wireless World*, vol. 64, p. 132; March, 1958.

621.385+621.375].029.65 3658
The Generation and Amplification of Millimetre Waves—Kleen and Pöschl. (See 3384.)

621.385.4:621.384.622 3659
The Resnatron as a 200-Mc/s Power Amplifier—E. B. Tucker, H. J. Schulte, E. A. Day, and E. E. Lampi. (Proc. IRE, vol. 46, pp. 1483–1492; August, 1958.) A description of the tubes used in the Minnesota linear proton accelerator. They are continuously pumped grid-pulsed amplifiers with a peak power output of 3.5 mw during 300-μsec pulses.

621.385.832.032.2 3660
Space-Charge-Grid High-Transconductance Guns—P. H. Gleichauf. (Proc. IRE, vol. 46, p. 1542; August, 1958.) Brief description of the development of a CR tube gun capable of delivering a screen current of 400 μa at a drive voltage of less than 7 volts.

621.385.832.032.36 3661
The Screen Efficiency of Sealed-Off High-Speed-Oscillograph Cathode-Ray Tubes—R. Feinberg. (*Proc. IEE*, vol. 105, pp. 370–372; July, 1958.) Factors affecting efficiency are summarized. Reduced screen efficiency is due to energy lost by nonradiative dissipation.

MISCELLANEOUS

551.58:621.3.002 3662
A Contribution to the Climatic Classification of Technical Apparatus—H. Burchard and G. Hoffmann. (*Elektrotech. Z., Ed. A*, vol. 79, pp. 315–321; May 1, 1958.) A world map of climatic zones is given which is based on a statistical analysis of maximum and minimum temperatures, and the distribution of population density in these zones is tabulated. A simplified classification of climates is derived so that des'gn and manufacture of equipment can be planned for the widest distribution combined with maximum economy.